Institute of Engineering Surveying and Space Geodesy (IESSG)

AN ASSESSMENT OF THE QUALITY OF GPS WATER VAPOUR ESTIMATES AND THEIR USE IN OPERATIONAL METEOROLOGY AND CLIMATE MONITORING

JONATHAN JONES, BSc.

Thesis submitted to the University of Nottingham

for the Degree of Doctor of Philosophy

May 2010

Abstract

The path delay between a GPS satellite and a ground based GPS receiver depends, after elimination of ionospheric effects using a combination of the two GPS frequencies, on the integral effect of the densities of dry air and water vapour along the signal path. The total delay in the signal from each satellite is known as the slant delay as the path is most likely to be non-azimuthal. The slant paths are then transferred into the vertical (or zenith) by an elevation mapping function, and this new parameter is known as the Zenith Total Delay or ZTD. ZTD gives a measure for the integrated tropospheric condition and is now widely accepted as a standard product from a network of dual frequency GPS receivers. With further calculation, taking into account surface pressure and temperature, we can then convert a portion of the ZTD into an estimate of the Integrated Water Vapour content of the atmosphere (IWV).

As IWV may potentially change rapidly on a very short timescale, it is the speed at which IWV can be calculated which is of critical importance to short term meteorological forecasting. Often, rapid changes in IWV are associated with high humidity conditions caused by extreme weather events such as thunderstorms. Extreme weather events such as these are typically difficult to predict and track under current operational meteorological systems and, as they have the potential to cause great damage, it is in the interests to both the public and Met Services to significantly improve nowcasting wherever possible. As such the requirement for dense near real-time GPS networks for meteorological applications becomes apparent. Furthermore water vapour is one of the most important constituents of the atmosphere as moisture and latent heat are primarily transmitted through the water vapour phase. As well as this, water vapour is one of the most important greenhouse gases, and as such accurate monitoring of water vapour is of great importance to climatological research.

This thesis assesses the quality of GPS water vapour estimates by comparison against a number of other remote sensing instruments to determine what the true value of the water vapour is and how well GPS water vapour estimates accurately represent real atmospheric fluctuations. Through these comparisons we can derive site specific bias corrections and thus, reconstruct a bias corrected time series of data for climate applications. Furthermore to ensure all biases associated with GPS processing changes are removed, a long time series of raw GPS data has been reprocessed under a consistent processing routine to again identify any climate trends in the data. Finally, this thesis addresses the question of whether near real-time GPS derived tropospheric estimates are of sufficient quality for climate applications without the need for time consuming reprocessing.

Acknowledgements

The work presented in this thesis has been carried out primarily at the Observations Development Department of the UK Met Office between 2003 and 2009. I wish to express my thanks to the Met Office for not only providing the time and flexibility to complete my studies but also the advice and expertise which has been essential for this work to be completed. I am very grateful to all staff at the University of Nottingham and in particular Dr Richard Bingley for his continued advice, expertise and support over the period of this work.

I would like to thank all of my colleagues both in the meteorological and geodetic worlds, in particular:

Paul Cruddace, Colin Fane and Mark Greaves at Ordnance Survey GB for all your ongoing assistance and for being a great source of both knowledge and of course, of GPS data.

All of my E-GVAP and EUREF colleagues for processing the SuperSites to assess inter-AC biases but particularly Siebren de Haan at KNMI and Henrik Vedel at DMI. Hopefully, we shall have many more years of fruitful collaboration between Geodesy and Meteorology.

All my colleagues across the Irish Sea. Ken Stewart and Geoff Bell at Ordnance Survey of Northern Ireland and Colin Bray and Ollie Finch at Ordnance Survey Ireland for your hard work in ensuring a continuing, timely and high quality data supply.

Adrian Jupp, Gemma Bennitt and Dave Offiler in the Met Office Satelllite Applications group. Without you there would be no customer for the data, thus no GPS project, and thus no thesis.

I wish to thank all of the co-authors of the papers and presentations published and pending for their input and expertise.

Finally I would like to thank my family. Special thank you to my wife Karen for all the time and patience you have given me to complete the writing up, and finally, a big thank you to my beautiful children, Thomas and Maggie Jones for all the joy they have brought me, for keeping me inspired and giving daddy time to ‘write his book’, and to you, my family, this work is dedicated…

Jonathan Jones
June 2009

Authors Contributions

Gaffard, C., and E. Walker, T. Hewison, J. Nash, **J. Jones** and E. G. Norton, 2007: High time resolution boundary layer description using combined remote sensing instruments, Proceedings of 11th International Workshop on technical and scientific Aspects of MST Radar (MST11) Gadanki/Tirupati, India.

Gaffard, C., and J. Nash, E. Walker/Blades, T. Hewison, **J. Jones**, and E. Grace Norton, 2008: High time resolution boundary layer description using combined remote sensing instruments, Ann. Geophys., 26, 2597-2612

Haan, S. de, **J. Jones** and H. Vedel, EUMETNET GPS Water Vapour (EGVAP), 2006: Presentation: EMS2006, 4/9/2006-8/9/2006, Ljubljana, Slovenia, European Meteorological Society (int.).

Jones, J., 2004: UK contributions in COST716 Final Report, Eds: G. Elgered, H. –P. Plag, H. van der Marel, S. Barlag and J. Nash, European Science Foundation.

Jones, J., 2005: Development of a UK National Water Vapour Processing System, Proceedings of WMO TECO2005 Technical Conference, Bucharest, Romania.

Jones, J., 2008: GPS Water Vapour – Operational Implementation and Recent Developments, Proceedings of WMO TECO2008 Technical Conference, St Petersburg, Russian Federation.

Nash, J., and C. Gaffard, T. Hewison, E. Norton, J. Agnew, E. Walker, **J. Jones**, M. Smees, M. Ramatschi, G. Dick, 2006: Humidity Evaluation using GPS, Radiometer, Wind Profiler and UV Lidar During CSIP Associated with Thunderstorms, Proceedings of COST720 Final Symposium, MeteoFrance, Toulouse.

Nash, J., and E. J. Orliac, A. H. Dodson, R. M. Bingley, **J. Jones**, and F. N. Teferle, 2006: On the use of near real-time GPS inferred humidity Fields for monitoring thunderstorm activity. Eos Transactions, 87(52), 2006. A11E-08.

Nash, J., and C. Gaffard, E. Yates and **J. Jones**, 2009: Preliminary thoughts on the relationships between lower troposphere profile data at individual sites and various spatial scales in the horizontal, Proceedings of 3rd COST/Net_ FAM Workshop, Olso, Norway, March 18th – 20th, 2009.

Glossary

AC	Analysis Centre
AMDAR	Aircraft Meteorological Data Reporting
ASI	Agenzia Spaziale Italiana (Italian space agency)
BSW5.0	Bernese GPS processing software version 5.0
CAPE	Convective Available Potential Energy
COST	Co-operation in the field of Scientific and Technical Research
COST716	Exploitation of Ground-Based GPS for Operational Numerical Weather Prediction and Climate Applications
CSIP	Convective Storm Initiation Project
DD	Double Difference (method of GPS processing)
DMI	Danish Meteorological Institute
E-GVAP	EUMETNET GPS Water Vapour Programme
ERP	Earth Rotation Parameter
EUMETNET	European Meteorological Network
FTIR	Fourier Transform Infra-red [Spectrometer]
Galileo	European GNSS
GFZ	The German GPS Analysis Centre, Geo Forschungs Zentrum
GIPSY-OASIS	GPS Inferred Positioning System Orbit Analysis Simulation Software
GLONASS	Russian GNSS
GNSS	Global Navigation Satellite System
GOP (or GOP_)	Geodetic Observatory Pecny, Czech Republic
GPS	Global Positioning System (US GNSS)
GTS	Global telecommunication System
HIRLAM	High Resolution Limited Area Model
IGS	International GNSS Service
IGU	IGS Ultra Rapid Products
IWV	Integrated Water Vapour
KNMI	Koninklijk Nederlands Meteorologisch Instituut
LPSNI	Land and Property Services of Northern Ireland (formerly OSNI)
METO	UK Met Office GPS processing system
MFRSR	Multi Filter Rotating Shadow-Band Radiometer
MSL	Mean Sea Level
NAE	North Atlantic and European NWP model (UK Met Office)
NGAA	The Nordic GNSS Analysis Centre
NMS	National Meteorological Service
NRT	Near Real Time

NWP	Numerical Weather Prediction
OSGB	Ordnance Survey of Great Britain
OSi	Ordnance Survey of Ireland
OSNI	Ordnance Survey of Northern Ireland
OSNet	Ordnance Survey's RTK GPS Network
OTL	Ocean Tide Loading
PCV	Phase centre Variations
PPP	Precise Point Positioning (method of GPS processing)
PTU	Pressure, Temperature and Humidity
PWV	Precipitable Water Vapour
RMS	Root Mean Square
RTK	Real Time Kinematic Positioning (method of GPS processing)
StDev	Standard Deviation
SVP	Saturation Vapour Pressure
TOUGH	Targeting Optimal Use of GPS Humidity Measurements in Meteorology
TWE	Total Water Equivalent
VP	Vapour Pressure
WE	Water Equivalent
WMO	World Meteorological Organization
WVR	Water Vapour Radiometer
ZD	Zenith Delay
ZHD	Zenith Hydrostatic delay
ZTD	Zenith Total Delay
ZWD	Zenith Wet Delay

Table of Contents

List of Figures

List of Tables

Chapter 1 Introduction

The use of Global Navigation Satellite Systems (GNSS) is becoming ever more widespread throughout the World every day. GNSS networks are being used in a diverse range of applications, particularly in developing countries where GNSS infrastructure is becoming a backbone for social and economic development. However if high precision GNSS is to be achieved, all errors in the GNSS signals must be mitigated.

The topics covered in this thesis are brought about by the delay imposed on Global Positioning System (GPS) signals specifically by the atmosphere. The delay caused by the uppermost part of the atmosphere, the ionosphere can easily be estimated by combination of the two GPS frequencies. The variability of delay due to the neutral part of the atmosphere (known as the troposphere) however is far more difficult to predict, both temporally and spatially as the variable component is directly proportional to atmospheric water vapour. The tropospheric delay is the difference between the actual travel time of the GPS signal through the atmosphere and the hypothetical travel time if the signal was traveling through a vacuum. i.e. if there was no atmosphere effecting signal propagation. In real terms the tropospheric delay is expressed as a unit of length which comes from the time delay of the signal multiplied by the speed of light. In general, tropospheric delay is normally in the range of between 2 and 3 metres, for a satellite at the zenith and a station at an altitude close to mean sea level. The actual tropospheric delay due to the refractive index of the atmosphere local to the GPS receiver must be estimated as accurately as possible if high precision GNSS positioning is to be possible.

From the work of Bevis et al., (1992) and others, it was shown that with a combination of specialist software and some atmospheric assumptions, atmospheric delay can be estimated accurately. Following on from this, with knowledge of the surface meteorological conditions, a more valuable meteorological quantity of Integrated Water Vapour (IWV) may be derived. IWV is a much more useful quantity to meteorology as it is directly linked to atmospheric humidity and can give us much more information concerning atmospheric state than a delay parameter alone. There have been a number of reports on the use of IWV in numerical models (Pacione et al., 2001; Falvey and Beavan, 2002; Geurova et al., 2006) as well as for short term forecasting applications (de Haan et al., 2004) but the main use of meteorological parameters derived from GPS observations is the assimilation of ZTD in numerical models, which is now used operationally at a number of European National meteorological services (Jupp et al., 2006; Poli et al., 2007).

1.1 GPS Meteorology in the UK

Since 1998 the Met Office has been evaluating the potential of extracting humidity information from the time delays in GPS signals received at the surface. In 2002 it was decided to develop a UK Met Office GPS processing capability with the main objective being to process as many GPS sites as possible in the British Isles delivering the results with the minimum time delay possible. Since this time the Met Office has worked in partnership with the Institute of Engineering, Surveying and Space Geodesy (IESSG) at the University of Nottingham to develop an automated processing system managed by Met Office staff. This system is referred to as METO and was successfully rolled-out for operational use in May 2007. A schematic of the data flow is shown for reference as Figure 1.1.

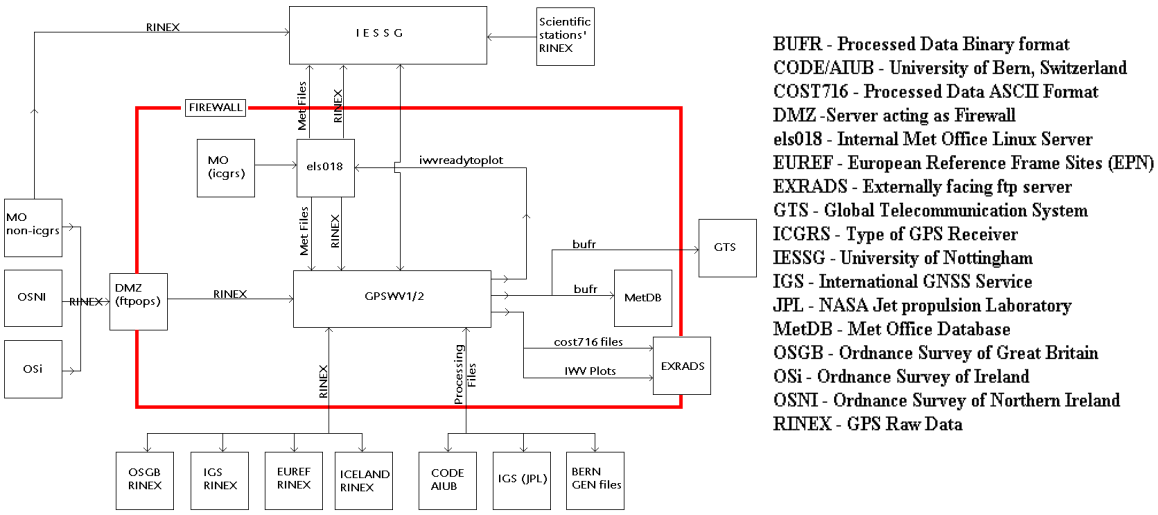

Figure 1.1 METO GPS processing data flow

The distribution of water vapour in the horizontal and vertical is required for the development of numerical weather prediction (NWP) in the UK. The information from the GPS signals at different sites constrains the horizontal distribution of water vapour in the model analyses. Since 2002 trials have been carried out by the NWP Satellite Applications group at the UK Met Office to assess the impact on NWP models of the assimilation of ground based GPS data. The conclusions suggest that in almost all cases neutral or positive impact is achieved. In some cases up to a 4% reduction in the standard deviation of model humidity, cloud cover and surface temperature is achieved by the assimilation of GPS data (Jupp, 2006).

Apart from NWP, the second main customer for GPS water vapour is the very short-term forecasting or ‘nowcasting’ community. Conditions which typically have high levels of water vapour are often associated with extreme weather events such as thunderstorms or very heavy rainfall and it is in

conditions such as these where near real-time water vapour monitoring systems, such as GPS, have the potential to become indispensable. High humidity convective thunderstorms which are typical of very high water vapour conditions can have a huge impact on national infrastructure as well as the risk to life, and as such any additional information on the location and structure of humidity fields is of great value to forecasters.

Water vapour is one of the most important greenhouse gases and from the work of Solomon et al., 2007, an estimated 70% of the recent rises in atmospheric temperature are attributed to water vapour feedback. Ground based GPS receivers could potentially be an excellent source for providing long term water vapour data for climate change studies. However, the quality of the data needs to be assessed to identify any biases introduced in the time series of data and the need for time consuming reprocessing of data is one of the questions addressed in this thesis. In the UK all raw GPS data are stored by the British Isles continuous GNSS Facility (BIGF), hosted by IESSG, at the University of Nottingham and are thus available for future reprocessing for climate applications.

1.2 GPS Meteorology in Europe

The COST (Co-operation in the Field of Scientific and Technical Research) organisation is an intergovernmental framework for European Cooperation in Science and Technology, allowing the coordination of nationally-funded research on a European level with Actions focusing on specific research topics. In 1998 the European COST Action 716 action entitled the 'Exploitation of ground-based GPS for Operational Numerical Weather Prediction and Climate Applications' began, which brought together geodetic and meteorological communities to assess the operational potential of ground-based GPS for meteorological applications on an international scale and specifically to provide near real-time observations for numerical weather prediction (Elgered et al., 2004). COST716 ended successfully in 2004 with positive NWP impact assessment trials indicating that zenith total delay estimates derived from a network of ground based GPS receivers would indeed be of use to operational meteorology.

A particular drawback of the observing system for near real-time ZTD, as it exists today, are inhomogineities, both in geographical coverage as well as in the quality and reliability of the ZTD and IWV estimates. The E-GVAP programme was established in April 2004 in order to establish an observing system capable of delivering near real time GPS ZTD of high quality and with good geographical coverage for use in operational meteorology (http://egvap.dmi.dk). The main topics of work within E-GVAP are the increase of the spatial coverage and density of observations as well as assisting Analysis Centres (ACs) by knowledge sharing, to improve the quality of their solution and increase homogeneity in processing solutions across Europe.

One noticeable outcome of the E-GVAP Project is the establishment of so-called GPS 'Supersites'. The Supersites are a small number of long established geodetic quality GPS sites which all have either a water vapour radiometer and/or an operational radiosonde station in close proximity. Also, the sites were chosen on the basis that they were within the same model layer in the main European NWP models as well as having a good geographical coverage to try and identify the role of network geometry and ocean tide loading models on processing. In the case of the most recent addition to the Supersite list, IZAN (Izana, Tenerife), there are a number of remote sensing instruments collocated which offer a great opportunity for further validation of GPS water vapour measurements and our understanding of what the real atmospheric moisture content is.

1.3 Thesis Aims and Objectives

This thesis aims to assess the accuracy of water vapour estimates derived from a network of ground based GPS receivers and look at the meteorological applications of the data, including the suitability of the data for climate applications.

The main objectives of the thesis are to answer the following questions:

a) What is the true accuracy of water vapour estimates derived from networks of ground based GPS receivers when compared against NWP and other remote sensing instruments?

b) Are GPS signals effected by falling snow and can the errors be used for snowfall monitoring?

c) How well do near real-time GPS water vapour estimates represent real, short term atmospheric fluctuations?

d) Are 2D water vapour maps derived from networks of ground based GPS receivers useful of use to short-term forecasting?

e) Are estimates of tropospheric parameters derived from GPS networks suitable for climate science and are near-real time estimates of sufficient quality?

1.4 Thesis Outline

Chapter 2 provides a background to the science and a review of the processing techniques involved. Also an overview of atmospheric water vapour is presented and its importance in the climate system. GNSS and particularly GPS are introduced, along with the established methods for the derivation of GPS water vapour estimates. Chapter 2 also looks at all the other instruments used in this thesis for comparison against GPS water vapour estimates to address instrument biases.

Chapter 3 addresses the question of accuracy of GPS water vapour estimates with a comprehensive comparison against a number of remote sensing and in-situ observation techniques, to determine what the true value of water vapour is and how well does the GPS water vapour estimates represent that 'true' value of atmospheric water vapour. Chapter 3 also addresses the questions of whether GPS signals are affected by falling snow and comparisons against other high temporal resolution remote sensing instruments determine what the limiting factors are in GPS water vapour estimates representing short-term atmospheric fluctuations.

If accurate estimates of water vapour can be derived from dense networks of GPS receivers, this constitutes a new observing system in itself. There is a limited value of a single observation from a single GPS receiver, but when large networks with a resolution useful to meteorology are available, smaller scale atmospheric structures can be identified by using GPS water vapour estimates. Chapter 4 addresses the usefulness of 2D water vapour maps to the forecasting community with the presentation of the development of these maps and examples of GPS derived water vapour fields.

Chapter 5 addresses the role GPS data can have in identifying and measuring long term climatological trends in atmospheric delay and water vapour. Bias corrections derived from Chapter 3 are applied to the data to ensure homogeneity of the time series and a long term GPS reprocessing campaign is presented. Furthermore, an assessment of the applicability of near real-time GPS water vapour estimates to climate studies is presented and determines whether time consuming reprocessing is necessary to determine accurate climate trends.

Chapter 6 contains conclusions and makes recommendations for future work based on the findings of this thesis.

Chapter 2 Background

Atmospheric water vapour observations may be measured directly by in-situ instruments such as from radiosondes or from instruments onboard aircraft or, alternatively, from remote sensing estimates from instruments such as microwave radiometers or GPS receivers. As with any instrument or observing technique, biases will exist to some degree or another. Radiosonde instrument changes can have profound effects on water vapour retrieval and GPS processing techniques can also have dramatic effects. In order to assess the extent of the biases we first must understand a little about the techniques themselves. Only when the biases have been assessed and quantified can we then apply the correct bias corrections to the data to ensure a homogenous time series.

Firstly in this Chapter, information on atmospheric water vapour and it's relevance to meteorology as well as its role in the climate system is presented. Then, an overview of GNSS and in particular GPS is presented along with the techniques required for ZTD and IWV estimation using GPS signals. A history and summary of GPS meteorology in the UK is also presented showing the development of the GPS networks over time as well as the development and final transition to operations of the Met Office GPS processing system METO. The fourth Section looks at each instrument which is used in this thesis for comparison with GPS water vapour estimates.

2.1 Atmospheric Water Vapour

Water vapour is one of the most significant constituents of the atmosphere since it is the means by which moisture and energy (as latent heat) are transported through the troposphere and lower stratosphere. Furthermore, apart from the role of water vapour in balancing the atmospheric heat budget, water vapour is obviously the source of precipitation, rain, snow, hail etc. In any vertical column of air, the amount of water vapour gives meteorologists a value of the maximum potential precipitation which could be retrieved from that air column under the right conditions. Also as water vapour is highly variable both temporally and spatially it poses a source of inaccuracy to the geodetic community, so the more accurately it can be estimated, the better the GPS derived coordinates.

Although the actual amount of atmospheric water is relatively low (~1%), the effect it has on the meteorology is very strong. It has the ability to cause small as well as large scale temperature anomalies and is the main mechanism for atmospheric latent heat exchange. Furthermore, when looking at water vapour's role in the climate system, recent studies have estimated that about 70% of the warming of the atmosphere is attributed to water vapour acting as a greenhouse gas (Houghton et al., 2001; Philipona et al., 2005).

In terms of definitions, water vapour is defined as the amount of water in gas phase (in grams per cubic metre) of air. Water vapour mixing ratio in a volume of air is the ratio of mass of water vapour and the mass of dry air. Specific humidity is the amount of water in gas phase (measured in grams in a total air volume with a mass of 1kg). A more commonly used parameter is relative humidity. This parameter is the ratio of the water vapour pressure to the saturation vapour pressure. The latter term is the pressure at which all water vapour condensates. When air has a relative humidity of 100% the air is said to be saturated and cannot absorb any further water vapour at that temperature and pressure.

Another way to express the water vapour content of an air parcel is to combine all the water vapour in the vertical column of air and in terms of water vapour it is this concept which is the topic of this thesis. The most commonly used terms are Integrated Water Vapour (IWV) and Precipitable Water Vapour (PWV). Both terms represent the absolute total amount of water in the vertical column of air which could, hypothetically precipitate out with units of kg/m^2. The term of Integrated Water Vapour, or IWV, will be used in this thesis. Also the unit, unlike the unit of mm which is commonly used for PWV, avoids any confusion with the units used in atmospheric delay which are units of length. The actual amount is exactly the same, as 1 kg of water spread out over $1m^2$ would be exactly 1mm in height.

It is important to remember that IWV is a cumulative total amount of water vapour, in principle all the way from the ground based GPS antenna in this case to the GPS satellite at an altitude of approx 20,200km. However, water vapour is by no means distributed evenly in the vertical. The vast majority of the water vapour is limited to the warmest, bottom most portion of the lowest section of the atmosphere known as the troposphere, see Figures 2.1 and 2.2.

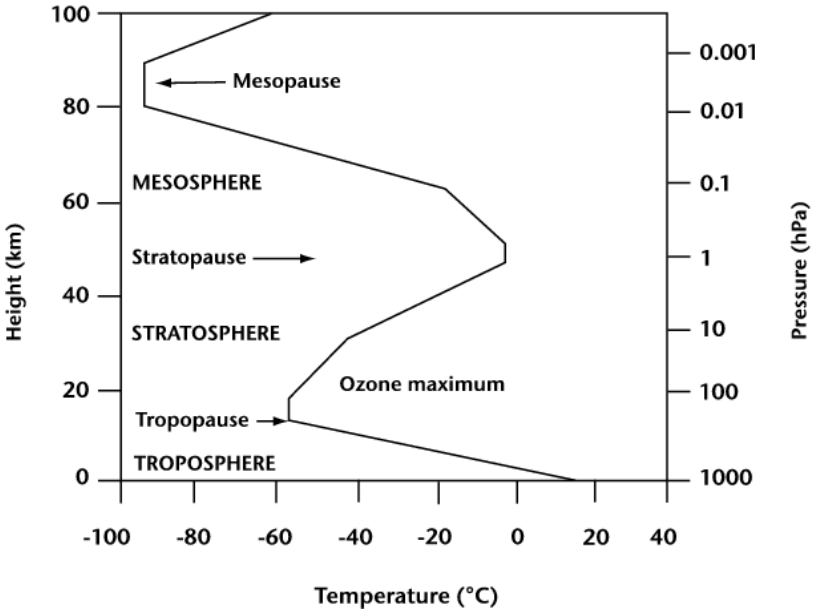

Figure 2.1 Typical atmospheric temperature profile

In real terms, the vast majority of all atmospheric water vapour is located in the bottom-most few km with a certain degree of variability depending on season, latitude and atmospheric conditions. A typical humidity profile for Camborne for July 2009 is shown in Figure 2.2.

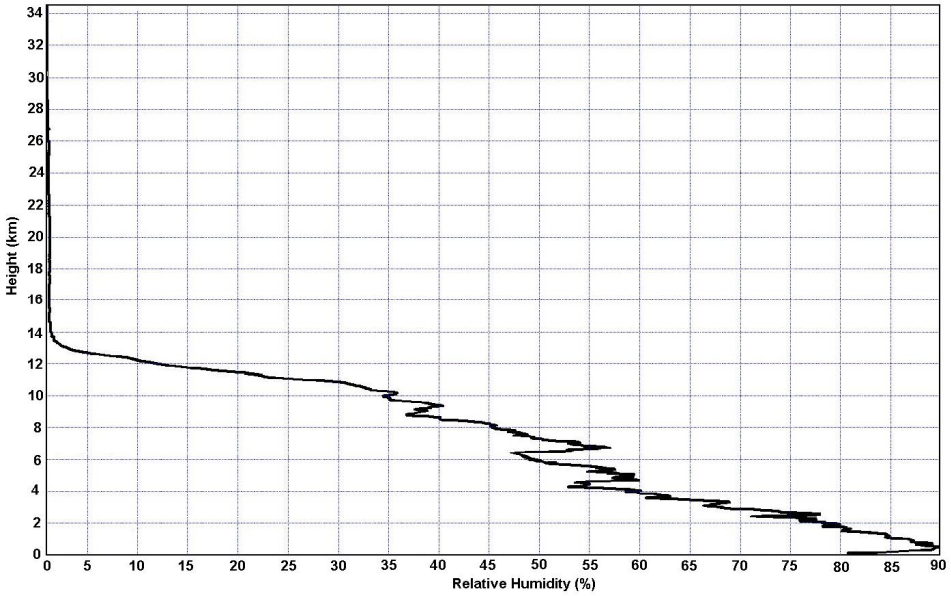

Figure 2.2 Average monthly humidity profile, Camborne, UK. Composite of all RS92 operational radiosonde ascents from July 2009.

Due to its high variability, both temporally and spatially, water vapour is one of the most difficult quantities to predict with numerical weather prediction (NWP) models. NWP models require three-dimensional temperature, moisture, pressure, and wind data (four dimensional in time). Typically a model field is initialised with existing model data coupled with observational data taken primarily from radiosonde ascents limited spatially and temporally, thus limiting the effectiveness of the forecast models. Unfortunately water vapour measurements are relatively scarce in meteorology with nearly all water vapour data obtained from operational radiosonde ascents. Given that approximately half the energy in the atmosphere is transported to that location by water vapour it becomes clear that other parameters such as cloud cover and surface temperature are also better forecast with superior water vapour information. Due to the importance of water vapour in operational meteorology, improved knowledge and understanding of water vapour fields is one of the prime focuses for future observing systems and is key to improving future forecasting capability.

Although modern NWP does typically estimate some atmospheric parameters with excellent accuracy (UK Met Office North Atlantic and European (NAE) domain model accurate to roughly 2hPa pressure), due to the reliance on spatially and temporally sparse observations to initialise the model schemes, other parameters such as water vapour are more difficult to predict. Figure 2.3 represents a time series of GPS zenith total delay (ZTD) and IWV estimates from the UK Met Office GPS system

(METO) compared against the HIRLAM 11km unified NWP model (Unden et al., 2002). This is just one example of an NWP model under estimating atmospheric zenith delay and water vapour (NB. The HL11 model does not currently assimilate the GPS estimates).

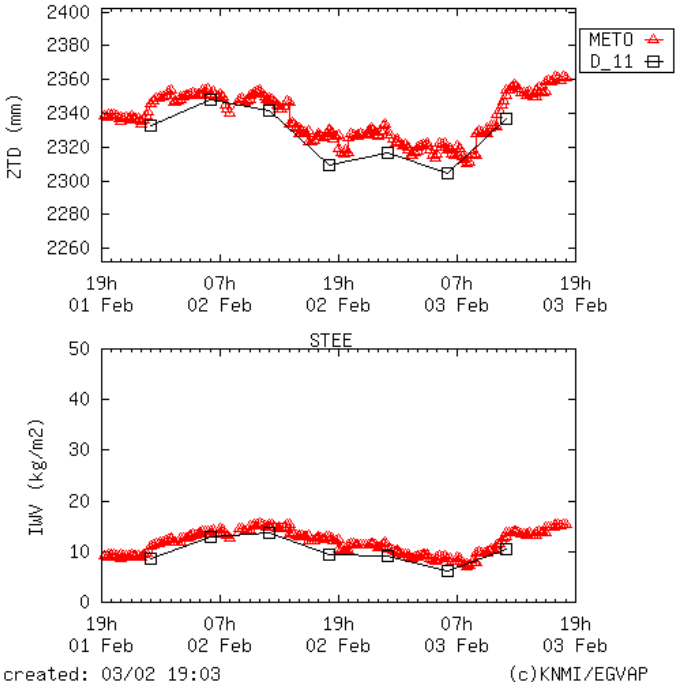

Figure 2.3 Time series of ZTD and IWV illustrating divergence of NWP from observations, Stevenage, UK, February 2010

In the future added computing power will permit NWP models with ever increasing resolution. As such with the advent of higher resolution NWP models will come the requirement for higher resolution observational data to be fed in to initialise the models starting conditions. For example, in the current UK 4km model, GPS ZTD data is only assimilated once every 3 hours (once per 3-hour model run). In the near future by contrast, the Met Office plans to introduce a new higher resolution model with a 1.5km grid square resolution and the need for higher rate GPS ZTD data.

Besides the importance to operational meteorology of accurate water vapour observations, water vapour is one of the most important controlling factors in mean atmospheric temperature by the absorption of radiation. Life on Earth is very much dependent on what is commonly referred to as the greenhouse effect. In general terms this effect is generally the absorption of solar radiation in the atmosphere which maintains the Earth's atmosphere at a habitable temperature in which life can exist. Earth has an average temperature of around 14^0C whereas if it were not for the presence of gases such as water vapour and carbon dioxide in the atmosphere, the Earth would have a mean atmospheric temperature of around -18 ^{0}C and life would not be possible as we know it.

Water Vapour is one of the most crucial greenhouse gases and plays a vital role in the global climate system. This role is not only restricted to absorbing and radiating energy from the sun, but has direct effects on the formation of clouds and aerosols and the chemistry of the lower atmosphere. Despite its importance to atmospheric processes over a wide range of spatial and temporal scales, it is one of the least understood and poorly described components of the Earth's atmosphere in current climate prediction models. Atmospheric water vapour in the atmosphere allows the short wavelength radiation of the sun to pass through the atmosphere, but absorbs long wavelength radiation emitted by the Earth's surface. This trapped radiation causes the temperatures to increase.

As air temperatures increase in association with global warming, atmospheric air parcels expand and can sustain a greater volume of water vapour. This additional water vapour can then absorb even more radiation, thus causing a positive feedback loop. The situation continues until some atmospheric equilibrium is reached and no further water vapour absorption can occur. Thus water vapour is generally thought of as a feedback rather than a cause of global warming. However, water vapour's role in the climate system is still not very well understood. In many climate models, details in the representation of clouds can substantially affect the model estimates of cloud feedback and climate sensitivity (e.g., Senior and Mitchell, 1993; Stainforth et al., 2005; Yokohata et al., 2005). Moreover, the spread of climate sensitivity estimates among current models arises primarily from inter-model differences in cloud feedbacks (Colman, 2003; Soden and Held, 2006; Webb et al., 2006) as such, water vapour and their attributable cloud feedbacks remain the largest source of uncertainty in climate sensitivity estimates.

With the advent of high precision ground based geodetic GPS networks however and high quality GPS processing schemes, we now have a new novel approach for the long term monitoring of atmospheric water vapour. GPS networks are increasing in their global coverage and if the data can be use for climate applications, they offer a huge resource in terms of monitoring atmospheric water vapour. Furthermore, due to the instruments' high level of reliability and the low level of maintenance, GPS sensors are especially suited to the more remote regions of the world which are typically data sparse. The applicability of GPS as a tool for climate applications is discussed further in Chapter5.

2.2 Global Navigation Satellite Systems (GNSS)

TRANSIT, was the first operational satellite navigation system. The system was developed to provide accurate location information to ballistic missile submarines. The system was rolled out for military use in January 1964 and subsequently to civilian users in July 1967. The system, using a constellation of five polar orbiting satellites in low Earth orbit (1075km) was comprised of 2 carrier frequencies (150 and 400MHz) which could be used to provide an hourly positioning estimate with an accuracy of between 200 and 400m.

However, it wasn't until 1993 when the Global Positioning System (GPS) achieved operational capability that continuous 3 dimensional positioning and timing information became widely available allowing positioning accuracy down to the sub decimetre level. The basic principle of GPS is that coded signals are transmitted by at least four satellites for the 3 dimensional position, plus the time element, to be determined. More information on the technique is given in the section below focusing on GPS basics.

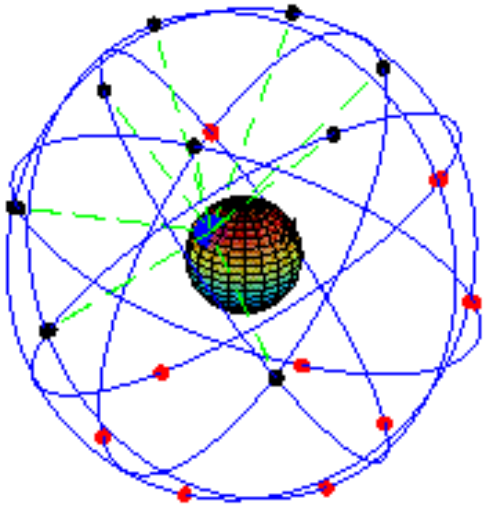

Figure 2.4 Representation of the GPS Satellite constellation

Although the focus of this thesis is GNSS data from the GPS, other GNSSs do exist. The Russian GLONASS system was complete in 1995 but rapidly fell into disrepair with the collapse of the Soviet Union. Beginning in 2001, the Russian Federation committed to restoring the system, with a goal of restoring global coverage by 2009. The Compass (or Beidou-2) system is a project by the Peoples Republic of China and is proposed to work on similar principles to GPS. Also, the European alternative to GPS, known as Galileo, is proposed to be operational by 2012. For the period of this thesis however, only GPS was fully operational and as such it was the only GNSS used and the only one referred to from this point forward.

2.2.1 GPS Basics

GPS consists of three primary segments; space, ground and user. The space segment consists of GPS satellites orbiting at an altitude of approximately 20,200km in orbital planes of 55 degrees to the equator. There must be at least 24 satellites operational to ensure any point on the Earth's surface can 'see' at least 4 satellites at any one time. The satellites transmit coded signals and other information (orbital parameters, satellite clock errors etc) to the user. The ground segment consists of a master control station in Colorado, USA as well as a number of global monitoring stations which are responsible for generating the satellite information such as orbits and clock errors.

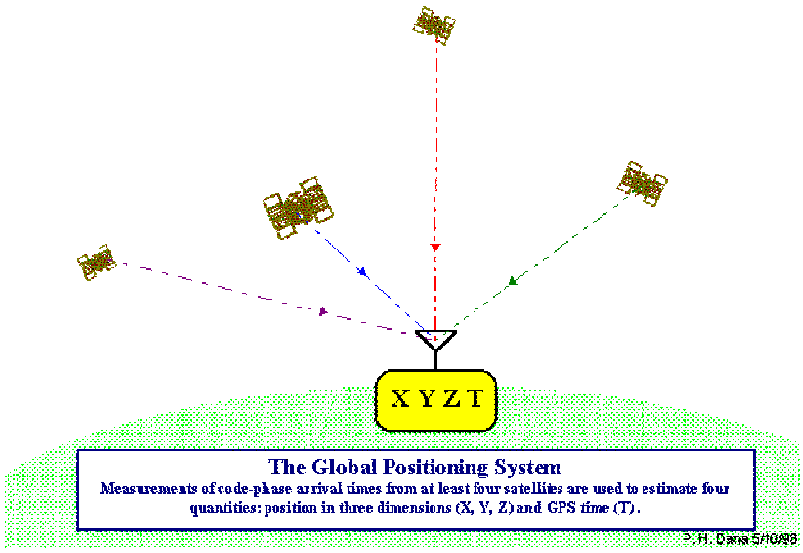

Figure 2.5 Illustration of GPS positioning

On each GPS satellite an onboard satellite oscillator generates the fundamental frequency (f_0) of 10.23MHz from which all other GPS signals are derived. The two sinusoidal carrier frequencies f_1 and f_2 (at 1575.42MHz and 1227.60MHz respectively) are right-hand polarized with respect to each other and are modulated with coded information. There are three codes imposed on the signal, the C/A (Coarse Acquisition or Clear-Access) code, the P (Precise or Protected) code and the navigation message. These codes have 2 states, a +1 or -1 state. As such if the phase-modulated L1 and L2 codes can be decoded by a ground based GPS receiver (the user segment) they may give the user positioning and velocity information, as summarised in Figure 2.5.

The C/A code has a code sequence of 1023 bits in length and is transmitted with a frequency of 1.023 MHz. As such it repeats itself once every millisecond and assuming the signal is travelling at the speed of light the distance between subsequent chips can be estimated to be ~300m. The generation of the P-Code is very similar with the length of the code sequence being approximately 2.3547 x 1014 bits which corresponds to a time span of approximately 266 days. The P-Code repeats

itself once every week and through a process known as anti-spoofing (AS), the P-code is encrypted to a Y-code.

After signals are received by a GPS receiver, the signals are initially split into their satellite specific PRN number based on the C/A codes. A carrier reference code is generated by the GPS receiver, modulated with a copy of the satellite specific PRN code and time shifted to compare against the received code. If the receiver and satellite clock errors are ignored this difference gives the travel time (τ) and when multiplied by the speed of light (c) gives the approximate range or pseudo-range to the satellite.

Phase positioning measurements are based on reconstructing the carrier phase of the signal and comparing against a signal copy generated by the GPS receiver. By observing the difference in the phase of the signals transmitted by the GPS satellite and those stored in the GPS receiver, the phase difference may be obtained which can be resolved to provide the user with a distance measurement. This expression may be written as:

$$\Delta\phi = \phi_{obs} - \phi_{rec} \qquad 2.1$$

Positioning using phase differencing has a much higher accuracy, although it does introduce what is known as an integer ambiguity (j_{amb}) which must be solved. Furthermore additional delays in the signal propagation such as ionospheric delay (ΔL_{ion}), tropospheric delay (ΔL_{trp}) and clock differences between the satellite and receiver $\left(\tau_{sat} - \tau_{rec}\right)$ must all be accounted for if precise, geodetic positioning is to be achieved. From Blewitt (1997) the pseudorange, multiplied by the frequency, λ , may be expressed as:

$$\lambda\Delta\phi = D + c\left(\tau_{sat} - \tau_{rec}\right) - \lambda j_{amb} + \Delta L_{trp} + \Delta L_{ion} + \mathrm{E} \qquad 2.2$$

Where D is the geometric range from receiver to satellite, c is the speed of light and E is the unknown errors such as receiver multipath. As there are more unknown parameters in equation 2.2 than known parameters, equations for a number of satellites are required if all parameters are to be solved for. Furthermore, satellite orbit and clock information must be known a-priori which can be obtained from the International GNSS Service (IGS), which is a voluntary federation of more than 200 worldwide organisations who generate and provide free of charge GPS products and services. With particular reference to this thesis, they provide satellite clock corrections as well as both predicted and past satellite orbit information.

Even though the clock files provided by the IGS are of high quality there still remain clock errors in both satellite and receiver as well as un-calibrated phase errors which must be accounted for. These errors are common to all receivers and satellites and they can be eliminated by observing a number of satellites and receivers and forming what are known as baselines. Single difference baselines are formed by observing the same satellite by two receivers, in this way the satellite clocks and phase errors can be eliminated. By observing two satellites by two GPS receivers the satellite clock, receiver clock and phase errors are eliminated. However, tropospheric errors can only be ignored if the baselines are relatively small and the stations are at the same altitude, as the effect from the atmosphere will affect all signals in the same way.

The alternative to forming baselines between receivers to remove the clock errors is to resolve the clock errors a-priori and thus introduce very accurate clock files into the processing in the first place. If this can be achieved a network of GPS receivers can be processed in a station specific way, which is commonly referred to as Precise Point Positioning or PPP. The main benefits of PPP are that it is, at least for the coordinate and tropospheric estimation part, faster because the sites can be processed individually and the processing load can be shared over a number off CPUs/PCs. Also as the sites are processed individually there is no risk of correlated errors as could be the case with the network solution. In reality however, any benefits in processing speed are often offset against the time it takes to generate the higher accuracy clocks and as such the overall processing time for a national scale (approximately 200-receiver) network is often comparable to that taken by a double difference solution. Also, while a PPP system might not have any correlated errors between sections of the network due to baselines, if any errors are introduced in the satellite clock determination with the PPP method, those errors will be applied to the whole network being processed. For more information on the PPP method, see Kouba and Heroux, 2001.

2.2.2 Tropospheric Delay

Once enough data has been collected from a number of satellites over a long enough time period, estimates can be generated of atmospheric delay as well as satellite clock errors and phase ambiguities. Due to the dispersive nature of the ionosphere it affects both GPS signals in the same way, by a mathematical combination of the L1 and L2 signals, a so-called ionosphere-free linear combination (L3) can be obtained and thus first order ionospheric delays can be eliminated. Second order effects are still present but their order of magnitude is so small they can be largely ignored for the purposes of this thesis.

$$L_3 = \frac{f_1^2}{f_1^2 - f_2^2} L_1 - \frac{f_2^2}{f_1^2 - f_2^2} L_2 \qquad 2.3$$

The atmosphere local to the GPS receiver is assumed to be horizontally homogenous and based on this assumption, slant path delays can be mapped into the vertical and the number of unknowns can be reduced further. There is not enough power in the least squares adjustment to solve for slant paths directly, thus limiting the use of slant delays and GPS tomography. Slant path delays are topics of research at a number of atmospheric and geodetic institutes, but use of a-priori atmospheric model information is necessary. For the purpose of this thesis, slant path delays are ignored and the focus is only on zenith path delays (see Figure 2.6)

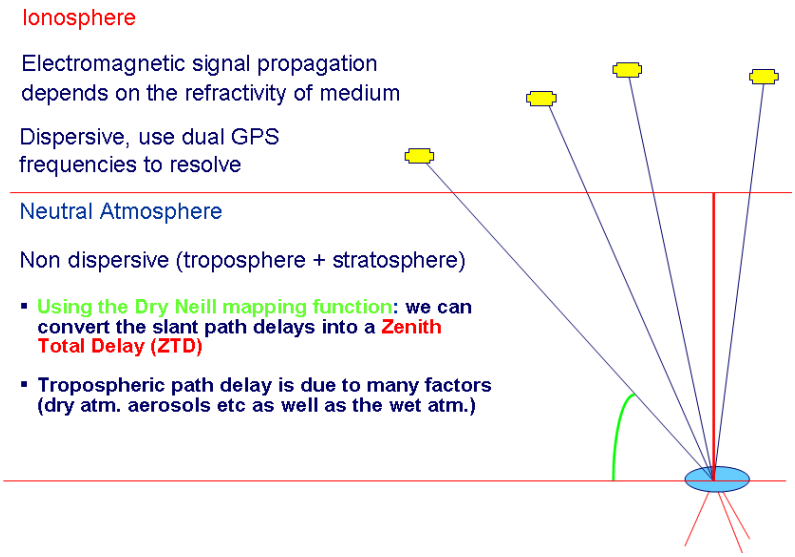

Figure 2.6 Schematic of Satellite signal path through atmosphere

Tropospheric delay can be expressed as:

$$\Delta^T = \int_s n ds - \int_g dg \qquad 2.4$$

where n is the refractive index, s is the actual signal path and g is the hypothetical geometric path. It is possible to rewrite this as

$$\Delta^T = \int_s (n-1) ds + \left(\int_s ds - \int_g dg \right) \qquad 2.5$$

This expression shows us that tropospheric delay is a combination of the excess geometric path length

as well as the slowing of the signal propagation speed.

Excess geometric path length caused by changes in refractive index, n, is only of relevance at very high zenith angles where the signal is effectively being bent by the atmosphere and a bending angle is introduced. At the vast majority of satellite zenith angles bending and thus excess path is very small when compared to the delay of the signal due to propagation. From McClatchey et al. (1971) geometric delay at a zenith angle of 80^o would only be in the region of ~4cm whereas at lower zenith angles (i.e. higher elevation angles) the delay due to slowing of the signal contributes to around 99.7% of the atmospheric delay. In current practice, most GPS receivers are set with an elevation cut off angles of either 5^o or 10^o which largely eliminates the geometric delay, as well as minimizing the multipath effect of signals being reflected off the Earth's surface or nearby objects.

As such we can we-write equation 2.5 to show that the tropospheric delay is due to the integrated refractivity along the signal propagation path:

$$\Delta^T = \int_s (n-1)ds = 10^{-6}\int_s N ds \qquad 2.6$$

where refractivity N is defined as $N=10^6(n-1)$ (according to Smith and Weintraub, 1953; Thomson et al., 1986). In the microwave range however refractivity is related to atmospheric parameters through:

$$N = k_1 \frac{p_d}{T} Z_d^{-1} + k_2 \frac{e}{T} Z_w^{-1} + k3 \frac{e}{T^2} Z_w^{-1} \qquad 2.7$$

Where p_d is the pressure of dry air, e is the water vapour pressure, T is the temperature, Z_d and Z_w are the compressibility factors of dry air and water vapour respectively and k1, k2 and k3 are thermodynamic coefficients with values of 77.6 $KhPa^{-1}$, 70.4 $KhPa^{-1}$ and 373900 $K2hPa^{-1}$ respectively, taken from Thayer, (1974).

2.2.3 Zenith Delay Estimates

One of the standard outputs from a number of geodetic GPS processing software is ZTD based on phase measurements from a network of ground based GPS receivers. In GPS meteorology it is useful to reduce the term of ZTD into its constituent parts, Zenith Hydrostatic Delay (ZHD) and Zenith Wet Delay (ZWD). ZHD is responsible for the vast majority of the ZTD delay (typically around 90%) and is easily modeled if surface pressures are known. It is the ZWD which is of interest to meteorology as it is this component which is related to humidity and can change rapidly both spatially and temporally. If we assume that the dry and wet components of equation 2.7 behave as ideal gases, Z_d

and Z_w are equal to 1 (Bevis et al., 1992) and can therefore be eliminated. Such that when we separate the pressure into its dry and wet partial pressures we can express these terms as:

$$\rho_d = \frac{p_d}{R_d T} \qquad \text{and} \qquad \rho_w = \frac{e}{R_w T} \qquad \text{2.8 and 2.9}$$

where R_d and R_w are the gas constants of dry air and water vapour respectively. The density of the 'real' air is simply $\rho_d + \rho_w$. Therefore the refractivity can be expressed as:

$$N = k_1 \frac{p_d}{T} + k_2 \frac{e}{T} + k3 \frac{e}{T^2} \qquad \text{2.10}$$

which can be further reduced to:

$$N = k_1 \rho R_d + (k_2 R_w - k_1 R_d)\rho_w + \frac{k_3 \rho_w R_w}{T} \qquad \text{2.11}$$

Since the path is assumed to be zenithal, ZTD is equal to Δ^T and therefore we can integrate equation 2.6, so that ZTD between the receiver altitude z_r and infinity is:

$$ZTD = 10^{-6} \int_{z_r}^{\infty} N dz \qquad \text{2.12}$$

And therefore:

$$ZTD = 10^{-6} \int_{z_r}^{\infty} k_1 \rho R_d dz + 10^{-6} \int_{z_r}^{\infty} (k_2 R_w - k_1 R_d)\rho_w dz + 10^{-6} \int_{z_r}^{\infty} \frac{k_3 \rho_w R_w}{T} dz \qquad \text{2.13}$$

2.2.4 Derivation of IWV from ZTD

The first term on the right hand side of equation 2.13 deals with the integration of the combined wet and dry air, The 2nd and 3rd terms integrate the water vapour density and ratio of water vapour density and temperature respectively. Furthermore by application of the hydrostatic equation:

$$dp = -g\rho dz \qquad \text{2.14}$$

where g is the local gravitational acceleration, allows us to transform the first term of equation 2.13

to:

$$ZHD = 10^{-6} \frac{k_1 R_d}{g^*} p_r \qquad 2.15$$

where g^* is the local gravitational acceleration and the centre of mass of the vertical air column and the integration is performed between 0 and pressure at the receiver p_r. Equation 2.15 shows the dependency between receiver pressure (i.e. receiver altitude) and ZHD. However, as is illustrated in equation 2.13, other atmospheric parameters need to be known (temperature, humidity etc) to determine the wet component of the delay. As this information is not necessarily available certain assumptions about the state of the atmosphere must be made.

By making additional assumptions about the vertical temperature and humidity structure we can transform ZWD into the more meteorological term of integrated water vapour (IWV):

$$\text{IWV} = \int_{z_r}^{\infty} \rho_w dz \qquad 2.16$$

So

$$\text{ZWD} = 10^{-6} \int_{z_r}^{\infty} (k_2 R_w - k_1 R_d) \rho_w dz + 10^{-6} \int_{z_r}^{\infty} \frac{k_3 \rho_w R_w}{T} dz$$

$$= 10^{-6} ((k_2 R_w - k_1 R_d) \int_{z_r}^{\infty} \rho_w dz + 10^{-6} k_3 R_w \int_{z_r}^{\infty} \frac{\rho_w}{T} dz \qquad 2.17$$

To derive a relationship between ZWD and IWV we must first derive a mean temperature the vertical column of air above the GPS receiver

$$T_m = \frac{\int_{z_r}^{\infty} \rho_w dz}{\int_{z_r}^{\infty} (\rho_w / T) dz} \qquad 2.18$$

And as this relation is identical to

$$\int_{z_r}^{\infty} \frac{\rho_w}{T} dz = \frac{\int_{Z_r}^{\infty} \rho_w dz}{T_m} \qquad 2.19$$

The ZWD equation 2.17 can now be rewritten as

$$ZWD = 10^{-6}(k_2 R_w - k_1 R_d + k_3 \frac{R_w}{T_m}) \int_{z_r}^{\infty} \rho_w dz \qquad 2.20$$

$$ZWD = 10^{-6}(k_2 R_w - k_1 R_d + k_3 \frac{R_w}{T_m}) IWV \qquad 2.21$$

The conversion of ZTD into IWV thus depends largely on the mean temperature of the air column (T_m), which in turn depends on the vertical temperature and humidity profiles. The estimation of vertical temperature and humidity introduces error into the ZWD to IWV conversion and for this reason ZTD is more commonly assimilated into NWP assimilation schemes as opposed to IWV.

2.3 GPS Processing for Meteorological Applications in the UK

In 2003 the IESSG at the University of Nottingham were contracted by the UK Met Office to carry out an investigation into the optimum GPS processing strategy for providing ZTD and IWV estimates for near real-time (NRT) meteorological applications (Orliac et al. 2003). After a series of trials, IESSG concluded that the optimum processing strategy would consist of running the Bernese processing software (developed by the University of Bern, Switzerland, (Rothacher, et al., 1996; Dach et al., 2007) utilising the double-difference (DD) GPS processing technique. For the NRT processing system, the predicted part of the International GNSS Service Ultra Rapid products (IGU) was to be used for the satellite orbit parameters and clocks. Although improved satellite orbit accuracy is achieved after the time of event, IESSG found that the IGU products were more than adequate for near real time processing using the DD strategy. The quality of the NRT processing was to be checked using the same DD network approach but using a more accurate first post processed update of the Ultra rapid orbit product, which was available with a 6 hour delay. Finally a Precise Point Positioning (PPP) strategy was also implemented using the most accurate IGS Final products, with a time delay of 20 days. Meteorological surface information would be retrieved from the Met Office Database (MetDB) for the ZTD to IWV transformation, and the conversion would carried out according to the method suggested by Saastamoinen (1972).

By 2004 the first development servers were delivered to the Met Office and were known as GPSMET1 and GPSMET2 respectively. The servers were for development of the system with the main aim to investigate the optimum processing strategy and reliability of GPS processing in a near real-time

environment. At this time automated near real-time GPS processing was only being trialled by a small number of European Geodetic institutes and the limitations of running such a system on an operational automated basis were largely unknown. Up until this point high accuracy GPS processing had primarily been done for geodetic applications on a daily basis and there were still a number of unknowns regarding data availability and processed data quality. When processing GPS data in a near real-time environment for NWP applications a balance needs to be found between the number of stations processed (geographical scope), and the quality of data against processing time. Data from a sufficiently large area needs to be delivered to NWP in as short a time as possible but providing data of high quality. These things are difficult to balance in GPS processing as an increased number of sites or higher quality of solution inherently take longer to process.

By 2005 the Met Office and IESSG had decided upon an optimum processing strategy and had also proved the reliability of processing GPS data in near real-time. At this point a further contract was placed with IESSG to deliver a new pair of processing servers by mid-2006 which would be responsible for the operational processing of GPS data at the UK Met Office. The new servers, GPSWV1 and GPSWV2 respectively, were quite different from the development servers in that they were more reliable and had the focus purely on NRT processing and not on the ability to reprocess past data. The main changes between the GPSMET and GPSWV servers was no major reliance on a MYSQL database as well as the dropping of the quality check solutions. As such the operational systems were based on an hourly NRT solution with a daily PPP solution for the generation of a-priori coordinates with a 30-day sliding window approach and with a 20 delay, using the IGS final orbits and clocks (IGS products). By December 2006 the new servers were delivered and by May 2007 had gained full operational status. The Met Office GPS processing system is known as METO and is the source of all the data used in this thesis unless stated otherwise. A table providing an overview of METO is shown as Table 2.1.

Software	Bernese v5.0
Raw Data	Hourly RINEX
ZTD/IWV Estimates	5 (00, 15, 30, 45 and 59)
OTL Model	FES2004
Reference System	IGS05
Antenna Phase Centre Model	Absolute
Orbits	Predicted half of IGU
A-priori Coordinate generation	30-day sliding window
Relative/Absolute Constraints	10mm/1.0m

Table 2.1 Overview of METO GPS processing parameters

The GPSWV1 and 2 servers were last updated in 2007 to take account the more up to date processing models including FES2004 OTL model, as well as absolute antenna phase centre models and the IGS05 reference system. The servers have since been running on a fully operational basis and process data from up to 300 European GPS sites on an hourly basis. Figure 2.7 shows the network of GPS sites processed by the METO servers as of May 2009.

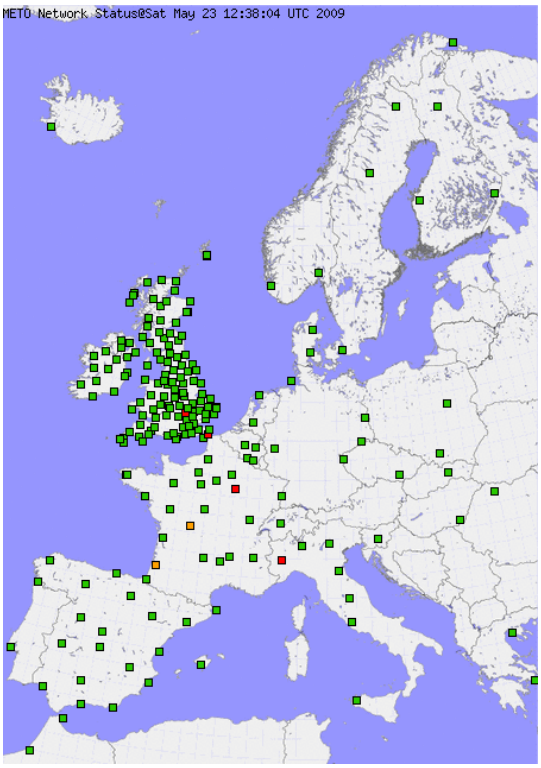

Figure 2.7 GPS network typically processed in NRT by METO. Colours represent latency of data. See E-GVAP website for more details, http://egvap.dmi.dk

In the UK the main GPS data provider is the Ordnance Survey of Great Britain (OSGB). Their OSNet network consists of around 100 sites operating continuously. For OSNet, data is routed to OSGB headquarters in Southampton in real time by way of broadband internet connections so that atmospheric and ionospheric corrections can be calculated and error corrections transmitted to their engineers in the field, allowing cm accuracy positioning in real time. In 2006 the Met Office and OSGB came to a resource sharing agreement whereby the Met Office would permit OSGB to install a number of GPS antennas and receivers on Met office sites around the UK in return for access to data from their network. Clearly without such an agreement the spatial resolution of the UK GPS network would not be dense enough for near real-time meteorological applications. Similar agreements are also in place between the Met Office and the national mapping agencies of both Northern Ireland and the Republic of Ireland, and without such agreements, the processing would be limited to a Great Britain network only.

2.4 IWV from Difference Sources

In order to validate any GPS water vapour estimates, data from a number of other remote sensing instruments is used. These include radiosondes, microwave radiometers, a sun photometer, a Fourier Transform Infra-red spectrometer, a Multi Filter Rotating Shadow-Band radiometer, NWP models and water vapour imagery from satellite data. Each one of these is briefly described in this Section.

2.4.1 IWV or TWE from Radiosonde Data

A radiosonde is an instrument designed to be launched under a weather balloon for in situ retrieval of atmospheric parameters. The radiosonde transmits the data back to a ground station for processing and quality control and subsequently the data can be used for operational meteorology as well as for climate applications. Radiosondes have been launched operationally in the UK since the early 20th century, however the technology employed, and as such their subsequent accuracy, has increased dramatically over time (Nash et al, 2006). Radiosondes play a vital role in operational meteorology as many NWP schemes are largely trained on radiosonde ascent data, and they have for some time been one of the only sources of high accuracy upper air measurement. However with the advent of modern remotes sensing techniques such as GPS, the two systems can be compared to assess the bias of each instrument.

Although a multitude of specialist sensors can be attached to radiosondes, most modern radiosondes used in operational meteorology are typically equipped with onboard pressure, temperature and humidity (PTU) sensors of varying types depending on the manufacturer and the intended use of the radiosonde. Height is either estimated directly by way of onboard code correlating GPS or inferred from atmospheric pressure using climatological models.

The Finnish manufacturer Vaisala has been the Met Office operational radiosonde provider for the period of this thesis. A pictorial history of Vaisala radiosondes is shown in Figure 2.8.


RS11 (1931 – 1983)

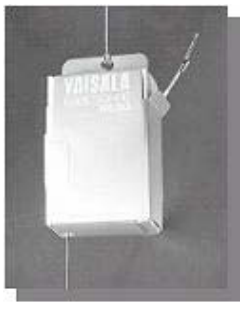

RS80 (1983 – 1999)


RS90 (1999 – 2003)


RS92 (2003 – Present)

Figure 2.8 Evolution of Vaisala radiosondes over time (images courtesy of Vaisala)

For the period of this thesis and the subsequent comparisons in Chapter 3 two main types of radiosondes were used operationally in the UK. In mid 2005 the Met Office upgraded their radiosonde type from the older RS80 (Leiterer, U., et al. 1997) to the more modern digital RS92 radiosonde. As we see later, major bias shifts exist when radiosonde types are renewed and this must be taken into account when performing long term comparisons against GPS or any other instrument. Both the RS80 and RS92 are high quality, self contained units with humidity sensor and temperature sensors located on a boom away from the radiosonde body to ensure minimal heat and air flow contamination. A schematic of a RS92 radiosonde is shown in Figures 2.9 and 2.10.

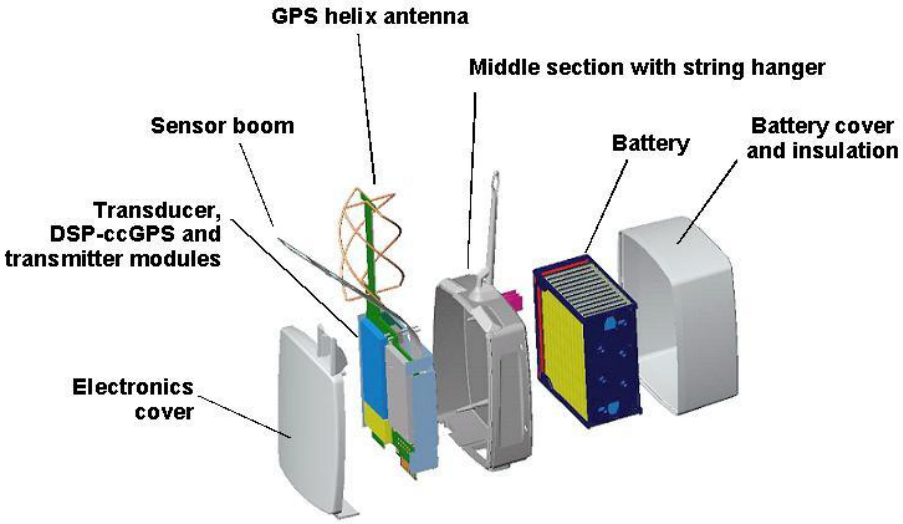

Figure 2.9 Vaisala RS92 radiosonde internals (Image courtesy of Vaisala)

Figure 2.10 The Vaisala Thermocap® (top) and Humicap® (bottom two) temperature and humidity sensors (Image courtesy of Vaisala)

Total Water Equivalent (TWE) is the term used for the equivalent measure of IWV but calculated from radiosonde ascents. The TWE is calculated by successfully incrementing the so-called water equivalent calculated at each 2 second layer of a radiosonde ascent (corresponding to approximately 10m height, depending on rate of balloon ascent) and then simply adding all the incremental layers to determine the total water equivalent for the column. In all the equations below suffix 1 refers to bottom of the layer and suffix 2 refers to top of layer. Firstly we need to calculate the mean vapour pressure for the individual 2 second layers. To complete this we must calculate the Vapour Pressure (VP) from Saturated Vapour Pressure (SVP) for top and bottom of each layer, where t_1 and t_2 are the temperatures at the bottom and top of the layer respectively, ρ_1 and ρ_2 is the humidity at the bottom and top of the layer respectively.

For bottom point

$$svp_1 = 6.11^{\left(\frac{19.7t_1}{273.16+t_1}\right)} \tag{2.22}$$

$$vp_1 = svp_1\left(\frac{\rho_1}{100}\right) \tag{2.23}$$

Similarly we need to perform the same calculation for the top of the layer

$$svp_2 = 6.11^{\left(\frac{19.7t_2}{273.16+t_2}\right)} \tag{2.24}$$

$$vp_2 = svp_2\left(\frac{\rho_2}{100}\right) \tag{2.25}$$

Next we must calculate the mean vapour pressure (VP_m) and mean temperature (T_m) for the layer which is simply:

$$VP_m = \left(\frac{vp_1 + vp_2}{2}\right) \tag{2.26}$$

And similarly we calculate the mean temperature

$$T_m = \left(\frac{t_1 + t_2}{2}\right) \tag{2.27}$$

As the layers are relatively thin (~10m) we can assume that by just calculating the mean temperature and vapour pressure we get representative data for the layer. Next we can calculate the so-called water equivalent (WE) for the layer. Firstly we must calculate the depth of the layer which is simply:

$$\delta h = h_1 - h_2 \qquad 2.28$$

With h_1 and h_2 being the height at the bottom and top of the layer respectively, and therefore we can calculate the wet equivalent for that layer:

$$WE = \delta h \left(\frac{VP_m}{4.615 T_m} \right) \qquad 2.29$$

Finally we can increment this procedure over successive layers to get the Total Water Equivalent for any radiosonde ascent:

$$TWE = TWE + WE \qquad 2.30$$

This process is carried out up to 12km after which it is assumed that the water vapour content is negligible. For comparison purposes the TWE is assumed to be vertical. The radiosonde flight in reality will hardly ever be vertical but as the radiosonde will generally stay in the same vertical column of air from which it was launched (i.e. the radiosonde is moving horizontally at the same velocity as the air mass itself) we can assume a vertical profile.

The main two sensors of importance in terms of calculating IWV are the radiosondes' humidity and temperature sensors. The Vaisala RS92 is equipped with the Vaisala Thermocap® temperature sensor working on the principles of electrical resistance for a given medium. The temperature sensor boasts an accuracy of 0.5^{o}C for the total radiosonde ascent with, as quoted by the manufacturer 'minimized solar radiation error'. However from studies completed in this thesis we can see that the effect of solar heating and the bias corrections applied in the Vaisala software are not negligible. The effect of solar heating on the radiosondes sensors is addressed in Chapter 3.

The RS92 is also equipped with the Vaisala Humicap® humidity sensor which again works on the principles of electrical resistance. The RS92 is equipped with two sensors which are in turn pulse heated to drive off condensation (cloud contamination) as well as any ice build up which might affect the reading. As such the manufacturer's quoted accuracy is 5% relative humidity for the complete ascent. Again solar radiation can drive off humidity and cause artificially low readings, causing artificially low TWE estimates.

As mentioned previously, during the period of this thesis, in around mid-2005, the radiosonde type was upgraded from the RS80 type radiosonde to the more modern RS92 radiosonde. Since the RS92 was introduced, the radiosonde has also had a number of instrument and software upgrades (Paukkunen et al., 2001 and 2002), all of which have to be taken into account when performing long time series comparisons against GPS water vapour. Table 2.2 is an overview of radiosonde upgrades over the time of the thesis for the four sites used for comparison in Chapter 3.

Site	RS80 data from	RS92 from	New Humidity (U) Sensor	New Temperature (T) Sensor
Camborne/CAMB	June 2001	April 2005	July 2007	July 2008
Herstmonceux/HERS	Jan 2002	Jan 2006	May 2007	July 2008
Lerwick/LERW	June 2001	April 2005	June 2007	July 2008
Watnall/IESG	Jan 2003	May 2005	June 2007	Aug 2008

Table 2.2 Overview of GPS processing and radiosonde upgrades during period of thesis

In July 2007 Vaisala updated their RS92 radiosondes with an improved humidity sensor coating in an attempt to reduce the effect of solar heating on the humidity sensor. In daytime soundings solar radiation causes an error in the humidity measurement. This is due to the fact that the humidity sensors and their contacts to the radiosonde are warmer than the surrounding air they are measuring. The effect is negligible in the lower troposphere. The effect becomes noticeable in the upper troposphere and lower stratosphere where solar radiation is strong, especially in high humidity conditions. This error is reduced by coating the sensor contacts with appropriate material. By doing this the error is estimated to be reduced by half.

Furthermore in July 2008 the Vaisala RS92 temperature sensor was strengthened with strong quartz fibre, which is firmly integrated into the current sensor structure. The added material to the structure is estimated to lead to five times better mechanical strength for RS92 radiosondes, without apparently degrading the response time or accuracy and solar radiation absorption by the sensor. The new structure makes the sensor less prone to damage during flight preparation and sounding. Also the protective boom frame has been removed to improve the air flow to the sensor.

To assess the impact, if any, on IWV estimates from radiosondes, biases both prior and post instrument changes are assessed in Chapter 3.

2.4.2 IWV from Microwave Radiometers

The use of water vapour radiometers (WVRs) for the retrieval of temperature and humidity profiles by microwave absorption has been demonstrated for some time (e.g. Westwater et al, 1965; Askne and Nordius 1987; Rosenkranz, 1998 etc). In addition to the retrieval of temperature and humidity profiles, IWV can also be extracted and as such they are an ideal tool for comparison against GPS water vapour. As with radiosonde data we can assess each instrument in terms of bias, but as WVRs typically observe at very high rates of observation (on seconds to minutes timescales) WVRs are a very useful tool for assessing how well GPS water vapour mirrors short term atmospheric fluctuations.

Figure 2.11 The Radiometrics Corporation MP3008
microwave radiometer. (Image courtesy of Radiometrics Corporation)

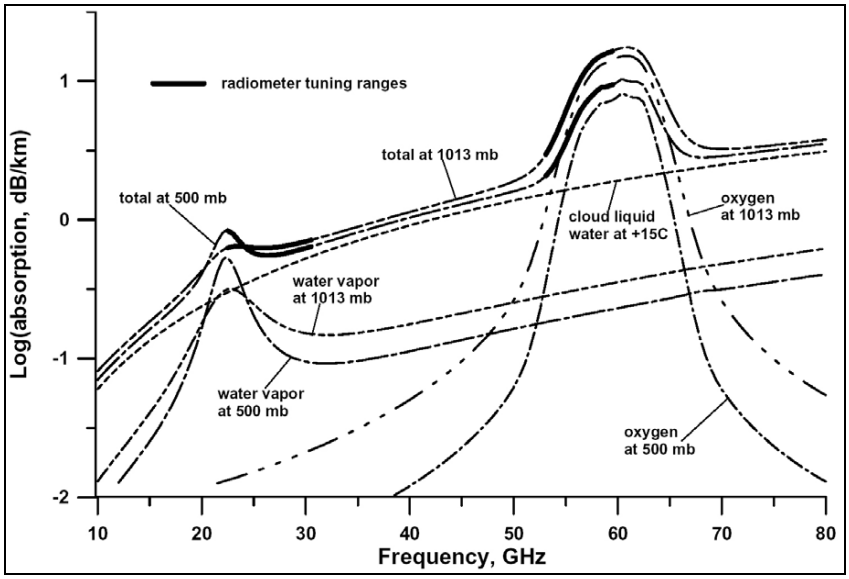

Figure 2.12 The microwave absorption spectrum. (Image courtesy of RPG HATPRO)

Ground based microwave profiling methods make use of atmospheric radiation absorption in the 22 to 60 GHz region. The zenith path atmospheric absorption spectrum at sea level for a typical mid latitude atmosphere with a 1 km thick, 0.5 g/m^3 cloud in this frequency band is shown in Figure 2.12.

Two altitudes and two water vapour densities are shown as well as typical microwave radiometer tuning bands, marked by bold lines. The feature at 22.2 GHz is a water vapour resonance that is broadened according to the atmospheric pressure, while the feature at 60 GHz is an assemblage of atmospheric oxygen resonances.

Temperature information can be obtained by measuring the radiation intensity, or brightness temperature, at points along the side of the oxygen feature at 60 GHz. By scanning downward from line centre, where the opacity is so great that all signals originate from just above the antenna, onto the wing of the line, where the radiometer "sees" deeper into the atmosphere, the instrument can obtain altitude information. As emission at any altitude is proportional to local temperature and density of oxygen; thus the temperature profile can be retrieved.

Water vapour profiles can be obtained by observing the intensity and shape of emission from pressure broadened water vapour lines. On satellites the water vapour line at 183 GHz is used for vapour profiling. The high opacity of this line hides the unknown emission emanating from the earth's surface, eliminating this error source, but precluding profiling to low altitudes. The 183 GHz line is too opaque for observations from the ground, except at very high altitudes or in extremely arid environments. The line at 22 GHz is too transparent for effective profiling from satellites, but is suitable for ground based profiling in most areas. The emission from water vapour is in a narrow line at high altitudes and is pressure broadened at low altitudes. The intensity of emission is proportional to vapour density and temperature. Scanning the spectral profile and mathematically inverting the observed data can therefore provide water vapour profiles.

Microwave radiometers typically use what are known as neural networks to determine atmospheric profiles. An Artificial Neural Network is an information processing system that is inspired by the human biological nervous system processes information. It is composed of a large number of highly interconnected processing elements (neurones) working in unison to solve specific problems. The benefit of neural networks over set climatic models is that a neural network can learn. For example, if a set of meteorological parameters occur, then the neural network can assimilate that information to improve future profiling estimates. The neural networks are derived using the *Stuttgart Neural Network Simulator* developed at the Institute for Parallel and Distributed High Performance Systems at the University of Stuttgart as well as from a history of radiosonde profiles. Profiles from the WVR are typically output in 100 meter altitudes up to 1 km and then in 250m resolution from 1 to 10 km. Above approximately 5 km, the atmospheric water vapour density and temperature approach the climatological mean values. Extensive analysis indicates that prior models of atmospheric structure

local to the microwave radiometer, known as ‘neural networks’ outperform other methods for retrieving water vapour, cloud liquid water, and temperature profiles from radiometric data (Hewison, 2006).

Data from the RPG HATPRO profiling microwave radiometer, owned and operated by the Met Office was used for comparison in this thesis unless stated otherwise. The RPG HATPRO is a 14 channel profiling radiometer, with 5 channels identifying the water vapour microwave absorption.

Like any instrument the microwave radiometer is susceptible to error. If the true value of water vapour is to be ascertained, then the potential error budget associated with each instrument must be identified. From Hewison (2006), we see that although the vertical resolution of profiling radiometers is not high enough for detailed vertical profiles, this should not effect IWV determination as it is by sheer nature an integrated product and not reliant on vertical resolution. Also from past studies (Duan et al, 1996) we have seen generally good agreement between radiosonde and water vapour radiometer IWV data.

With regards to the ongoing use of the radiometer, great case has to be taken not to record false data from direct solar radiation. The Sun is a 6,000 K Black Body radiator and has an angular area of approximately ~ 1% of the antenna, and if the radiometer is pointed directly at the sun the brightness temperature will increase by approximately ~ 60K. Also, if the sun is within the first antenna side lobe (~ 10 degrees off the antenna pointing axis), it will cause an increase in brightness temperature of ~ 1K. Observations should therefore be avoided in directions within ~15 degrees of the Sun position. At both the Camborne and Herstmonceux test sites, much care was taken in the positioning of the radiometers to ensure zero contamination from solar radiation.

As neural network retrieval algorithms are somewhat site dependent, especially for retrieval of water vapour and liquid water, the operator should ensure that the retrieval coefficients are representative for the observation site. Such retrieval coefficients are generated from a history of radiosonde data from the same or a representative site.

Furthermore great care must be taken in the installation and calibration if accurate IWV information is to be retrieved from the atmospheric brightness temperatures recorded by the WVR. Calibration error will degrade the inherent instrument accuracy. Internal Noise Diodes provide an accurate, high stability operational gain reference, but they are only as accurate as the accuracy of the primary standards used to calibrate them. Care should be taken when calibrating the Noise Diodes. The internal ambient Black Body target provides a means to calibrate the system temperature, from which the receiver temperature is derived. The receiver temperature is very stable, so observations of the Black Body target can be relatively infrequent. For the data used in this thesis, calibration was carried out for all WVRs according to the manufacturer’s recommendations both against the WVR’s internal black body target as well as periodically against a cold body target (liquid Nitrogen).

Furthermore liquid water on the radiometer radome can result in artificially high radiometer brightness temperature measurements. However a hydrophobic coating on the radome and a heated fan which blows across the microwave window minimize the accumulation of liquid water on the radome.

The microwave radiometer is an excellent instrument for very high resolution water vapour estimates. It still has to be fully resolved as to beyond which temporal resolution the radiometer starts just recording system noise, however, for comparison against GPS in Chapter 3, the radiometer estimates are only used for overall bias comparison, in which system noise would be averaged (and thus eliminated) over the longer time periods used. Also, the radiometer is used for assessing how much constraint should be imposed on a GPS solution, and in this case it is the identification of main features which we can compare against GPS and again, system noise is not of particular importance here.

2.2.3 The Fourier Transform Infrared Spectrometer

A Fourier Transform Infrared Spectrometer is a device which collects the infrared solar absorption spectra for the determination of the quantity of a specific gas, water vapour in this case. Instead of recording the amount of energy absorbed when the frequency of the infra-red light is varied (as in a monochromator), the IR light is guided through an inferometer. After passing through the sample, the measured signal is the interferogram. Performing a mathematical Fourier transform on the signal results in a spectrum identical to that from conventional (dispersive) infrared spectroscopy.

FTIR spectrometers are cheaper than conventional spectrometers because building of interferometers is simpler than the fabrication of a monochromator. In addition, measurement of a single spectrum is faster for the FTIR technique because the information at all frequencies is collected simultaneously. This allows multiple samples to be collected and averaged together resulting in an improvement in sensitivity. Because of its various advantages, virtually all modern infrared spectrometers are FTIR instruments.

The retrieval of atmospheric parameters from the FTIR have been previously well documented (Rodgers 2000). However due to atmospheric water vapour being so variable both temporally and spatially, the standard retrieval methods are not well suited. Vertical profiles of atmospheric water vapour from FTIR were firstly reported by Hase et al. (2004) and in more recent years the retrieval algorithms have been further developed (Schneider et al, 2006; Schneider and Hase, 2009) at the Institute for Meteorology and Climate Research, Karlsruhe, Germany to provide reliable water vapour retrieval.

2.2.4 Sun Photometer

A sun photometer is an automated sun and sky scanning filter radiometer. A typical sun photometer such as the CIMEL in operation at Izana, Tenerife (as used in Chapter 3 for comparison against other remote sensing instruments) measures at 8 different passbands between 340 nm and 1020 nm. Its field of view is 1.2^o with the pointing of the instrument being automatically controlled by astronomical calculations. Direct sun measurements are made typically every 15 minutes and the sky is scanned regularly at a large number of different angles with respect to the sun, which allows the user to determine many different aerosol properties. The theory regarding the use of sun photometers is relatively well established with several hundred globally distributed photometers being used regularly as part of AERONET (Aerosol Robotic Network) (Holben et al., 1998).

The photometer IWV is calculated from the 940 nm passband direct sun observations applying the modified Langley technique (Schmid et al., 2001). In this thesis level 1.5 AERONET data is used. Data is automatically cloud screened as per Smirnov et al. (2000).

2.2.5 The Multi Filter Rotating Shadow-Band radiometer (MFRSR)

A multifilter rotating shadow-band radiometer (MFRSR) detects irradiances at six narrow wavelength passbands (between 410 nm and 940μm) including the global horizontal, the diffuse horizontal, and the direct normal solar irradiances. The first is measured directly, whereas the latter two are calculated from a sequence of three measurements. For the middle measurement a shadowing band blocks a strip of the sky where the Sun is located and for the other two the shadowing band blocks strips of the sky 9o to either side. These side measurements permit a correction of the excess sky blocked during the middle (Sun-blocking) measurement necessary to determine the diffuse horizontal irradiances. The direct normal irradiances are than calculated by subtracting the diffuse horizontal from the global horizontal irradiances. For more details please refer to Harrison et al. (1994).

The PWV is calculated from the direct normal irradiances determined for the 940 nm passband. At Izana, Tenerife the IWV data is calculated by the modified Langley plot method. Therefore, the relationship between the slant optical depth and the water vapour slant column amounts is approximated by a power law parameterisation (e.g., Bruegge et al., 1992). Uncertainties in this parameterisation and uncertainties in the Langley regression (due to variable atmospheric water vapour amounts) are the major error sources of MFRSR's water vapour data. A good overview of MFRSR's water vapour retrieval technique and the error sources is given by Alexandrov et al. (2009).

In this thesis, in addition a data post processing to screen low quality measurements is performed, which is similar to the method applied by Alexandrov et al. (2004) for an automated cloud screening

of the MFRSR irradiance measurements and consists in analysing the inhomogineity of the atmospheric water vapour field as determined by the MFRSR.

2.2.6 Water Vapour Images from Satellites

Water vapour imagery is a valuable tool for weather analysis and forecasting, because it represents flow patterns of the upper troposphere. Water vapour is transparent to radiation at visible and 10-12 micron wavelengths. This is why visible and IR satellite imagery is used to observe surface features and clouds. However, water vapour is a very efficient absorber and emitter of radiation with wavelengths between 6.5 and 6.9 microns (Figure 2.13) and as such satellite radiometers measuring the amount of radiation emitted by the atmosphere at these wavelengths can be used to detect water vapour in the atmosphere (Grody et al., 2001). The water vapour satellite image displays the water vapour concentration in the atmospheric layer between 600 and 300hPa, (approximately 4000 to 9000 meters above the surface of the earth) representing the middle and upper part of the troposphere.

Water vapour images (Weldon, et al 1991) from remote sensing instruments aboard satellites such as Meteosat 8 show emitted radiation from the Earths atmosphere and cloud tops at a spatial resolution equivalent to 3km at the sub-satellite point, but increases for higher latitudes and longitudes away from the meridian, and are available with typically a 15 minute temporal resolution.

White areas on water vapour images (Figures 2.15 and 2.16) denote moist areas of the upper troposphere (or cloud tops where high cloud is present) where most of the emitted surface and atmospheric radiation has been absorbed and re-emitted according to the amount of water vapour that is present. Dark areas denote drier regions of the upper troposphere where little absorption/re-emission has occurred. Radiation from this channel is received from a narrow spectral band centred at 6.2 microns. The second water vapour channel at 7.3 microns is in the wings of the WV absorption band and hence radiation detected in this channel is lower in the atmosphere than the 6.2 micron channel (Figure 2.14). As such, channel differences between the two water vapour channels can give an indication of vertical atmospheric water vapour distribution.

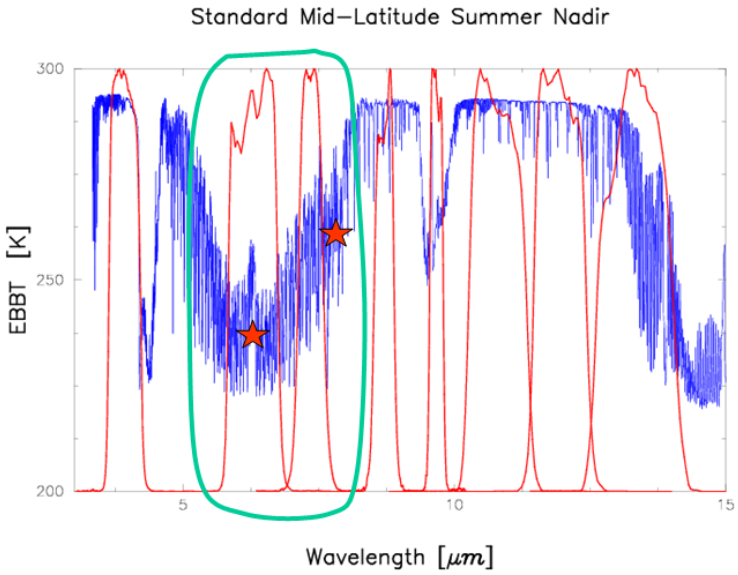

Figure 2.13 Energy Spectrum showing water vapour absorption band, with 6.2micron channel being roughly identified by the bottom red star and the 7.3micron channel being in the wing of the absorption band and illustrated by the upper star. (Image courtesy of EUMETSAT)

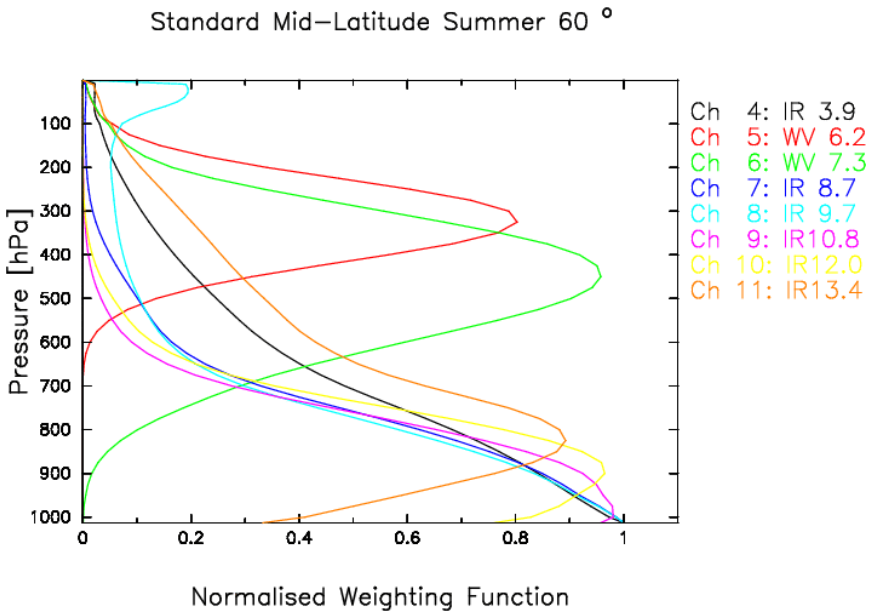

Figure 2.14 Typical atmospheric absorption weighting function. Water vapour absorption at 6.2micron and 7.3micron roughly represent absorption at ~300hPa and ~500hPa respectively (Image courtesy of EUMETSAT)

The main limitation of satellite water vapour is due to the strong water vapour absorptions at approximately 300hPa and 500hPa, little water vapour information is ever retrieved from below these pressure levels. As such satellite water vapour can be thought of primarily as an upper to mid

troposphere tool as it effectively 'sees' the top of the atmosphere and cannot penetrate further down into the atmosphere than the point at which the absorption takes place. In contrast GPS water vapour relates to the cumulative amount of water vapour from the entire column. Furthermore, as the vast amount of water vapour (90%+) is situated in the lowest 3-5km of the troposphere, GPS can generally be thought of as a lower atmosphere tool. By combination of the EUMETSAT 6.3micron, 7.3micron and the GPS water vapour estimates, we can therefore determine some vertical information regarding the tropospheric water vapour structure. An example of when a combination of satellite water vapour and GPS water vapour adds information to the forecaster is given in Chapter 4.

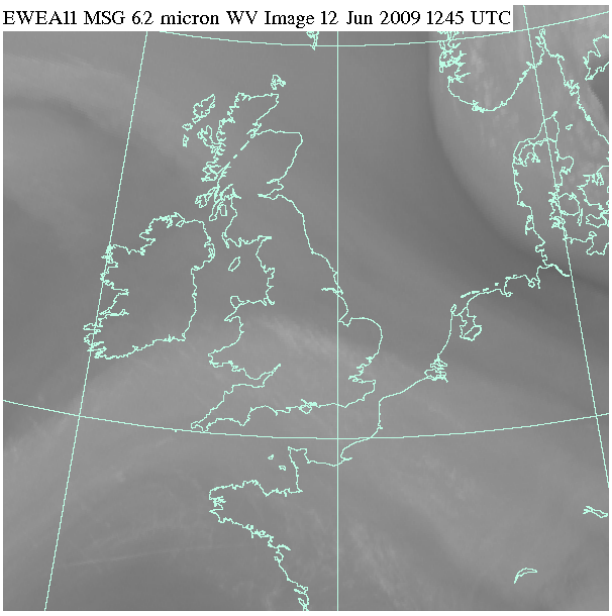

Figure 2.15 Example Meteosat 8, 6.3micron water vapour image. (Image courtesy of Meteosat)

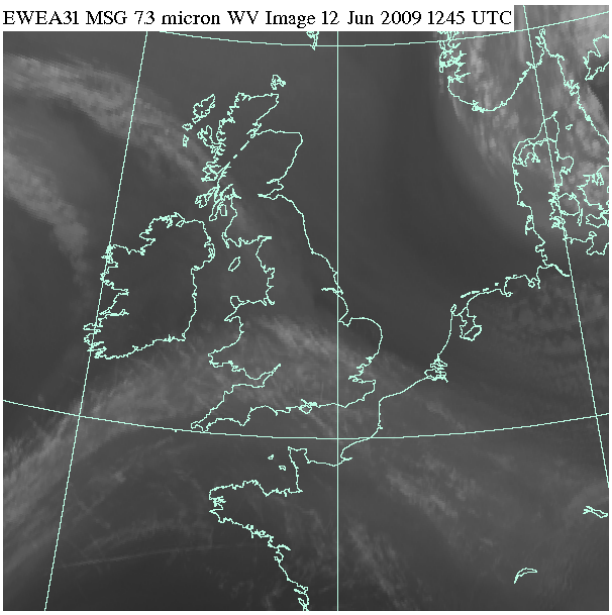

Figure 2.16 Example Meteosat 8, 7.2micron water vapour image. (Image courtesy of Meteosat)

2.2.7 Derivation of ZTD from Numerical Weather Prediction Models

Numerical weather prediction (NWP) models play an essential role in modern weather forecasting. The NWP process involves assimilation of observations to provide the starting conditions for a numerical weather forecast model. The model is essentially a computer simulation of the processes in the Earth's atmosphere, land surface and oceans which all affect the weather. Once starting conditions (wind, temperature, pressure temperature, humidity etc) are known, the parameters are transformed onto a 3-dimensional grid and a number of model runs are performed with slight changes to starting conditions to produce an ensemble of model forecasts.

The Met Office runs three primary unified models on an ongoing, operational basis. The most coarse numerical model in terms of spatial resolution is the Global model. The Global model has a grid resolution of approximately 40km at mid-latitudes and is run twice daily at 00 and 12:00 UTC and, as the name implies, has full global coverage. Apart from its obvious use in predicting global and large scale meteorology, the Global model is essential to provide the smaller scale models with conditions at their boundary. The next higher resolution model is the North Atlantic and European (NAE) model which covers the majority of Europe with 12km grid squares centred on the UK. The NAE has a higher temporal resolution than the global model also with model runs every 6 hours at 00, 06, 12 and 18:00 UTC. The NAE is typically used for the identification of mesoscale events over the European region and was the first model in which GPS ZTD was operationally assimilated in the UK. The highest operational resolution model is the UK regional model, the UK4, with a resolution of 4km. This model is run every 3 hours from 00UTC and is primarily used for the identification of smaller scale features over the UK adding detail to the output from the NAE. Further even higher resolution models can be run on an ad-hoc basis for example to track pollutant emissions. Table 2.3 and Figure 2.17 summarise the Met Office unified numerical weather prediction models.

	Global	NAE	UK4
Resolution	0.5625° x 0.375° (~40 km in mid-lats).	0.11° x 0.11° ~12 km	0.036° x 0.036° ~4 km
Grid points	640 x 481	600 x 360	288 x 360
Model levels	50 lid ~63 km	38 lid ~39 km	70 lid ~40 km
Forecast length	144 hrs	48 hrs	36 hrs

Table 2.3 Overview of the Met Office NWP models.

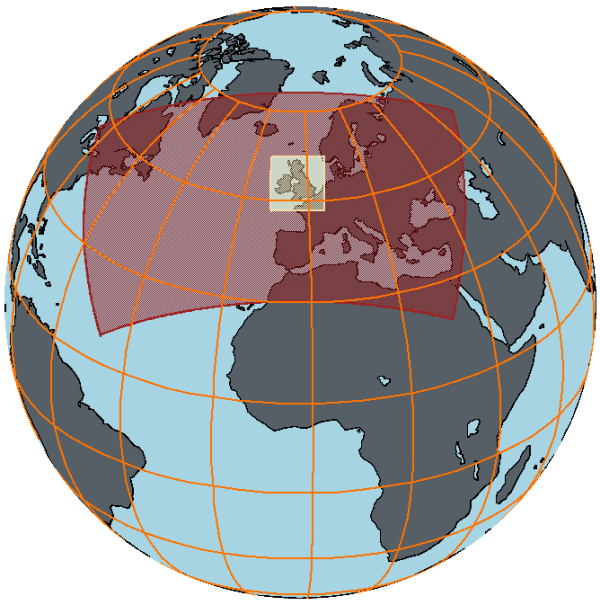

Figure 2.17 Met Office NWP Unified Model domain areas (whole globe = Global Model, red = NAE model, yellow area UK4 high resolution model)

Combined, the models assimilate approximately half a million observations daily. However, even with such a high amount of data, there are still regions of the world which are very observation sparse. Numerical models are particularly valuable for weather prediction over more remote and oceanic regions where it has typically been very difficult and/or expensive to provide reliable observations. Through the process of combining observations with previous model output, the Met Office can provide weather forecasts in areas or for times without many observations. This process commonly known as data assimilation is a recursive process of adding an observation to improve the forecast output; the new, improved model forecast is then combined with further observations for successive forecasts.

In order to derive ZTD from NWP models we need to calculate discrete refractivity for each model layer. Firstly, as we have seen ZTD may be expressed as;

$$10^{-6}\int_{z=0}^{z=\infty} N dz \qquad 2.31$$

where z is the height above the surface and N is the refractivity, given by

$$\frac{ap}{T}+\frac{be}{T^2} \qquad 2.32$$

where p is the pressure, e is the water vapour pressure, T is the temperature and a and b are the dry and wet refractivity constants, given as 0.776 K Pa^{-1} and 3.73 x 10^3 K^2 Pa^{-1} respectively. In order to calculate an estimate of ZTD from a model field, a discrete version of equation 2.32 must be developed. Potential temperature and specific humidity on $\theta(B)$ levels are considered to be constant within each model layer bounded by the $\rho(A)$ levels immediately above and below each θ level. The pressures on the ρ levels immediately above and below the θ level under consideration and given by

$$\prod_a = \left(\frac{p_a}{p_{ref}} \right)^{\frac{R}{c_p}} \tag{2.34}$$

And are linearly interpolated to the height of the i^{th} θ level as follows:

$$\prod_{b_i} = \alpha \prod_{a_i} + (1-\alpha) \prod_{a_{i+1}} \tag{2.35}$$

where

$$\alpha = \frac{z_{a_{i+1}} - z_{b_i}}{z_{a_{i+1}} - z_{a_i}} \tag{2.36}$$

Furthermore pressure on the i^{th} θ level is then given by

$$p_i = p_{ref} \left(\prod_{a_i} \right)^{\frac{c_p}{R}} \tag{2.37}$$

The mean layer virtual temperature is then found by solving the hydrostatic equation assuming constant potential temperature across the model layer.

$$T = \frac{T_v}{1.0 + q_i C_{virtual}} \tag{2.38}$$

It is assumed that refractivity is constant within each model layer. This assumption appears to be reasonable as the majority of the signal contribution by ZTD is made by lowest model levels where layer thickness is relatively small. Refractivity for the i^{th} level is then given by

$$N_i = \frac{ap_{\theta_i}}{T} + \frac{bp_{\theta_i} q_{\theta_i}}{T^2\left(\varepsilon + (1-\varepsilon)q_{\theta_i}\right)} \tag{2.39}$$

The Zenith Delay for each layer (ZD) is then calculated by taking the difference between the heights of the ρ levels immediately above and below the θ levels as follows:

$$ZD_i = 10^{-6} N_i \left(z_{a_i+1} - z_{a_i}\right) \tag{2.40}$$

The forward model starts at the top θ level, and iterates downwards, adding the delay for each layer to the total until the model layer such that

$$z_{a_i} < GPSantennaheight < z_{a_i+1} \tag{2.41}$$

or, the bottom model layer is reached. In either case, a correction is likely to be required in order to account for the difference in height between the first ρ level and the true GPS antenna height. When attempting to estimate ZTD from model fields however a complication arises as a result of there being a height difference between the model layer (ρ) and the actual station height. If one simply calculates the delay through the entire model column, one is likely to observe biases when comparing against observations. Height difference corrections are divided into two distinct categories: where the antenna lies above or below the first model layer (Figures 2.19 and 2.20 respectively).

As with the calculation of refractivity for the full layers, it is assumed that the potential temperature and specific humidity is constant within the model layer bounded by the ρ levels. Pressure is linearly interpolated to the GPS station height, denoted z_{gps} as follows:

$$\prod_{gps} = \alpha \prod_{a_i} + (1-\alpha)\prod_{a_{i+1}} \tag{2.42}$$

Where

$$\alpha = \frac{z_{a_i+1} - z_{gps}}{z_{a_{i+1}} - z_{a_i}} \tag{2.43}$$

Pressure at the station height, p_{gps}, is then given by

$$p_{gps} = p_{ref}\left(\prod_{a_i}\right)^{\frac{c_p}{R}} \tag{2.44}$$

The calculation of ZD for the partial layer bounded by z_{a+1} and z_{gps} then proceeds as with the calculation for a complete layer, except that the height difference is that between z_{a+1} and z_{gps}.

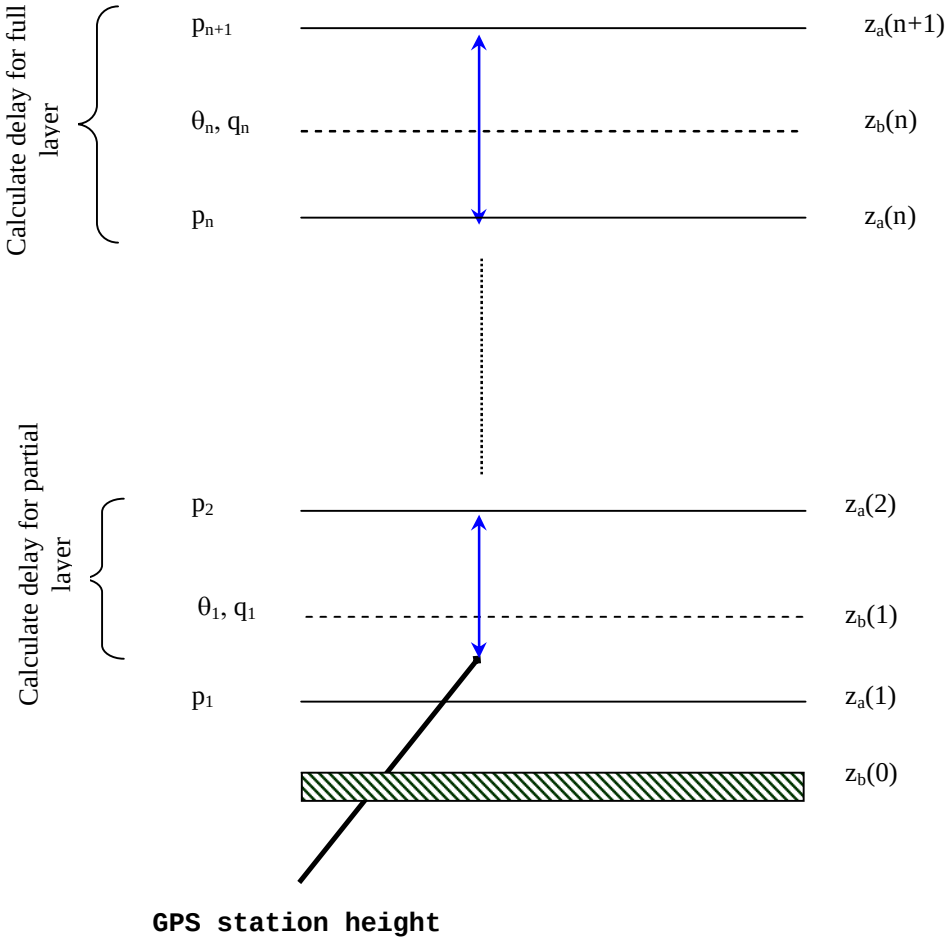

Figure 2.18 Schematic of model boundary layers for the condition where the GPS antenna is above the lowest NWP model layer

In the case of an observation which lies below the model surface, certain assumptions must be made about the temperature, pressure and humidity below the model bottom. The ZD forward model assumes that potential temperature and specific humidity are the same value as those at z_{b1}, and uses the same approach as described previously to linearly extrapolate Exner pressures to the observation height except that z_{a+1} and z_a are used. The delay is then calculated as previously using the difference between z_a and z_{gps}.

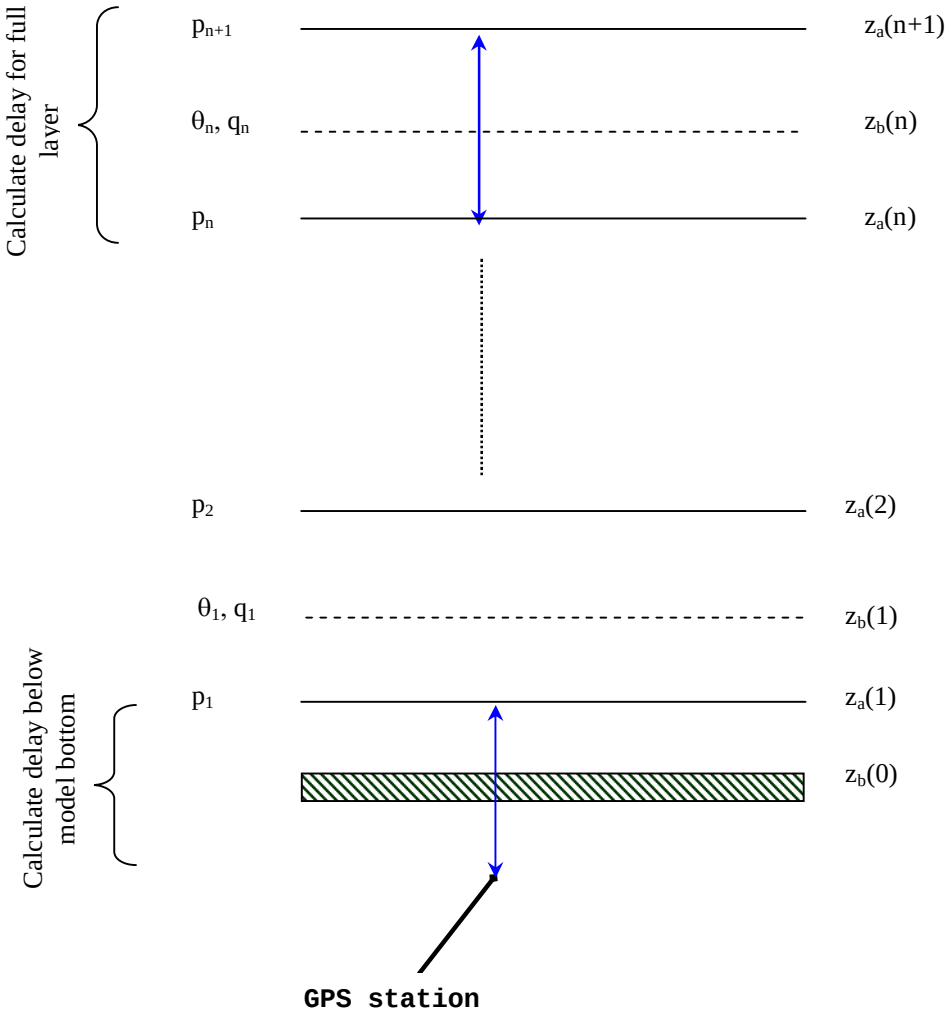

Figure 2.19 Schematic of situation where GPS antenna is below bottom NWP model layer

Furthermore, as the GPS signal, and thus atmospheric delay contribution is to the absolute top of the atmosphere, a further small correction must be made for the signal delay above the model top. This is calculated by using the assumption of hydrostatic equilibrium to evaluate the integral

$$10^{-6}\int_{z=z_{top}}^{z=\infty}\frac{aP}{T}dz \qquad 2.45$$

which yields

$$10^{-6}\frac{aRP_{top}}{g} \qquad 2.46$$

Where R is the gas constant, g is the gravitational acceleration and P_{top} is the pressure on the uppermost ρ level of the model.

The above estimation of ZTD from NWP models is fairly well defined and the same technique is used in a variety of NWP models both in terms of scale and across Europe

2.5 Summary

As we have seen in this Chapter, there are a variety of systems which are capable of producing atmospheric water vapour estimates, however as summarized by this Chapter, each system has distinct advantages and disadvantages. If we are to truly determine the real value of atmospheric water vapour to assess how well GPS water vapour estimates represent the real atmosphere, a multi-instrument comparison must be carried out to determine the biases of each instrument.

Even numerical models have biases due to the assumptions made when determining ZTD at distinct model layers. To determine how well models represent atmospheric delay, we need to assess the spatial bias against NWP to have an understanding if there are any NWP biases at different locations.

Finally, as we have seen in this Chapter, any number of instrument upgrades or GPS processing changes have the ability to influence ZTD, and thus, IWV estimates. If we are to determine a long term climate data set from GPS data, we must assess the instruments, primarily radiosondes and GPS to determine bias corrections which will allow us to reconstruct a climate time series for the identification of climate trends over the UK and Europe.

Chapter 3 Validation of GPS Water Vapour Measurements

As we have seen in Chapter 2, water vapour can be measured directly with radiosonde ascents and indirectly with remote sensing instruments such as GPS, microwave radiometers as well as with a number of other instruments. With any instrument the accuracy of the data must be thoroughly assessed before it can be trusted and used operationally in providing meteorological models with starting parameters. In order to truly validate GPS water vapour estimates, in this thesis data is compared against as many other different remote sensing instruments as is possible from a number of European sites at varying latitudes and altitudes.

Absolute accuracy of ZTD and IWV estimates is not necessarily a problem for operational meteorology as all NWP schemes will apply a bias correction to the data. However, in terms of assessing which is the correct model to apply in GPS processing or for when using GPS water vapour as a tool for monitoring climate change, data biases need to be addressed and estimated. Also it is essential to know, as far as possible, what the 'true' value of the water vapour is. Only once we have an estimate of the real atmospheric water vapour content will we know which are the most applicable models to apply in GPS processing schemes.

Since the beginning of this study in 2003, a number of remote sensing instruments have been used to validate GPS water vapour estimates. The primary source of data for comparison in the UK is from operational radiosonde ascents. Radiosonde data has been extracted from the Met Office database from 2001 to 2008, giving us a 7-year time scale in which to identify biases, and to define bias corrections for radiosonde and GPS data so that we have the potential to identify any long term trends.

To assess inter-instrument biases in this Chapter, not only radiosonde data was used. Data from all other instruments outlined in Chapter 2 has also been assessed to identify each instruments' characteristics at a number of European integrated observing sites. In order to understand the potential source of biases in the GPS data itself we also have to consider the models used in GPS processing with particular reference to the role of Ocean Tide Loading (OTL) models as well as how the geometry of the network can effect data quality. Furthermore, if we are to eliminate biases in the time series to be able to determine climatological trends, we must also assess the biases introduced with GPS processing changes such as the introduction of absolute antenna phase centre variation (PCV) models in late 2006.

Fortunately, with the advent of the E-GVAP Supersites there exists a unique opportunity to study the question of GPS water vapour accuracy. Not only are all the Supersites with GPS collocated with other

remote sensing instruments but as all E-GVAP Analysis centres (ACs) process data from all Supersites, we may also assess the relative accuracy of each processing solution at each AC. Biases can exist between many aspects of GPS processing solutions including different relative constraints imposed on the tropospheric outputs of processing as well simply from different processing software, for example comparing outputs from the Bernese processing software (Dach, et al., 2007) against the GIPSY-OASIS software (Webb and Zumberge, 1993) developed by the NASA Jet propulsion Laboratory, JPL.

Through access to data from the E-GVAP Supersites as well as from data recorded by other remote sensing instruments this Chapter will address the quality of GPS IWV and ZTD estimates compared to other remote sensing instruments' data as well as against other European ACs solutions and against NWP data. An assessment of inter AC biases will be carried out looking at the effects of processing changes between ACs and finally a long term comparison study against radiosondes and other remote sensing instruments is carried out to try and determine the correct bias corrections to apply in order that we can have a consistent time series of data to try and assess climate trends.

3.1 Assessment of Inter-GPS Receiver Quality

Throughout the world a large number of GPS receivers and antennas are used in large GPS networks for geodetic and meteorological applications. The relative biases introduced with signal reception and processing at the receiver end are taken care of with the use of the correct antenna phase centre models and in theory any such biases are removed. However it has been noted that coordinate shifts can occur when models are changed. The question of bias shifts due to using different antenna phase centre models is assessed later in this Chapter as it is more relating to GPS processing software and models as opposed to the hardware itself.

To assess how well receiver biases are modelled out by the GPS software, data is compared at the Met Office site at Camborne, Cornwall, UK which has two collocated GPS receivers connected to the same GPS antenna by way of a cable splitter. Even though the receivers use the same antenna, the GPS sites are effectively different and they have the names CAMB and CAM2 respectively. The antenna and mount is a relatively long-term installation being installed in 1998 and is owned and operated by the Met Office. The GPS receiver CAMB is an Ashtech iGGRS type and is owned and operated by the Met Office. CAM2 is a Leica SR530 type GPS receiver and is owned and operated by the OSGB as part of their OSNet network. The antenna is a Dorne Margolin Choke-ring type and the antenna cable is split to connect to the two different GPS receivers. The fact that two receivers are connected to the same antenna gives us the opportunity to directly compare the quality of the GPS receivers to see if any biases exist in the data.

The data was processed as part of the operational METO processing system in a double difference network approach.

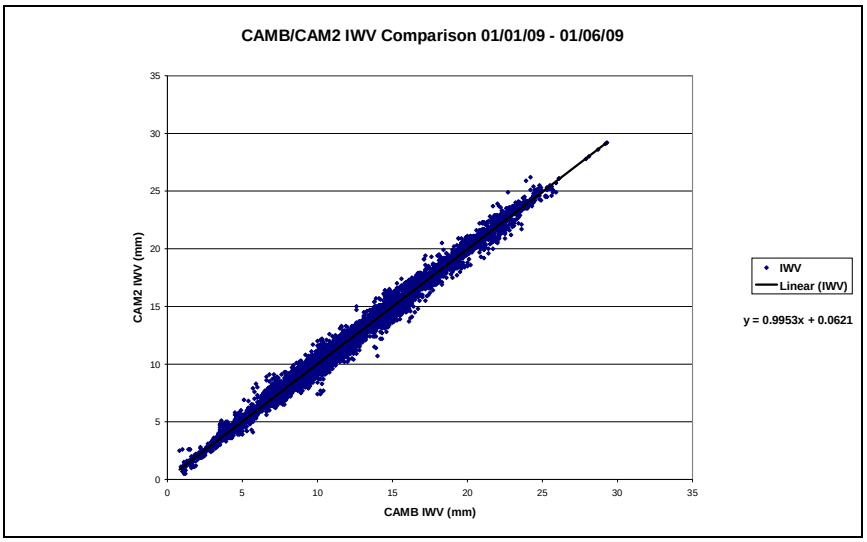

Figure 3.1 CAMB/CAM2 IWV comparison, 1st Jan 2009 – 1st June 2009

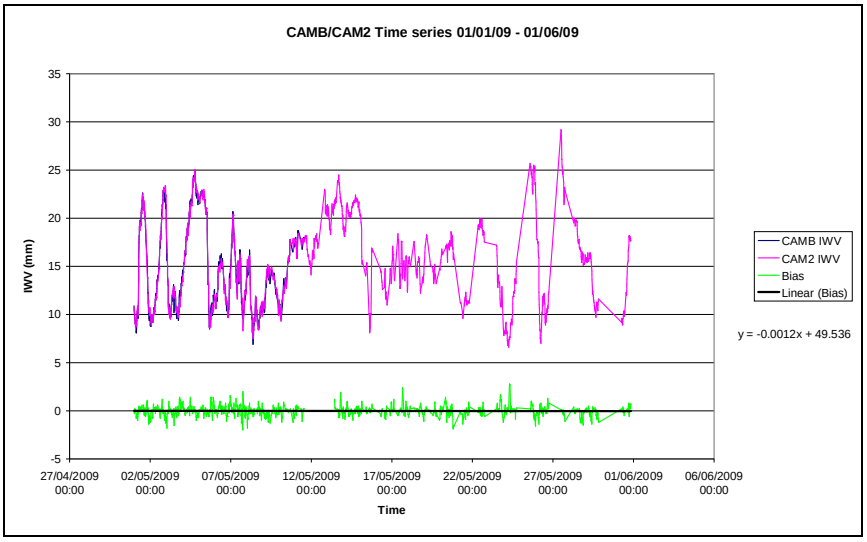

Figure 3.2 Time series of CAMB vs. CAM2 IWV, 1st Jan 2009 to 1st June 2009

In Figures 3.1 and 3.2 data is compared from the 1st of Jan 2009 through to 1st June 1009, comparing almost 15,000 estimates. A negligible bias of only -0.014kg/m^2 IWV (CAMB minus CAM2) exists between the two receivers and as such it is fair to assume that at least in this example, receiver biases are negligible when using the Bernese software.

The question of how well the GPS processing software accounts for antenna phase centres and changes in antenna are dealt with later in this Chapter when results from schemes using relative vs.

absolute antenna phase centre models are assessed. The question of how much bias is introduced when new antennas are installed at a site is also studied later in this Chapter.

3.2 GPS Water Vapour Processing Errors

In the production of GPS water vapour a number of models and assumptions are introduced into the GPS processing routine which will inevitably lead to biases between different processing solutions. The E-GVAP Supersites offer a novel opportunity to study, in parallel, atmospheric delay estimates from a number of European Analysis Centres (ACs). Each AC processes data in a geographically unique network, using different processing software and processing schemes applicable to their own region and requirements. In this section we assess data from a variety of E-GVAP ACs to identify the scale of any biases and to investigate where in the processing routines the biases are generated.

The E-GVAP Supersites were selected specifically for the purpose of validating GPS water vapour against other instruments as well as for AC vs. AC comparisons. The criteria used for selecting a Supersite are listed below:

1. Supersites had to either have a radiosonde or microwave radiometer at a collocated (<20km separation) meteorological station for IWV validation; 20km was chosen as the spatial separation limit, as pressure which is critical for ZTD to IWV conversion would not vary over such a small distance.
2. Supersites had to be long term, stable geodetic quality GPS installations, ideally conforming to EUREF EPN or IGS installation standards
3. The GPS and radiosonde stations had to be within the same Met Office NWP model layers – this eliminates potential errors introduced when estimating ZTD/IWV in adjacent model layers.
4. Sites were chosen in geographically diverse locations to assess the biases introduced from differing network geometries and OTL models; some sites were chosen on the periphery of networks and some in the centre of networks, while others were chosen because they were coastal sites where one would expect a larger importance of OTL models.

All E-GVAP ACs were requested to process the data from all Supersites and the GPS processing comparisons in this Chapter use the data courtesy of the E-GVAP Project to compare inter AC biases and determine how consistent ZTD and IWV processing is across the European region.

3.2.1 Different Processing Strategies – PPP vs. DD

In terms of GPS processing there are two main accepted methods – Double Difference (DD) and Precise Point Positioning (PPP). The main difference between the two is that PPP is a station-wise solution whereas DD is a network approach. In PPP, if there is a problem with one station, it will not affect the solutions of other nearby stations. Also, as the processing is station specific, the load of processing can be run in parallel on a number of CPU's or even on parallel servers. In this way the actual GPS processing part of PPP is much quicker than DD. However for PPP to be effective very precise satellite clock values have to be available. At the time of publication the globally produced IGS satellite clock products are not available at a high enough temporal resolution for PPP positioning and therefore if an AC wishes to process GPS data using PPP, satellite clocks have to be calculated by the AC themselves. Additionally another risk to processing in PPP is that if an error has been made in the satellite clock estimation, this error will be translated to every station. Both the German and Nordic ACs in E-GVAP, GFZ and NGAA respectively, process GPS data in this way.

In DD processing, baselines between GPS stations in the network are formed and in this way the clock errors in the phase GPS equations can be eliminated. There are however negatives to DD processing. Firstly the processing is much slower, as baselines as well as the receiver-satellite distances have to be estimated. Also, if there is a problem with one GPS station, this error will be introduced to the other stations which it is connected to by way of the baselines.

In terms of the efficiency of PPP vs. DD processing, for smaller or medium sized networks (<200 stations) the additional time saved by not having to calculate baselines is often replaced by the time it takes to estimate satellite clocks. As such the time taken to process a 200 station network is comparable between the PPP and DD strategies. However due to the fact that the time it takes to process in DD compared to number of stations is non-linear, as you process ever larger networks, the time savings of a PPP strategy can become apparent. Figures 3.3, 3.4 and 3.5 are presented showing the average receipt times of processed GPS ZTD into the Met Office database for a comparable sized METO (DD) and GFZ (PPP) network as well as that for a much larger NGAA network.

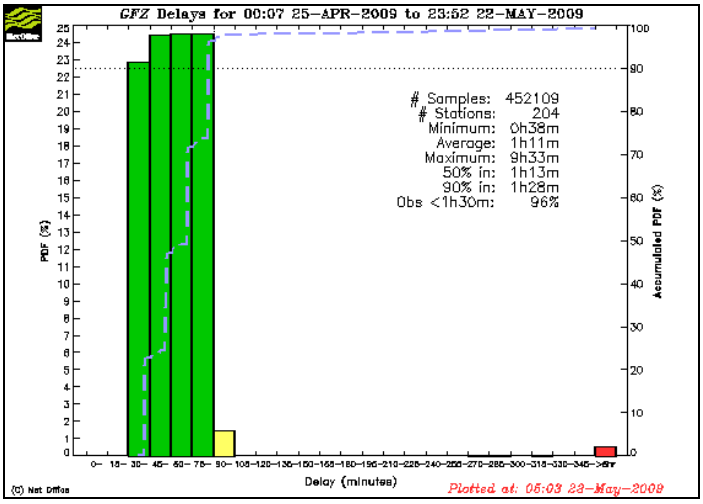

Figure 3.3 Typical MetDB Receipt times for GFZ (PPP) processing

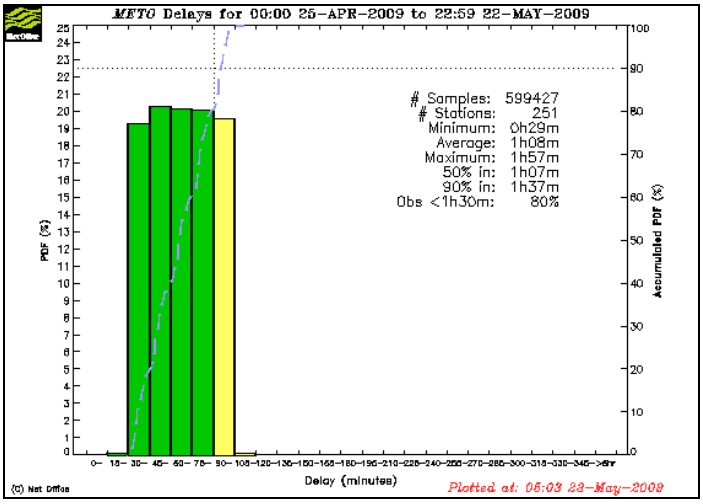

Figure 3.4 Typical MetDB Receipt times for METO (DD) processing

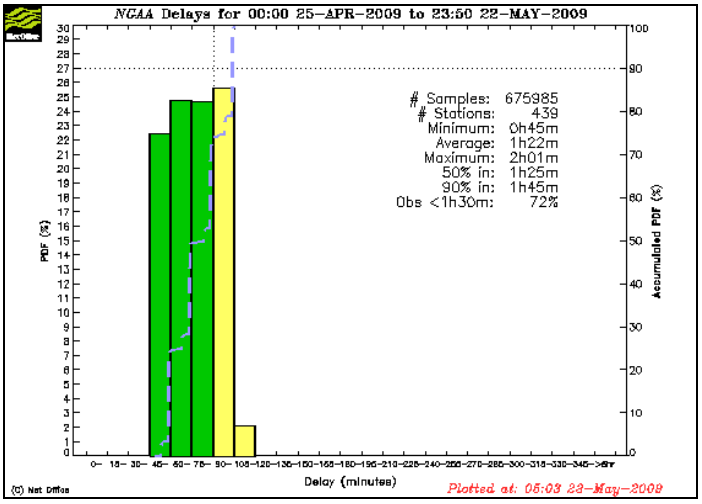

Figure 3.5 Typical MetDB Receipt times for NGAA (PPP) processing

As mentioned previously, the METO system employs a DD processing strategy. The decision to use a DD strategy was based on investigations carried out by IESSG at the University of Nottingham (Orliac et al., 2003), on the achieved accuracy of ZTD estimates using IGU satellite orbits and clocks. At the time of assessment the IGS products were not sufficiently accurate for PPP processing and it was not known that other ACs were intending to generate their own satellite clock products. As such it was decided that for network sizes likely to be processed by the Met Office a DD strategy was the only option. Since this time however, ACs such as GFZ have, partly through the E-GVAP Project, made their enhanced products available to other members of the scientific community, thus making a PPP solution more achievable by other ACs and offering a solution which may well be used by the Met Office in the future.

Although the speed of delivery of GPS data from PPP and DD networks varies and can be simply monitored, the quality of the respective solutions needs to be assessed. Through the E-GVAP project we have the opportunity to directly compare data from difference ACs and identify relative biases and variability of the solutions. As there are a number of variables between ACs such as network geometry, processing strategy etc, these factors have been assessed individually below to assess the scale of the errors which can be attributed to each variation between AC. Data is compared from all ACs for the geodetic quality installation ZIMM at Zimmerwald, Switzerland and data is shown as a time series as figure 3.6. We can see that if polynomial trend lines are plotted for each AC the average spread of data is in the order of 2kg/m^2 IWV. Even though the spread of IWV is comparable with other remote sensing instruments such as microwave radiometers and radiosondes (Rocken et al., 1995 and 1997; Liou et al., 2001; Guerova et al., 2003) the bias is still substantial considering all data has come from the same observing system, just processed in a different manner. In order to better understand the biases we need to look at how each AC processed their data and to see where any biases can be assigned. Only when more consistent IWV data from a variety of ACs can be produced will the forecasting community have additional confidence in the data. As we see later, separate to this, biases of up to 15kg/m^2 can be introduced by simply using an inconsistent approach to the meteorological data used for ZTD to IWV conversion!

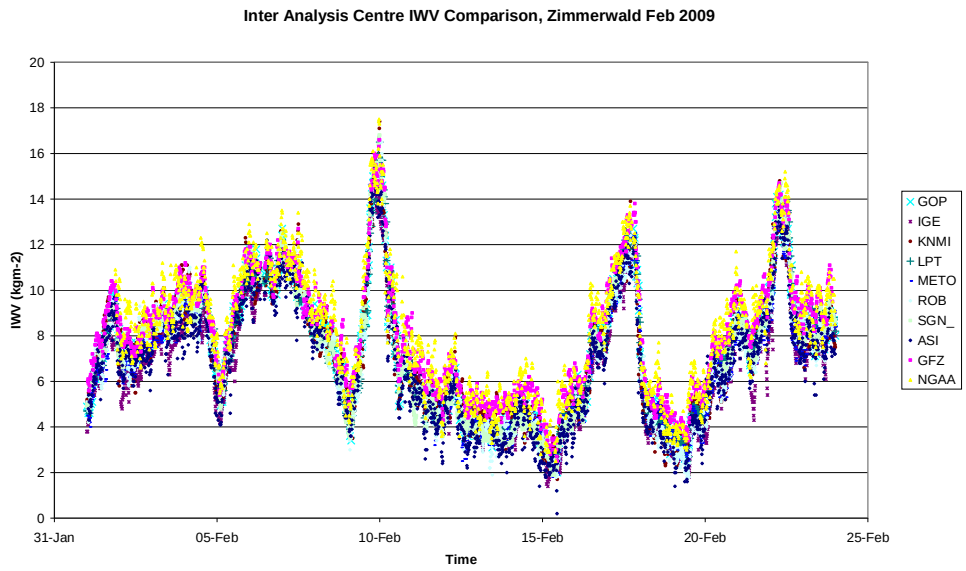

Figure 3.6 Comparison of all E-GVAP AC's IWV, ZIMM, February 2009

The majority of ACs within E-GVAP produce ZTD estimates within the quality requirements of NWP assimilation schemes, which are typically based on the mean 28-day StDev against the NWP model and not bias. Bias can be easily corrected for in NWP assimilation schemes and thus is not of utmost importance to NWP. However if we are to truly know which processing scheme produces IWV estimates that most accurately represent the real atmosphere we need to understand how AC biases are generated. Historically observational data has always been compared against NWP. ZTD data from NWP however has always been known to be too slow in representing real atmospheric phenomena and real events tend to get smoothed in assimilation schemes (Healy et al., 2005). This is a result of the limits of computing power dictating model grid-squares which are too large to represent small-scale atmospheric events such as convective thunderstorms, for example. With the advent of increased computing power comes the ability to run assimilation schemes with ever decreasing model grid sizes and thus increased resolution. In 2009 the Met Office, like a number of other national met services are carrying out trials on further high resolution (1.5km) NWP models and as such ZTD estimates will be needed to represent the real atmosphere with much greater accuracy and temporal resolution also. However, for the period of this thesis, most synoptic scale NWP models (covering a European-scale area) have a resolution of anything down to around 10km. So, for the purposes of comparison in this Chapter, ZTD data from the European HIRLAM 11km NWP model is used.

Through the E-GVAP project each AC provided details of their processing schemes and a comparison of processing technique against biases and variability of ZTD estimates was completed by the author. Table 3.1 gives an overview of each ACs processing scheme.

Analysis Centre	Software	PPP vs. DD	Satellite Orbits and clocks, and ERPs	Phase Centre Model	OTL Model	Relative Constraint	Bernese Normal Equation file window
ASI	GIPSY-OASIS II 4.04	DD	IGU	Absolute	FES2004	10mm	24hr window, 1h moving forward
GFZ_	EPOS.P.V2	PPP	GFZ Calculated	Relative	Pagatakis	Random walk	N/A
GOP_	BSW5.0	DD	IGU	Absolute	FES2004	15mm	12 hours
IGE_	BSW5.0	DD	IGU	Absolute	FES2004	1mm	12
LPT_	BSW5.0 +	DD	IGU	Absolute	FES2004	Loose	8 hours
METO	BSW5.0	DD	IGU	Absolute	FES2004	1mm	5 hours
NGAA	GIPSY-OASIS II	PPP	NGAA Calculated	Absolute	FES2004	Random Walk	N/A
ROB_	BSW5.0	DD	IGU	Absolute	FES2004	2mm	6 hours
SGN_	BSW5.0	DD	IGU	Absolute	FES2004	10mm	5 hours

Table 3.1 Comparison of processing schemes of all ACs involved in E-GVAP (+ for LTP_ processing software indicates additional improvements, mainly GLONASS ambiguity resolution)

Of particular note in Table 3.1 is that fact that out of all the European ACs involved in E-GVAP only GFZ and NGAA use PPP whereas all the other ACs use DD with the same software and processing models. The only exception to this is the Italian AC, ASI, who use the GIPSY-OASIS software. So the main difference between the majority of ACs using DD are the geographical scope of the network processed and the relative constraints and number of NEQ files added together in the processing. As the processing schemes are so similar it would be expected that the results from each AC should also be very similar, however as can be seen in Figure 3.7, even if the PPP ACs and ASI are excluded from the comparison there is still a 2kg/m^2 bias between ACs IWV estimates.

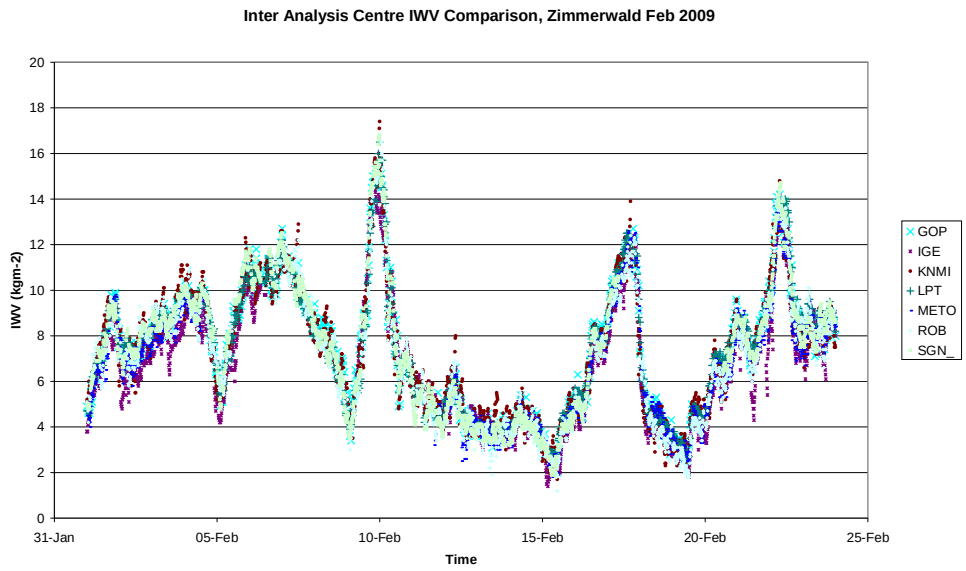

Figure 3.7 Time series of all BSW 5.0 DD E-GVAP AC's IWV, ZIMM, February 2009

To assess the inter AC biases further, all ZTD data from all ACs involved in E-GVAP were compared and biases and quality, in terms of StDev against the HIRLAM 11km NWP model assessed. The data used here was for a 2-week period in May/June 2009 and the results are shown in Table 3.2.

AC	No of ZTD estimates	No of sites processed	Mean ZTD bias (mm)	Mean ZTD Site StDev for period vs. HL11 model (mm)	StDev. of all estimates for period vs. HL11 model (mm)
ASI	2762	59	2.6	14.4	17.3
GFZ	10011	202	-1.7	10.8	12.2
GOP	3822	72	2.2	11.2	12.1
IGE	7159	154	6.2	14.9	31.2
KNMI	2624	49	3.7	10.5	11.8
LPT	5021	93	2.3	12.4	13.9
METO	11154	222	4.0	11.4	16.5
NGAA	18244	431	0.3	9.7	15.1
ROB	8709	172	3.1	11.6	13.6
SGN	9068	171	3.0	12.7	14.9

Table 3.2 Average quality statistics for E-GVAP ACs 2009/05/19 - 2009/05/25

When Tables 3.1 and 3.2 are compared it can clearly be seen that the two ACs who process in a PPP have the 'lowest' estimates of ZTD with GFZ having a dry bias in the ZTD estimates of -2.7mm and NGAA having a very low bias with respect to the model. All other ACs overestimate ZTD with respect to the model, with a bias ranging from +2.2mm ZTD (GOP_) to +6.2mm (IGE_) with an overall mean (PPP ACs excluded) of +3.4mm ZTD. Considering the different solutions and different networks processed, the mean biases are very close suggesting they represent the atmosphere well and indicate that the NWP model may well underestimate atmospheric delay by approximately 3mm.

As we will see later in this Chapter, although it is very useful to measure GPS ZTD against NWP data to verify the stability of an AC solution, if we are to determine the real atmospheric moisture content and the variability of atmospheric conditions, we must compare GPS water vapour estimates against those from other instruments.

3.2.2 Network Geometry

It is widely accepted, but not well quantified, that GPS sites at the extremes of a network processed using DD produce coordinate data of lower quality than sites within the centre of a network largely due to the network geometry. The assumption being that if a GPS site was within a larger network, any biases created through the production of GPS baselines would generally even out if it was connected to baselines in a number of directions. However, if a site is on the extremity of a network and all the baselines are in one general direction, any biases created in baseline production would this time not necessarily be cancelled out. The effect on ZTD quality is however largely unknown. To assess the relative quality of ZTD data from GPS sites at the extremes of a network, a comparison was completed looking at variability of bias of METO ZTD estimates compared against the Met Office North Atlantic and European (NAE) NWP model.

A study of this kind is important as assessing GPS and NWP quality based on geographical location might indicate a lack of NWP representivity in certain areas or might indicate GPS processing errors such as biases in ocean tide loading models. A comparison of this nature is also important as it could also influence ACs on the scale of the network they choose to process and could also influence projects such as E-GVAP in advising the member countries on the geographical extent of the network which they should process.

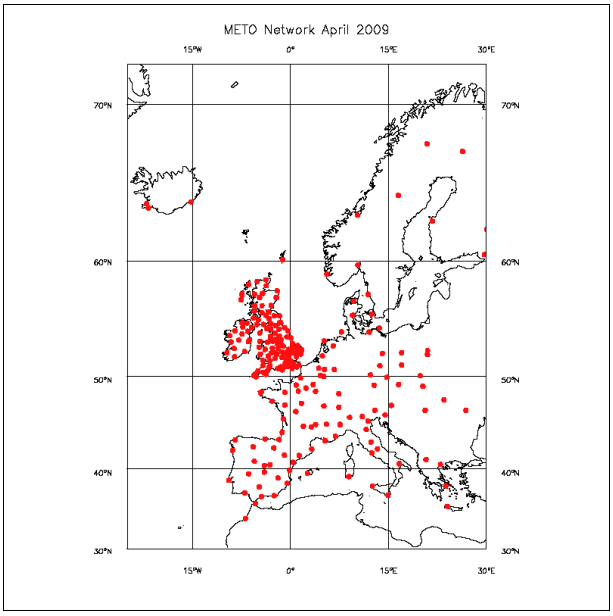

Figure 3.8 GPS sites processed by the METO, April 2009

A comparison study was carried out to assess the quality of ZTD data against model data for the nominal network processed by METO. For reference the whole of the METO network processed in April 2009 is shown in Figure 3.8. GPS ZTD - NWP ZTD biases from all GPS sites assimilated by the Met Office NAE NWP model were taken for the month of April 2009. Data was sorted with any sites with less than 20% data availability were eliminated as they would not give a representative data set. Data was then sorted by StDev and the 20 sites with the lowest StDev and the 20 sites with the highest StDev were identified to see if there was any correlation between StDev and geographical location. The sites with the 20 lowest and 20 highest StDev are shown in Figures 3.10 and 3.11 respectively.

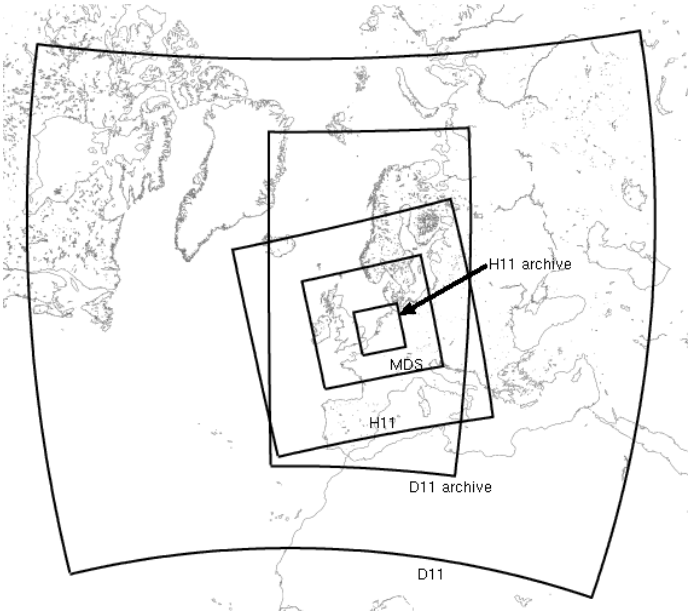

Figure 3.9 HIRLAM 11km model domain. HL11 is the model used for comparisons in the E-GVAP project.

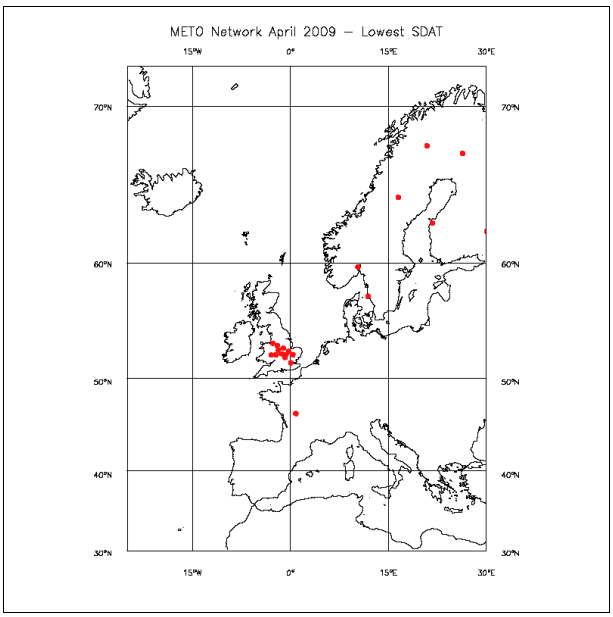

Figure 3.10 GPS sites processed by METO with the lowest StDev vs. Met Office NAE NWP model, April 2009

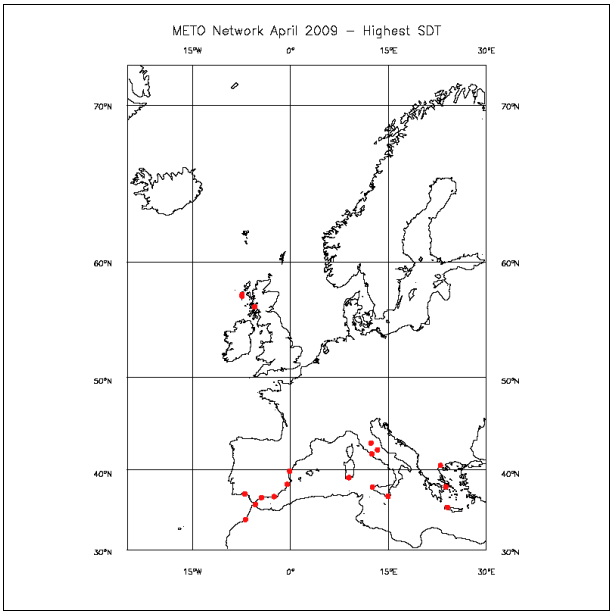

Figure 3.11 GPS sites processed by METO with the highest StDev vs. Met Office NAE NWP model, April 2009

From Figures 3.10 and 3.11 it is clear that the vast majority of the sites with the highest StDev are all located at the southern extreme of the network. This is a surprising result as it illustrates that there is not a simple correlation between ZTD quality compared and sites being at the extreme of a network. In fact, some of the sites in the Nordic region which are at the northeast extreme of the network

processed by METO are some of the highest quality sites (Figure 3.10). To investigate further the apparent pattern of sites at the southern extreme having the highest StDev a statistical analysis of StDev compared against latitude and longitude was carried out. Again all data for April 2009 was taken into account excluding those with less than 20% estimates. Figures 3.12 and 3.13 are plots of StDev against latitude and longitude respectively for all sites assimilated for April 2009.

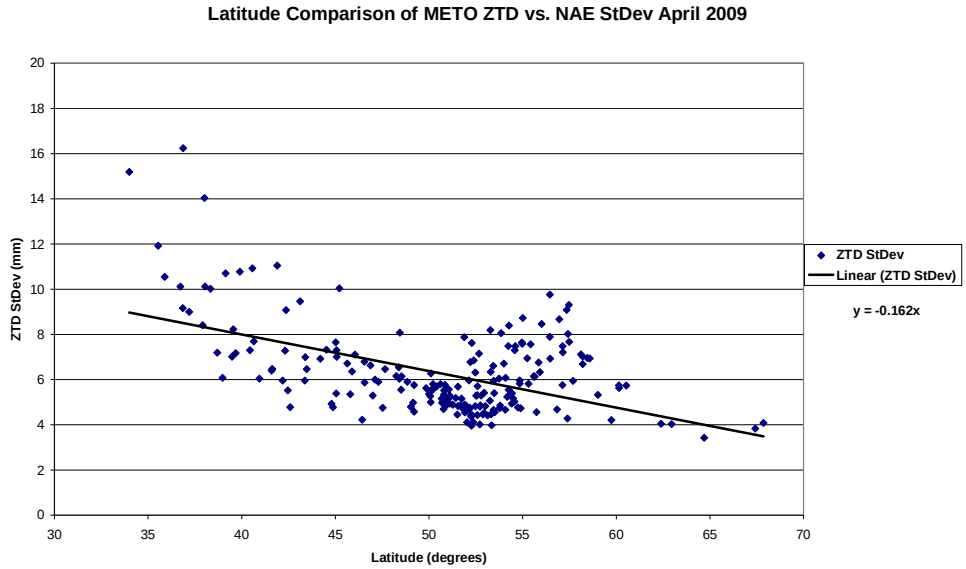

Figure 3.12 METO ZTD minus NAE NWP ZTD StDev as a function of latitude

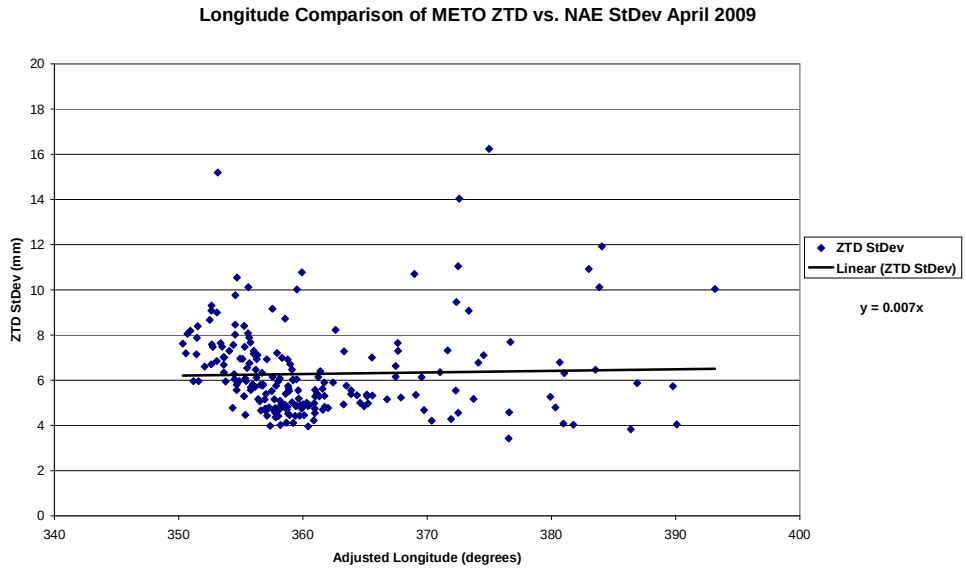

Figure 3.13 METO ZTD minus NAE NWP ZTD StDev as a function of longitude

From Figure 3.12 it can clearly be seen that the trend of increasing SD with decreasing latitude is reflected through the whole network and not just limited to a smaller number of sites being of poor quality on the southern extreme of the network. If a linear trend is drawn we can see that on average a

trend of an increase in StDev of approximately 1.6mm per degree of latitude. The concept that the quality is not related to sites being at the extremes of networks is further demonstrated by the fact that there is no deterioration of quality either with higher latitudes or against longitude. It may be concluded, therefore that ZTD quality from a DD network does not necessarily deteriorate at the extremity of the network. Rather, in the case of the data processed by METO the error specifically increases in a southerly direction.

To determine whether the trend is simply a systematic bias in the ZTD estimation, data quality has been assessed as a function of ZTD (StDev/ZTD). This is essentially a percentage error of the ZTD estimates and indicates again that sites at the southern extreme are the worst quality when compared to the Met Office NAE model.

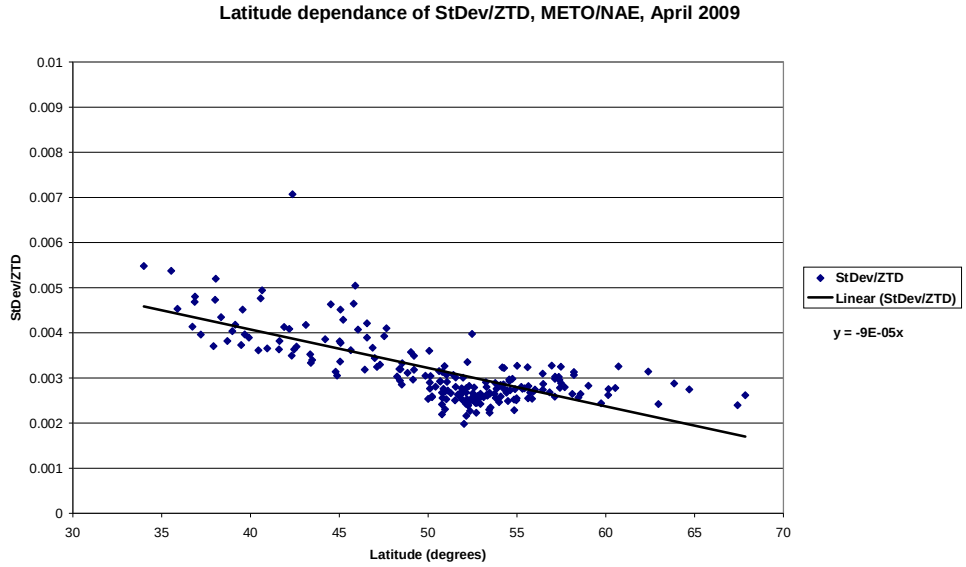

Figure 3.14 Trend of StDev / ZTD as a function of latitude. All METO sites, April 2009

However, it is important to remember that this comparison is only against the Met Office NAE model and the bias might indeed lay in the model itself not accurately representing humidity fields at lower latitudes. To assess where the source of the bias lies data was also compared against the HIRLAM 11km NWP model. As we can see from Figures 2.17 and 3.9, the HIRLAM 11km model has a smaller domain size than the NAE model. As such one would expect the bias to be more evident in the HL11 model. To assess the bias against the HL11 model, data was again compared in a similar manner and the results are shown as Figures 3.15 and 3.16.

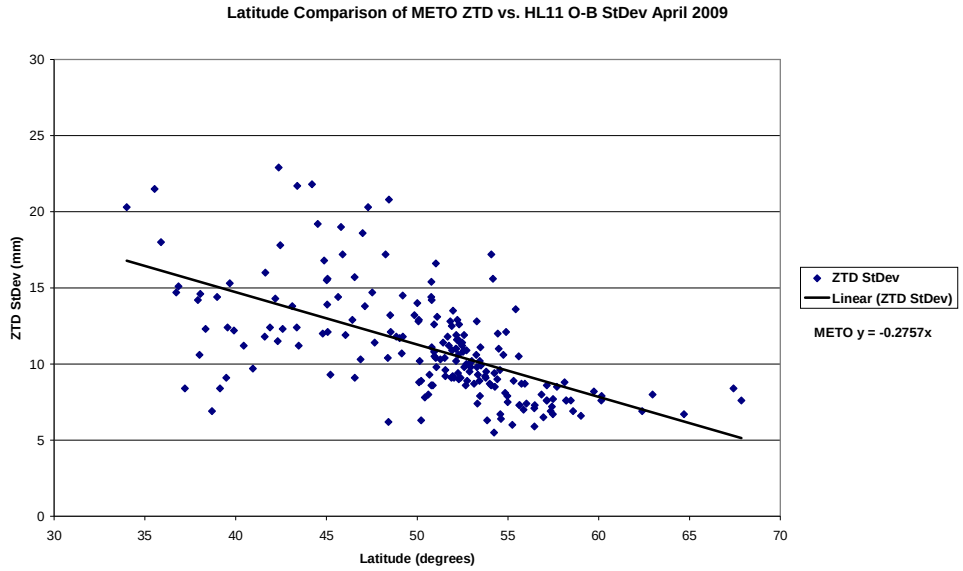

Figure 3.15 METO minus HL11 NWP ZTD StDev as a function of latitude, April 2009

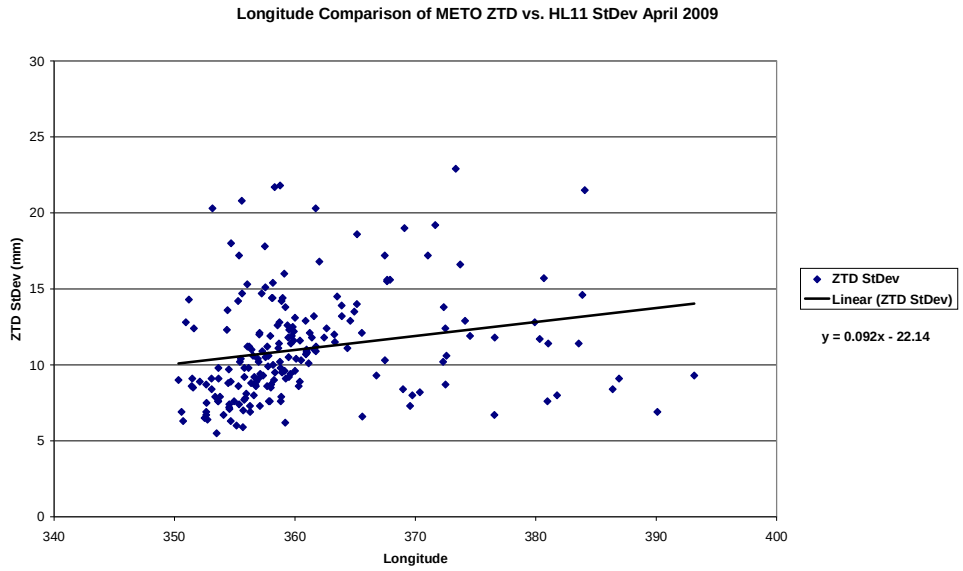

Figure 3.16 METO minus HL11 NWP ZTD StDev as a function of longitude, April 2009

It is clear from the comparison against latitude (Figure 3.15) that again, the NWP model has an increased variance from GPS ZTD data at lower latitudes with a linear trend of approximately 2.6mm StDev per degree of latitude. Due to the increased error per degree of latitude for the HL11 model with its smaller domain size, this might indeed suggest that ZTD quality is related more to the model domain and the parameters available to initialise the model from larger scale NWP models, rather than with the GPS solution. However we could also conclude that from Figures 3.12 and 3.15 that there is some function in the METO processing, such as the FES2004 OTL model, or higher order ionospheric effects, which is providing poorer quality ZTD estimates at the southern extreme of the network.

To assess the bias further, we can compare ZTD from a different AC, using a different OTL model, against numerical model data. This should eliminate any bias introduced specifically in the METO processing system. From Table 3.1 we see that the German analysis centre GFZ is the only centre using a difference OTL model (the Pagatakis model) and thus we can compare ZTD against the HL11 NWP model to see if the biases are still evident and make some judgements on the how representative the FES2004 OTL model used by METO is. Data was compared in a similar method but for May 2009. A latitudinal comparison is completed plotting StDev against latitude for GFZ PP ZTD against the HL11 model and the results are shown as Figure 3.17.

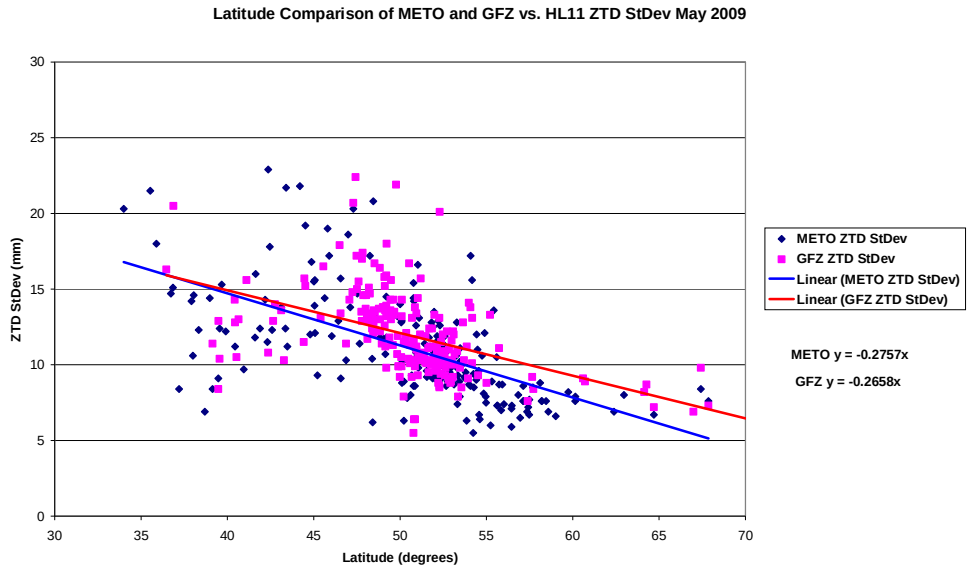

Figure 3.17 METO and GFZ minus HL11 NWP ZTD StDev as a function of latitude

From Figure 3.17 we can see that GFZ has a trend of increasing StDev with decreasing latitude which is almost identical to that from METO data for May (linear trends of an increase in StDev of 0.2658mm per degree of latitude for GFZ data and 0.2757mm METO). It may also be noted that there exists a slightly higher bias offset for GFZ also which one can assume is an artefact of the differences in the processing strategies (PPP vs. DD).

When assessing how well each model compares against a common data set (METO) we see a linear trend of 0.2757mm comparing against the HL11 model but only a linear trend of 0.162mm per degree against the Met Office NAE model (Figure 3.12). Therefore we may assert that the NAE model is indeed more representative of humidity at lower latitudes with respect to the HL11 model. This is most likely a result of the extended geographical scope of the NAE model when compared to the HL11 model.

In all the comparisons completed here of GPS ZTD against model ZTD, data sets show a common theme of increasing error with decreasing latitude. As both METO and GFZ solutions are very different in terms of how ZTD is estimated and also due to the fact that both systems use different OTL models it is a fair assumption that the source of the bias is not within the GPS processing. However the increasing StDev with decreasing latitude might just be a scale factor in the ZTD as the farther south the GPS site is located, the greater ZTD they are generally going to have due to the atmospheric water vapour distribution. The mean ZTD observed by a site from April to May 20009 is plotted against latitude in Figure 3.18.

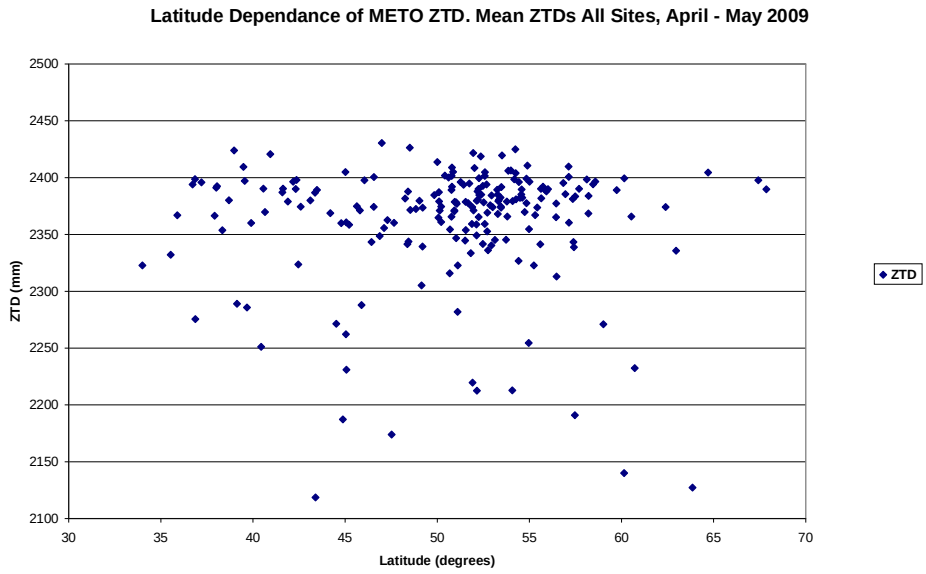

Figure 3.18 METO ZTD as a function of latitude, April 2009

If a scale error in ZTD were to be the source of the increase in error with decreasing latitude we would expect to see generally higher ZTD at lower latitudes. From Figure 3.18 we can see that this is not the case. There is no such latitude dependency as ZTD is more influenced by altitude and the increase in ZTD with decreasing latitude is small by comparison.

Now that a systematic bias due to latitude has been eliminated we need to assess whether there is a systematic bias in the data itself. An assessment therefore was carried out by plotting the error against increasing ZTD. The comparison was carried out for all the sites processed by METO for April 2009. The results are shown as Figure 3.19.

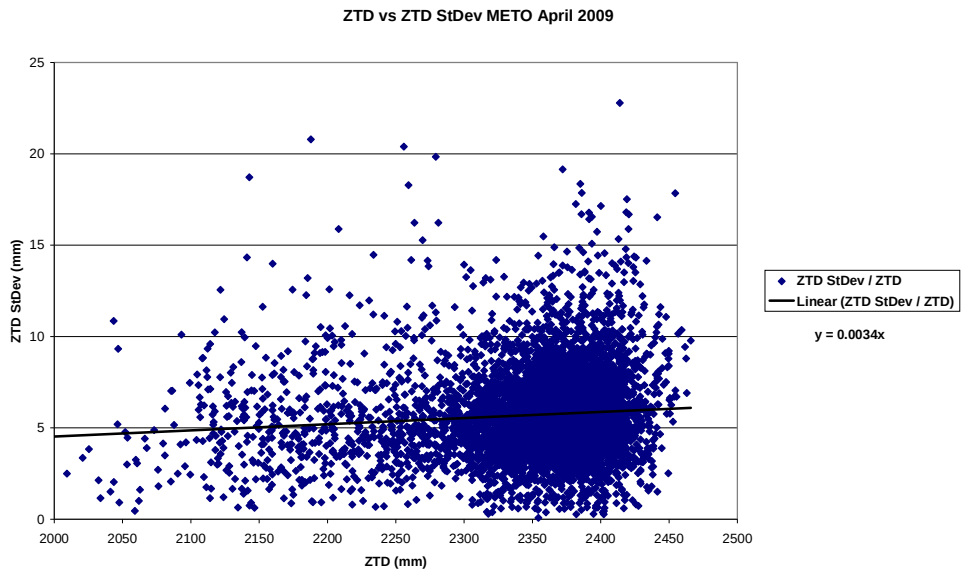

Figure 3.19 Systematic trend of METO minus NAE ZTD StDev, April 2009

From Figure 3.19 we can see that there is a small systematic bias of increasing StDev with increasing ZTD, with a linear trend of 6.4mm increase in StDev per metre increase in ZTD or a 3.2mm increase over the 0.5m range in ZTD.

This is small when compared to the 10mm increase as a function of latitude, over the 35^{o} range of latitude. As such we can say with a fair degree of certainty that both NWP models are having difficulty estimating ZTD at the southern extreme of their domain areas. This is most likely due to the lack of boundary conditions to initialise the models to the South, and might indicate the models need improvement in this geographic area or that the domain area needs to be increased if ZTD estimates from numerical models are to be improved in the Mediterranean area.

3.2.3 Relative Constraints

In the Bernese processing software, tropospheric parameters are estimated using a least squares adjustment. The resulting normal equation files may be added together from subsequent campaigns to give a better estimate of the parameter in question. This is carried out with the Bernese ADDNEQ2 program. The tropospheric parameters themselves are constrained by using both absolute and relative constraints which effectively limit the variability of the tropospheric parameters estimates as a piece-wise linear function. Relative constraints imposed in GPS processing therefore have a direct effect on the variability of the IWV estimate from one observation to the next. The tighter the relative constraint, the lower the variability from epoch to epoch and the smoother the IWV estimates appear. Relative constraints are necessary to limit the variability of tropospheric parameters because otherwise there is not enough observation data to constrain successive tropospheric estimates. However, finding

the optimum relative constraint is essential to ensure the real atmospheric structure is represented while at the same time GPS processing 'noise' is filtered out.

Comparison against NWP models is one of the most established techniques used for validating GPS water vapour estimates. However, NWP models are limited in the scale of events which they can adequately model primarily by the size of their grid squares. As such, sub-model square scale events, such as small scale convection, are typically not represented well by NWP. It is these very such events for which near real time GPS water vapour data could be most useful in identifying and quantifying, due to the spatial resolution of ground based GPS networks and the temporal resolution of GPS data. As such, comparisons against NWP should be more relevant for comparing larger scale atmospheric phenomena or identifying AC biases/trends etc and are of limited use when trying to establish how well GPS water vapour estimates mirror the real atmosphere. As comparison against NWP is the most common validation technique, it is tempting for ACs to over constrain their GPS solutions and this will normally give good results in terms of StDev etc when compared against NWP, but at the expense of providing real atmospheric information. To truly assess the correct amount of variability of a GPS IWV solution, data has to be compared against another source of data with a much higher temporal resolution. The WVR is a perfect instrument for this type of analysis due to its very high observation rate (every few seconds). Bias between the two instruments is not of prime focus here, but more the identification of small scale atmospheric fluctuations.

During the Convective Storm Initiation Project (CSIP) campaign (see Chapter 1) the German GPS AC, GFZ, installed a number of temporary GPS sites in the south of England in addition to those of OSGB. The additional sites consisted of four, high quality sites employing choke ring antennas and dual frequency GPS receivers, centred around the main observations platform at Chilbolton. A map of the CSIP campaign area is shown as Figure 3.20.

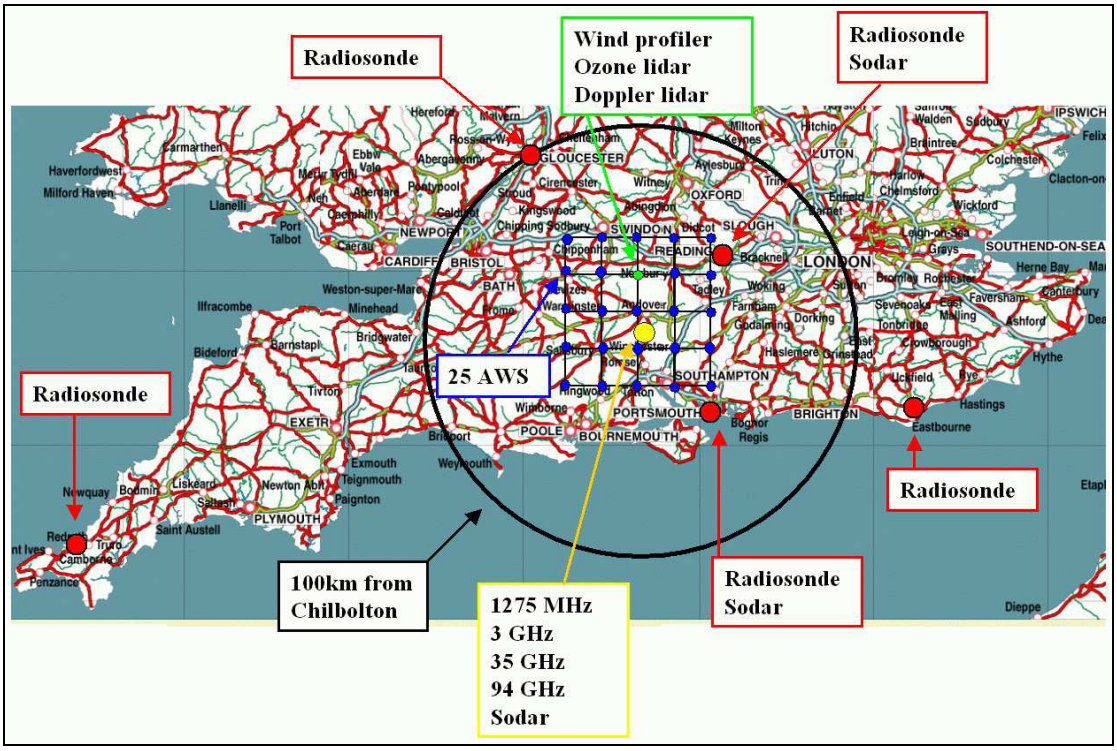

Figure 3.20 Map of CSIP campaign region. Courtesy of CSIP Project.

Data was recorded and processed by GFZ, and ZTD was estimated under their operational PPP processing campaign (as per Table 3.1). Data was then converted to IWV by the Met Office using the method as suggested by Saastamoinen (1972) and with surface meteorological parameters extracted from the Met Office database. Data from the temporary sites was compared against those from nearby sites processed by METO as well as against a Radiometrics MP3008 microwave radiometer which was installed at Chilbolton (collocated with the GPS receiver CSI3). Data is plotted as a time series in Figure 3.21.

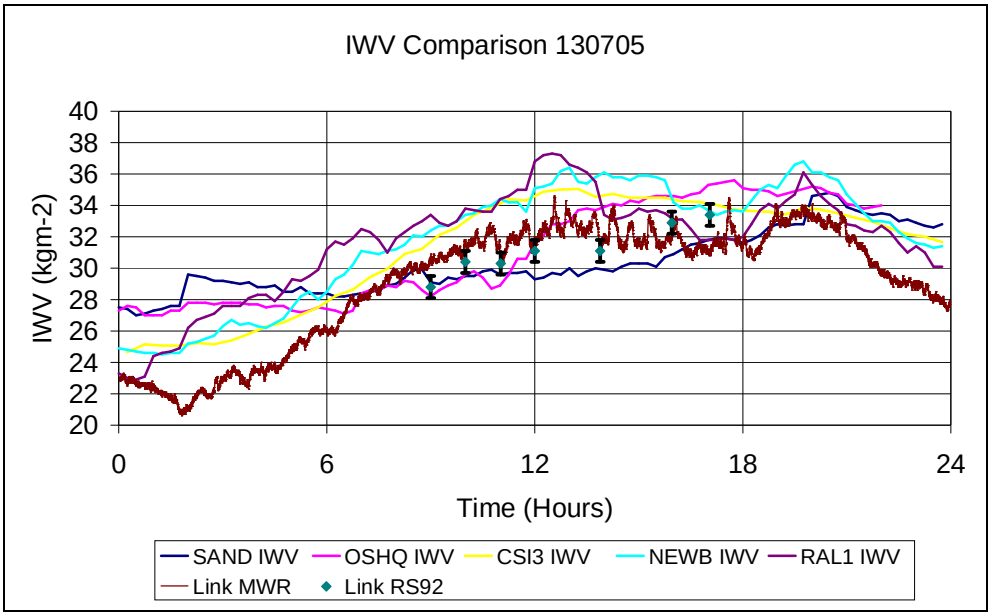

Figure 3.21 Time series of IWV showing GFZ IWV estimates for CSI3 appearing smoother than the METO IWV estimates for SAND, OSHQ, NEWB and RAL1.

From Figure 3.21 it can be seen that there is far less variability in the GFZ IWV estimates for CSI3 than the METO IWV estimates from the other nearby GPS receivers such as NEWB (Newbury) or the WVR data. The CSI3 data appears to be 'smoother' in relation to atmospheric variations identified by the other GPS receivers. Furthermore when compared against the microwave radiometer, observing at a 30 second time interval, all of the GPS data is far less variable suggesting that there is either noise in the WVR signal or the constraints applied to the GPS solutions need be assessed. In this example the data from the CSI3 site would most likely compare very well against NWP IWV data in terms of bias, but as we see here, the data does not necessarily represent the real atmosphere very well.

When the Met Office operational GPS processing servers (GPSWV1/2) were delivered by the University of Nottingham in October 2006, the relative constraint imposed on the processing was 1.5mm. Before operational assimilation of GPS ZTD from the Met Office systems could begin a thorough assessment of data quality (variability of StDev) against the North Atlantic and European (NAE) NWP model had to be completed to ensure StDev of the data was within operational targets of 15mm ZTD. Data was compared from December and January 2007/2008 and it was found that the StDev was too large (~21mm ZTD) and as such the ZTD data could not be assimilated operationally. To ensure data was brought within the operational limits, the relative constraint imposed on tropospheric parameter production was reduced to 1mm and subsequently the StDev decreased markedly to within operational targets. For example the StDev for April 2009 from METO was 11.4mm which is now typical of METO.

To assess the difference in variability of IWV resulting from different tropospheric relative constraints in the Bernese software, data was reprocessed for a 1 week period in 2008 for the GPS site PAYE (Payerne, Switzerland) with varying relative constraints at 0.5mm, 1mm, 2mm, 5mm and 10mm increments. IWV estimates were then compared against RPG HATPRO microwave radiometer data which is collocated at the site at Payerne. The radiometer records data approximately every 30 seconds and as such should represent real atmospheric fluctuations well. All data recorded by the radiometer whilst it was raining was excluded from the comparison due to the known problems associated with using WVRs in rain (Chapter 2). IWV data from all relative constraint solutions as well as from the WVR are shown as Figure 3.22.

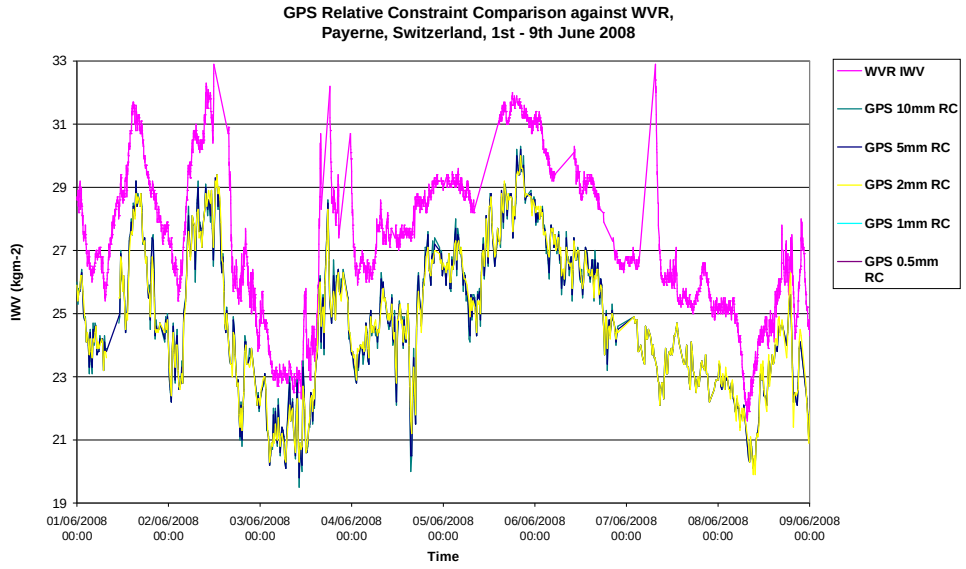

Figure 3.22 Time series of all IWV data from Payerne

The most noticeable observation from Figure 3.22 is the consistent offset of the WVR data compared to all GPS solutions. A mean bias for the time period assessed exists of approximately 2.5kg/m^2. As mentioned previously, the bias is not being assessed here, more the fluctuation of the atmosphere. For ease of comparison of the WVR data against GPS IWV a bias correction of 2.5kg/m^2 was applied to the WVR data and the data is henceforth known as bias corrected WVR (BC-WVR). Also from Figure 3.22 we can see that although there is a relatively wide range of relative constraints applied to the various GPS solutions (between 0.5mm and 10mm), there is overall no great difference between the IWV from the different solutions when viewed on such a large scale. The bias and StDev between the different solutions is displayed in Table 3.3.

	10 - 5mm RC	5 - 2mm RC	2 - 1mm RC	1 - 0.5mm RC
Bias (kg/m^2)	0.0029	-0.0058	0.0029	-0.0027
StDev (kg/m^2)	0.1010	0.2213	0.2030	0.1904
Max. Bias (kg/m^2)	0.5	0.9	0.8	0.7

Table 3.3 Summary of biases and variability of biases between solutions with varying relative constraint

Although the overall bias between solutions is small, when we compare the differences at a smaller scale do we see how the less constrained solutions compare better against WVR data than the estimates with tighter relative constraints. Figures 3.23, 3.324 and 3.25 are example from the period of reprocessing where instances have been identified illustrating the variability of the GPS estimates against the WVR data.

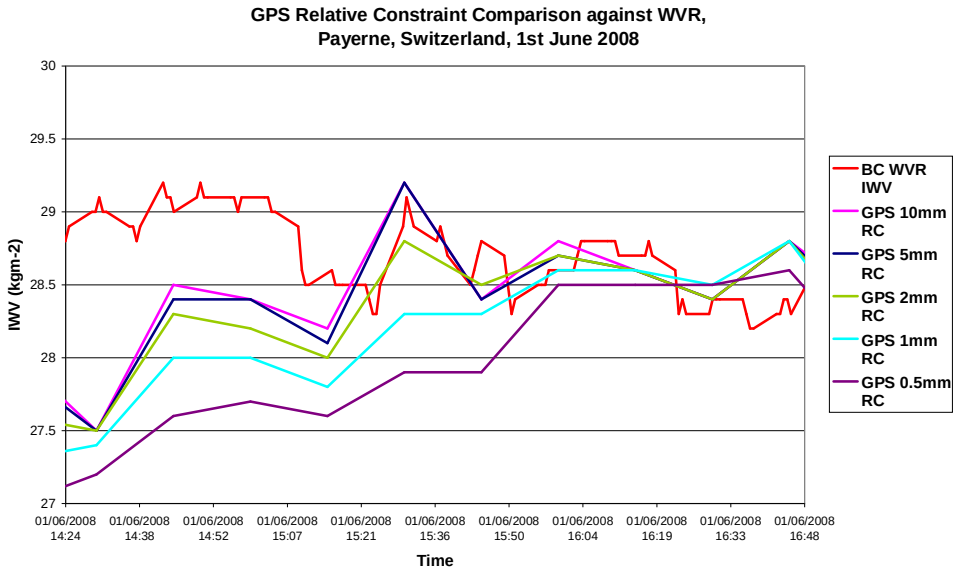

Figure 3.23 IWV time series from all RC GPS estimates and bias corrected WVR IWV, Payerne, Switzerland, June 1st 2008

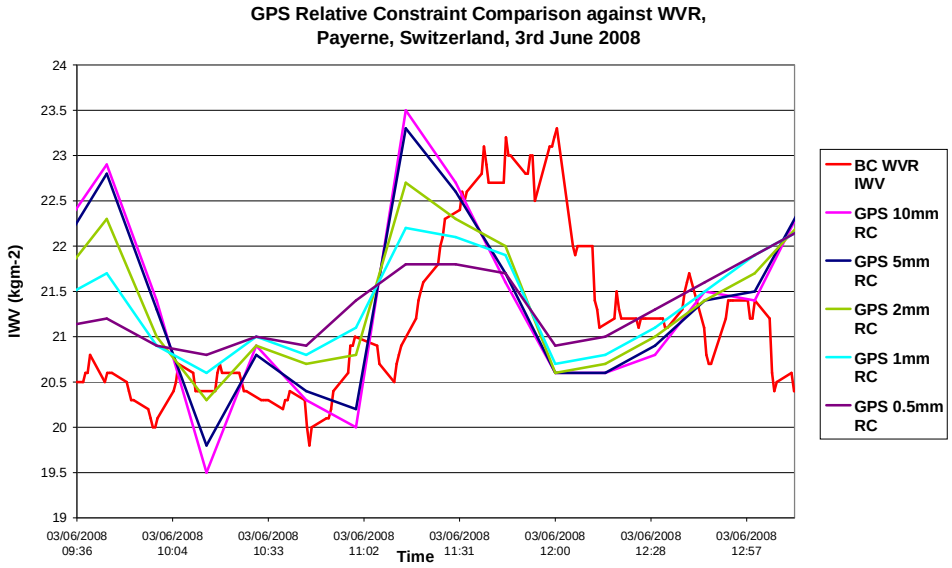

Figure 3.24 IWV time series from all RC GPS estimates and bias corrected WVR IWV, Payerne, Switzerland, June 3rd 2008

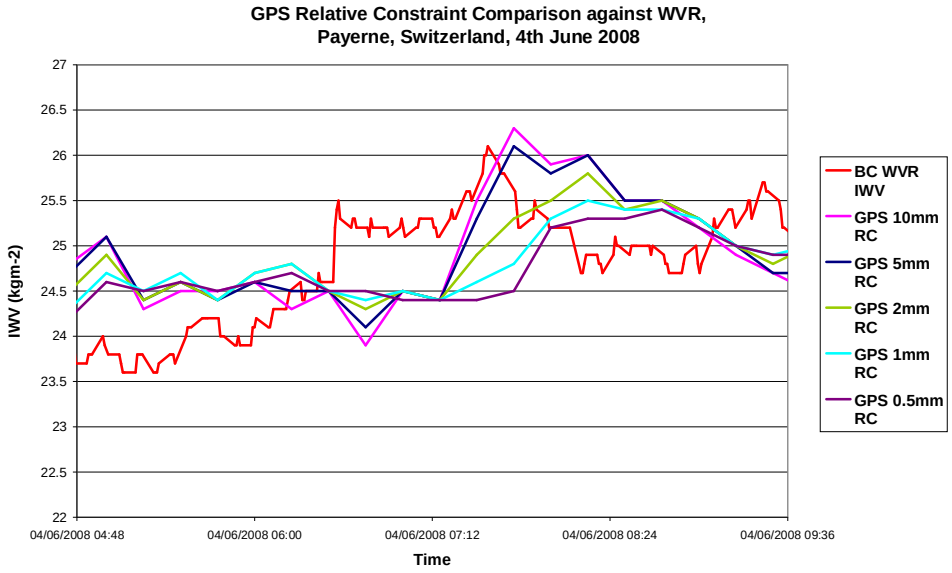

Figure 3.25 IWV time series from all RC GPS solutions and bias corrected WVR IWV, Payerne, Switzerland, June 4th 2008

From the three examples shown in Figures 3.23 to 3.25, we can see the least constrained solutions (10mm and 5mm shown by the pink and dark blue lines respectively) at times representing the real atmospheric fluctuations with the greatest degree of accuracy. For example, at approximately 15:30 UTC on June 1st, we see a peak in the BC-WVR data (orange line) which is broadly reflected in both the 10mm and 5mm GPS solutions, whereas all other solutions underestimate the rise in IWV over

this period. Of all the solutions, the 2mm constrained IWV solution seems to be the best compromise of representing the real atmospheric fluctuations and comparing well against the BC-WVR data whilst at the same time still restraining the random walk of the water vapour data to a sensible degree. Similar patterns can again be seen for the peak in water vapour at ~ 11:30 on the 3rd of June and again at ~08:00 on the 4th of June. It is important to note that the operational GPS estimate with a constraint of only 1mm does not mirror fluctuations as represented by the BC-WVR data particularly well suggesting that the relative constraints imposed on the UK operational processing servers may need to be relaxed if the data is to be used more for nowcasting focused activities.

However, it can also be seen that on a number of occasions through the comparison period that all GPS solutions diverge from the WVR data, and in these instances it is of course the least constrained solutions which diverge the most. An example is shown as Figure 3.26 where at about 12:43, the GPS solutions' IWV diverge away from the WVR solution.

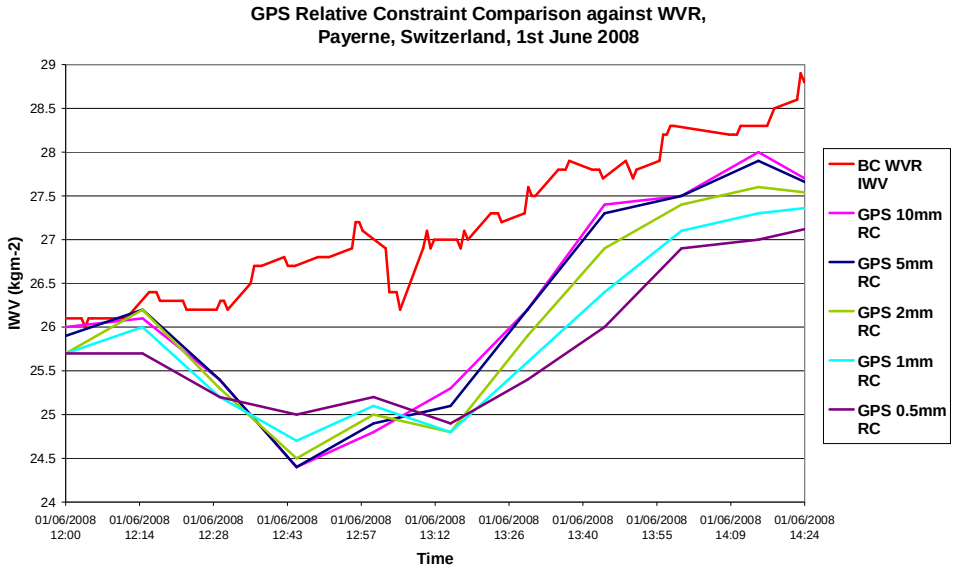

Figure 3.26 IWV time series from all RC GPS solutions and bias corrected WVR IWV, Payerne, Switzerland, June 1st 2008

The balance of constraining versus allowing the data to represent real atmospheric fluctuations is an important question for the application of GPS water vapour. If the data is to be solely used for assimilation into NWP models, then the constraint imposed on the data will be largely dictated by the NWP resolution. However, if GPS water vapour data is to be used for nowcasting purposes, the data must be more loosely constrained to allow the estimates to best mirror the real atmosphere. From the comparison study it can be seen that even a small change in relative constraint imposed during the ADDNEQ part of the Bernese processing can have large effect on IWV estimation. The standard deviation of the biases between the solutions were all small, ranging from ~0.1 to ~0.2 kg/m^2

indicating that all the solutions followed the same trends of increasing and decreasing IWV very well. From further comparison however we see that, at least in this case study, if the atmospheric fluctuations are to be best captured by GPS a relaxation of the METO operational relative constraint is needed, most likely to 2mm. However from previous comparison against the NAE model from when the METO system had a more loosely constrained solution, the results suggest that the noise in the data was too great for NWP to adequately resolve.

In the near future the solution to this problem might be to have two processing solutions, one with a more tightly constrained solution providing ZTD estimated for NWP, representing larger scale atmospheric features, and another more loosely constrained providing information to the short term forecasting community. Also, with the advent of higher resolution NWP models, it remains to be seen whether the higher temporal and spatial resolution of the new NWP models can successfully assimilate data from a more loosely constrained GPS solution. In the future, further trials will be carried out to assess the optimum balance of relative constraints for input into the new high resolution NWP models and it may prove that one GPS solution can satisfy both customers of the data, but for now these tests show that the current METO solution is effectively 'tuned' for input to the current NWP model.

3.2.4 Introduction of Absolute Antenna Phase Centre Models

In December 2006 a new set of processing models were introduced relating to the way in which GPS antennas are represented in the processing system. High precision GPS positioning is based on measurements of the carrier phase typically using a geodetic quality choke-ring antenna. Every antenna has an individual phase pattern which can be expressed as the contribution of the antenna to the signal phase measured by the receiver. This antenna phase contribution is a function of the direction of the recorded GPS signals reaching the antenna for a given GPS satellite constellation geometry. Since GPS processing software estimates tropospheric delay parameters by mapping the slant delays from each satellite to the vertical to retrieve ZTD and IWV, an uncorrected antenna phase centre can significantly distort the detected phase change with elevation that is attributed to the troposphere. The results are poor quality troposphere delay estimates as well as poor height repeatability.
As the satellite moves, even though keeping a constant distance to the phase centre, the phase centre of the antenna will rotate around the physical centre of the antenna and will trace out a pattern known as the Phase Centre Variation or PCV.

To produce absolute antenna phase centre models a reference antenna is used to create a short differential baseline with the test antenna. Now, clock, orbit, and propagation effects are eliminated. If the test antenna is tilted in a variety of directions, the phase differences seen between the two antennas

should reflect the phase difference due to the elevation and azimuth dependence of the PCV since the same satellites are seen at different elevations and azimuths with respect to each antennas horizon and orientation. A least squares solution for the surface describing the PCV and the phase centre offsets with respect to the antenna reference point can be obtained from continuous tilting of the test antenna over several hours to include observations from as many directions as possible. If the reference and test antennas are the same, this procedure yields the absolute phase centre offsets and their variation as a function of the direction for that antenna. Once these calibration parameters are known, this reference antenna may be used to find the absolute calibration parameters of other antenna models.

Before this absolute calibration had been established, antennas were calibrated in a relative sense. The procedure was similar to that described for the absolute calibrations except the test antenna is not tilted but remains pointing at the zenith like the reference antenna. As the GPS satellites move across the sky, the phase differences due to differences between the test and reference antennas will again be traced out. This procedure can only determine the PCV of the test antenna relative to the reference antenna. In this case phase centre offsets and a constant null PCV are assigned to the reference antenna. Because the test antenna is held fixed, this procedure also suffers from a lack of adequate sky coverage. These relative calibrations can be turned into absolute calibration, once the absolute calibration of the reference antenna is independently determined, by replacing the previously assumed reference value with absolute values.

In practice relative antenna calibrations are perfectly acceptable over shorter baselines (< several hundred km) because the elevations from each antenna to the same satellite are not significantly different. However, on longer baselines (> a few thousand km) the curvature of the earth causes the elevations to the same satellites to be significantly different and knowledge of the absolute PCV becomes essential. In either case, ignoring the PCV leaves the mainly elevation-dependent antenna effects imbedded in the GPS data. If the GPS solution includes an adjustment of a tropospheric delay parameter, the uncorrected antenna effects will significantly distort the elevation dependence of the data causing erroneous tropospheric delays.

Vespe and Pacione. (2007) showed a dry shift in ZTD to the extent of 5mm with the introduction of absolute antenna phase centre models as well as a bias reduction against radiosonde water vapour. However for correct bias corrections to be determined, we need to firstly determine the bias correction in a site specific nature as it will relate to the specific antenna at that site. Furthermore any biases introduced might also be proportional to the local atmospheric conditions giving even more requirement for site specific bias corrections to be determined. To assess if any difference in bias was introduced due to the change from relative to absolute antenna phase centres, we can use the bias against the operational radiosonde ascents in the UK as a common IWV reference, assuming no radiosonde upgrades took place during the period of comparison. In January 2007 the Met Office GPS processing servers were updated from relative to absolute antenna phase centre models. To assess the

impact of the update, data was compared from before and after the point of upgrade. Radiosonde minus GPS IWV data was then taken and mean biases calculated. Data was compared before the update point back to the point when RS92's were introduced for each particular site, as no radiosonde instrument updates had been made during this time. For the data used for comparison after the upgrade to absolute antenna models, consistent radiosonde data was available up to June 2007 when the humidity sensor was upgraded, as detailed in Chapter 2. The results for Camborne, Herstmonceux, Nottingham and Lerwick respectively are shown in Figures 3.27 to 3.30 inclusive, where RAPCV means relative antenna phase centre models and AAPCV means absolute antenna phase centre models.

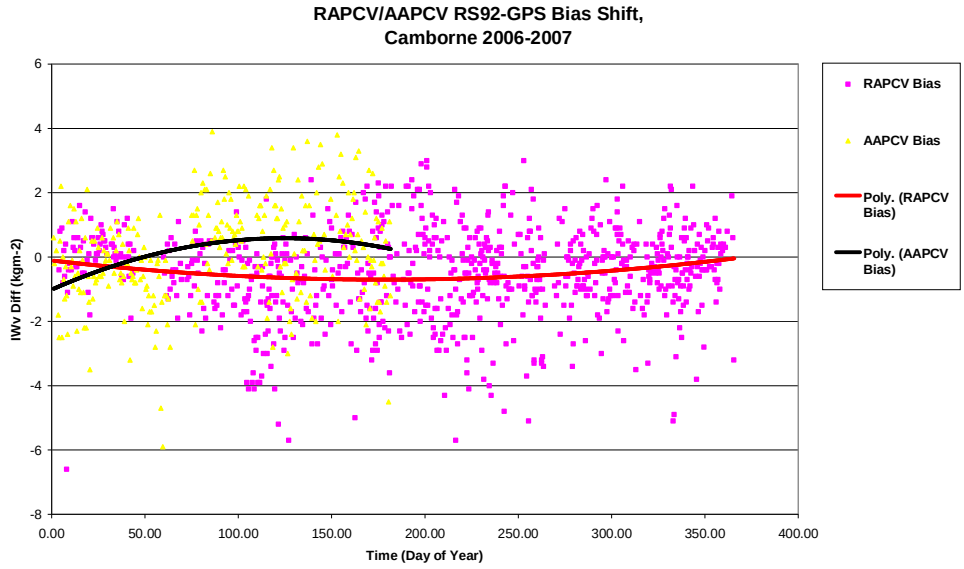

Figure 3.27 Bias shift from RAPCV to AAPCV models, Camborne 2006 - 2007

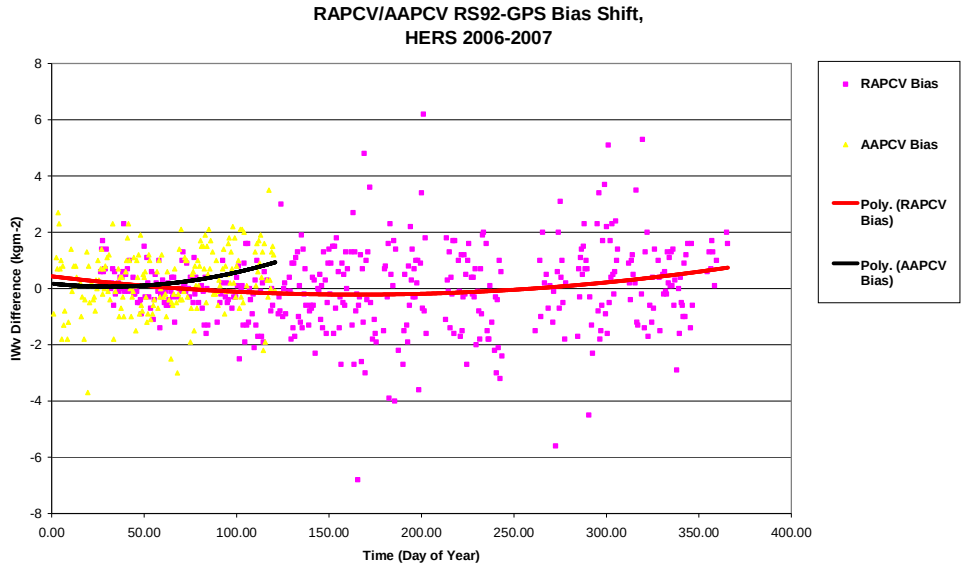

Figure 3.28 Bias shift from RAPCV to AAPCV models, Herstmonceux 2006 – 2007

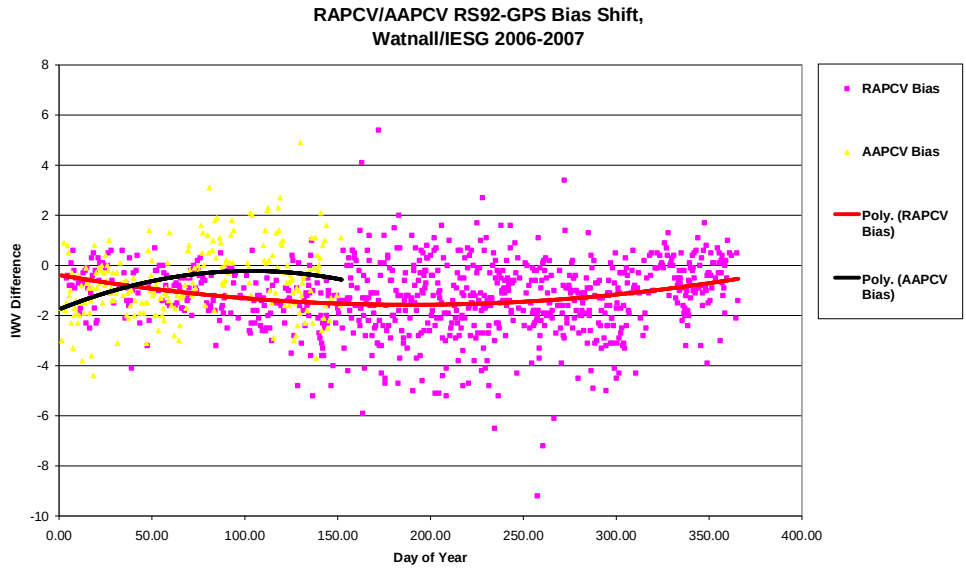

Figure 3.29 Bias shift from RAPCV to AAPCV models, Nottingham 2006 – 2007

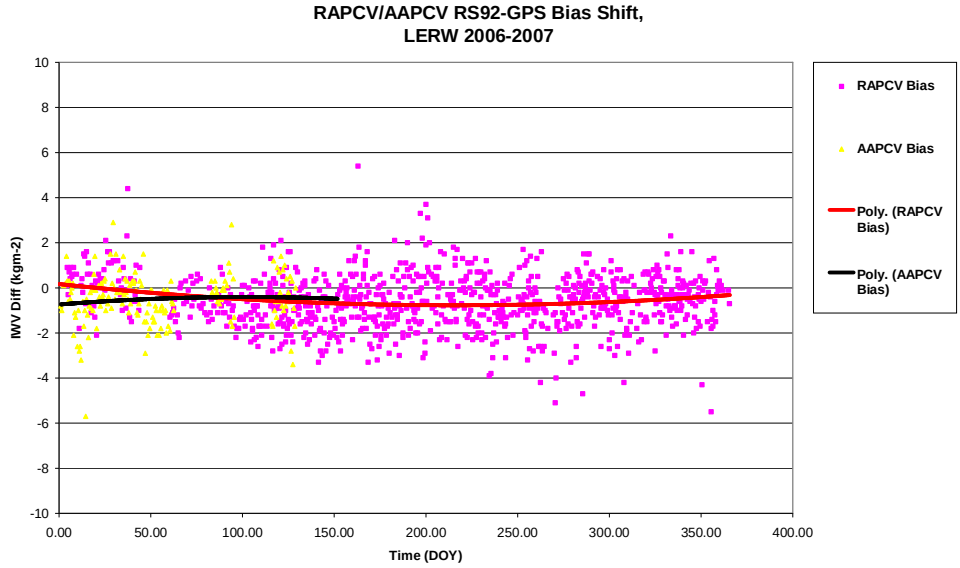

Figure 3.30 Bias shift from RAPCV to AAPCV models, Lerwick 2006 – 2007

It is clear to see from the results, that the bias did indeed move in the positive direction for all sites. For the case of Camborne, the negative bias has actually been reversed leaving a positive RS-GPS IWV bias. For Nottingham and Lerwick the negative bias was reduced leaving a smaller but still negative bias. For the case of Herstmonceux, the bias was already very small and as such, the positive shift actually increased the overall bias, moving it further from zero. However for all sites with the exception of Herstmonceux the change to AAPCVs resulted in a reduction in the negative dry radiosonde bias. The results from the comparison are shown as Table 3.4.

Site	RS92 (old T, old U) vs. GPS (RAPCV) Bias (kg/m^2)	RS92 (old T, old U) vs. GPS (AAPCV) Bias (kg/m^2)	Bias Shift (kg/m^2)
Camborne	-0.5075	+0.2896	+0.7971
Herstmonceux	+0.0134	+0.2918	+0.2784
Nottingham	-1.2627	-0.6340	+0.6287
Lerwick	-0.5944	-0.5242	+0.0702

Table 3.4 RS92 vs. GPS bias from before and after AAPCV GPS processing update in January 2007

From Table 3.4 we can see that the introduction of absolute antenna phase centre models in January 2007 did have a dramatic effect on the bias against radiosonde IWV. The RS-GPS bias following the introduction of the new antenna phase centre models is significantly less than the bias with relative antenna phase centre models suggesting, assuming radiosonde data is correct, that the upgrade adjusted biases in the right direction. If Herstmonceux is excluded, the overall shift in bias is around 0.7 kg/m^2 for all other sites. Due to the range of the bias shift, with particular reference here to the smaller bias shift at Herstmonceux, we see the importance of estimating bias corrections on a site by site basis which needs to be completed for any site from which data is to be used for climate analysis. However, as we will see later in this Chapter all other biases such as instrument upgrades also need to be taken into account before a consistent time series of data can be produced.

3.2.5 DD NEQ Addition – Speed vs. Quality

The three most important considerations for GPS meteorology are the size and geometry of the network, the quality of the solution, and the speed of which the data (ZTD) can be delivered to NWP. All three factors are interlinked as the speed of the GPS processing solution is dictated by the number of sites processed and the quality of the solution which in turn, if number of sites is excluded, is dictated by the number of normal equation files (NEQs) added in the final stages of a Bernese DD processing. From studies carried out by the University of Nottingham (Orliac et al., 2003) it was found that the optimum number of NEQs to be stacked was 7; 6 previous hours plus the current hour's normal equation file and the operational servers were delivered to the Met Office under this configuration. Subsequently, as the number of sites processed by METO increased the time delay under the 7-NEQ processing strategy became too great and delivery of data from a 200+ station network could not be delivered to NWP within the operational timeliness targets. As such, in an effort to speed up delivery of observations to NWP the number of NEQs to be stacked was reduced to 6 with no attributable loss of quality, and the systems have been running operationally in this configuration since January 2007. As the network expanded further and processing slowed again, the number of NEQs to be stacked needed to be reduced further to 5; 4 previous hours plus the current hour. As the NEQs were being reduced further, the outcome with regards to the effect on data quality was unknown

therefore as assessment needed to be carried out to determine the effect on data quality with the NEQ reduction. At the beginning of January 2008 the configuration of the nominal back-up server at the Met Office, GPSWV2, was altered to use 5 NEQs whilst the configuration of the operational server, GPSWV1, was left unaltered running with 6 NEQs. Data was assessed for the following 1 month period to try and determine if there was any appreciable bias between IWV data from the two solutions. Data was compared (over 1600 data points) was collected and compared and a time series of this data set is illustrated in Figure 3.31.

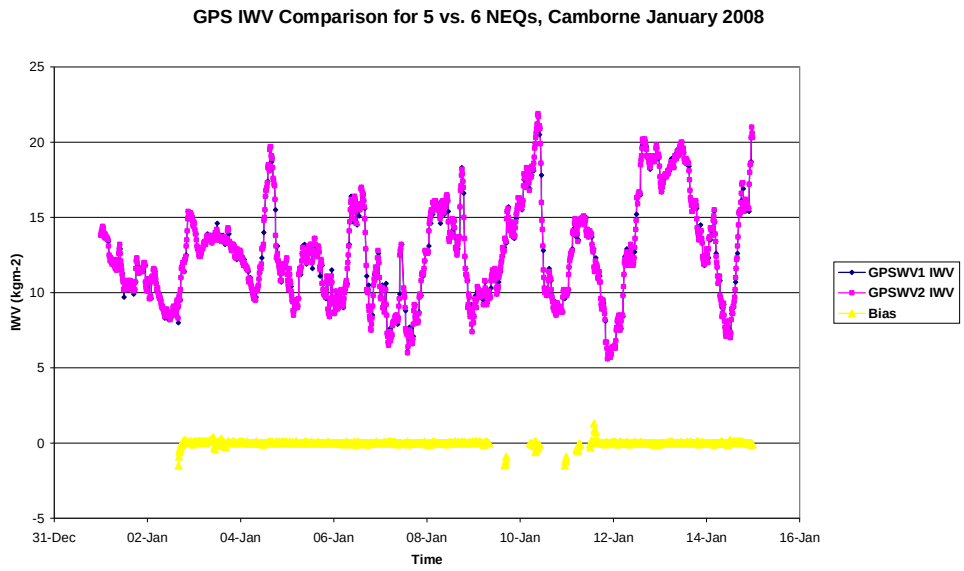

Figure 3.31 METO 5-NEQ IWV vs. 6-NEQ IWV, Camborne, January 2008

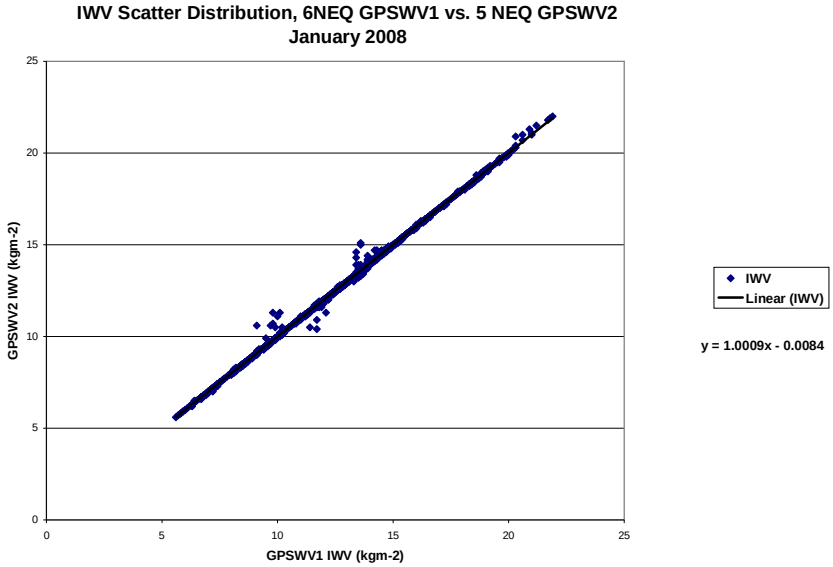

Figure 3.32 Scatter distribution of 5NEQ IWV vs. 6NEQ IWV, Camborne, January 2008

As can be seen from Figures 3.31 and 3.32, there is generally no appreciable loss of data quality in a 5-NEQ solution (GPSWV2) when compared against the 6-NEQ solution (GPSWV1). There were a small number of examples where the GPSWV1-GPSWV2 bias was in excess of 1 kg/m^2, however overall the comparison showed that there was only a very small mean bias of 0.00138 kg/m^2 for the period (StDev of 0.149 kg/m^2 IWV). From the occasional larger biases between the solutions it appears that reducing the number of normal equation files further may have adverse effects on data quality and if in the future the time delay of high quality ZTD and IWV data to the users has to be reduced further, either the number of sites would have to be reduced or the network would have to be processed as two sub-networks, one on GPSWV1 and one on GPSWV2.

In GPS meteorology, the time delay between observation time and the time at which the data is available is crucial. For data assimilated into numerical models, the time delay between observation and assimilation is currently 90minutes for the NAE model, for nowcasting however the timeliness requirements would be much more critical. For nowcasting applications, data must be available to the forecaster within 12minutes to be considered to be useful and real time. To deliver high quality GPS estimates on these timescales would have to involve a new sub-hour processing strategy, but the optimum sub-hour strategy would require much investigation to ensure the optimum balance is delivered of data quality against speed of data delivery.

3.3 Inter-Instrument Comparison of IWV

To further assess how well GPS water vapour estimates represent the real atmosphere and to assess the absolute accuracy of GPS water vapour it is essential to compare such data against water vapour data retrieved from other remote sensing and in-situ measurements. Radiosondes are used globally for providing retrievals of atmospheric profiles and are one of the most heavily weighted observations in numerical models. As described in Chapter 2, column total water estimates can be retrieved from humidity and temperature measurements from radiosondes and as such they are an invaluable tool for water vapour comparison against GPS. In the UK we have four sites where GPS receivers are collocated with operational radiosonde sites. Due to their collocation as well as the relatively high quality and stability of radiosonde data, radiosondes are the most widely used observation type for comparison in this thesis.

Before using long radiosonde time series for comparison against GPS water vapour however, any biases in either the radiosonde or GPS time series need to be addressed. As mentioned in Chapter 2 the radiosondes used for comparison over the period of this thesis have undergone a number of hardware and software upgrades and the influence of the upgrades on IWV estimates must therefore, be assessed. To correlate radiosonde upgrade against launch date, data was provided by Vaisala (the radiosonde manufacturer) relating radiosonde batch number to instrument updates. Furthermore, using radiosonde batch number information extracted from the Met Office database it was possible to correlate batch number (and hence sensor upgrade) against date of launch. In this way it has been possible to assess any bias shift at the point of upgrade. If a raw time series is plotted of all radiosonde data compared to all GPS (Figure 3.33) for January 2001 to December 2008 it is clear that there are major shifts in RS-GPS bias over the period. All sensor and processing upgrades must be accounted for if long term RS-GPS biases and any trends in the water vapour are to be resolved.

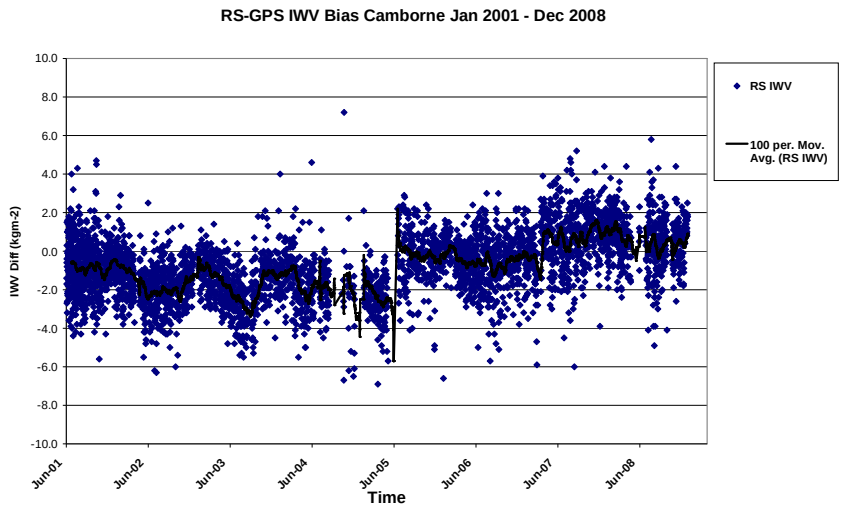

Figure 3.33 Raw Time series (no bias correction applied) for Camborne 2001 - 2008

A comparison of data was carried out from the four operational radiosonde stations in the UK which are collocated with GPS receivers. The sites are Lerwick on Shetland, Watnall near Nottingham, Herstmonceux in Sussex and Camborne in Cornwall. Table 3.5 provides an overview of the main GPS processing and radiosonde upgrades that took place during the period of analysis. In addition to the radiosonde upgrades, if the data is to be used for comparison against GPS water vapour estimates, any major changes in the GPS processing system also have to be addresses. Fortunately no antenna changes occurred during the comparison at any of the four sites eliminating any bias shifts which might have been introduced through equipment change. The only GPS processing changes which took place over the period have already been addressed above through the bias analysis relating to the change from relative to absolute antenna phase centre models.

Site	RS80 from	RS92 from	Absolute antenna phase centre models Since	New Humidity (U) Sensor	New Temperature (T) Sensor
Camborne/CAMB	June 2001	April 2005	Jan 2007	July 2007	July 2008
Herstmonceux/HERS	Jan 2002	Jan 2006	Jan 2007	May 2007	July 2008
Lerwick/LERW	June 2001	April 2005	Jan 2007	June 2007	July 2008
Watnall/IESG	Jan 2003	May 2005	Jan 2007	June 2007	Aug 2008

Table 3.5 Overview of GPS processing and radiosonde upgrades during period of thesis

3.3.1 Introduction of the Vaisala RS92 Radiosonde

The first major change to the radiosonde data set was the introduction of the newer RS92 radiosonde taking over operational duties at the four sites used for comparison which occurred in 2005/06. If a time series of the older RS80 IWV as well as the newer RS92 IWV are plotted taking into account the radiosonde upgrade, the bias shift between instruments is very clear. Figure 3.44 is the raw radiosonde IWV time series from Camborne.

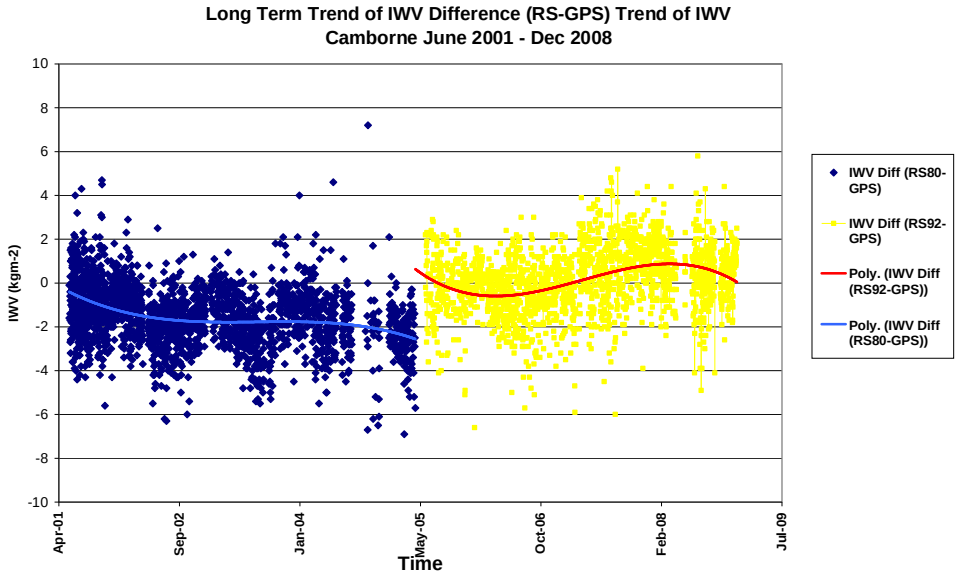

Figure 3.34 Example time series of Camborne RS-GPS IWV Bias

If RS-GPS bias from prior and following the upgrade is assessed, the change in bias is negative for all four sites. The mean RS80 bias for Camborne for example was approximately -1.5 kg/m^2 (RS-GPS) whereas the mean RS92-GPS IWV bias following the upgrade was reduced to around -0.5 kg/m^2. A similar bias shift was observed for all other collocated radiosonde/GPS sites in the UK used for comparison with a mean bias shift for all sites of 0.74 kg/m^2. The RS80 and RS92 (RS minus GPS) IWV biases as well as the bias shift per site are given in Table 3.6.

Site	RS80 - GPS Bias* (kg/m$^{2)}$	RS92 - GPS Bias** (kg/m$^{2)}$	Bias Shift (kg/m^2)
CAMB	-1.5033	-0.5075	+0.9958
HERS	-0.7838	0.0134	+0.7972
IESG	-1.8275	-1.2627	+0.5648
LERW	-1.2060	-0.5944	+0.6116

Table 3.6 Bias reduction (RS-GPS) following introduction of RS92 radiosonde

*There is no record of any instrument changes which occurred in the RS80 time series. As such we have to assume that all data for the RS80 is consistent.

**It is important to note that the data used for the RS92 comparison is from the point of upgrade only until any further changes were made to either the radiosonde or the GPS processing system. In this case the next change in the time series was the upgrade to absolute antenna phase centre models which is described in more detail previously in this Chapter. Also the data used here is before any further radiosonde humidity or temperature sensor upgrades.

From the results in Table 3.6 we see that RS80 IWV measurements were typically in the order of ~1.5 kg/m^2 less than those from coincident GPS water vapour estimates. Following the upgrade the RS92 estimates of water vapour are much more in line with those from GPS with a mean bias for all sites of only -0.5878 kg/m^2. However with the exception of Herstmonceux there is still a dry bias in the radiosonde data with respect to GPS water vapour. A number of assessments have been carried out to assess this radiosonde dry bias such as Wang and Zhang (2007) and it has been asserted that the bias is a result of solar radiation heating the radiosonde humidity and temperature sensors, driving off humidity and causing the radiosonde to record too low temperature and humidity measurements. As was demonstrated in Chapter 2 these translate directly into water vapour estimates. GPS water vapour offers a relatively new, novel application which is unaffected by moisture (as is the case with microwave radiometers).

To assess if there is indeed a systematic bias between the data types (i.e. a percentage error) data is plotted as a scatter plot to assess the slope of a linear trend and see if either system over or underestimates IWV at low/high water vapour levels. These results are given as Figures 3.35 to 3.38 inclusive.

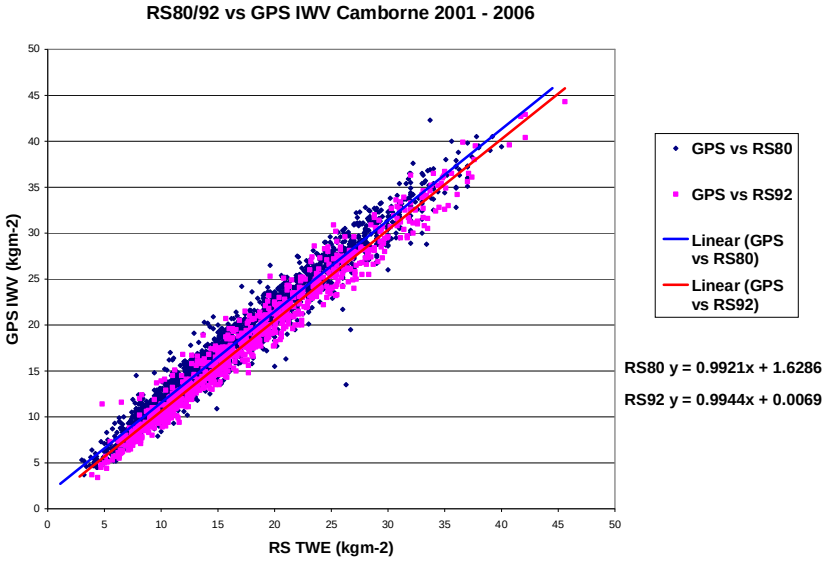

Figure 3.35 Scatter plot of RS80 and RS92 IWV vs. GPS IWV, Camborne, 2001-2006

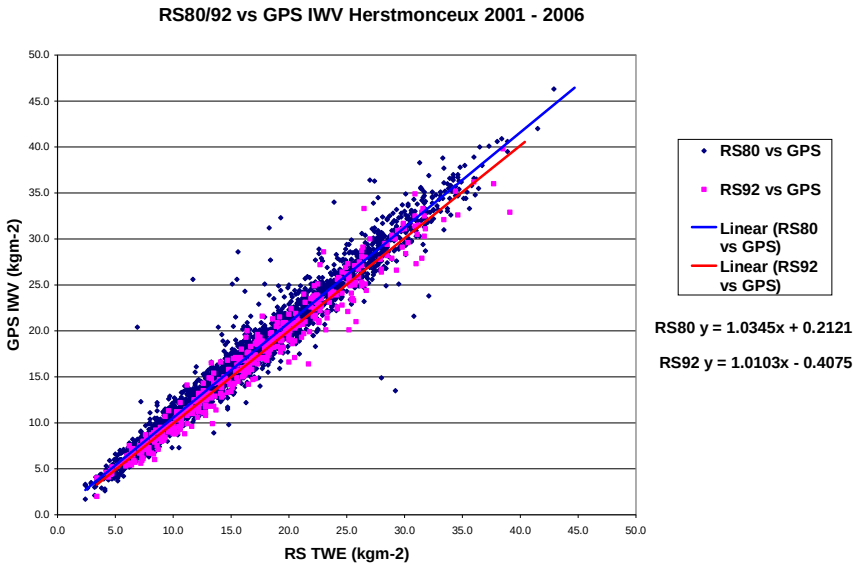

Figure 3.36 Scatter plot of RS80 and RS92 IWV vs. GPS IWV, Herstmonceux, 2001-2008

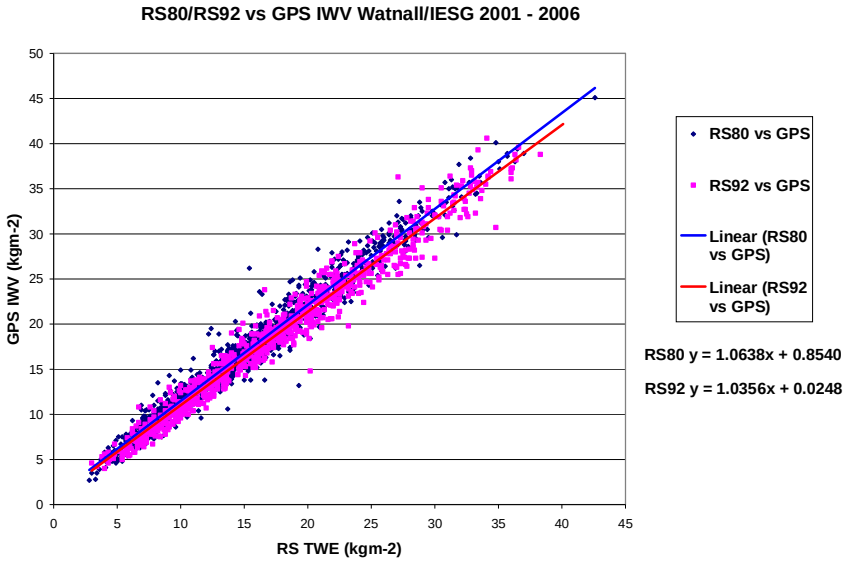

Figure 3.37 Scatter plot of RS80 and RS92 IWV vs. GPS IWV, Nottingham, 2001-2008

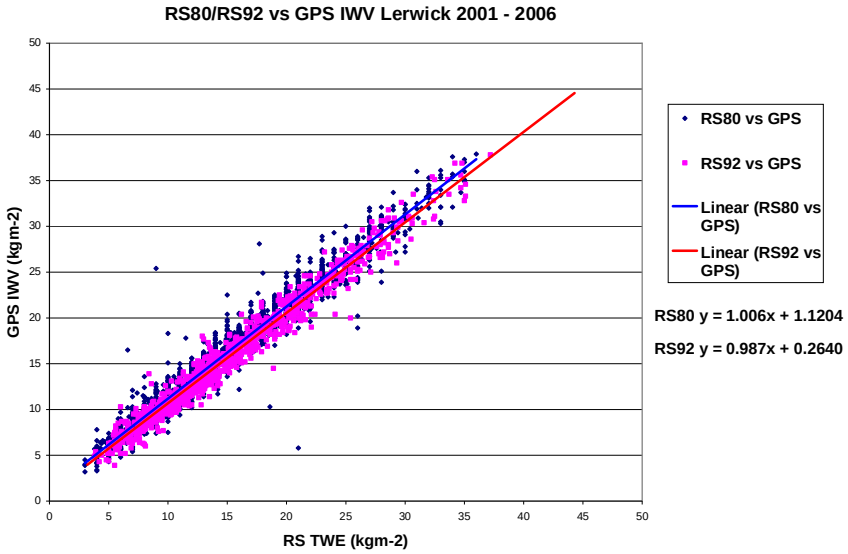

Figure 3.38 Scatter plot of RS80 and RS92 IWV vs. GPS IWV, Lerwick, 2001-2008

From the intercepts of the linear trend lines in Figures 3.35 to 3.38 and from Table 3.6 we can see that although the RS-GPS bias has been reduced by the introduction of the newer RS92 radiosonde (intercept closer to 0), with the exception of the site at Herstmonceux, the radiosondes still measure too low IWV with respect to GPS (intercepts are all positive and RS92-GPS bias is still negative). The slope of the linear trend lines is summarised in Table 3.7 from which we can see that all linear trends from the scatter plots are close to 1 indicating that there is generally good agreement between radiosonde and GPS and that there appears to be no systematic bias related to increasing water vapour.

Site	RS80 Trend	RS92 Trend
Camborne	Y=0.9921x	Y=0.9944x
Herstmonceux	Y=1.0345x	Y=1.0103x
Watnall	Y= 1.0638x	Y=1.0356x
Lerwick	Y=1.0060x	Y=0.9870x

Table 3.7 Overview of RS80 and RS92 vs. GPS

In short then, the introduction of the RS92 was a large improvement on the RS80, with a decrease in the radiosonde dry bias, but there does still exist a dry bias of the radiosonde which is thought to be down to solar radiation heating up the radiosonde instruments and is assessed in more detail later in this Chapter.

3.3.2 Introduction of a new coating on the RS92 Humidity Sensor

As mentioned above, the first RS92 upgrade during the time of study was during May/July 2007 when a new coating was applied to the RS92 humidity sensor in an attempt by the manufacturer to try and reduce the effect of the dry bias from solar radiation. The assumption is that in general the higher the sun is above the local horizon, the greater the heating of the radiosonde by solar radiation (Lorenc et al., 1996). The sensor is then at an artificially high temperature and some humidity will be driven off by the heating effect. As temperature and humidity are of course used in IWV estimation, any bias in the humidity sensor would be translated to an error in IWV estimates. According to the manufacturer, the bias induced by solar radiation should only be noticed at higher altitudes (upper troposphere and lower stratosphere) at which the amount of humidity is so low that the impact on radiosonde derived IWV should be minimal. Before assessing if the instrument upgrade had the desired effect on solar influenced bias at higher solar elevations we must first assess what the overall impact of the upgrade had on radiosonde IWV estimates.

To assess if the upgrade caused a shift on general RS92-GPS IWV bias, data was compared from prior and post sensor upgrade and the mean bias calculated from a comparison with GPS water vapour estimates from a consistently processed GPS system using absolute antenna phase centre models. Data is compared from January 2007 when absolute antenna phase centre models were introduced through to the point at which the radiosonde sensor upgrade took place (~May/July 2007 depending on radiosonde site) all the way to the point at which the next radiosonde instrument upgrade took place with the new temperature sensor, introduced in July 2008. The results for Lerwick, which exhibits the most apparent bias shift, are presented as Figure 3.39.

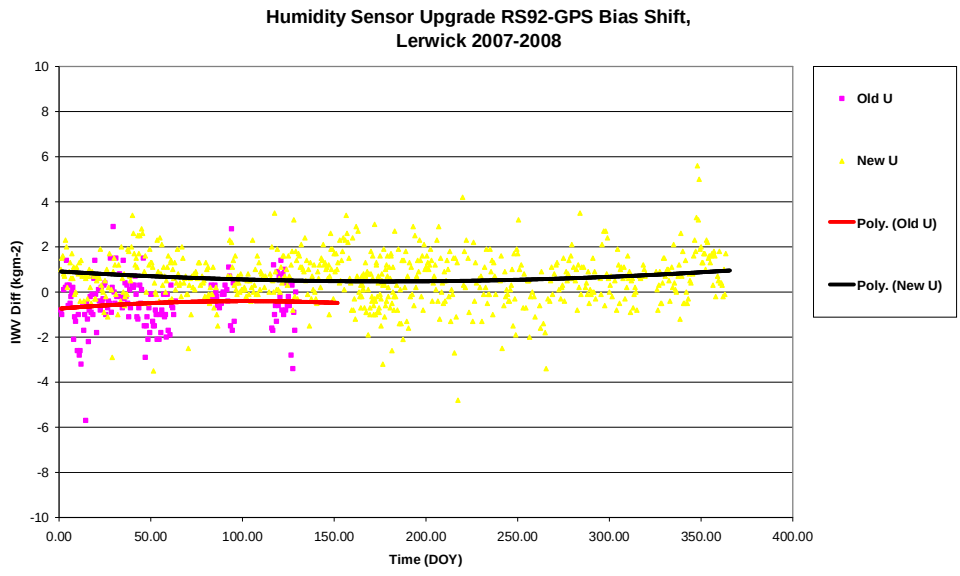

Figure 3.39 Bias shift due to new humidity sensor coating, Lerwick 2007 - 2008

It can be seen from the comparisons (with the results summarised in Table 3.8) that for all sites with the exception of Watnall/IESG, the introduction of the new humidity sensor coating caused the bias to shift in the positive direction. Following the upgrade, the biases were all shifted to the positive but the shift in bias was so large that the overall effect was actually an increase in bias against GPS. For all sites except Watnall/IESG this now resulted in RS92 now measuring higher values with respect to GPS.

Site	RS92 (old U, old T) vs. GPS Bias (kg/m^2)	RS92 (new U, old T) vs. GPS Bias (kg/m^2)	Bias Shift (kg/m^2)
Camborne	+0.2896	+0.8323	+0.5427
Herstmonceux	+0.2918	+0.3803	+0.0885
Nottingham	-0.6340	-0.9665	-0.3325
Lerwick	-0.5242	+0.6136	+1.1378
Mean Bias	-0.1442	+0.2149	+0.3591

Table 3.8 Summary of results from RS92-GPS comparisons relating to the introduction of the new RS92 humidity sensor

To assess whether the new humidity sensor coating had the desired effect with respect to bias induced by solar heating, the IWV data were compared against solar elevation calculated for all sites. Solar elevation is calculated mathematically based on time of day/year as well as latitude (see Appendix 1 for derivation routines).

A comparison was carried out using consistent data (no GPS or radiosonde changes) for as long a time series as possible on either side of the upgrade. In this example data is compared from January 2007 when absolute antenna phase centre models were first used for METO until June 2007 when the sensor upgrade took place. This data was compared against data from post June 2007 up to July 2008 when the temperature sensor was upgraded. Although there is of course no heating from solar radiation at night, solar elevations of less than zero are still taken into account as they might give us further information concerning the performance of the new sensor at night. The results are shown in Figures 3.40 to 3.43 inclusive.

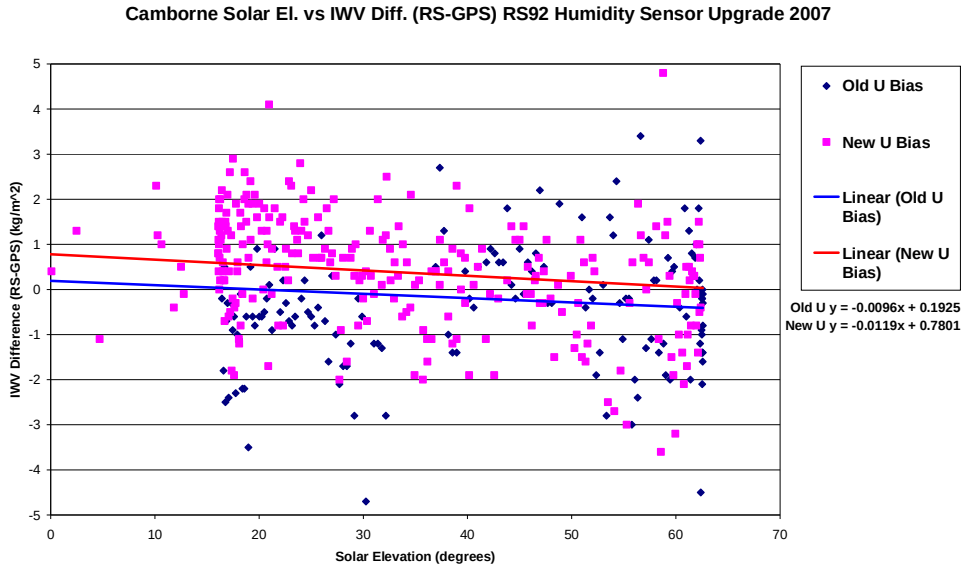

Figure 3.40 RS-GPS bias correlated against solar elevation for old and new humidity sensor types, Camborne 2007-2008

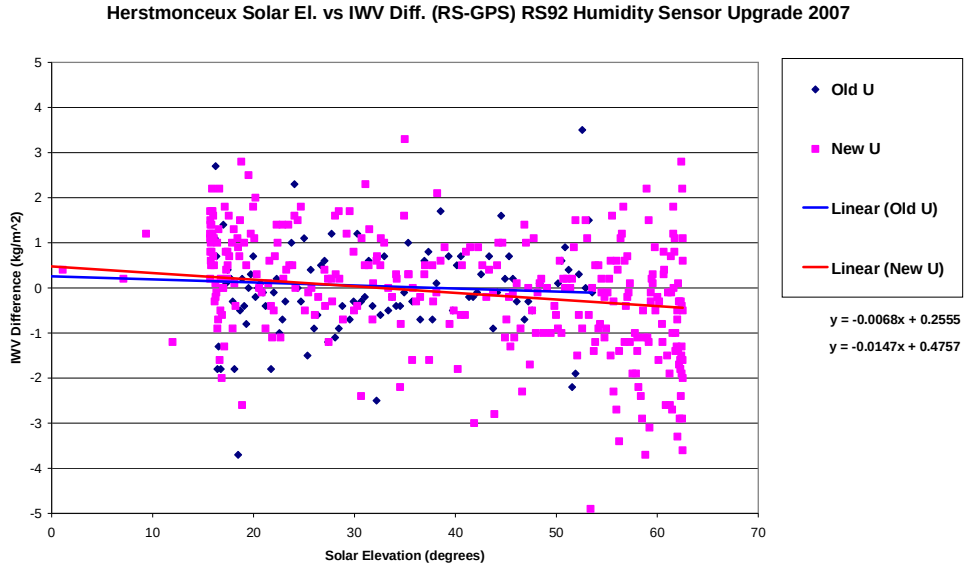

Figure 3.41 RS-GPS bias correlated against solar elevation for old and new humidity sensor types, Herstmonceux 2007-2008

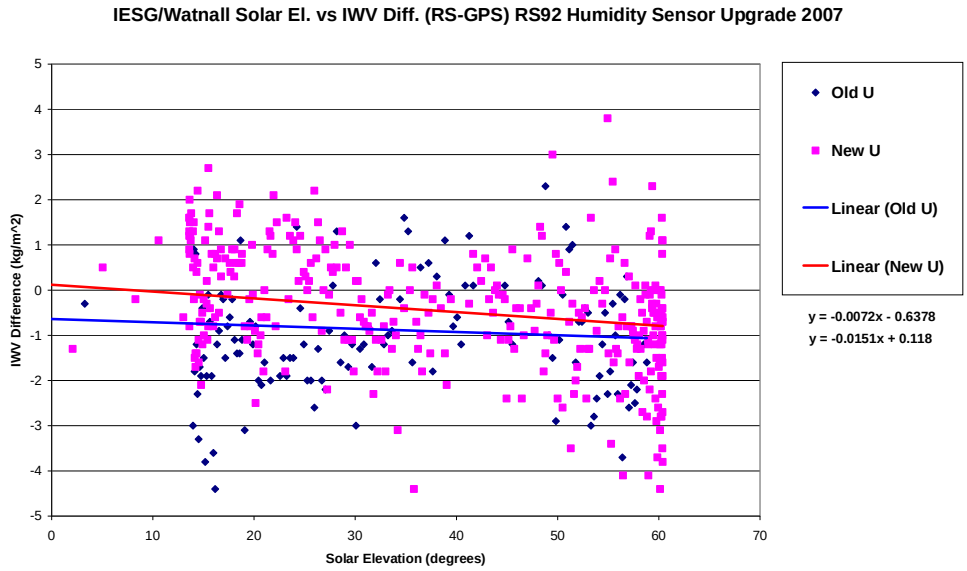

Figure 3.42 RS-GPS bias correlated against solar elevation for old and new humidity sensor types, Nottingham 2007-2008

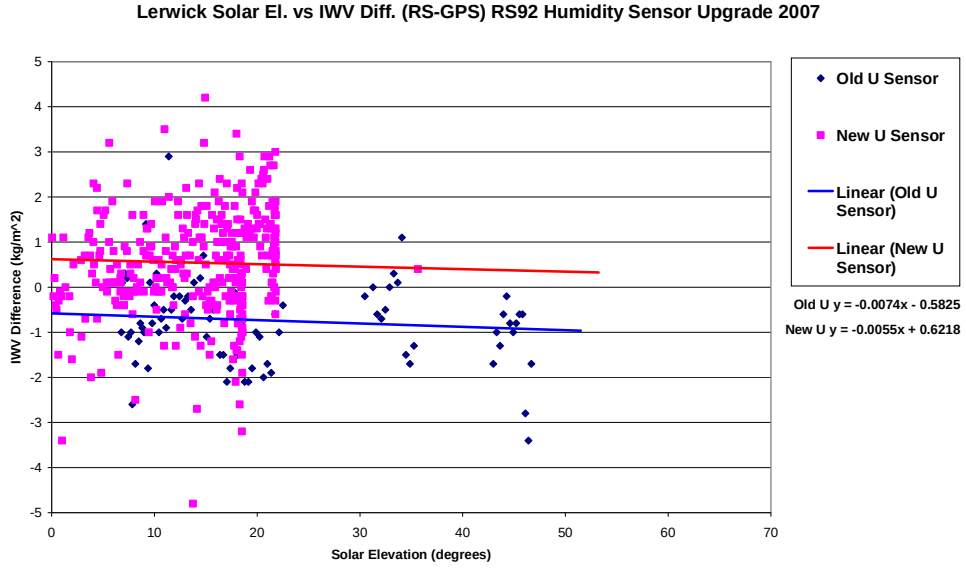

Figure 3.43 RS-GPS bias correlated against solar elevation for old and new humidity sensor types, Lerwick 2007-2008

Site	Old U Sensor Linear Trend	New U Sensor Linear Trend
Camborne	0.0096x	0.0119x
Herstmonceux	0.0068x	0.0147x
Watnall	0.0072x	0.0151x
Lerwick	0.0074x	0.0055x

Table 3.9 Summary of linear trend of RS92-GPS IWV bias prior and post radiosonde humidity sensor upgrade

The most obvious result in Figures 3.40 to 3.43 is that in all cases, with the exception of Herstmonceux, the overall bias against solar elevation has been shifted in the positive. This is consistent with the results in Table 3.8, with the introduction of the new humidity sensor causing a bias shift to the positive. It may also be observed from Figures 3.540 to 3.43 (and summarised in Table 3.9), that the slope of the linear trend lines for all sites actually increased since the upgrade. Thus, it appears that the upgrade by Vaisala in 2007 was more of a bias shift, rather than an upgrade which actually reduced the effect of solar radiation heating of the humidity sensor.

3.3.3 Introduction of a new temperature sensor structure on the RS92 Humidity Sensor

In July 2008 the Vaisala RS92 radiosonde temperature sensor structure was modified with a quartz fibre added to the structure of the temperature boom to add strength and reduce breakage. Radiosonde-GPS bias can be used to assess any bias shift due to the upgraded temperature sensor. Data is compared from a consistent data set from as far prior and post the sensor change. Data is compared in this case from the previous radiosonde instrument upgrade (humidity sensor change in June 2007) to the end of 2007 and compared against the equivalent time period after the temperature sensor upgrade in July 2008 to the end of 2008. The results are presented in Figures 3.44 to 3.47.

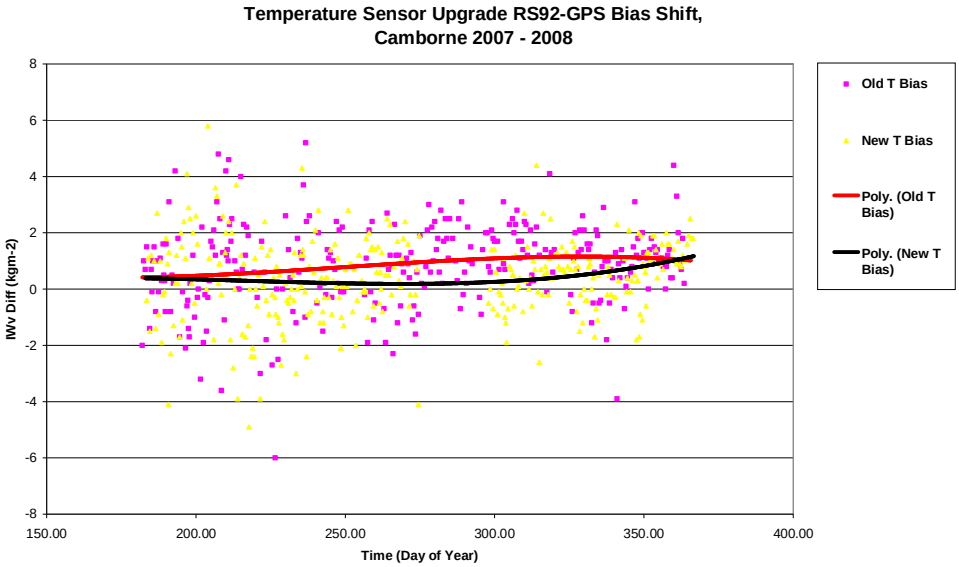

Figure 3.44 Bias shift due to new temperature sensor, Camborne July 2007- July 2008

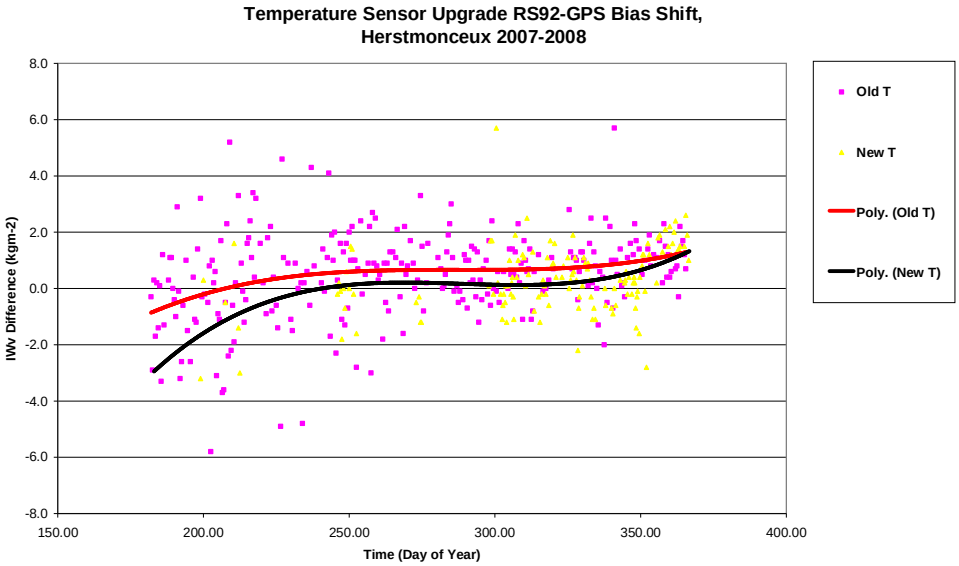

Figure 3.45 Bias shift due to new temperature sensor, Herstmonceux July 2007- July 2008

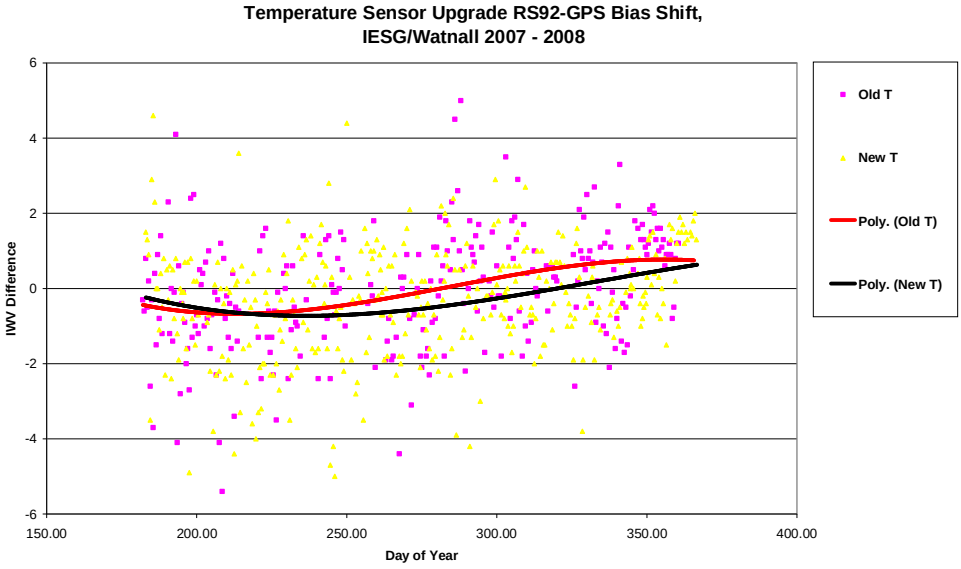

Figure 3.46 Bias shift due to new temperature sensor, Nottingham July 2007- July 2008

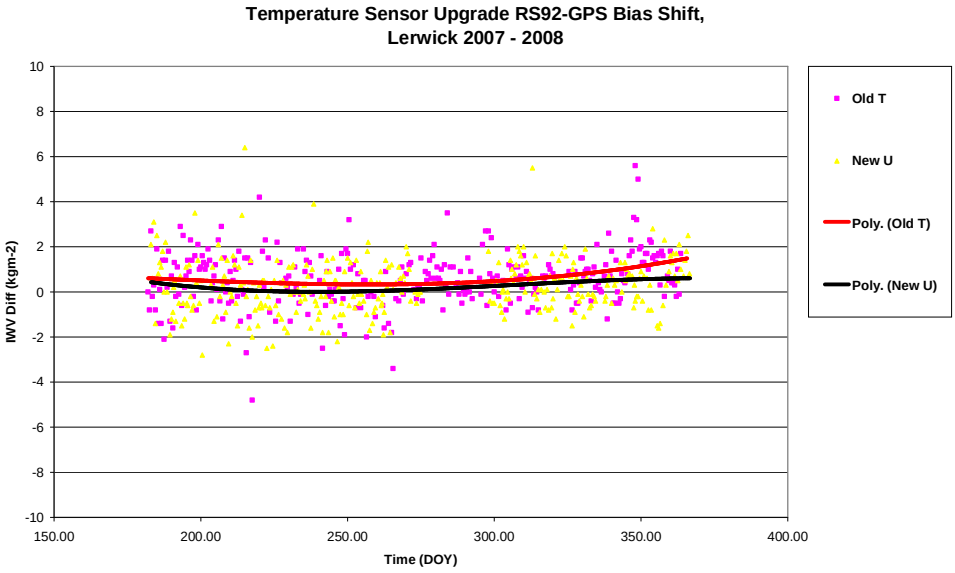

Figure 3.47 Bias shift due to new temperature sensor, Lerwick July 2007- July 2008

Site	RS92 (new U, old T) vs. GPS(AAPCV) Bias (kg/m^2)	RS92 (new U new T) vs. GPS(AAPCV) Bias (kg/m^2)	Bias Shift (kg/m^2)
Camborne	+0.8323	+0.3975	-0.4348
Herstmonceux	+0.3803	+0.3118	-0.0685
Watnall	-0.9665	-0.3107	+0.6558
Lerwick	+0.6136	+0.2416	-0.3720
Mean Bias	+0.2149	+0.1601	-0.0549

Table 3.10 Summary of RS92-GPS biases and relative bias shift relating to the introduction of the new temperature sensor

It can be seen from Figures 3.44 to 3.47, and summarised in Table 3.10, that the bias shifts in the negative direction by about 0.3 kg/m^2 for all sites, excluding Watnall/IESG, with the introduction of the new temperature boom. This is contrary to the information supplied by the manufacturer (Vaisala) who advised that the new temperature boom structure would not affect temperature. The bias shift we see here must have come from the new boom as there were no other factors which changed during the period of analysis. As it happens, this further bias shift was interesting as the bias at all sites reduced, taking the mean bias closer to zero when compared with GPS. As we can see, that final bias (i.e. the bias between GPS water vapour using the most up to date processing models against the most up to date RS92 incarnation) is, with the exception of Watnall/IESG, approximately a 0.3 kg/m^2 bias with GPS water vapour measuring too low with respect to the Vaisala RS92 radiosonde. As mentioned previously, the Watnall/IESG bias may be a result of not true collocation between the sites leading to local differences in temperature and humidity fields leading to IWV biases inconsistent with the other sites under analysis here.

3.3.4 Summary

From initial consideration it would appear that the introduction of the absolute antenna phase centre models into the processing in January 2007 brought about a bias reversal of radiosonde TWE vs. GPS water vapour, with GPS now underestimating water vapour with respect to radiosondes. However it has been demonstrated in this Chapter that when more care is taken in comparing radiosonde data, taking into account the various radiosonde upgrades which have taken place over the time period, the results are not so clear. While it is true that the introduction of the absolute antenna phase centre models did have an effect on RS-GPS bias, it was a positive effect taking the mean biases for all sites used here for comparison, with the exclusion of Herstmonceux, closer to zero. Herstmonceux is exceptional here as it already had a very low mean dry bias of only about -0.78 kg/m^2 IWV (RS80) compared to other sites whose mean bias combined was about -1.51 kg/m^2 IWV. It is unclear why this

difference existed, but since the recent radiosonde upgrades its mean bias is in line with that from the other sites, with the exception of Watnall/IESG. In the case of the Watnall/IESG bias, a difference exists most likely from the fact that the two sites are not collocated. IESG GPS receiver is at the University of Nottingham which is approximately 10km from the radiosonde site at Watnall. Whereas at all other sites used for comparison here the GPS and radiosonde site are within a few hundred metres at most (Lerwick and Camborne significantly less) and it is the spatial separation and more accurately the difference between surface parameters used in the ZTD to IWV conversion which are most likely the source of the error. A summary of all the biases at different stages of the comparison is shown as Table 3.11 and an overview of the relative shift in bias with each GPS processing or radiosonde change/upgrade is shown as Table 3.12.

Site	RS80-GPS Bias (kg/m^2)	RS92 (old T, old U) vs. GPS (RAPCV) Bias (kg/m^2)	RS92 (old T, old U) vs. GPS (AAPCV) Bias (kg/m^2)	RS92 (new U, old T) vs. GPS(AAPCV) Bias (kg/m^2)	RS92 (new U new T) vs. GPS(AAPCV) Bias (kg/m^2)
Camborne	-1.5033	-0.5075	+0.2896	+0.8323	+0.3975
Herstmonceux	-0.7838	+0.0134	+0.2918	+0.3803	+0.3118
Watnall	-1.8275	-1.2627	-0.6340	-0.9665	-0.3107
Lerwick	-1.2060	-0.5944	-0.5242	+0.6136	+0.2416
Mean Bias	-1.3302	-0.5878	-0.1442	+0.2149	+0.1601

Table 3.11 Overview of RS vs. GPS Bias evolution over the period of this thesis

Site	RS80 – RS92 Bias Shift	RAPCV-AAPCV Bias Shift	Old U-New U sensor Bias shift	Old T-New T sensor Bias shift
Camborne	+0.9958	+0.7971	+0.5427	-0.4348
Herstmonceux	+0.7972	+0.2784	+0.0885	-0.0685
Watnall	+0.5648	+0.6287	-0.3325	+0.6558
Lerwick	+0.6116	+0.0702	+1.1378	-0.3720
Mean Bias Shift	+0.7423	+0.4436	+0.3591	-0.0549

Table 3.12 Overview of relative bias shifts between GPS and radiosonde upgrade points

As can be seen from Table 3.12 the largest and most consistent bias shift for all sites was with the introduction of the RS92 radiosonde in 2005/6, followed by the introduction of the absolute antenna phase centre models in January 2007. For both cases, the mean bias was influenced in the positive direction but as the previous bias was negative, the bias shift from both upgrades caused the overall

mean bias for all sites to be reduced. Since this time, the changes in bias caused by radiosonde instrument upgrades have not been so clear. When assessing the humidity sensor upgrade in 2007 the linear trend of IWV bias vs. solar elevation indicates that the humidity sensor upgrade seems more like a bias shift upgrade as opposed to a successful upgrade of the sensor to combat solar heating. The overall bias was then moved to the positive, with the radiosonde now measuring greater IWV than GPS. With the temperature sensor upgrade in July 2008 the mean bias shift was in the negative, bringing the overall bias down to a small positive bias, closer to zero. The exception here is Watnall/IESG which is left with a negative bias, now suspected to be related to spatial separation of the sites. If the Watnall/IESG results are excluded, the final overall bias between RS92 and GPS is +0.317 kg/m^2 with GPS now underestimating IWV with respect to the latest incarnation of the Vaisala RS92 radiosonde, or the latest incarnation of the Vaisala RS92 radiosonde overestimating IWV with respect to GPS.

In summary, one cannot underestimate the importance of taking into account all instrument upgrades when comparing data and trends over long timescales. On initial comparison there seems a definitive GPS-induced bias shift with the introduction of the absolute antenna phase centre models in January 2007. However, on further analysis, radiosonde-induced bias shifts almost equal to that have occurred since with the RS92 humidity and temperature sensor upgrades. Anyway, as a result of this comparison, site specific bias corrections can now be made on the data, and Chapter 5 uses these to reconstruct long term time series over this period, as a first attempt to try and identify any climate trends in the data.

3.4 Integrated Observing of IWV

To further assess inter-instrument biases we cannot rely solely on data from radiosondes. While the radiosonde and GPS do give high quality water vapour observations as demonstrated above, without additional instruments' data we still do not know which data is correct. If we are to determine the true value of water vapour, data from other independent instruments must also be used for comparison. Furthermore, while radiosonde data is of course a very valuable source of data for comparison, radiosonde data are sparse both temporally and spatially compared to more automated instrument types such as GPS. Due to the cost of maintaining radiosonde stations, the number of operational sites in Europe has decreased markedly over the past decade with ever more emphasis on remote sensing instruments such as microwave radiometers for the purpose of retrieving water vapour estimates.

In this thesis water vapour estimates from as many diverse data sources as possible are compared to try and identify the true water vapour values. Through the Supersite concept from the E-GVAP project we have a number of sites which have GPS receivers collocated with other remote sensing instruments which are perfect for comparisons such as this. Two Supersites were chosen for the purpose of comparison in this thesis, Payerne (PAYE), Switzerland and Izana, Tenerife.

Courtesy of MeteoSwiss, we have a whole 1-year WVR time series which we can compare against the collocated GPS to address any radiometer/GPS biases. The second Supersite used here for comparison, Izana, Tenerife is truly an integrated observing station with a GPS receiver collocated with a number of other instruments and from comparison the aim is to determine the inter-instrument biases in this section.

3.4.1 Comparison against WVR at Payerne, Switzerland

The Swiss meteorological service, MeteoSwiss' aerological station at Payerne. is the primary MeteoSwiss centre for the testing and development of meteorological instruments as well as being one of MeteoSwiss' operational radiosonde stations. The site houses a RPG HATPRO microwave radiometer owned by MeteoSwiss as well as a geodetic quality GPS receiver operated by the Swiss mapping agency, SwissTopo as part of their national (AGNES) GNSS network.

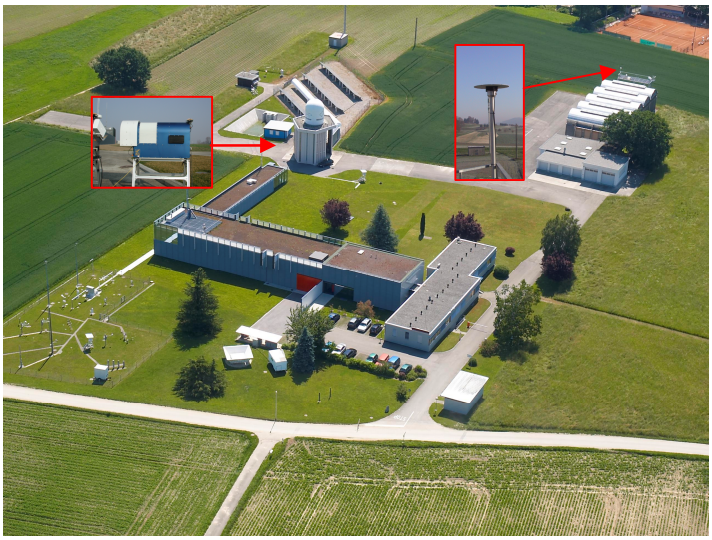

Figure 3.48 Payerne Aerological Station, Switzerland

Data was compared from the WVR and GPS for the whole of 2008. Due to the size of the data set only data at 12:00hrs were compared. Data from 12:00 should give us the best opportunity to measure inter-instrument biases as the maximum IWV would expect to be detected at around this time. Data from the radiometer from periods during rain were excluded for the reasons outlined in Chapter 2 concerning the limitations of using microwave radiometers in rain. An annual time series of data is shown as Figures 3.49 and 3.50.

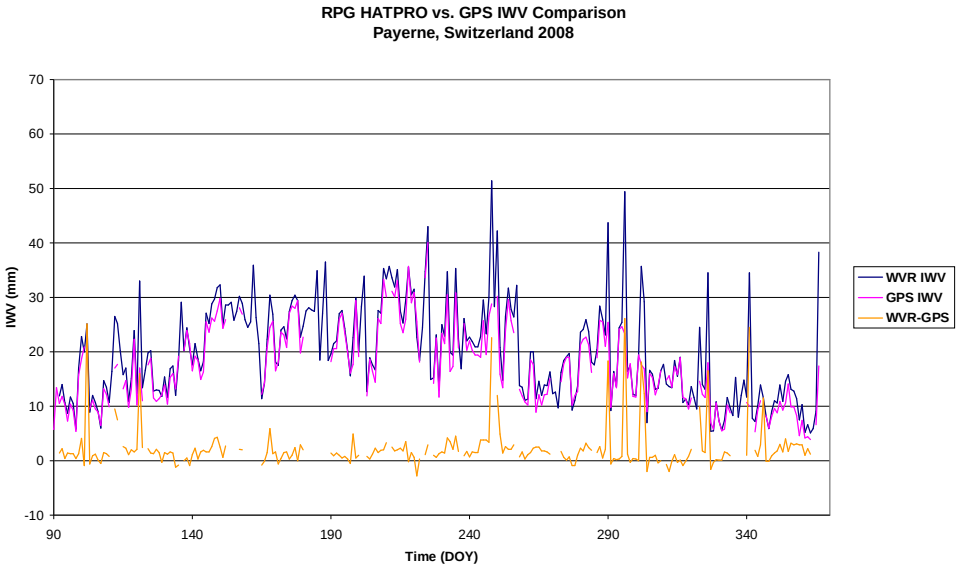

Figure 3.49 Comparison of GPS IWV against WVR IWV. Payerne, Switzerland 2008

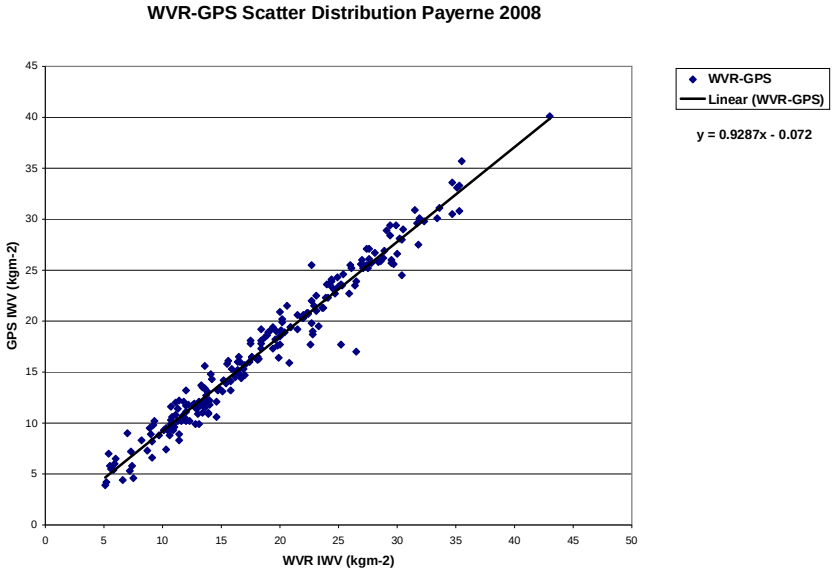

Figure 3.50 Distribution of WVR and GPS IWV coincident data, Payerne 2008

From Figures 3.49 and 3.50 we can see a distinct bias between WVR and GPS IWV, with once again, as with the radiosonde comparison in Section 3.3, the GPS measuring too low with respect to the WVR. If a mean bias is calculated for coincident data during the period of comparison we detect a GPS dry bias of approximately 1.4 kg/m^2. From the slope of a linear trend drawn on the scatter distribution in Figure 3.50, we can see that the GPS dry bias appears to be consistent throughout the range of IWV values indicating no systematic bias against WVR IWV.

3.4.2 Integrated Observing at Izana, Tenrife

The site at Izaña, Tenerife is operated by the Spanish Meteorological service (AEMET) in association with the Institute for Meteorology and Climate Research (IMK), Karlsruhe, Germany. The observatory at Izaña is one of the premier Spanish observing sites and in May 2008 a dual frequency GPS receiver was installed making it an ideal addition to the list of E-GVAP Supersites. In terms of GPS water vapour observations the site at Izaña is quite unique because of the altitude. At 3718m above MSL, Izaña offers an opportunity to study instrument biases at very low water vapour levels. Collocated with the GPS receiver, the site has a number of instruments capable of measuring IWV, including Fourier-Transform Infrared Spectrometer (FTIR), a CIMEL sun photometer, a MFRSR radiometer as well as an operational radiosonde station with twice daily radiosonde flights. The main aim of the comparison here is to study a long term time series to see how the RS92 compares against the other instruments at the site. If we can identify inter-instrument biases, we then would have a better understanding of where the radiosonde bias lies in comparison with these other remote sensing instruments and furthermore we can then apply that knowledge to the radiosonde-GPS bias. Although the GPS site was installed in May 2008, the data supply since this time has been inconsistent. As such the only comparison against GPS data here is for a ~3 week period from 14th of July to the 4th of August 2008

Figure 3.51 The integrated observing site at Izaña, Tenerife.

For the comparison at Izaña, data was taken from all instruments and coincident data was compared from mid-day data for the whole of 2007. Data had to be thinned as radiosonde data is only available from the twice daily flights (mid-day and mid-night). Radiosondes are released at approx 11:15 and 23:15 so that they reach the meteorological standard 100hPa level at the nominal time of 12:00 and 00:00 respectively. Also data had to be thinned as some of the instruments such as the MFRSR microwave radiometer observe data at one or two second intervals which results in data files too large

to be sensibly handled for a long term comparison. Data was also chosen from mid-day for comparison because the site at Izaña is at such high altitude that the typical night-time IWV observations would be so low that any biases between instruments would be too small to be sufficiently measured. Data from the Vaisala RS92 radiosonde temperature sensor is bias corrected for solar heating according to Vomel et al., (2007). Data was compared with Vaisala RS92 IWV as the control, therefore the comparisons consisted of RS92 minus CIMEL sun photometer (RS-C) and RS92 minus FTIR (RS-F) A time series of all instruments IWV and a time series of instrument bias compared to the RS92 are presented as Figures 3.52 and 3.53 respectively.

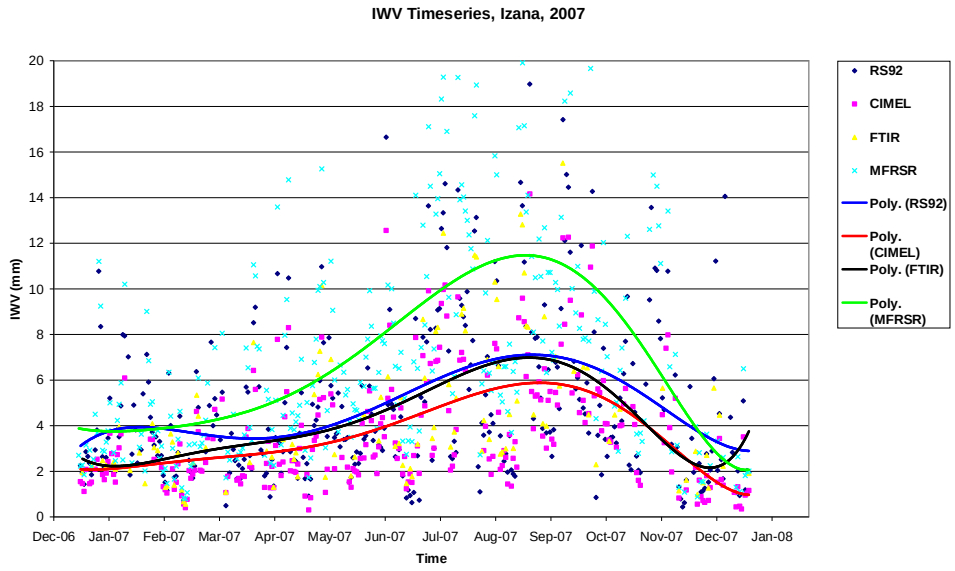

Figure 3.52 Time series of IWV, Izaña, 2007

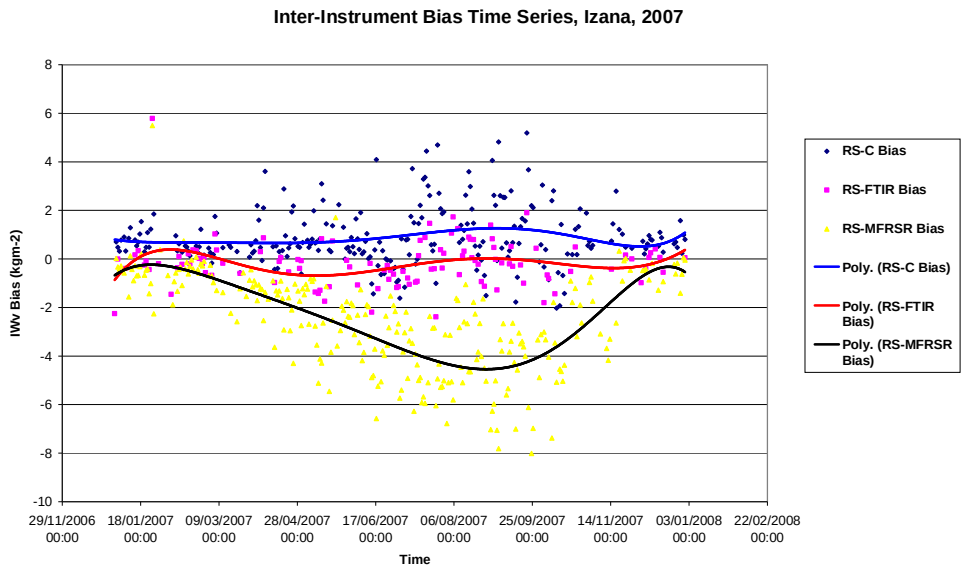

Figure 3.53 Time series of Instrument Biases, Izaña, 2007

From the time series comparisons (Figures 3.52 and 3.53) it is clear to see that when polynomial trend lines are plotted we have a fairly stable bias between the radiosonde and both the CIMEL sun photometer and FTIR, but we see a clear seasonal trend in the MFRSR microwave radiometer data. For the period of 2007 the MFRSR measures the highest IWV with a mean bias of -2.53 kg/m^2, ranging from -0.29 kg/m^2 in the winter (for the month of January) to -3.94 kg/m^2 in the summer (for the month of August). As mentioned previously, the mean bias against the other instruments is far less variable with the mean RS-FTIR bias being -0.20 kg/m^2 and the RS-CIMEL mean bias for 2007 is +0.87 kg/m^2.

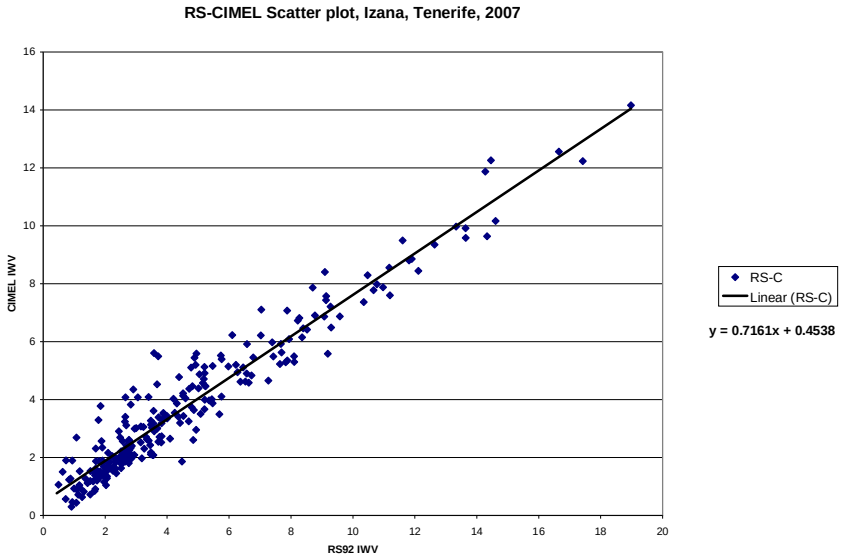

Figure 3.54 RS-CIMEL scatter distribution plot, Izaña, 2007

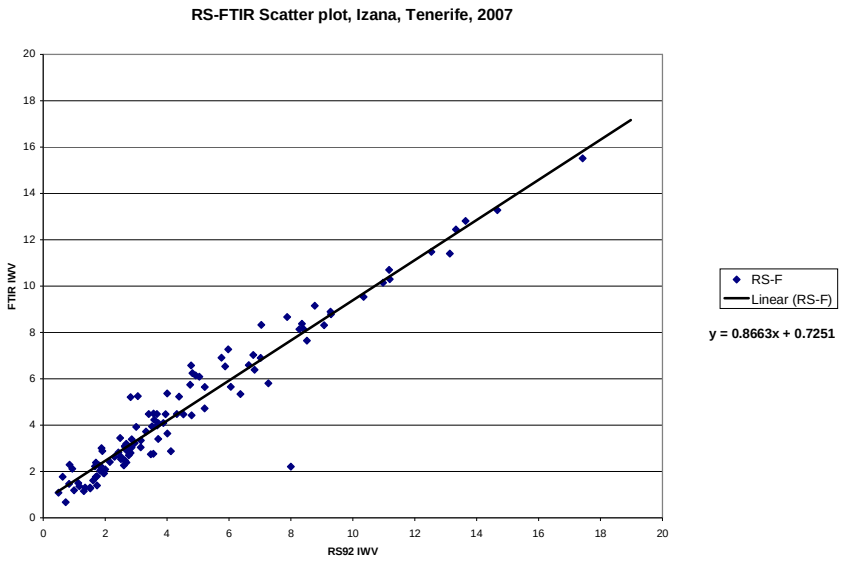

Figure 3.55 RS-FTIR scatter distribution plot, Izaña, 2007

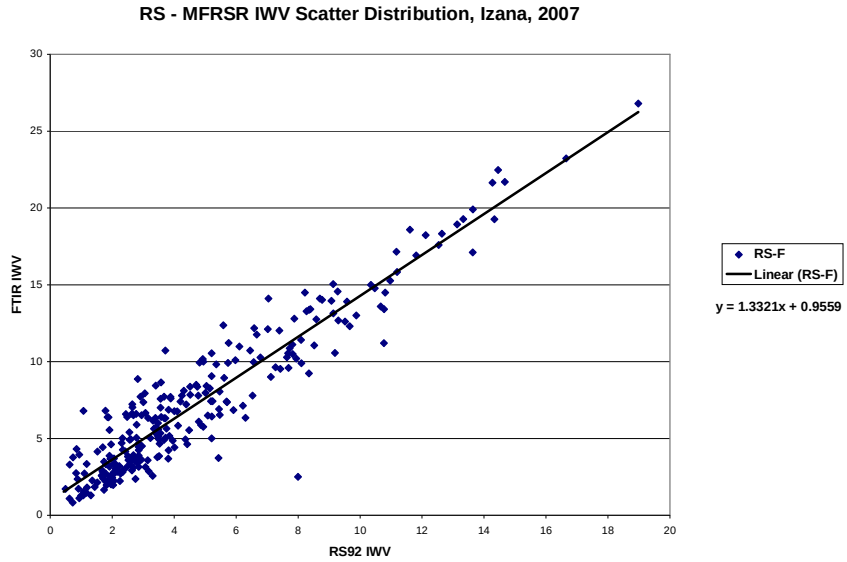

Figure 3.56 RS-MFRSR scatter distribution plot, Izaña, 2007

From the scatter distribution plots, (Figures 3.54 to 3.56) we see the agreement between instruments is fair with a moderate spread of data points about the linear trend lines. Also when the RS92 is compared against the CIMEL and FTIR in this way we see for both plots a linear trend of <1 for RS92, suggesting the RS92 is over estimating water vapour at high IWV levels. When RS92 data is compared against the MFRSR, the linear trend is >1 suggesting that there is a systematic bias in the MFRSR over estimating IWV at high IWV levels. When the RS-instrument IWV biases are plotted against IWV we see how the bias increases at higher levels of IWV. Figures 3.57, 3.58 and 3.59 illustrate the systematic nature of this trend.

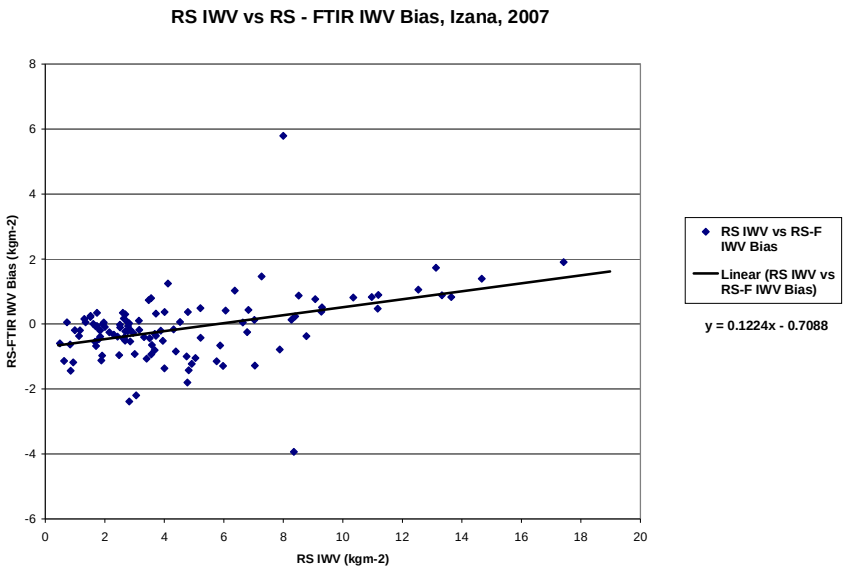

Figure 3.57 Increase in RS-FTIR bias with increasing IWV

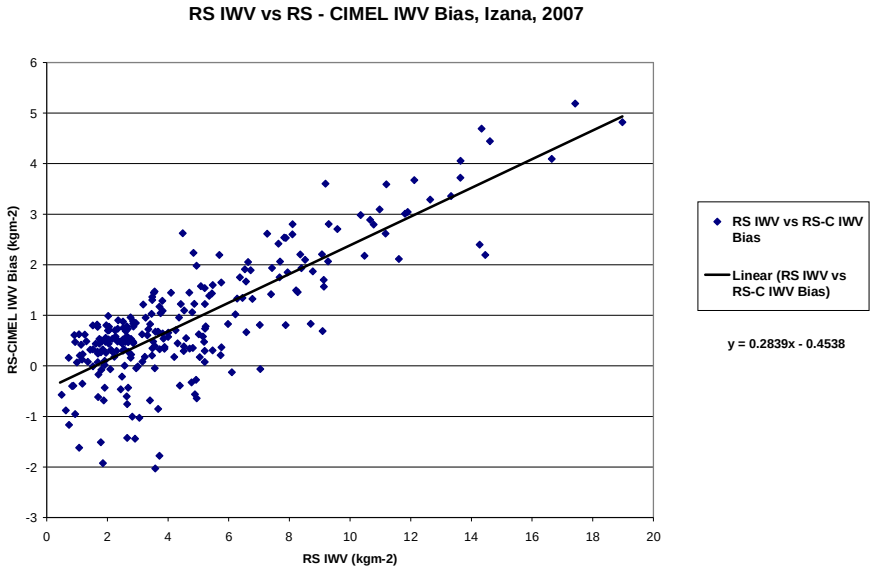

Figure 3.58 Increase in RS-CIMEL bias with increasing IWV

The smallest systematic bias with increasing IWV is between the RS92 and FTIR with a positive trend and the bias increasing by 0.1224 kg/m^2 per 1kg/m^2 increase in IWV (Figure 3.57).When comparing the RS-CIMEL bias with increasing IWV, we see a strong positive trend with bias increasing by 0.28 kg/m^2 per 1kg/m^2 increase in IWV (Figure 3.68). As the FTIR and RS92 agree relatively well with no great systematic inter-instrument bias, the larger trend against the sun photometer indicates a strong systematic bias within the sun photometer, with a larger increase in bias with increasing IWV.

When comparing the MFRSR sun photometer against the RS92 (Figure 3.59) we see a strong negative trend with bias becoming more negative by roughly 0.3kg/m^2 per 1kg/m^2 increase in IWV.

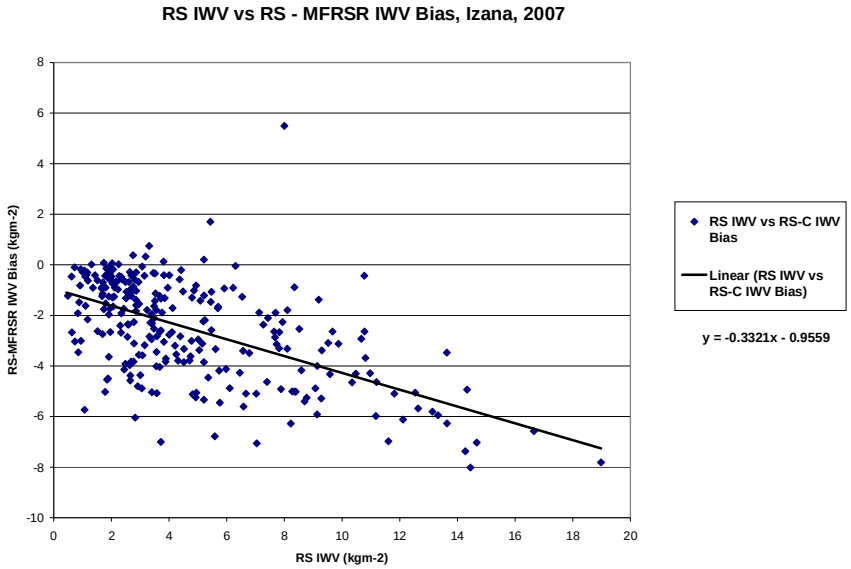

Figure 3.59 Increase in RS-MFRSR bias with increasing IWV

Comparatively, the CIMEL under estimates IWV the most, with a strong systematic nature and the bias increasing with increasing IWV. When compared to the CIMEL and RS92, the FTIR appears to underestimate a little again with a systematic nature of the bias with increasing IWV. The MFRSR over estimates the most at high IWVs with very large biases (~8kg/m^2) at higher IWVs.

To compare the instruments' data against GPS water vapour estimates we can use the data from the period in July/August 2008 when GPS data were delivered regularly as mentioned above. From a time series plotted as Figure 3.60 we can see that the GPS under estimates IWV when compared to all of the other instruments, with a mean bias of 3.28 kg/m^2 compared to radiosonde data and 5.89 kg/m^2 compared to the MFRSR.

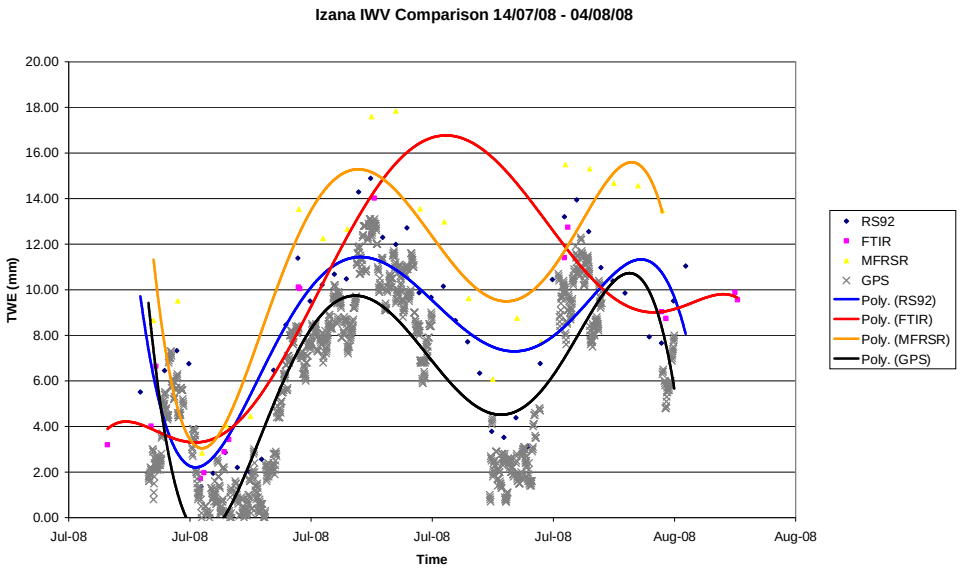

Figure 3.60 Time series of IWV, 14th July – 4th August, 2008, Izaña, Tenerife.

3.4.3 SUMMARY

From the comparisons at Izaña we can see that with respect to all other instruments GPS estimates too low water vapour values. The stability of the biases throughout the period of comparison indicates that the MFRSR greatly over estimates water vapour in the summer and as such should be excluded from comparison. When compared against RS92 data both the CIMEL sun photometer and FTIR show no seasonality to the biases and as such can be considered stable with relation to their bias range over the period. When the bias of RS-CIMEL and RS-FTIR are assessed we see a fairly consistent bias of around +0.87 kg/m^2 and -0.2 kg/m^2 respectively. From the comparison carried out in Section 3.3, we see a RS92-GPS bias of 0.3 kg/m^2 suggesting that the GPS water vapour estimations should be between those of the FTIR and CIMEL. However, from the comparison above, we can see that the GPS water vapour sensor at Izaña estimates water vapour lower than all other instruments with a dry bias of 3.28 kg/m^2 when compared to RS92 data. The cause of the exceptional dry bias at Izaña is unclear. Further investigation needs to be carried out to assess where the source of the bias may lie. If older radiosondes are being used, then as shown in Section 3.3, this could lead to additional, unexpected biases. However, at the time of this thesis, we can only assume that the radiosondes are of the latest variety and there is indeed a large dry bias in the GPS water vapour estimate.

To fully address the apparent dry bias further, comparisons from GPS at high altitudes need to be carried out. Hopefully with the recent inclusion of IZAN as an E-GVAP Supersite, further analysis of the GPS data from this site will be possible in the future to try and identify the source of the apparent bias.

3.5 The Effect of Falling Snow on GPS Signals

Although GPS water vapour measurements are not affected by falling rain (Solheim et al., 1999) the evidence of the effect on GPS signals of falling snow is less well understood. From anecdotal evidence within the Met Office there seems to be uncertainty concerning the effect of falling snow on GPS signal propagation. A number of events have been reported where GPS signal reception has been lost during heavy snowfall. The proposition is, that if the falling snow is dense enough, then it can actually block GPS signal reception. From previous studies (Jaldehag et al., 1996), it has been suggested that snow, at least in accumulations; does have a scattering affect on GPS signals. The suggestion is that if there is indeed a correlation between falling snow and satellite drop-out or signal to noise (S/N) ratio then it might be possible to use poor quality GPS signals as a new observing system for the real-time monitoring of falling snow and in particular the determination of the snow/rain melting point in cloud, which is notoriously difficult to determine by other remote sensing instruments. If the technique were possible, near real time 2D maps of snow could be produced from GPS signals much in the same way as water vapour maps already are(see Chapter 4) and would constitute a completely new observing system to meteorology.

During early February 2009 parts of the UK suffered the heaviest snowfall since February 1991. Data from this time period was analysed to determine if there is any correlation between satellite drop-out/signal quality and falling snow. During the period of analysis (31st Jan – 6th Feb), snow fell periodically with accumulations exceeding 20cm in a number of locations in the Southern UK. A plot of snow depth accumulations is shown as Figure 3.61, based on data taken from the Met Office database.

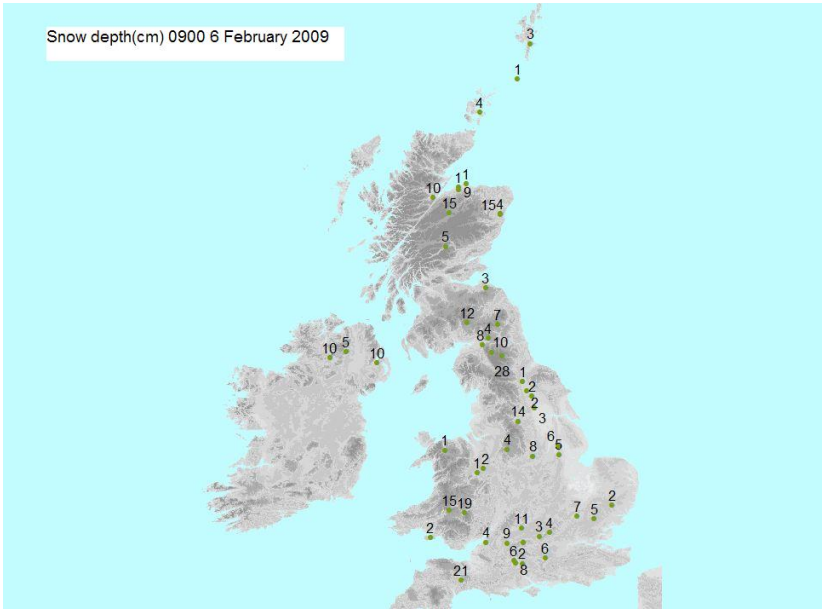

Figure 3.61 Snow accumulations on the 6th of February 2009

The first assessment was carried out to determine if there was any satellite drop-out during periods of snow. Hourly RINEX data was firstly concatenated into daily files using the UNAVCO Translation, Editing and Quality Check or TEQC software (http://facility.unavco.org/software/teqc/teqc.html) and then the number of observed satellites was determined and plotted against time of day to identify any patterns which might relate to snowfall. The results for a number of sites in the Southern UK are presented in Figure 3.62.

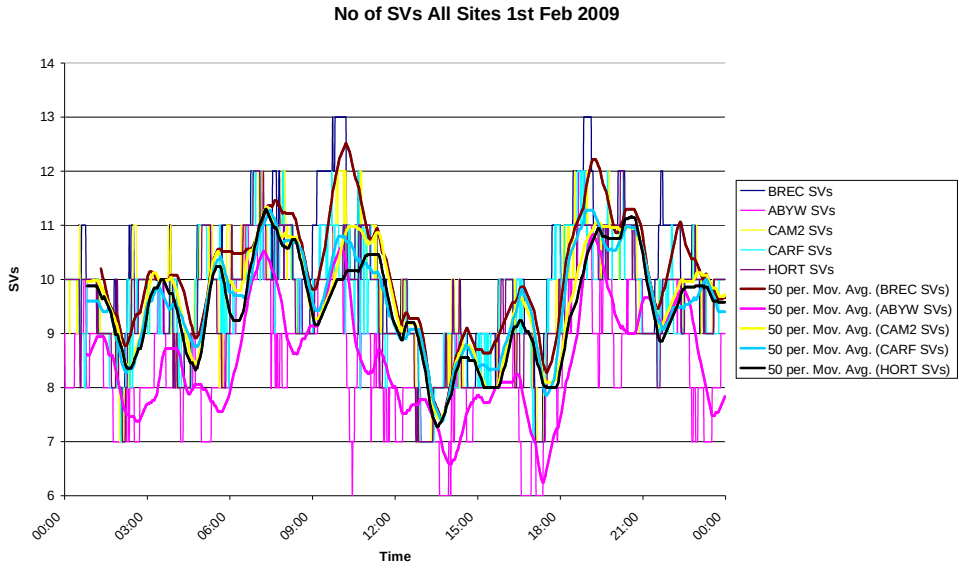

Figure 3.62 Number of satellites observed at a number of sites in the Southern UK, 1st February 2009

When the number of satellites is plotted for a number of sites we do see periodic satellite dropout over this period of intermittent snow. However, Figure 3.63 shows that when satellite drop out is plotted on subsequent days for one site (BREC in this case study) we see identical plots indicating that the drop in the number of satellites observed is just the 'natural' satellite dropout throughout the day due to the constellation geometry and the local horizon. The thick dark line is a composite of all the moving average of the data points for successive days. It is dark because all the moving average trend lines overlie each other indicating that for the period of the study there was very little difference between the number of satellites observed at the same time on successive days, which is to be expected due to the geometry of the GPS satellite constellation and seemingly unaffected by the period of snowfall.

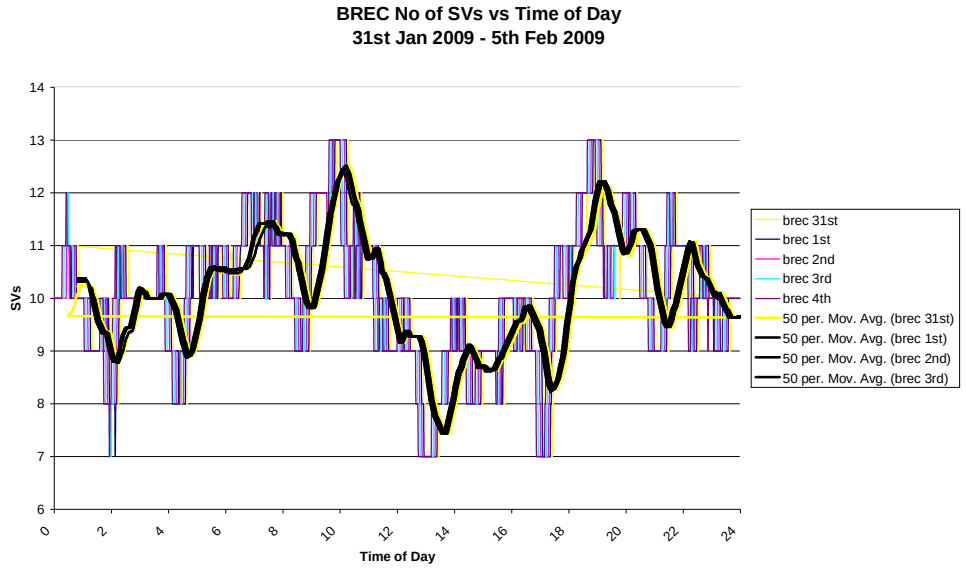

Figure 3.63 Number of satellites observed at BREC, 31st Jan – 6th February 2009

To further assess if there was any loss of satellite reception, the number of satellites visible was plotted against the specific times when there was snowfall, as reported in the Met Office database. The time series over the entire period is shown as Figure 3.64. We can see that there is the daily frequency pattern of the number of satellites observed and there is no deviation from the standard pattern during times of snow (blue diamonds). Also the deviation in the number of satellites from the mean for the time of day (in 30 seconds batches) was calculated to assess if any divergence from the mean could be correlated against snowfall, Figure 3.65.

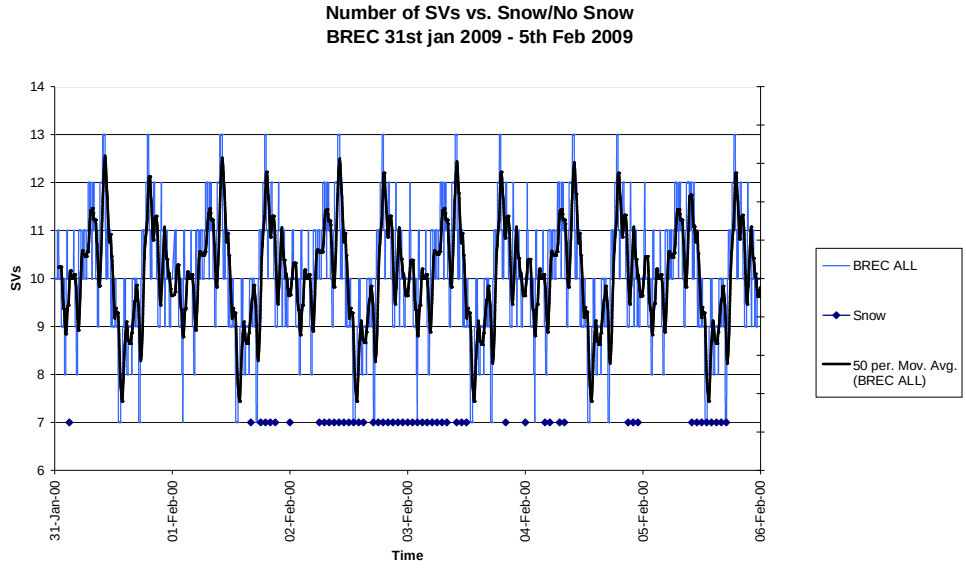

Figure 3.64 Daily satellite number and snowfall, Brecon (BREC) 31st Jan – 6th Feb 2009

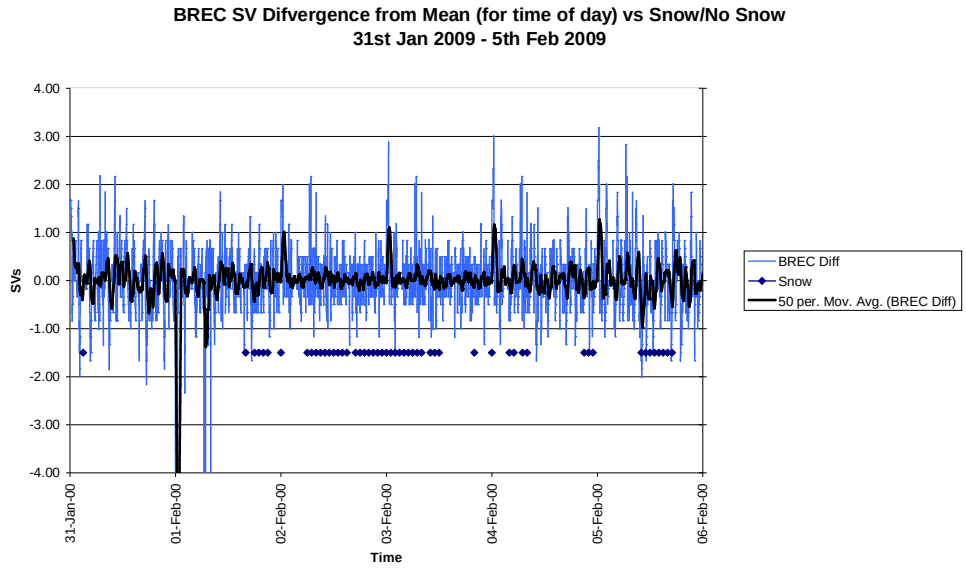

Figure 3.65 Observed satellite divergence from mean per time of day and snowfall, Brecon (BREC), 30th Jan – 6th Feb 2009

Again, from the divergence from mean number of satellites observed (Figure 3.65) there is no meaningful correlation between snowfall and number of satellites observed, even at 30 second intervals.

So, the number of satellites observed is in no way correlated with snowfall. However, this says nothing of the received signal quality. From the studies of Jaldehag et al., (1996) and Larson et al., (2008) it has been demonstrated that snow and standing water respectively have an effect on the scattering properties of GPS signals. As such a further assessment was carried out to assess the quality of the GPS signals in terms of signal to noise ratio, as calculated using the UNAVCO TEQC software.

Daily RINEX data from BREC was retrieved from the British Isles Continuous GNSS Facility (BIGF) and the data was pre processed using TEQC to retrieve signal to noise ratios. The daily files contained observation data at a 30 second epoch rate. As such, for each day 2880 signal to noise S/N ratio values for each GPS frequency were retrieved (SN1 and SN2 for L1 and L2 respectively). Such a high resolution is more than adequate to identify any periods of snowfall.

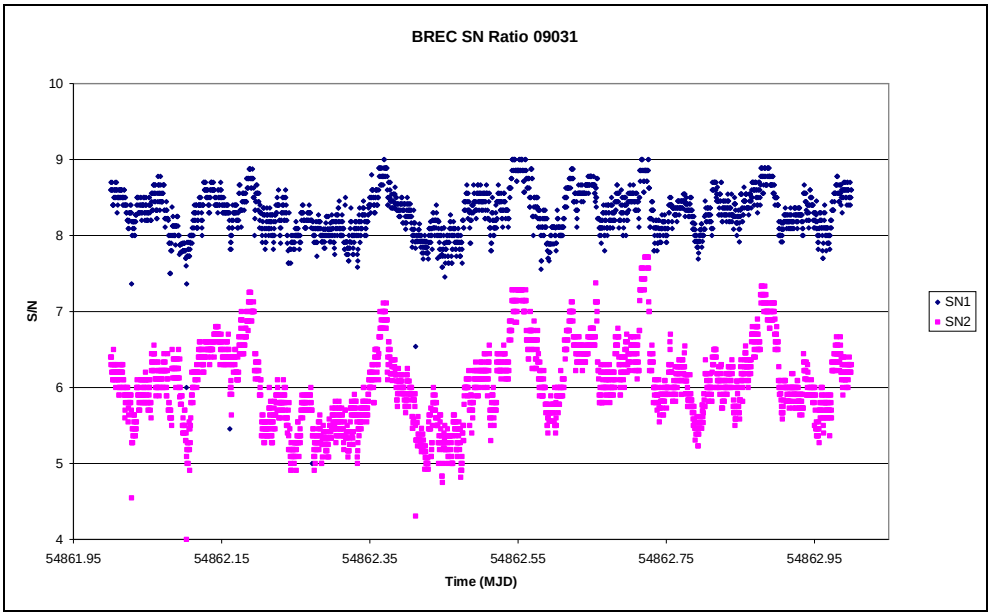

Figure 3.66 Example daily signal to noise ratio plot for Brecon (BREC) 31st Jan 2009

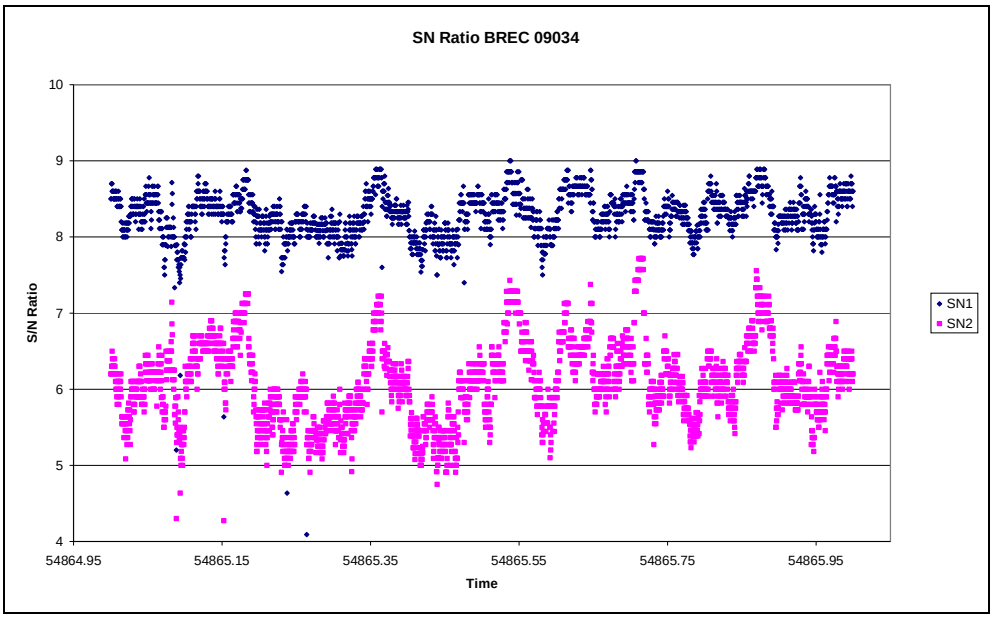

Figure 3.67 Example daily signal to noise ratio plot for Brecon (BREC) 3rd Feb 2009

When days with no snow (DOY031) are compared against days with almost continuous snow (DOY034) in Figures 3.66 and 3.67 respectively, we see no correlation between falling snow and signal quality. Signal to noise ratio appears to be largely dependant on satellite geometry and the environment local to the GPS antenna, as we see almost identical S/N ratios on successive days. To help to identify any deviance from a mean due to short term factors such as snowfall, an average S/N ratio per time of day (in 30 second batches) was calculated using all available data from DOY030 to DOY040. The individual S/N values were then compared against the mean to determine if there was

any significant divergence from the mean during snow. Examples are shown from DOY031 (no snow) and DOY034 (heavy snowfall) as Figures 3.68 and 3.69 respectively. Although there are differences between the plots, there is no correlation between day of snow and time of day when it was snowing and the divergence from the signal to noise mean.

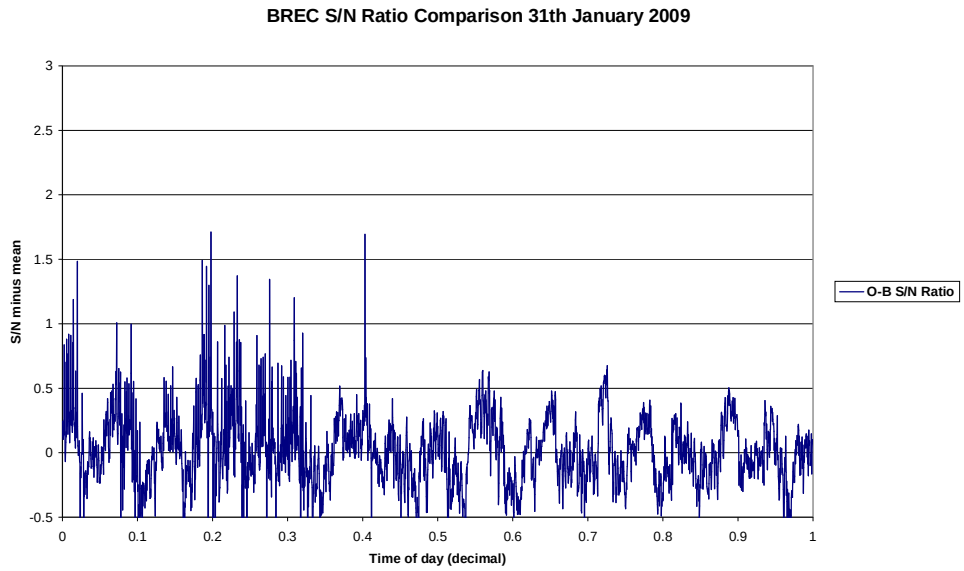

Figure 3.68 Signal to noise divergence from mean, 31st Jan 2009 (no snow)

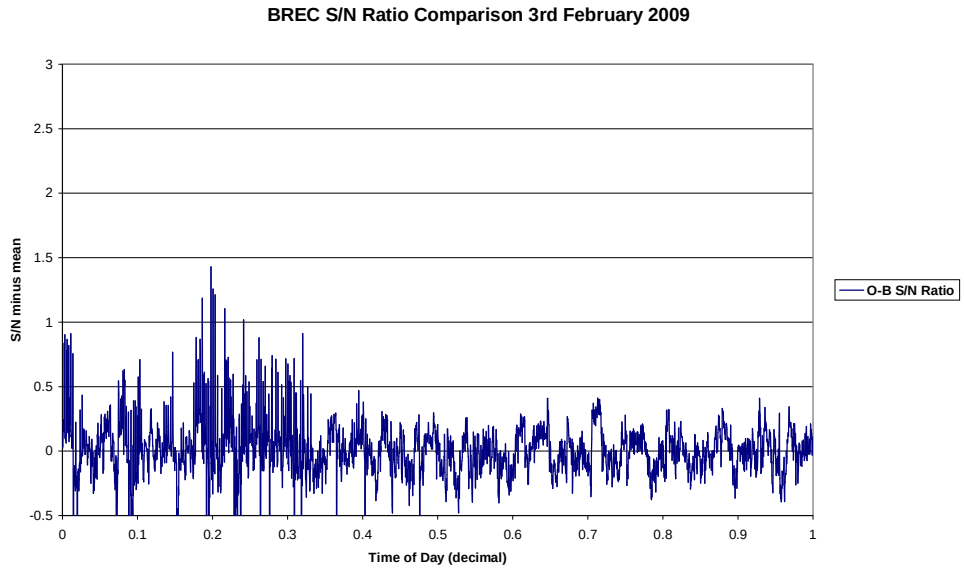

Figure 3.69 Signal to noise divergence from mean, 3rd Feb 2009 (snow)

As a further quality check, the coordinates from METO were also plotted to ensure site stability and the results are plotted as Figures 3.70, 3.71 and 3.72.

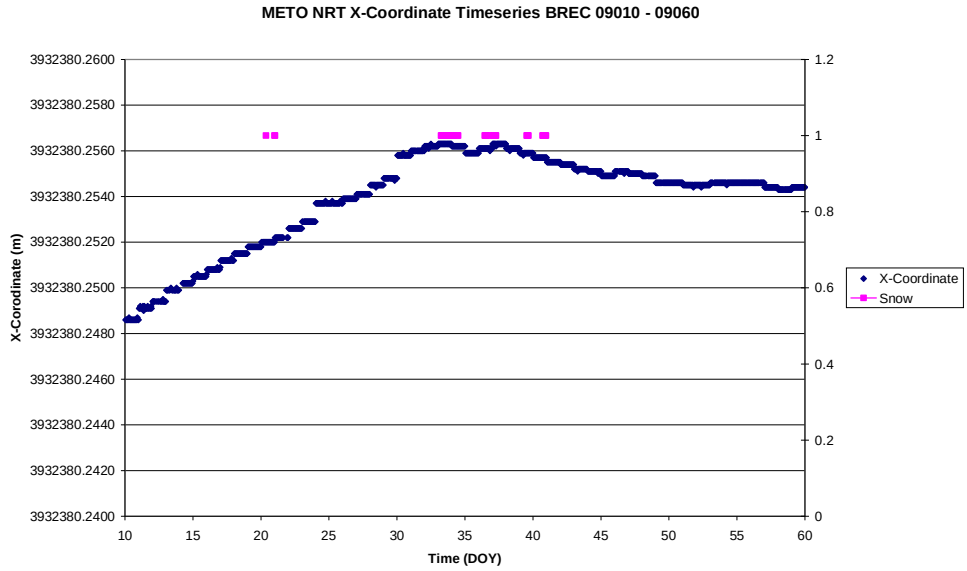

Figure 3.70 Plot of X-Coordinate, BREC DOY010 – DOY060, 2009

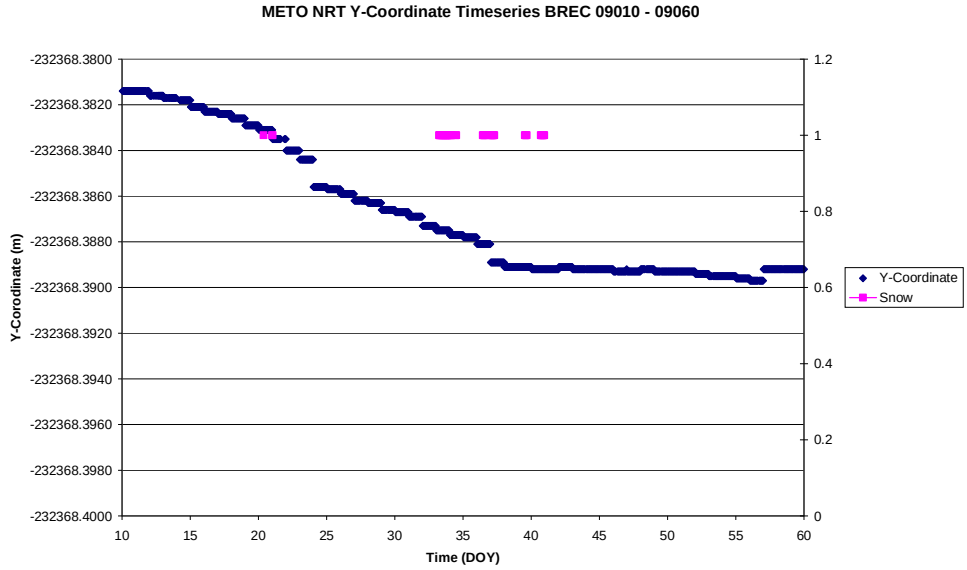

Figure 3.71 Plot of Y-Coordinate, BREC DOY010 – DOY060, 2009

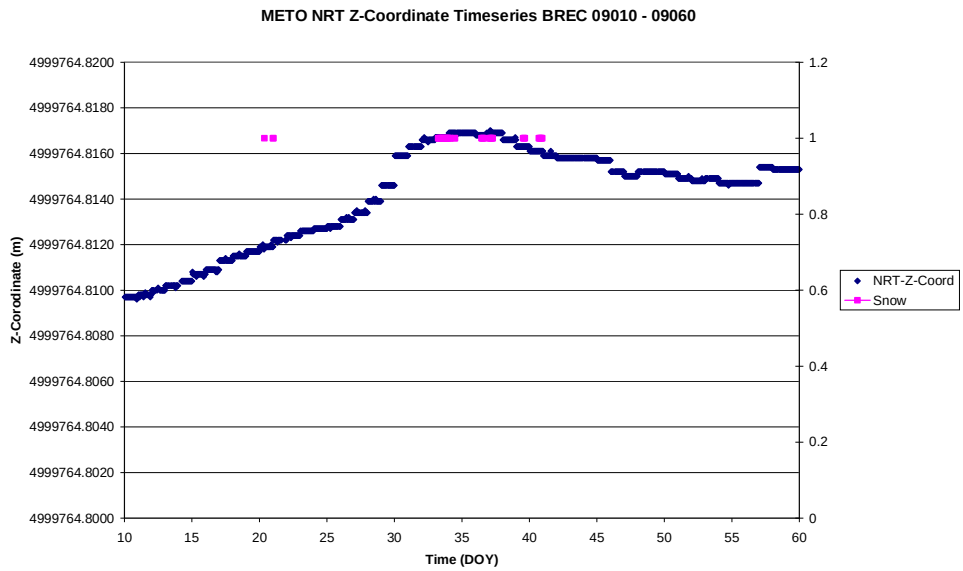

Figure 3.72 Plot of Z-Coordinate, BREC DOY010 – DOY060, 2009

When the X, Y and Z coordinate are plotted and periods of snow are plotted over the top (pink squares) there appears, at least in the X and Z direction (relating to height), a correlation between the coordinate maxima and snow. It is important to note that the scale of the plot on the vertical axis in Figures 3.70 to 3.72 is only 20mm. Also, apart from snow, the error in this case might be attributed to the fact that the GPS site at Brecon is part of the OSGB OSNet network and is not a geodetic quality installation. As such it may be that the coordinate movement is due to thermal expansion and contraction on the scale that we see here. As well as the possible correlation between falling snow and the coordinate movement it is also interesting that the coordinate movement began long before any snow fell suggesting that the coordinate shift may be more related to some longer scale phenomenon such as atmospheric pressure loading not being mitigated in the GPS processing algorithms.

To further assess the stability of the GPS antenna daily PPP coordinates taken from METO were also assessed. The PPP coordinates are processed using the highest quality IGS orbit parameters. Although coordinates generated by a PPP campaign using the highest quality orbital products do represent the highest quality, due to the fact that the coordinates are not constrained as with the NRT coordinates, the time series appears somewhat more random. The coordinates from both processing routines are plotted, on a timescale from the beginning of 2008 to assess if there is a similar short term trend in PPP coordinates as there appears to be in the NRT coordinates. The results are shown as Figures 3.73 and 3.74.

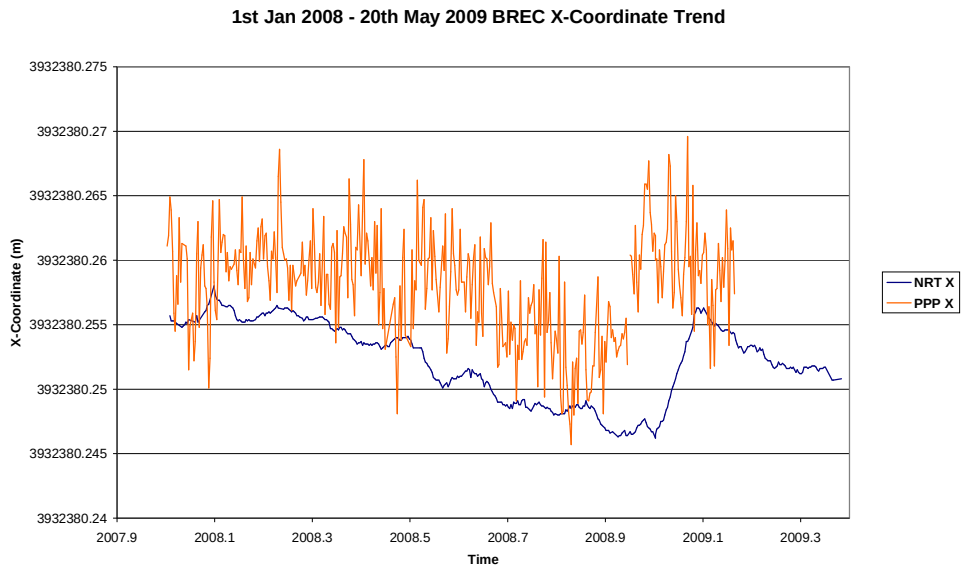

Figure 3.73 BREC seasonal X-coordinate trend, 1st Jan 2008 – 20th May 2009

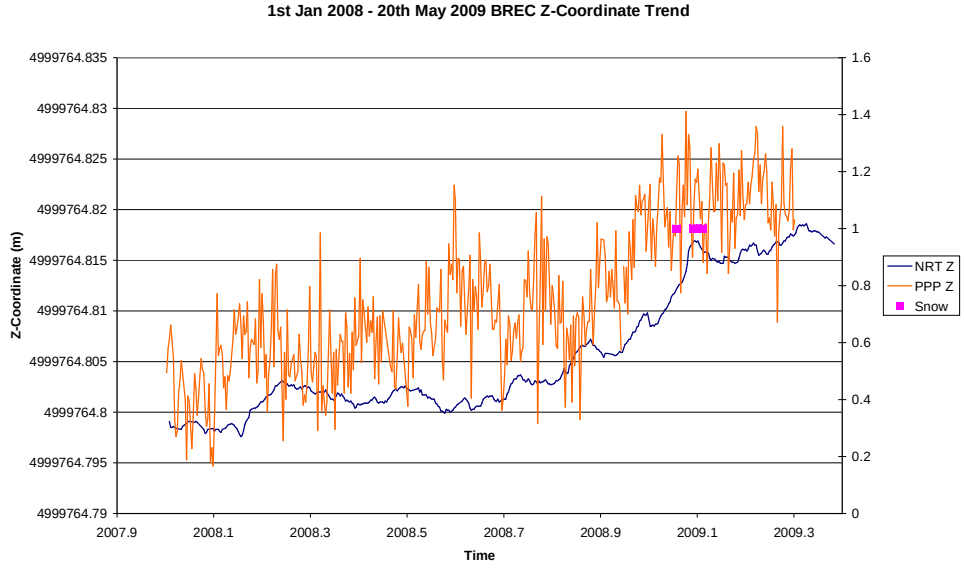

Figure 3.74 BREC seasonal Z-coordinate trend, 1st Jan 2008 – 20th May 2009

From Figures 3.73 and 3.74 we can see the greater amount of variability in the PPP Z-coordinate, but there appears to be no correlation with snowfall. Also when looking at the X and Z-coordinates on a longer time scale we see that the PPP coordinates do generally follow the same pattern as the NRT coordinates with the antenna apparently going up (an increase in X and Z) during the winter months. To assess if there is any correlation between the X and Z coordinate movements with atmospheric conditions such as temperature and pressure, these were also plotted against NRT and PPP Z-Coordinates and the results are shown as Figures 3.75 and 3.76 respectively.

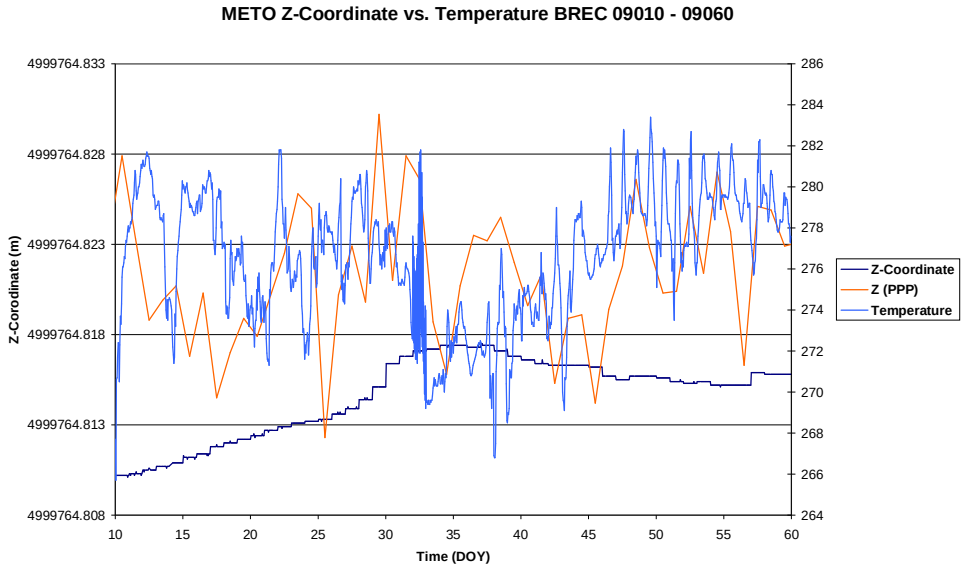

Figure 3.75 Plot of NRT Z-Coordinate (dark blue), PPP-Z-Coordinate (orange) and surface temperature (in Kelvin), BREC, 10th Jan 2009 – 1st March 2009

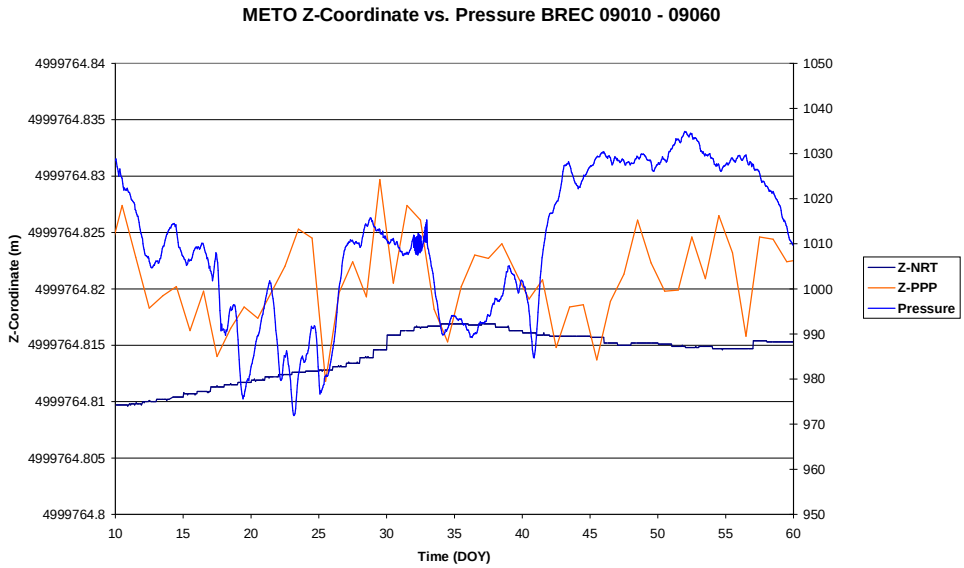

Figure 3.76 Plot of NRT Z-Coordinate (dark blue), PPP-Z-Coordinate (orange) and surface pressure in hPa (blue), 10th Jan 2009 – 1st March 2009

From Figures 3.75 and 3.76 there does indeed appear to be a correlation between surface temperature and pressure and the PPP Z-coordinate drift with the more pronounced correlation with pressure. However, it is important to note that the correlation with pressure is seemingly not related to atmospheric pressure loading, where one would expect to see an anti-correlation.

Figure 3.77 OSNet GPS installation BREC, Brecon, Powys, Wales

As states previously, the variation in the BREC coordinate time series may be linked with the fact that the GPS installation is not of geodetic quality as it is installed on the building of Brecon Leisure Centre. The variation in Z-coordinate may be linked to thermal expansion and contraction of the building it is mounted on and may be attributed to thermal expansion during the winter due to the building's heating being used more frequently.

To further assess whether the coordinate shift is site dependent or more widespread the same comparison was completed for 2 more sites in the UK. The first additional site is another Ordnance Survey OSNet site at Shobdon Airfield, (SHOB) and the second additional site for comparison is the Met Office geodetic quality GPS installation at Camborne (CAMB). The Met Office site at Camborne is a much higher quality GPS installation with the antenna mounted on a carbon fibre pole anchored to >1m3 of concrete laid directly on to bedrock or at which all sedimentary settlement under the GPS monument has already taken place. Z-coordinate data is again compared against pressure retrieved from the Met Office database and the results are shown as Figures 3.80 and 3.81.

Figure 3.78 OSNet GPS installation at Shobdon Airfield (SHOB)

Figure 3.79 Met Office GPS installation at Camborne (CAMB)

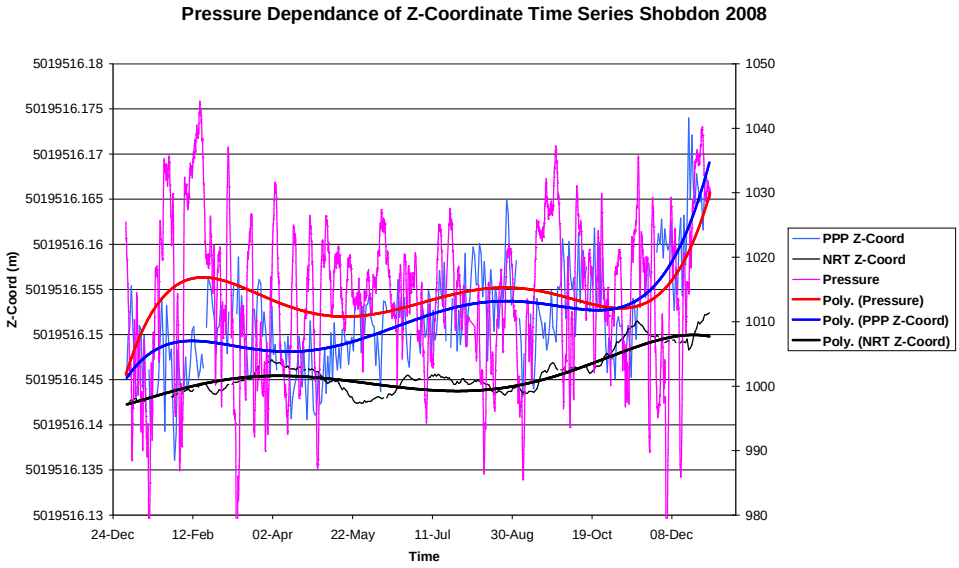

Figure 3.80 Plot of Z-Coordinate against MSL pressure, SHOB 2008

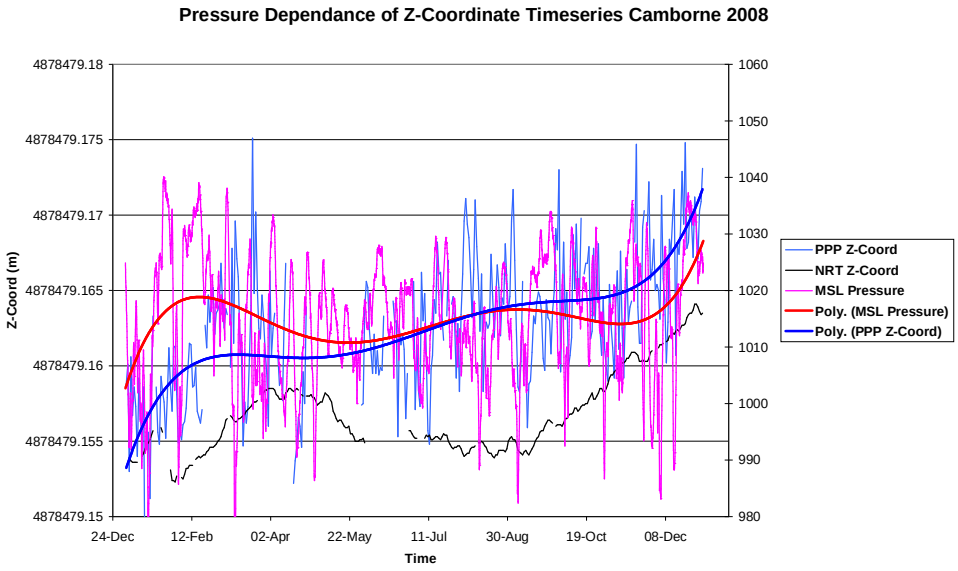

Figure 3.81 Plot of Z-Coordinate against MSL pressure, CAMB 2008

As we can see from Figures 3.80 and 3.81 there again appears to be a relationship between surface pressure and Z-coordinate, albeit not in the way that would be expected for atmospheric pressure loading. Instead it is possible that this is a function of using Bernese to solve for ZTD with no a-priori atmospheric pressure input, leading to biases that are directly related to shifts in the coordinates for the sites. The introduced error is relatively small and would pose no particular problem to GPS meteorology, especially as the a-priori coordinates for METO are based on a 30-day average of PPP coordinates from 20 to 50 days previous. However, determining whether a-priori atmospheric pressure changes the ZTD output from Bernese software and whether this is significant for GPS meteorology may be something worthy of further investigation.

3.6 The Sensitivity of ZTD to IWV Conversion to Meteorological Data

At the current time, the primary focus of GPS processing schemes for meteorological applications has been for ZTD assimilation into NWP models. As such, when assessing the quality of GPS water vapour data, much time and consideration is given to assessing the quality of the output of the GPS processing, i.e. ZTD. Often, little attention is then given to the data which is used by which ZTD estimates are converted into IWV. However, if GPS water vapour is going to be used in operational meteorology it is important to assess the method by which IWV is estimated.

The resolution and accuracy of meteorological data used for the conversion, as described in Chapter 2, can have profound effects on IWV estimates. The resolution of meteorological data, both temporally and spatially, is assessed in this Chapter to make recommendations for future ZTD to IWV conversion methods. At the current time there are no standards on the resolution of meteorological data used for ZTD to IWV conversion. The actual method is well defined, (Chapter 2) but the source and resolution of the meteorological data is not fixed.

Within the E-GVAP Project only a limited number of European ACs actually convert ZTD into IWV. The majority just produce ZTD as the ACs involved are generally geodetic institutes and it is then left to the national meteorological service (NMS) to retrieve surface meteorological information and covert to IWV. The technique by which ACs perform the conversion is not specified within GPS meteorology and is one of the topics of analysis in this Chapter. Only METO and GFZ routinely perform an IWV conversion and include the information in the COST716 format files submitted to the E-GVAP project, as such ZTD and IWV estimates from GFZ and METO are used for comparison.

In this chapter the question is whether hourly meteorological observations are adequate for the ZTD to IWV conversion or whether higher temporal resolution data is required so that IWV estimates more accurately represent real atmospheric fluctuations? Also an assessment is made on whether the technique of using meteorological data from the nearest surface station is adequate or whether a spatial interpolation provides more accurately estimated surface observations at the GPS antenna site.

3.6.1 Spatial Resolution of Meteorological Data

As described in Chapter 2, surface pressure is the critical meteorological parameter in ZTD to IWV conversion. Thankfully surface pressure does not normally vary greatly over the distances between a GPS site and the nearest SYNOP site. As such, the assumption of no horizontal pressure gradient is made for the METO ZTD to IWV conversion and which uses data taken from the nearest available SYNOP site with temperature and pressure adjusted to the height of the GPS antenna. If this is not available, the system then takes data from the next nearest site and so on. The ZTD to IWV conversion at the German analysis centre, GFZ, is a little more sophisticated in that it triangulates the SYNOP data to the GPS receiver location and estimates the surface parameters for the GPS site. Furthermore NWP model data can be used in this way providing NWP surface data for the exact location of the GPS receiver. A comparison was carried out looking at ZTD and IWV from two European GPS sites, BRUS and LDB2 for May 2009. The results are shown in Figures 3.82 and 3.83.

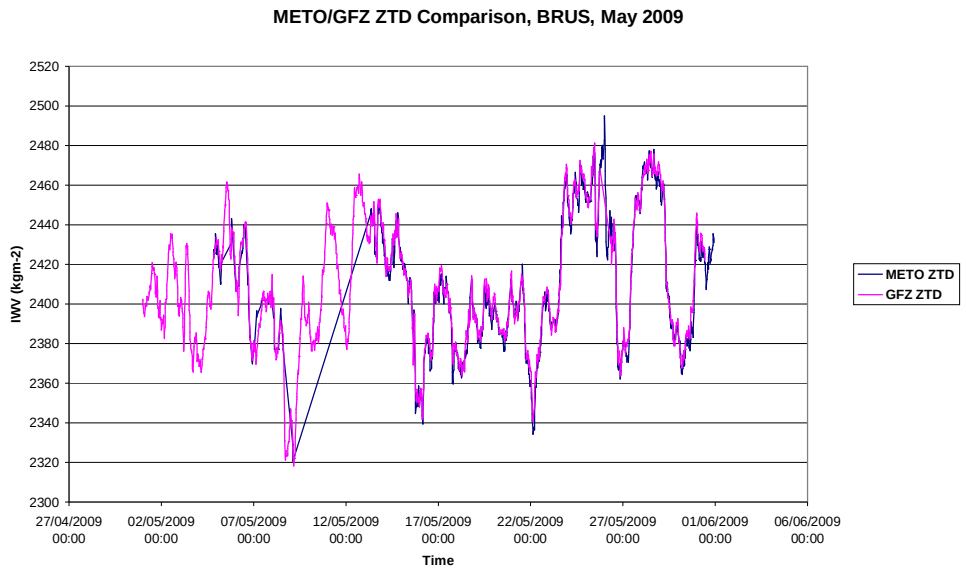

Figure 3.82 Time series of BRUS ZTD from GFZ and METO, May 2009

When the ZTD time series is compared (Figure 3.82) we see a very good agreement indeed. However, the results of IWV time series comparison are quite startling with a large bias between the two solutions. Both sets of data were contributed to the E-GVAP server for use in operational meteorology. If the forecasting community are to have confidence in IWV data derived from GPS networks, such large biases cannot exist. Consideration of both Figures 3.82 and 3.83 clearly indicates that the source of the differences is related to the ZTD to IWV conversion.

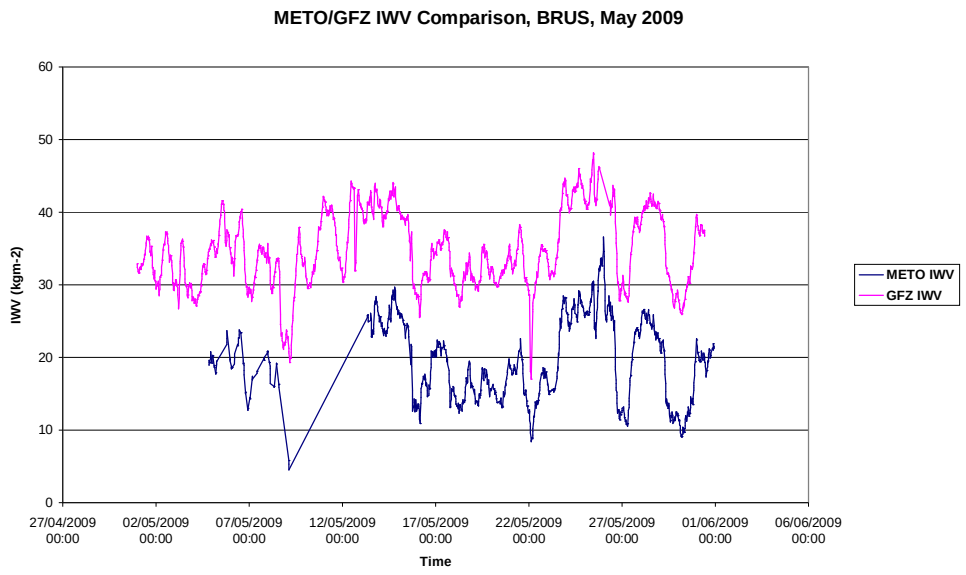

Figure 3.83 Time series of BRUS IWV from GFZ and METO, May 2009

As well as ZTD and IWV estimates, the standard ASCII format COST716 files also contain data used for ZTD to IWV conversion, if this conversion was indeed made by the contributing AC. When the surface parameters (temperature and MSL pressure) which were used for the conversion are plotted (Figures 3.84 and 3.85) we see the pressure from the GFZ solution is unrealistically low. The GFZ which uses triangulated data obviously has a problem in this case and this highlights the dangers of using a mathematically derived interpolation of surface data rather than actual surface observations for IWV calculations. Of course, individual surface sensors do also go wrong, as was the case with a METO processed site in the North of England earlier in 2009. However, in this case, the problem site was immediately identified as the IWV was so high it was unfeasible, rather than being high, but within realistic limits as in this case.

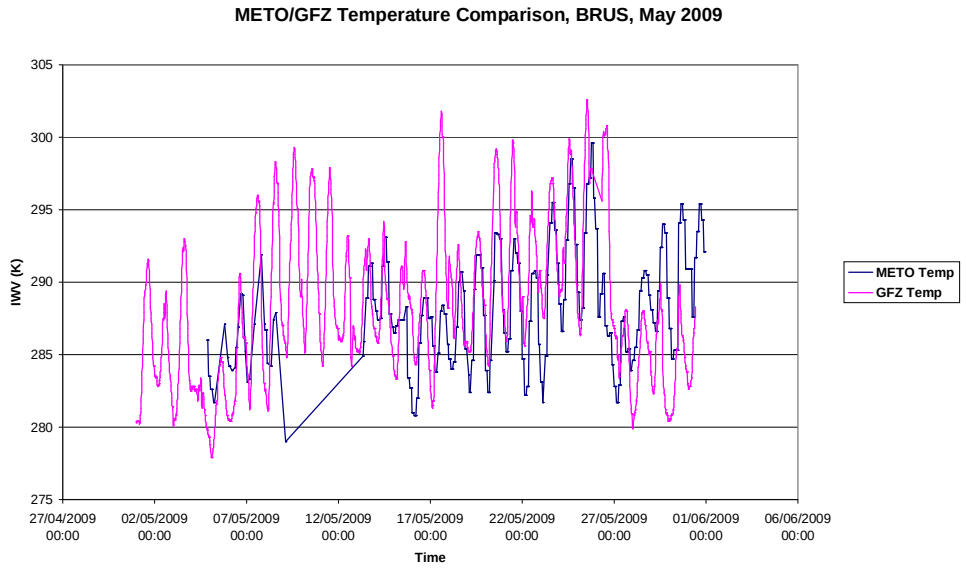

Figure 3.84 Time series of BRUS surface temperature from GFZ and METO, May 2009

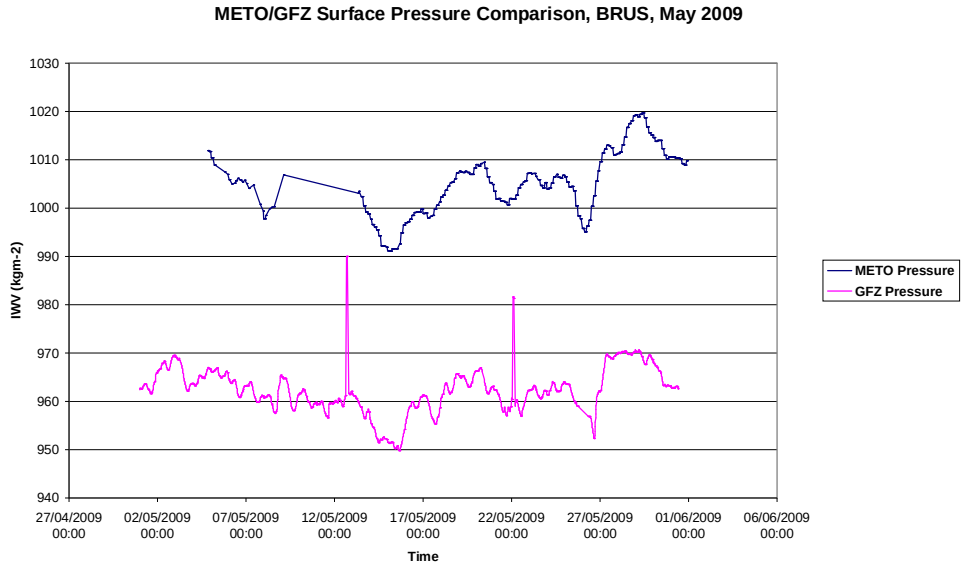

Figure 3.85 Time series of BRUS surface pressure from GFZ and METO, May 2009

By contrast, when another site is compared, this time Lindenberg (LDB2) in Germany, the meteorological data interpolation scheme appears to work fine and the two solutions agree very well, Figure 3.86)

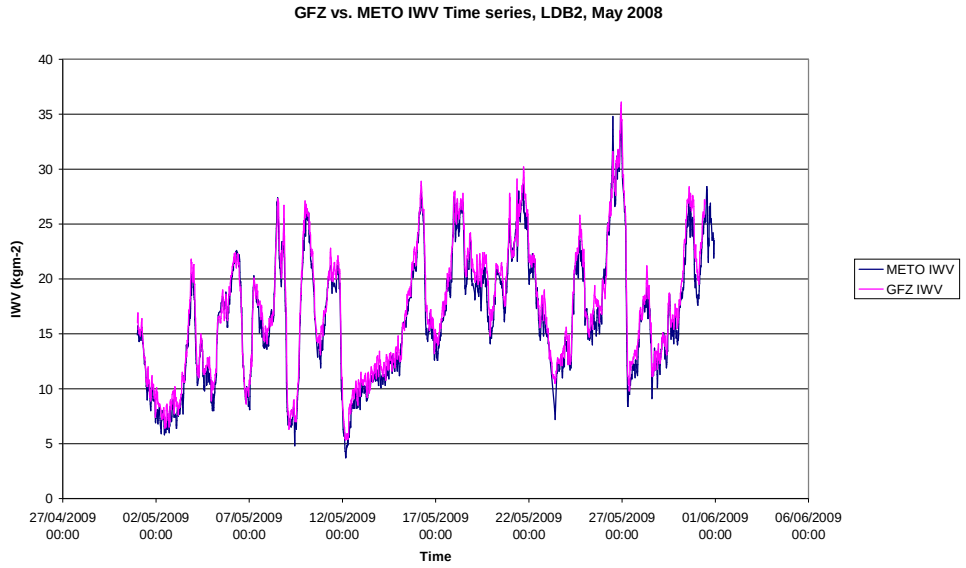

Figure 3.86 Time series of LDB2 IWV from GFZ and METO, May 2008

For the METO solution of both sites, the meteorological surface data was retrieved from surface sites only 730m away (BRUS) and 835m away (LDB2). The danger by contrast of the METO solution is that if the nearest few surface sites' data isn't available, the solution might be using surface data from too far away to be representative of the atmosphere local to the GPS receiver.

To ensure such biases are removed from future data, a consistent ZTD to IWV conversion approach needs to be adopted on a large scale e.g. European. Only if an agreement can be made across a number of ACs and national meteorological services relating to ZTD to IWV conversion will a consistent approach be adopted which will be essential for operational use of IWV data across Europe.

Further examples are given in Annex 2 of this thesis.

3.6.2 Temporal Resolution of Meteorological Data

As part of the study of the integration of GPS IWV with data from other instruments (Chapter 4) a series of programs were developed by the author to plot GPS water vapour onto 2D maps to try and assist the forecasting community to better understand water vapour fields and the potential usefulness of near real-time GPS water vapour estimates from dense GPS networks.

From analysis of the water vapour maps it became evident that there existed jumps in water vapour estimates from one hour to the next. More precisely, the jumps occur between the HH:45 minute water

vapour map and the first map from the following hour i.e. HH+1:00. If the maps are to be used by the operational forecasting community, an assessment of the jumps in water vapour fields must be carried out to determine if this is due to shifts in ZTD estimates from successive hours or whether they are a result of the relatively poor resolution of the meteorological surface data used in the ZTD to IWV conversion.

For the METO GPS water vapour solution, meteorological parameters are extracted from the Met Office database on an hourly basis. This introduces limitations on the ZTD to IWV conversion as the met data is only representative for the HH:00 GPS estimate, i.e. for the HH:15 GPSWV estimate, the met data is now 15minutes old etc. The problem continually gets worse the further you go from the time of met observation and is only rectified when the HH:00 surface observations are coincident with the HH:00 ZTD estimates in the next hour. Although 1 hour is a relatively short amount of time and meteorological parameters may not normally change greatly on these timescales, it is precisely the extreme cases where atmospheric parameters are changing rapidly when GPS water vapour could be most useful to forecasters, such as in convective thunderstorm events etc.

If we again use the case study of BRUS for May 2009, and look more closely at the time series we can see jumps in the data between data from HH:45 estimates to the HH+1:00 estimates in the next hour, (Figure 3.87); these jumps occur between turquoise (HH:45) and blue (HH+1:00) dots.

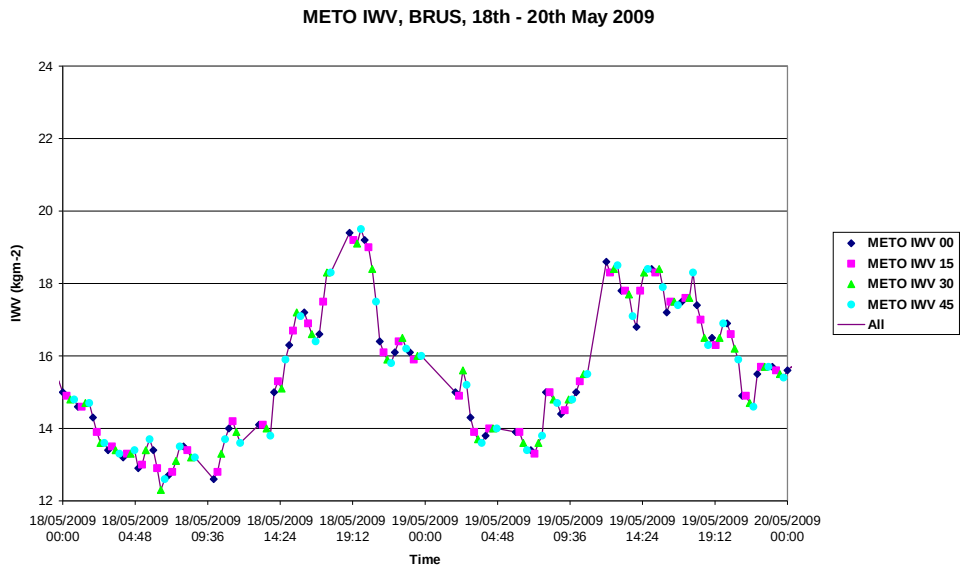

Figure 3.87 Time series of IWV, BRUS, May, 2009, showing jumps between successive IWV estimates from HH:45 to HH+1:00

However, when we plot ZTD on the same plot we see that the jumps in IWV are a direct result of associated jumps in ZTD (Figure 3.88).

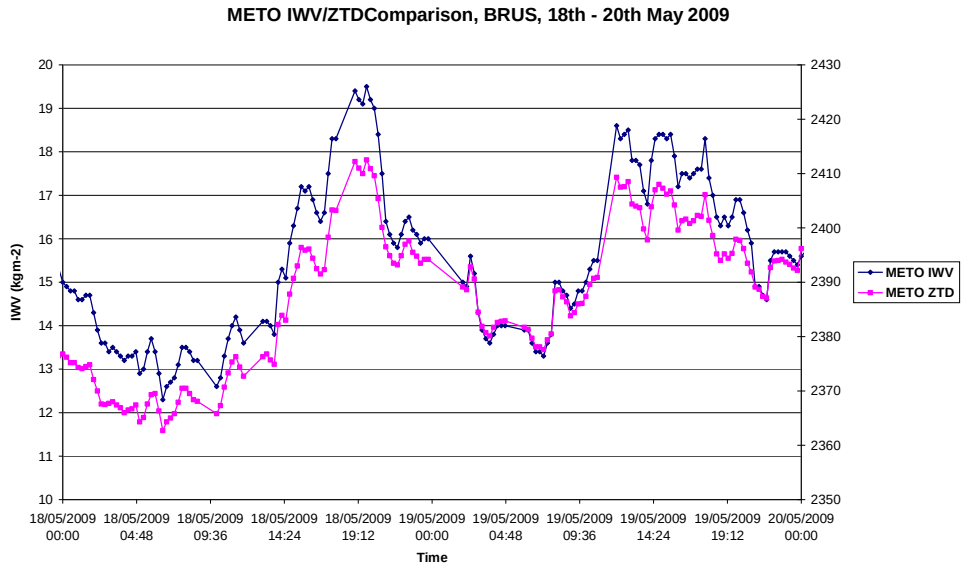

Figure 3.88 Time series of IWV and ZTD for BRUS, 18th – 20th May 2009

From the comparisons here we can see that the hourly meteorological data is not the source of the IWV jumps between the estimates from one hour to the next. The jumps in data are in fact introduced from the GPS processing scheme and output in the ZTD estimates. Further assessment needs to be carried out to assess the source of the jumps, which may be related to the number of normal equation files used in the process or the relative constraints imposed on the processing. However, as shown previously both of these are critical in ensuring that a sensible result of sufficiently high quality is obtained over a long period of time, selection may have to be a trade off between not over constraining whilst accepting some jumps.

3.7 Summary

From the long term comparisons of radiosonde against GPS in the UK we can now quantify the biases introduced with the number of radiosonde upgrades over the period of assessment and hence reproduce a bias corrected time series of data for the four sites analysed in this study. Since the most recent radiosonde upgrade in 2008, the most recent incarnation of the Vaisala RS92 radiosonde has a mean bias of around 0.3 kg/m^2 with the radiosonde measuring higher IWV estimates than GPS.

When considering inter-instrument comparisons in an attempt to try and identify the true value of water vapour, as we have seen in this Chapter we have, through the E-GVAP Project a number of integrated observing sites which are very valuable assets for a comparison of this nature. At Payerne, Switzerland we compared a full annual data set of WVR data against GPS WV. From the comparison we see a large dry bias in the GPS compared to the WVR data of around 2.5kg/m^2.

From the 2007 comparison at Izaña, we can see that there are a number of clear signals within the data. The most obvious is the very large summer time bias in MFRSR data, overestimating IWV compared to all other instruments during this time with an mean summer bias < 4 kg/m^2 and as such is excluded for further comparisons and bias conclusions. The CIMEL, FTIR and RS92 generally compare well at Izaña with an overall spread of biases against the RS92 radiosondes of around 1 kg/m^2. The RS92 does appear to over estimate systematically with an increasing bias with increasing IWV when compared to both the FTIR and CIMEL sun photometer. The CIMEL appears to have the highest positive systematic bias of 0.28 kg/m^2 increase in bias per 1mm kg/m^2 of IWV when compared against RS92 measurements. The results of the brief GPS comparison at Izaña are interesting as the GPS does appear to have a much larger bias when compared to radiosondes than with the previous analysis. At Izaña the RS92-GPS bias is in the order of 3.3 kg/m^2 whereas in the UK it is more like 0.3 kg/m^2. This large bias at high altitude needs further investigation at other high altitude sites before any firm conclusions can be drawn.

When assessing how well the hourly meteorological surface data meet the needs of operational meteorology in terms of the temporal resolution for ZTD to IWV conversion we can see that the limiting factor in ZTD conversion is not so much the resolution of the surface data, but the ZTD data itself. Jumps in ZTD data from successive hours are evident and again more study needs to be carried out here to assess the source of the bias in the processing system. In terms of spatial resolution of the meteorological surface data, we see how large biases in IWV data can arise from different techniques in surface data determination. In the case study shown, biases of up to 15mm IWV can be introduced by using non-representative pressure data. Much care must be taken with the quality of the surface data if IWV estimates from GPS networks are going to be used, and trusted, for operational meteorology.

From the comparisons carried out in Chapter 3.5 we have seen that falling snow has no appreciable effect on the GPS signals, both in terms of losing track of satellites or with regards to signal strength illustrated in signal to noise ratios.

Chapter 4 Integrating GPS IWV with Other Remote Sensing Instruments for Nowcasting

Two of the main benefits of GPS IWV over other instruments capable of measuring IWV, are the network's spatial coverage and the speed at which the data can be made available to the forecasters. As such GPS IWV is potentially an extremely useful tool for very short term forecasting (also known as nowcasting) in the prediction and monitoring of extreme weather events such as the convective initiation of thunderstorm cells. A number of case studies are examined illustrating the usefulness of water vapour obtained from GPS networks when combined with other data types and assessing the best combination of instruments for improved 3 dimensional understanding of atmospheric processes.

The main customer as yet of GPS derived meteorological data is the NWP community. The operational output of the METO processing servers is ZTD which, as mentioned previously, is assimilated in the NWP models at the Met Office. The conversion to IWV and its usefulness are still in the early stages of development as the usefulness to operational forecasting has not been demonstrated to the extent where GPS IWV is used on an operational basis. Aside from the input of ZTD to NWP models, if the full benefits of GPS derived meteorological parameters are to be fully realized, a tool to visualize water vapour fields needed to be developed in order to illustrate the usefulness to the forecasting community.

As a result, a suite of programs were developed using IDL (http://www.ittvis.com/ProductServices/IDL.aspx) through the course of this thesis to visualize water vapour fields on 2D maps of Europe to assist in weather forecasting. The conversion and display of IWV data are tools developed through the course of this thesis and are not operational Met Office tools, as they are still in development. Through the development of the GPS water vapour visualization software, however, we have a new tool in which we can visualise observations from other systems, such as wind and lightning data, to form an integrated observing package for forecasting.

Chapter 4 is primarily concerned with identifying the benefits to operational meteorology by the integration of GPS IWV with other remote sensing instruments and the improved meteorological understanding gained with an integrated observing approach when assessing meteorological phenomena in a 2-dimensional field.

4.1 History of GPS Water Vapour Imagery

The development of a display tool for near real-time GPS IWV is essential to maximising its usefulness to nowcasting, simply providing the data as numerical values obviously does have value e.g. for input to NWP models etc, but for nowcasting applications the visualisation of GPS IWV fields in near real time is a desirable tool to give forecasters better understanding of GPS IWV fields over the UK and Europe. In addition to plotting GPS IWV values, value may be added to any plots by integrating other observing systems such as wind and lightning data. This facility is thus far unused by operational meteorology but was developed as part of this thesis and as a demonstration within the Met Office.

In the past there had been relatively poor spatial resolution of GPS receivers in the UK, and as such plotting IWV values in near real-time would have had limited impact due to the high amount of interpolation necessary. However, as a result of the resource sharing agreement between the Met Office and OSGB, the Met Office now has access to data from approximately 150+ GPS receivers in the UK and Ireland with a mean spatial resolution of around 50km. With GPS networks at this kind of spatial resolution, the development of a GPS IWV visualisation tool becomes sensible as smaller scale meteorological features may now be identified using GPS water vapour alone.

Initially, when the network of GPS receivers in the UK was of relatively poor spatial resolution, the decision was taken to advect IWV data up and downwind to add data points to the map for contouring of water vapour fields. It was thought at that time that spatial changes of water vapour fields did not occur on such a sufficiently small scale that advecting water vapour data in space by 1 hour (according to the wind fields at the time) would add error to the plots. Wind information was taken from Doppler wind profilers and weather radar winds (5 in UK at the time) (Holleman, 2005), operational radiosonde ascents (6 sites in UK at the time) as well as from Aircraft Meteorological Data Reporting (AMDAR). This additional information not only enabled the advection of IWV values but also provided additional wind information in the form of wind barbs which could be plotted also adding value to the displays. Further data was also added to the plots in the form of lightning data taken from the Met Office ATD (Arrival Time Difference) lightning detection system. As the vast majority of water vapour is located in the lower troposphere, winds were taken from 2km for advection and for plotting on the maps as they would best represent the water vapour fields.

During initial phases of development of the water vapour imagery, it was noted that water vapour fields do indeed fluctuate on a sub-hour basis over the typical inter-station distances in the UK. As such it was deemed not sensible to advect water vapour up and down wind by the 1 hour as previously thought. Furthermore since the time of initial development, the GPS network density in the UK improved to a reduced mean inter-station distance of around 50km, following to the roll-out of the OSGB OSNet. This means that advection of GPS water vapour data was not necessary any more and so the advection part of the water vapour imagery was dropped in 2005. Figure 4.1 shows the current GPS network density in the UK and Ireland (at the time of publication) of sites contributing to METO.

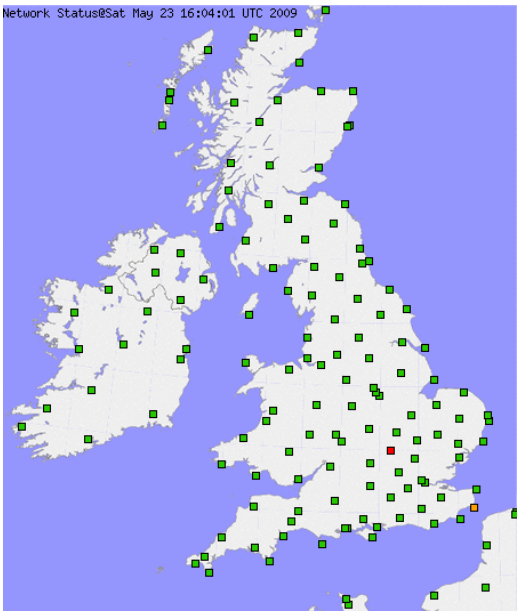

Figure 4.1 Typical NRT GPS network, May 2009. Colours represent latency, see E-GVAP website for more details, http://egvap.dmi.dk

The main aim of case study work is to try and interpret the 3D atmospheric processes by the combination of a number of remote sensing instruments including 2D GPS water vapour fields.

To date, two main case studies have been examined to review the potential of GPS IWV estimates for operational meteorology. Both cases were chosen as the atmospheric conditions led to extreme weather in the UK which was poorly forecast, primarily due to a lack of understanding of the atmospheric processes at work. Thunderstorms have the capacity for great damage and disruption to society and are such an extremely important area of study for meteorologists, but unfortunately the convective initiation of thunderstorm cells is not yet well understood and forecasting thunderstorms still provides great difficulty to meteorologists.

4.2 Meteorological Case Studies

4.2.1 24th June 2005 – Cold Pool Case Study

Between 12:00 and 18:00 on 24 June 2005 an upper-air trough (i.e. a weak front) moved across the central and southern UK bringing with it associated convective thunderstorms and heavy rainfall which led to flash-flooding and much disruption over Southern UK. The synoptic situation at 12:00UTC and the 7.3 micron satellite water vapour imagery is shown as Figures 4.2 and 4.3 respectively.

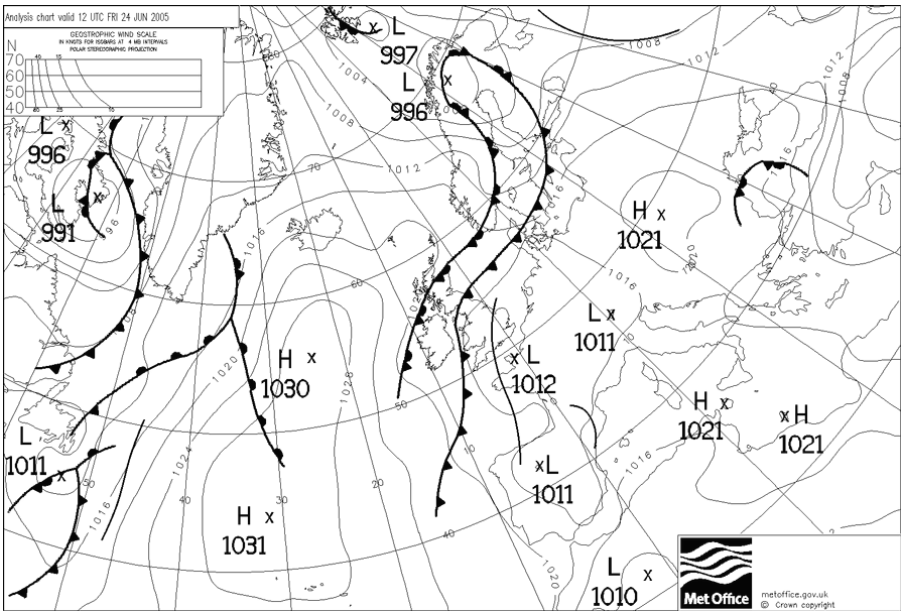

Figure 4.2 Synoptic chart for 12:00 UTC, 24th June 2005. Note North-South trough line over SE UK. Plot taken from Met Office NAE NWP model.

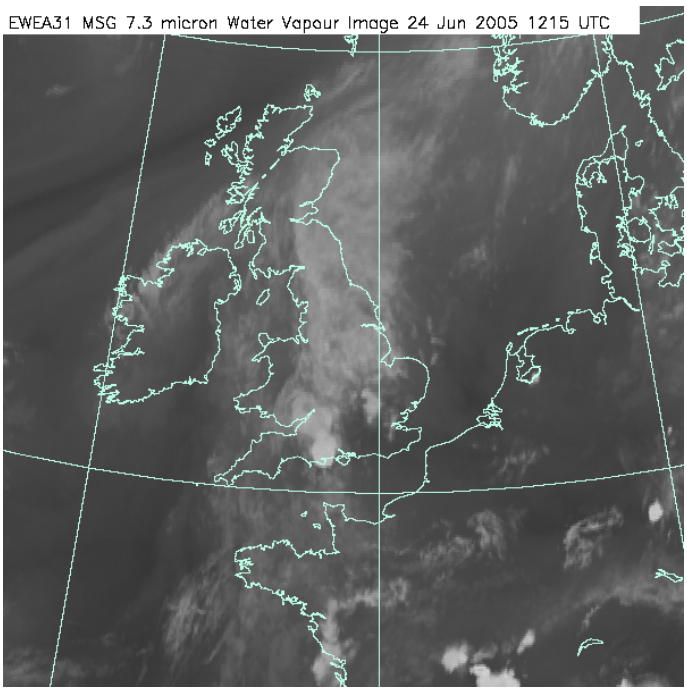

Figure 4.3 7.3micron Water Vapour Image from Meteosat 8, 12:15UTC, 24th June 2005.
Image courtesy of EUMETSAT

From Figures 4.2 and 4.3 it is possible to identify the weak frontal feature which is on the satellite water vapour image as the band of grey clouds over the southern UK. As we can see from Figure 4.3 although we can see drier air ahead and behind the trough, identified by the darker areas, there is no further detail in the image to identify any smaller scale features. However, by around 13:00 UTC the GPS IWV estimates had identified a small area of drier air to the immediate west of the centre of the convective storms (Figure 4.4). In the following hours, this area of relatively dry air intensified and by 14:30 the value of water vapour in the dry area was approximately 9kg/m^2 drier than the area of the storms, which was only 10-20km to the East (Figure 4.5).

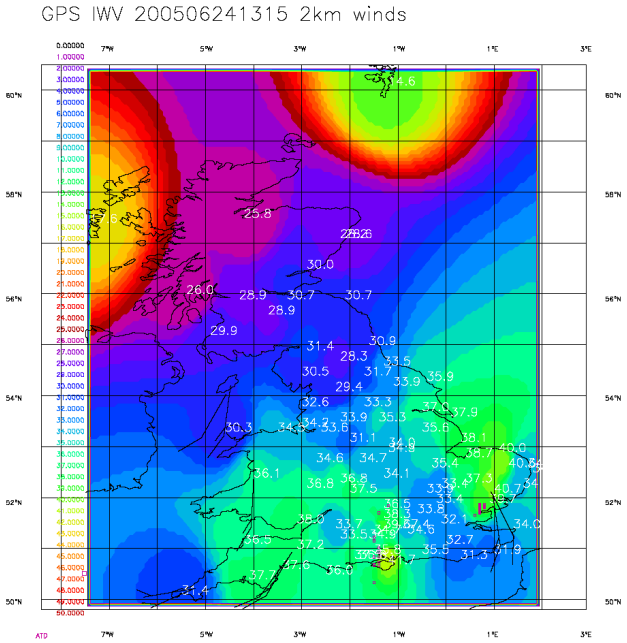

Figure 4.4 UK GPS water vapour map, 13:15 UTC, 24th June 2005

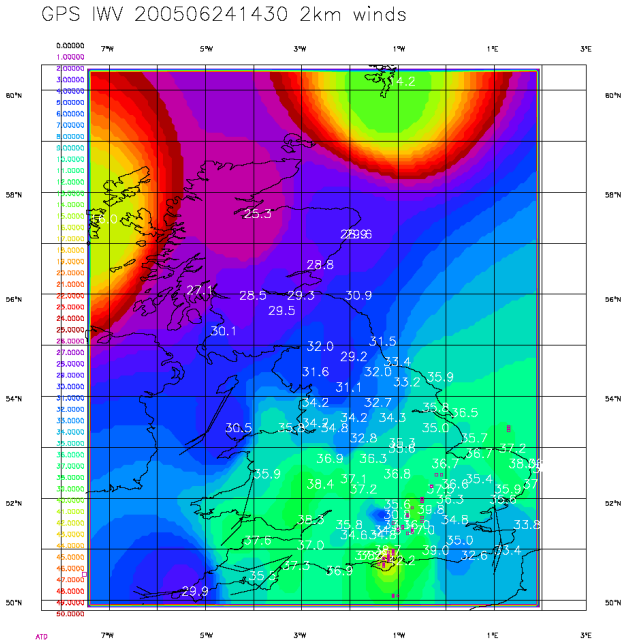

Figure 4.5 UK GPS water vapour map, 14:30 UTC, 24th June 2005

This relatively dry (~30 kg/m^2), cold area behind the storm may be attributed to the down-welling of colder drier air known as a 'cold pool'. In a normal, relatively stationary convective situation, the warmer up-welling air will continue to rise until all the convective potential energy or CAPE (Moncrief and Miller, 1976) is exhausted and then the air parcel will begin to cool and descend. In

this situation the up-welling air meets the down-welling, colder air and further convection is mitigated to some degree. However, if the convective cell is moving at such a speed that the colder down-welling air is offset with respect to the up-welling air, they will never meet and convection will not be mitigated. Furthermore, this dry, cold air will now reach the surface and spread out forcing surface air upwards (due to buoyancy) which in turn could lead to the initiation of further convective instability. Thus, a cold pool as in this example has the potential to perpetuate a convective cell for a much greater time than would normally be possible if the additional instability were not being sustained. A storm of this type would be very difficult to forecast as it would have the potential to sustain itself and cause much greater damage and disruption than would normally be associated with a storm of this size.

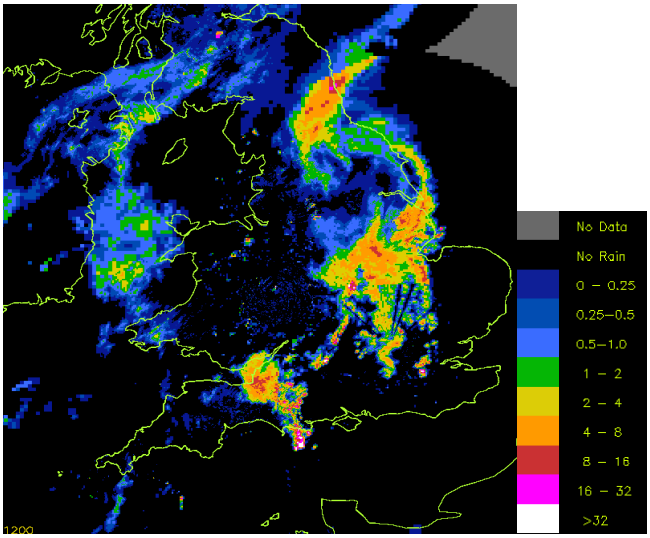

Figure 4.6 Weather radar returns for 12:00UTC, June 24th 2005. Taken from Met Office RADARNET, weather radar network

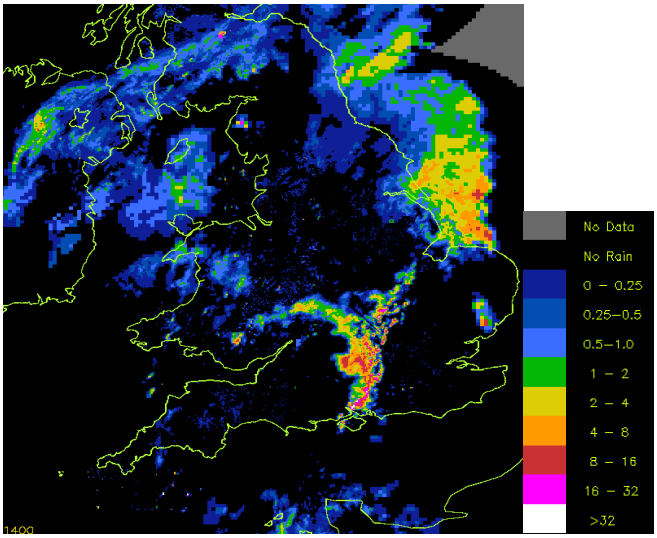

Figure 4.7 Weather radar returns for 14:00 UTC, June 24th 2005. Taken from Met Office RADARNET, weather radar network

As can be seen from Figures 4.6 and 4.7, typical observing systems such as weather radar cannot identify anything in the area of the down-welling, colder air. This illustrates the importance of GPS water vapour maps as a new, novel observation technique which, if adopted by operational meteorology, could offer insight into atmospheric phenomena which is currently unavailable.

This is an excellent example of how integrated observing systems can be used to give the forecaster previously unidentified information. In this case GPS IWV identified a feature which when investigated with other instruments was identified as a cold pool. Hopefully in the future improved timeliness of GPS IWV maps will allow the forecasters to view such features in the very near real-time and thus improve their forecasts accordingly.

4.2.2 13th July 2005 – Sea Breeze Case Study

On the 13th July 2005 a depression to the North West of Iceland developed and gradually moved south west towards the UK creating a succession of cold fronts. Throughout the day, the two fronts progressed southwards, and by 12:00UTC the surface analysis identified a ridge of high pressure extending across the central UK (Figure 4.8). The forecast for the day from the Mesoscale 12km NWP model (forerunner to the NAE), showed a line of convergence over the Southern UK extending from Cornwall to around London (Figure 4.9) at 15:00UTC. The convergence zone was a result of the weak northerly winds from the high pressure meeting southerly winds associated with sea breezes.

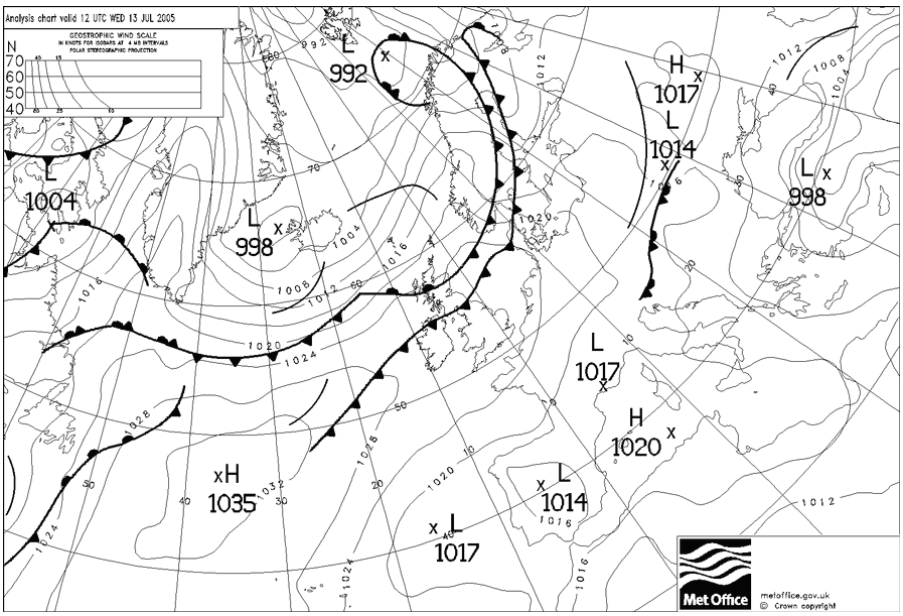

Figure 4.8 Synoptic chart, 12:00 UTC 13th July 2005

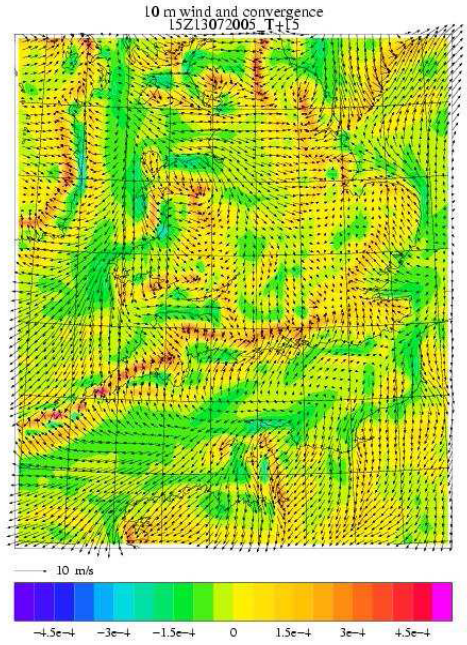

Figure 4.9 NWP forecast of 10m wind and convergence, 15:00 UTC, 13th July 2005

The development of a sea breeze is well understood, (Pielke, 1981; Atkins and Wakimoto, 1997). A sea breeze is a wind caused by temperature differences between land and water as a result of sea having a greater specific heat than land. The temperature differential creates a pressure minimum over the land due to its relative warmth and forces higher pressure, cooler air from the sea to move inland (Figure 4.10). A sea breeze front is a zone of convergence between the sea breeze and another air mass. The sea-breeze meets the warmer air over the land and creates a boundary like a weak cold front which, if the sea breeze is strong enough, can trigger convection and thunderstorms.

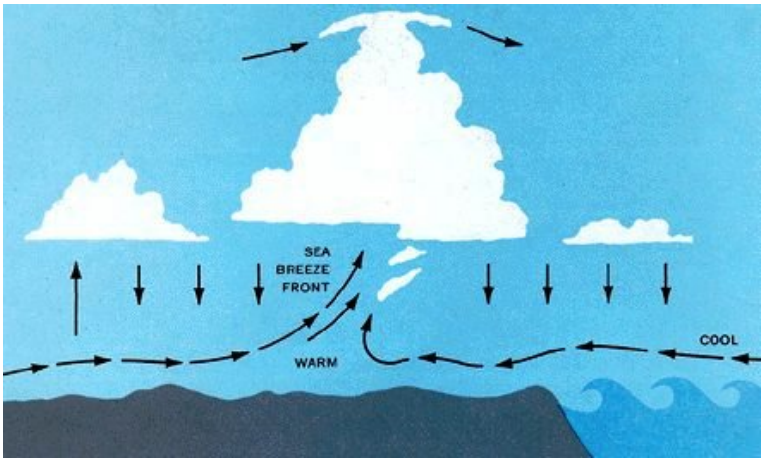

Figure 4.10 Schematic of a typical sea-breeze front (Image courtesy of U.S. Federal Aviation Administration)

Sea breezes are known to be low-level features, so to assess the vertical extent of the sea breeze and associated convergence zone, wind data at 500m and 3000m from radiosonde, AMDAR and wind profiling radar data are compared, Figures 4.11 and 4.12 respectively.

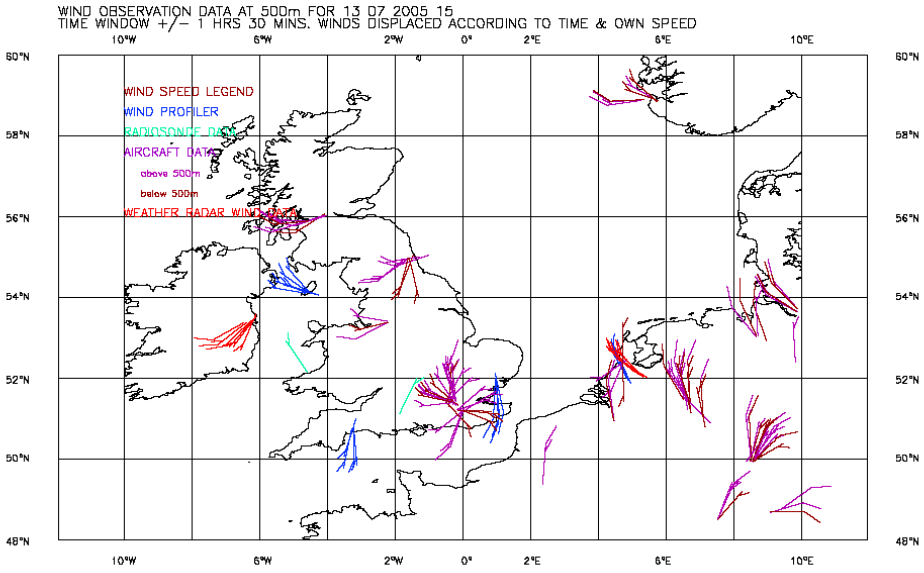

Figure 4.11 Wind chart showing southerly sea breeze winds at 500m over southern UK, 15:00 UTC 13th July 2005

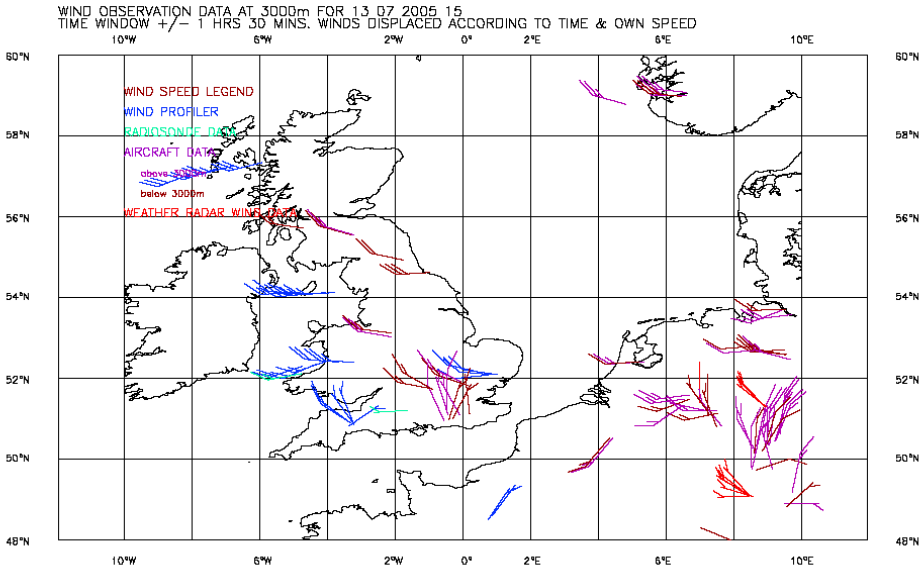

Figure 4.12 Wind chart showing no southerly sea breeze winds at 3000m over southern UK, 15:00 UTC 13th July 2005

When the wind information is assessed at different altitudes we can see the sea breezes as southerly winds over southern UK at 500m, however we see no such feature on the 3000m plot. Furthermore, when satellite water vapour imagery is compared (Figure 4.13), we can see no evidence of the sea breeze convergence zone in the upper level water vapour fields, confirming that the sea breezes are confined to lower levels.

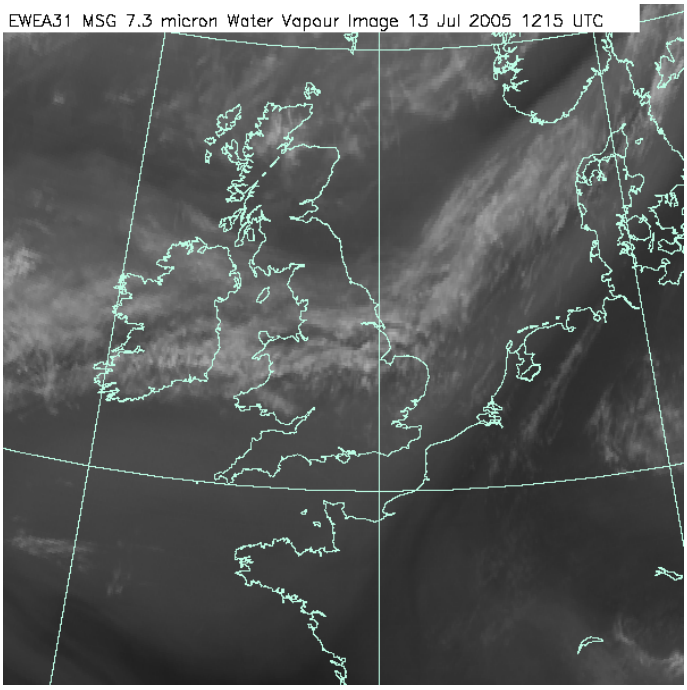

Figure 4.13 EUMETSAT 7.3 Micron WV Image, 12:15 UTC 13th July 2005

When hourly GPS water vapour images are compared (Figures 4.14 to 4.17), the GPS water vapour field associated with the convergence zone is well defined. Throughout the day we can see a band of high levels of water vapour progressing over the UK, reaching the south coast of the UK at around 15:00. The sea breezes appear to slow down the progression of the high water vapour field southwards and effectively dissipate the high zone of water vapour by 18:30 (Figure 4.17).

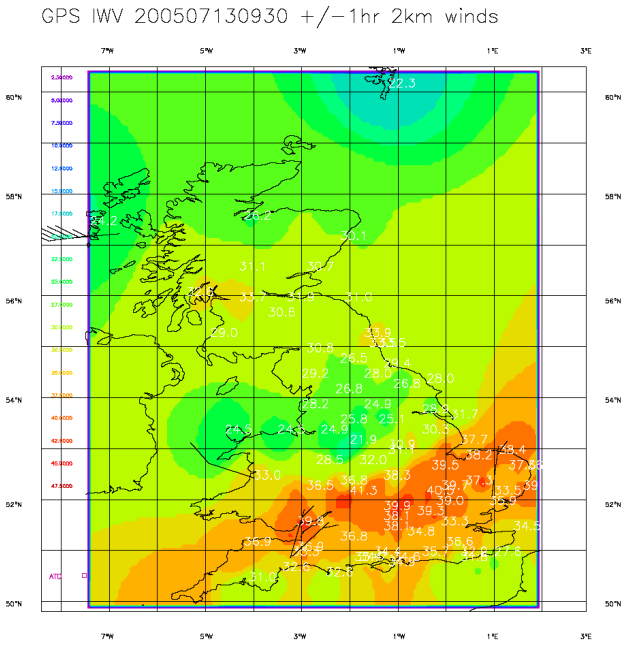

Figure 4.14 GPS water vapour plot, 09:30 UTC, 13th July 2005

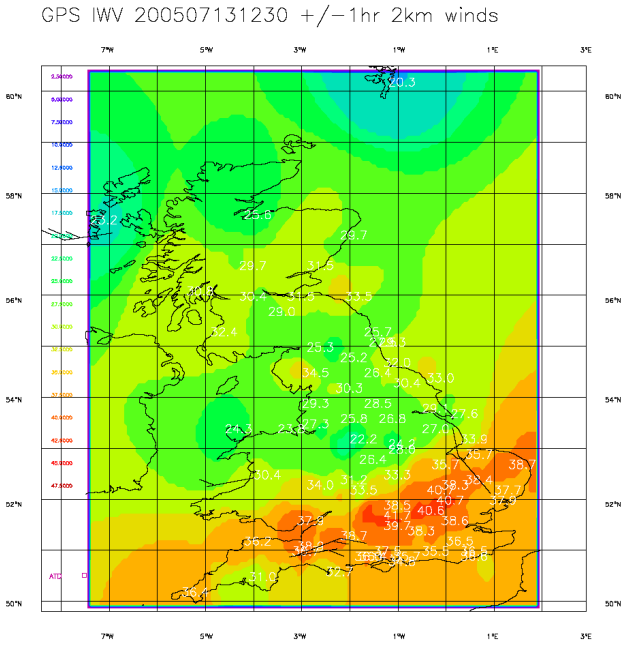

Figure 4.15 GPS water vapour plot, 12:30 UTC, 13th July 2005

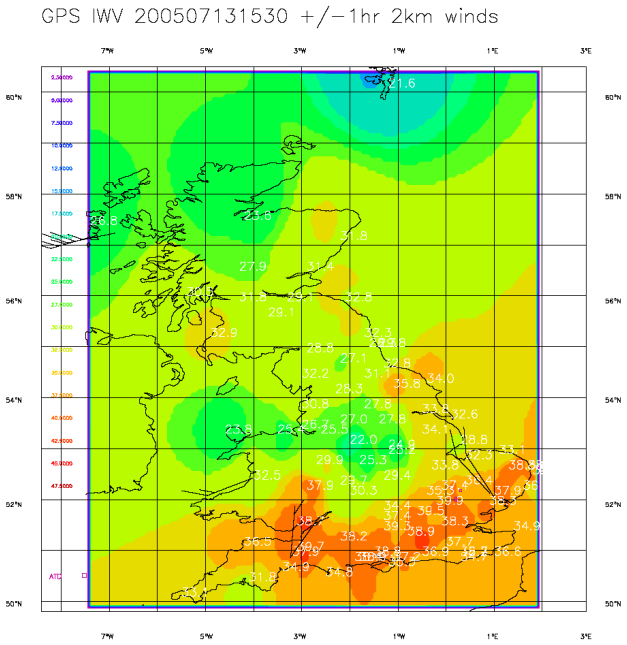

Figure 4.16 GPS water vapour plot, 15:30 UTC, 13th July 2005

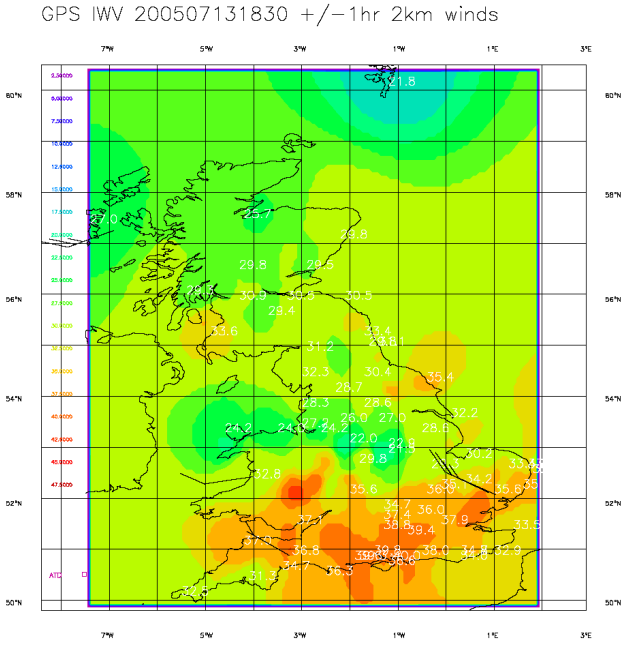

Figure 4.17 GPS water vapour plot, 18:30 UTC, 13th July 2005

If we compare the water vapour images derived from ground based GPS against the visible channel of the METEOSAT 8 satellite (Figure 4.18) we can clearly see the extent of the sea breeze on the visible image, is approximately in the same location as the high areas of water vapour at the same time (Figure 4.16)

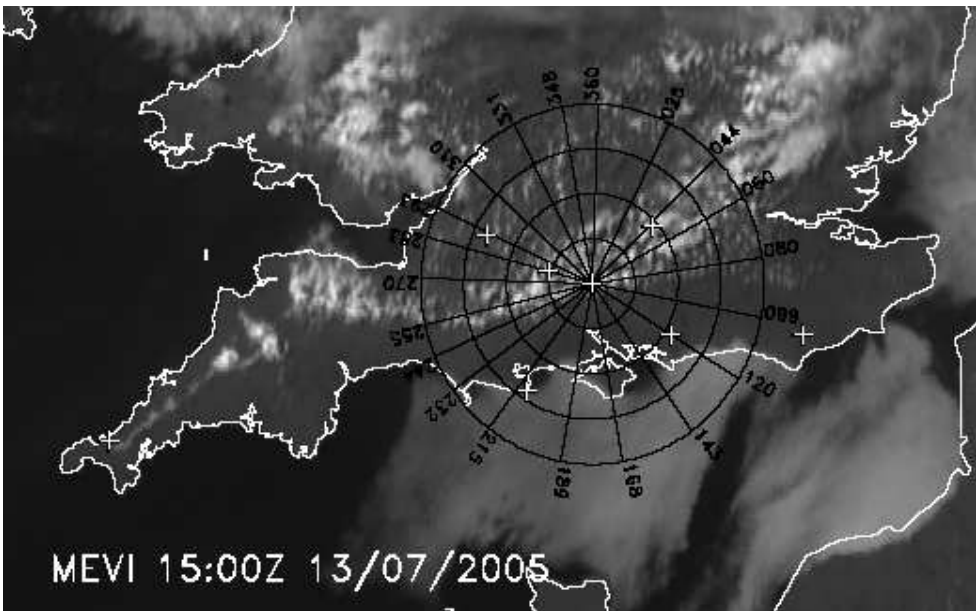

Figure 4.18 METEOSAT high-resolution visible imagery for 1500 UTC, 13th July 2005

This example clearly illustrates the ability of water vapour estimates derived from networks of ground based GPS receivers to identify low level features such as sea-breeze fronts. Furthermore if we compare the GPS water vapour plot against the coincident 7.3micron satellite image (Figure 4.13), we see that the satellite cannot resolve low level features such as sea breeze fronts and as such, we see the value to the forecasting community of near real-time plots of water vapour derived from networks of GPS receivers.

4.2.3 28th July 2005 – Dry Tongue Intrusion Case Study

Between 11:00 and 18:00 on 28th July 2005 a dry tongue of air intruded over the south east UK with associated thunderstorms and even a tornado touching down in Peterborough at around 17:00. The general synoptic situation, illustrated in Figure 4.19, was focused around a low pressure system centred over the Southern Irish Sea with generally southerly winds. As can be viewed in Figure 4.21 the weather radar returns do not show any significant rainfall over the area in which the tornado occurred at around 17:00UTC, and as such this event was very difficult to forecast.

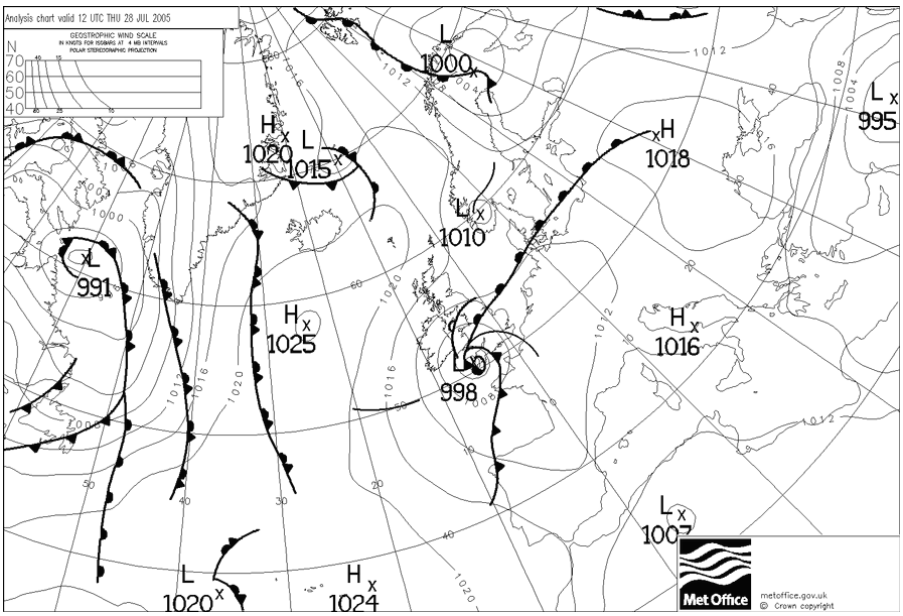

Figure 4.19 Synoptic chart, 12:00 UTC 28th July 2005

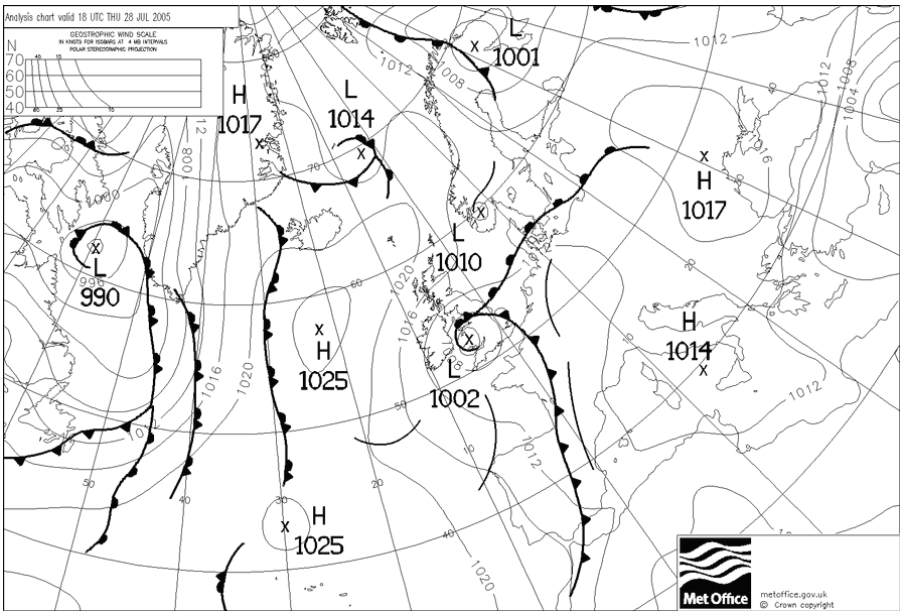

Figure 4.20 Synoptic chart, 18:00 UTC 28th July 2005

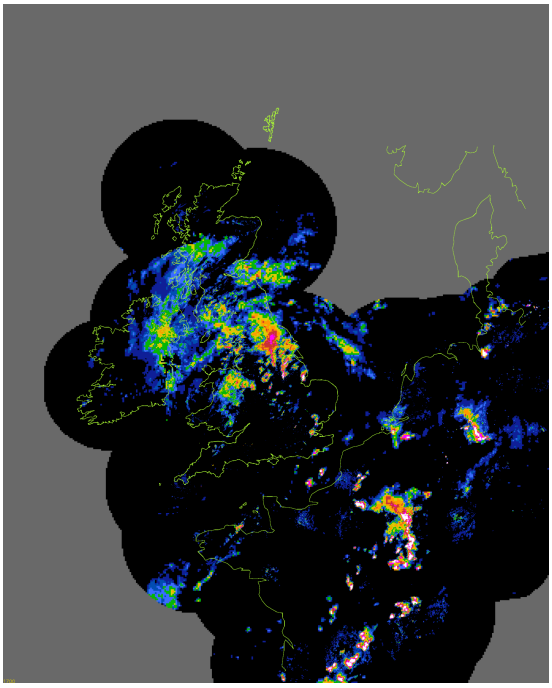

Figure 4.21 Weather radar returns for 17:00, 28th July 2005. Image taken from Met Office RADARNET, weather radar system

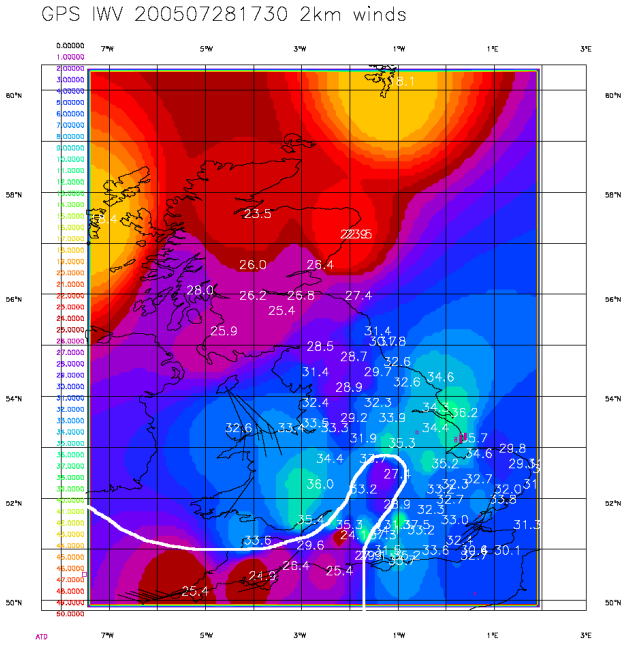

Figure 4.22 GPS Water Vapour plot, 17:30, 28th July 2005. White line on plot is manually drawn extent of dry intrusion

If we study the GPS water vapour imagery for 17:30 on the 28th July (Figure 4.21), we can identify the dry tongue of air intruding over the southern UK. However when we observe the satellite water vapour imagery we can see the dry tongue intruding more to the east over the south east UK, this is consistent for both the 7.3 micron and 6.2 micron water vapour channels, Figures 4.23 and 4.24.

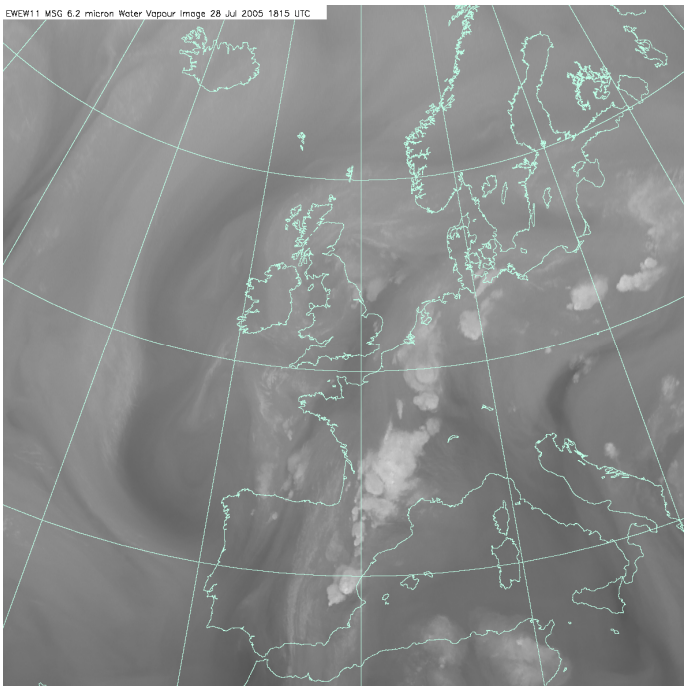

Figure 4.23 6.2micron Meteosat 8 water vapour image, 18:00UTC 28th July 2005

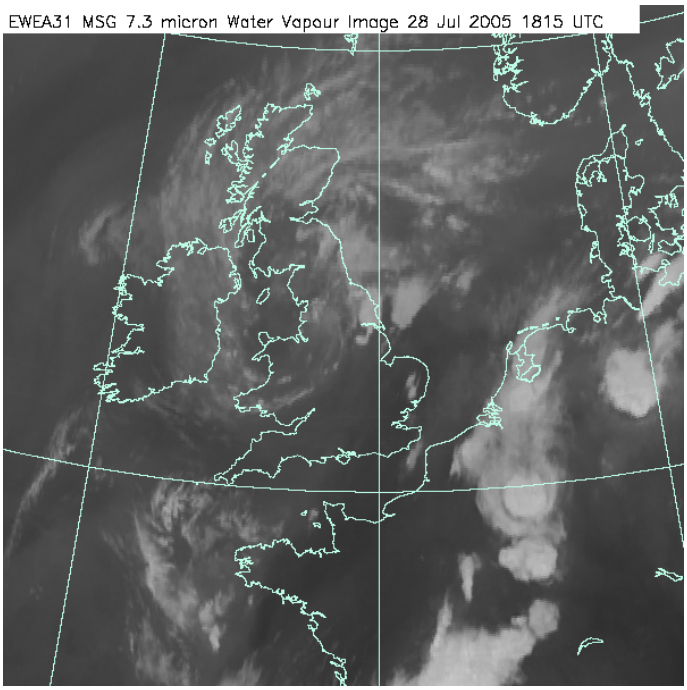

Figure 4.24 7.3micron Meteosat 8 water vapour image, 18:00UTC 28th July 2005

Satellite water vapour is effectively a downward looking tool and as such 'sees' primarily the water vapour in the top-most layers of the atmosphere, conversely GPS water vapour 'sees' the whole of the atmosphere but as the vast majority of water vapour is contained in the bottom-most 3-5km, GPS can be regarded as a system for identifying primarily lower atmospheric water vapour. From a

combination of satellite water vapour and ground based GPS IWV it can be seen, that there is a displacement in the position of the dry tongue with height, from this it may be inferred that the dry tongue is slanting in a easterly direction with height. The effect of the slant would be that the air beneath the tongue would be forced down as the dry intrusion consists of a relatively colder, denser air mass possibly inducing shearing in the upper atmosphere which is most likely the source of the tornado and the convection around the edge of the intrusion.

If we manually overlay the location of the satellite dry tongue on the GPS water vapour plot for the same time, we can clearly see the offset, Figure 4.25.

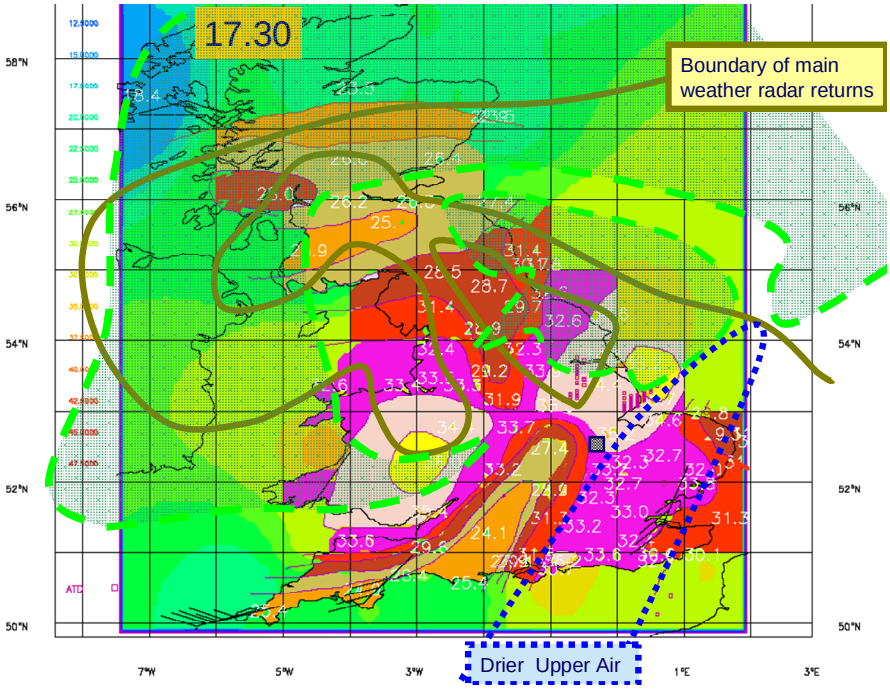

Figure 4.25 Manual interpretation of combined GPS IWV, satellite WV and weather radar plot illustrating horizontal offset between upper air and lower air dry intrusion.

This example shows that when GPS water vapour imagery is used in conjunction with satellite water vapour images, additional atmospheric information can be determined that would have previously been unknown. In this example, without the GPS water vapour knowledge, the forecaster would have no way of telling that the dry tongue was in fact sloping with height and that there is an increased likelihood of atmospheric shearing most likely in the upper troposphere. This again illustrates the GPS water vapour maps as a novel observational instrument in their own right. The additional information one can determine when using a network of GPS receivers adds new insight to water vapour fields, more than one sensor on it's own could ever be used for.

4.2.4 22nd July 2006 – Large Scale Convection Case Study

During 22nd July 2006, a large, mesoscale thunderstorm developed over the English Channel and proceeded to track north-eastwards over the UK, causing a large amount of damage and disruption. The main convective cells were typical of intense summer thunderstorms, with periods of intense rainfall causing local flash flooding, followed by longer periods of steady rainfall. The storm is of particular note as it was poorly forecast and caused a great deal of damage, particularly to a regatta what was taking place in 'The Wash' (north of King's Lyn, East Anglia) with a number of boats overturned. The synoptic situation at 12:00 is presented as Figure 4.26.

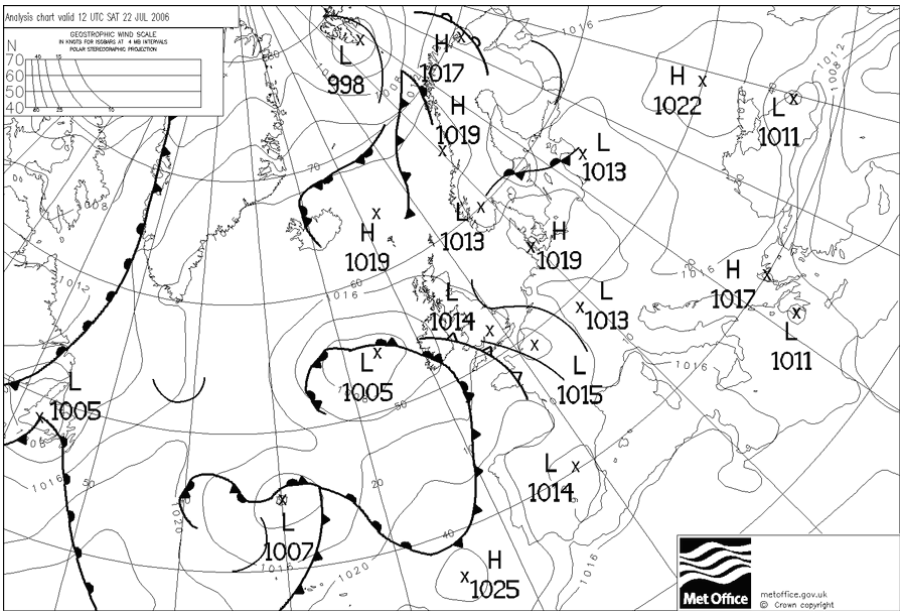

Figure 4.26 Synoptic chart, 12:00 UTC 22nd July 2006

If we assess the satellite imagery at around mid-day, in both the visible and 7.3micron wavelengths (Figures 4.27 and 4.28 respectively), as well as the water vapour imagery from ground based GPS (Figure 4.29), we can clearly see the developing convective storm over the central southern UK. Also, to the north-east of the convective centre, a dry intrusion of clear, drier air is identified.

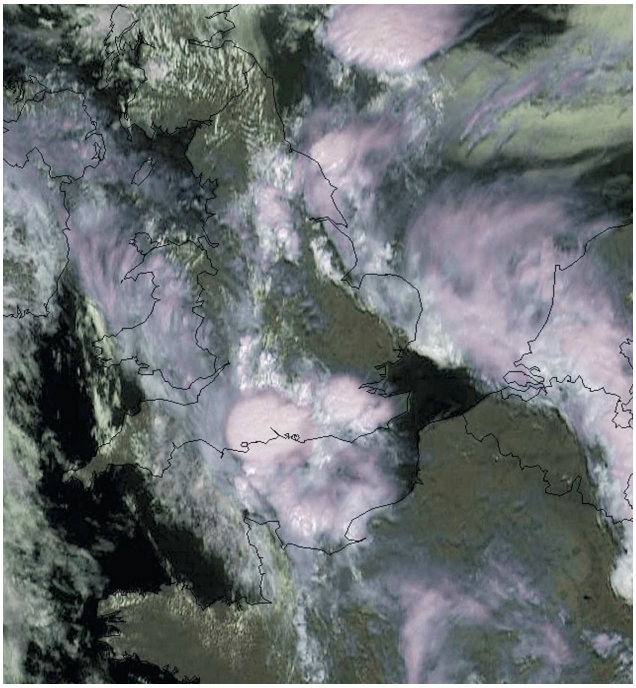

Figure 4.27 METEOSAT8 visible channel image, 1130UTC, 22nd July 2006 (Image courtesy of EUMETSAT)

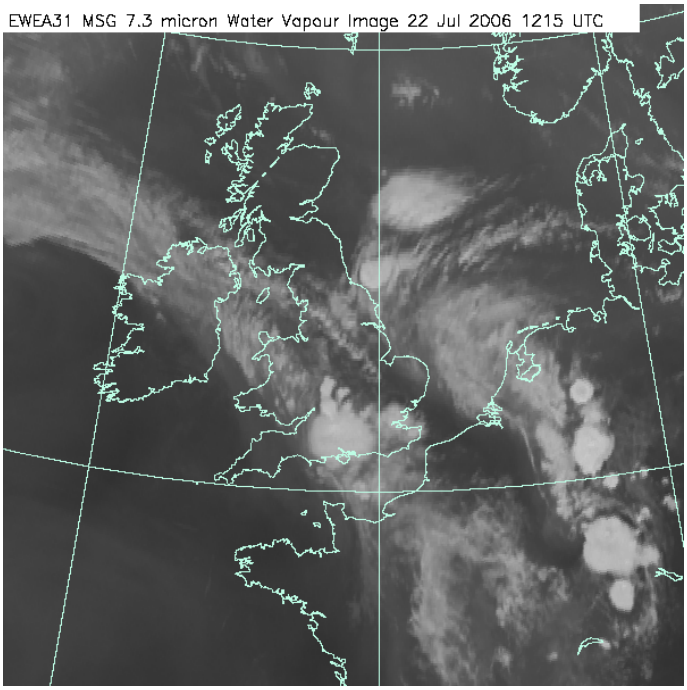

Figure 4.28 METEOSAT8 7.3micron water vapour image, 12:15UTC 22nd July 2006 (Image courtesy of EUMETSAT)

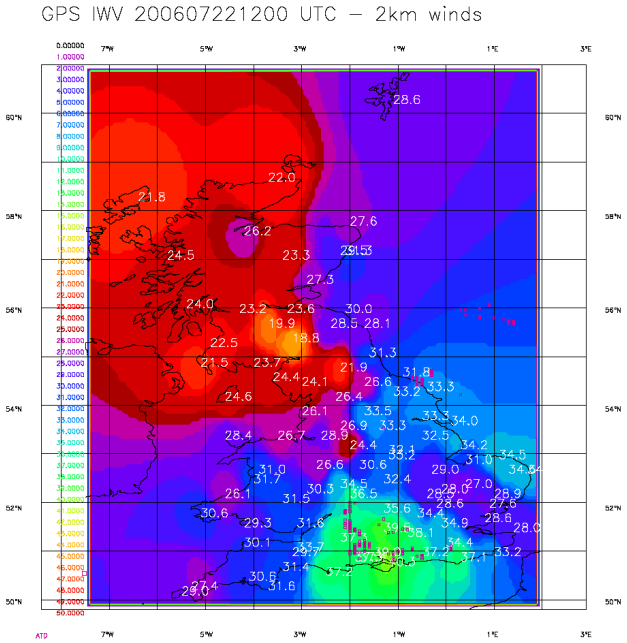

Figure 4.29 UK GPS water vapour map, 12:00UTC, 22nd July 2006 (purple squares are the location of lightning taken from the Met Office lightning detection system).

If the hourly GPS water vapour images are studied (Figures 4.30 to 4.35), the evolution of the water vapour fields can be followed throughout the day. As was presented in detail in Figure 4.29, at around mid-day there was a large, dry intrusion of air over the south east UK. This air mass would have consisted of cold, dry, dense air, and would be in direct contrast with the warm, moist air associated with the convective cell immediately to the west.

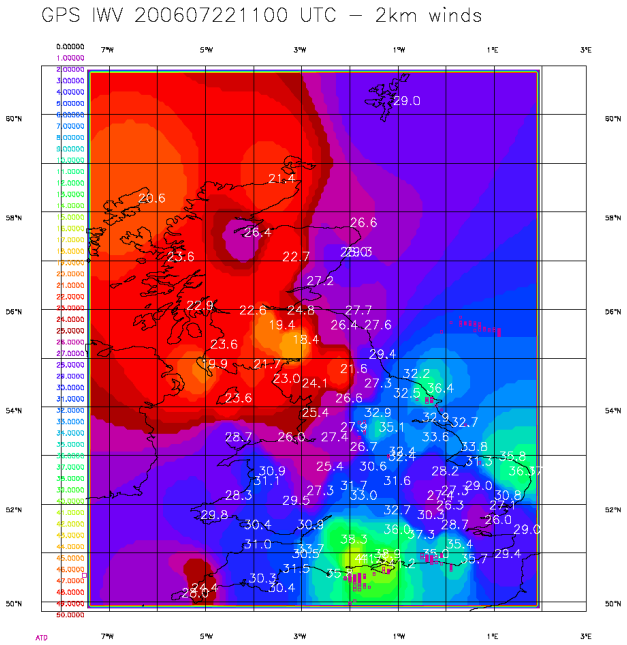

Figure 4.30 GPS water vapour plot, 11:00 UTC, 22nd July 2006

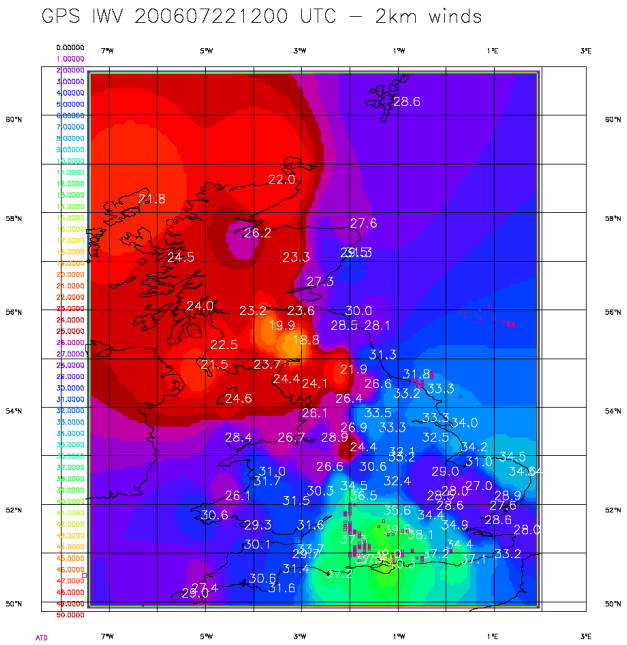

Figure 4.31 GPS water vapour plot, 12:00 UTC, 22nd July 2006

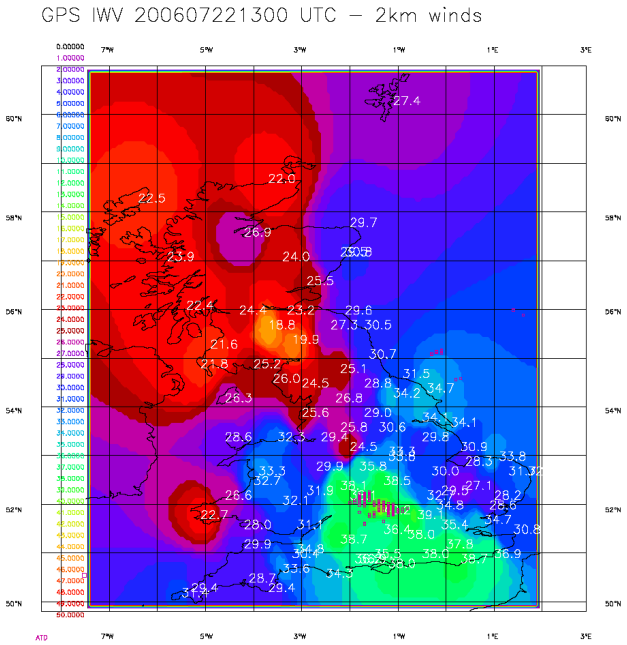

Figure 4.32 GPS water vapour plot, 13:00 UTC, 22nd July 2006

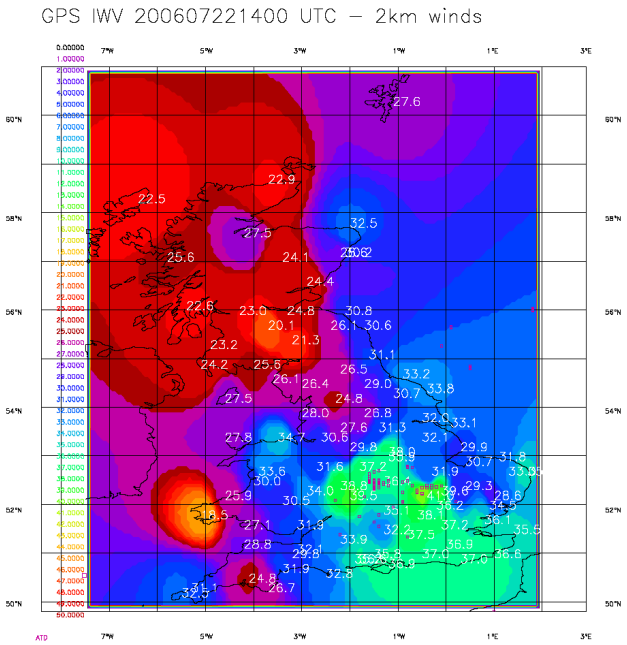

Figure 4.33 GPS water vapour plot, 14:00 UTC, 22nd July 2006

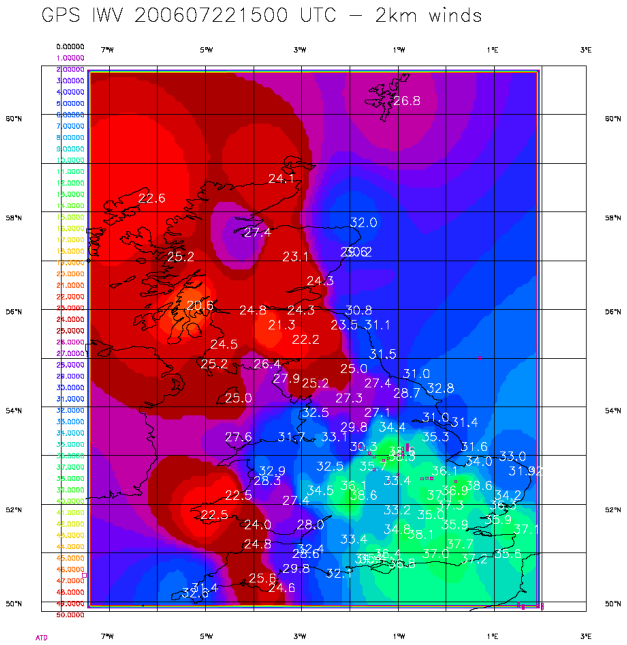

Figure 4.34 GPS water vapour plot, 15:00 UTC, 22nd July 2006

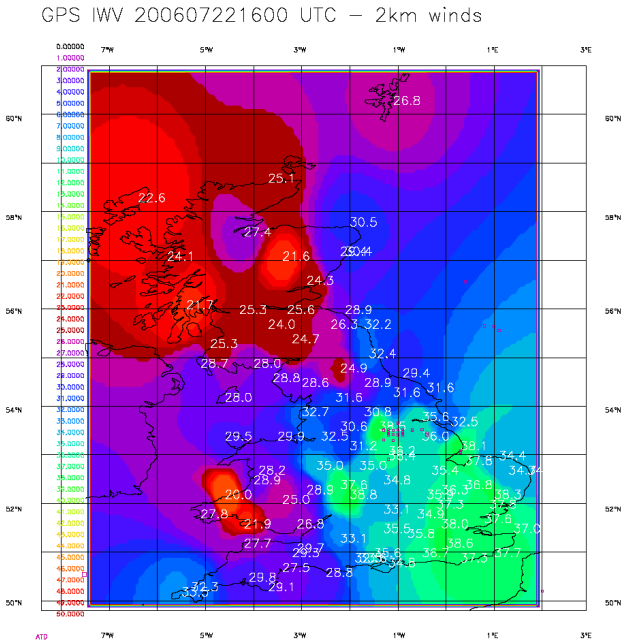

Figure 4.35 GPS water vapour plot, 16:00 UTC, 22nd July 2006

From Figures 4.30 to 4.35, the progression of the high water vapour to the north east of the storm can be identified with the high water vapour area associated with the storm moving to areas of lower water vapour associated with the dry intrusion. In this situation the warmer, moist air would have moved on top of the denser, cold, dry intrusion forming a capping inversion with warm air overlying cold air. This would add to instability and could be the cause of further convection to the east. The main storm centre does move more directly to the north (Figure 4.36), but possibly because of the water vapour field moving more to the north east, we saw more than expected convective initiation to the east, in the general area of The Wash

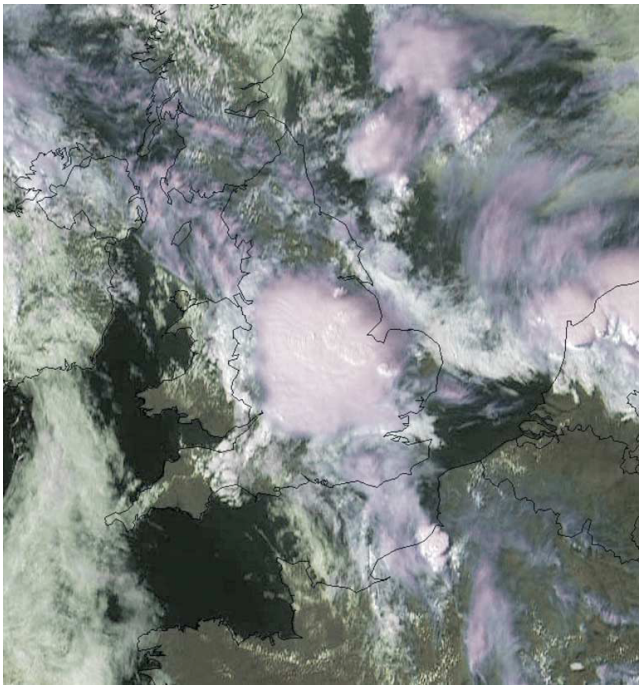

Figure 4.36 METEOSAT8 visible channel image, 1130UTC, 22nd July 2006 (Image courtesy of EUMETSAT).

This is an example of where water vapour images derived from a network of ground based GPS receivers can give additional information to the forecaster. From just assessing the water vapour fields from traditional observing systems such as satellite imagery (Figure 4.28) we do not see the horizontal detail in the water vapour fields, nor do we know the scale of the gradient between the two air masses. Only by using networks of GPS receivers to estimate water vapour, can the detail and the actual values of water vapour estimates be estimated on larger scales.

4.2.5 30th October 2008 – Ottery St Mary Case Study

Early in the morning of the 30th of October 2008, a freak storm occurred over the village of Ottery St Mary in Devon depositing over 30cm of hail in around 2 hours. The small, localised storm was not well forecast by the Met Office and caused a large amount of damage and disruption and led to floodwaters of 1.2m (Figures 4.37 and 4.38) in the area.

Figure 4.37 Image of hail, Ottery St Mary, Devon, 30th October 2008

Figure 4.38 Image of hail and floodwater, Ottery St Mary, Devon, 30th October 2008

If time series of GPS water vapour data are plotted for the three most local GPS receivers to Ottery St Mary (Exmouth, Dunkeswell and Taunton, Figures 4.39, 4.40 and 4.41 respectively) a rise in atmospheric water vapour overnight can clearly be observed, however, no radical feature can be observed which would be representative of such a severe event.

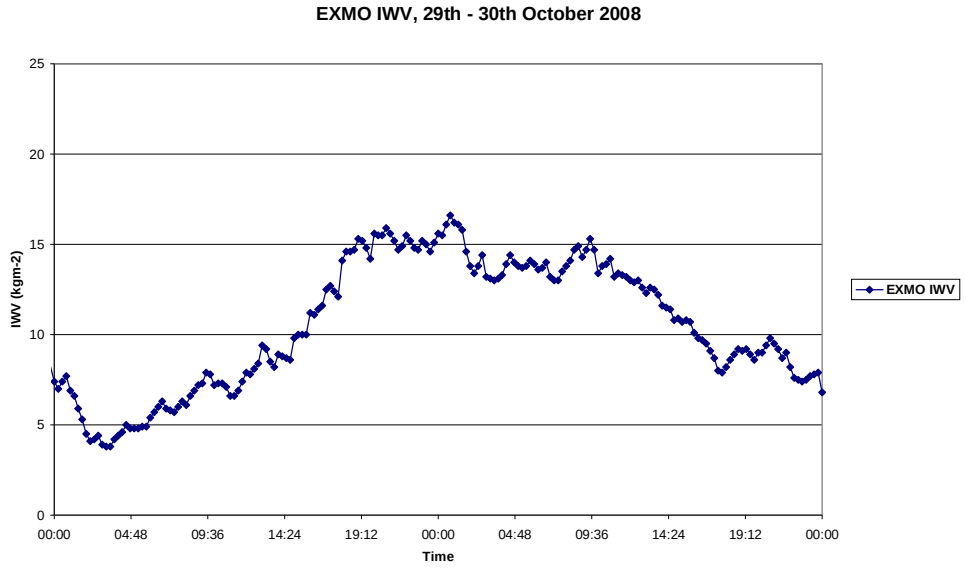

Figure 4.39 IWV time series, EXMO, 29th and 30th October 2008

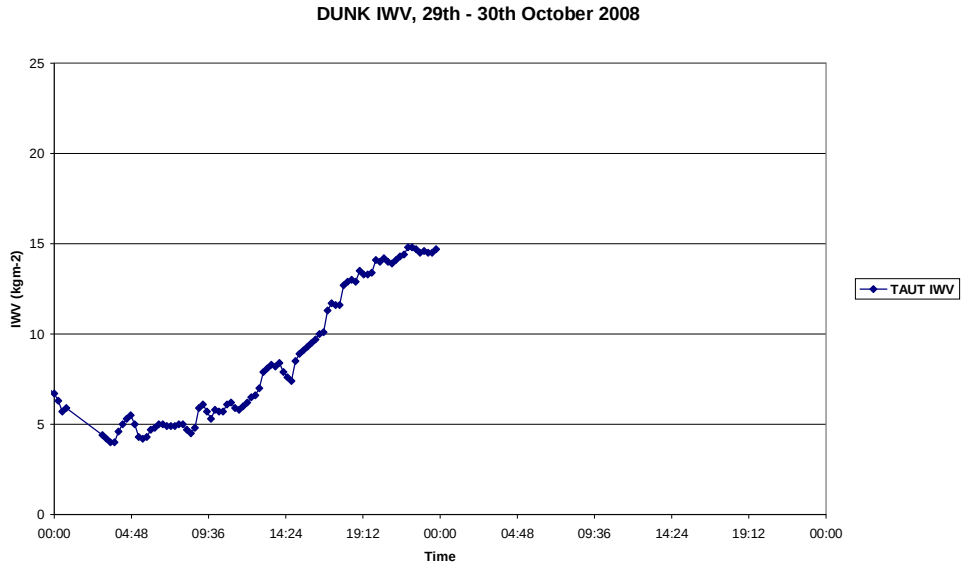

Figure 4.40 IWV time series, DUNK, 29th October 2008

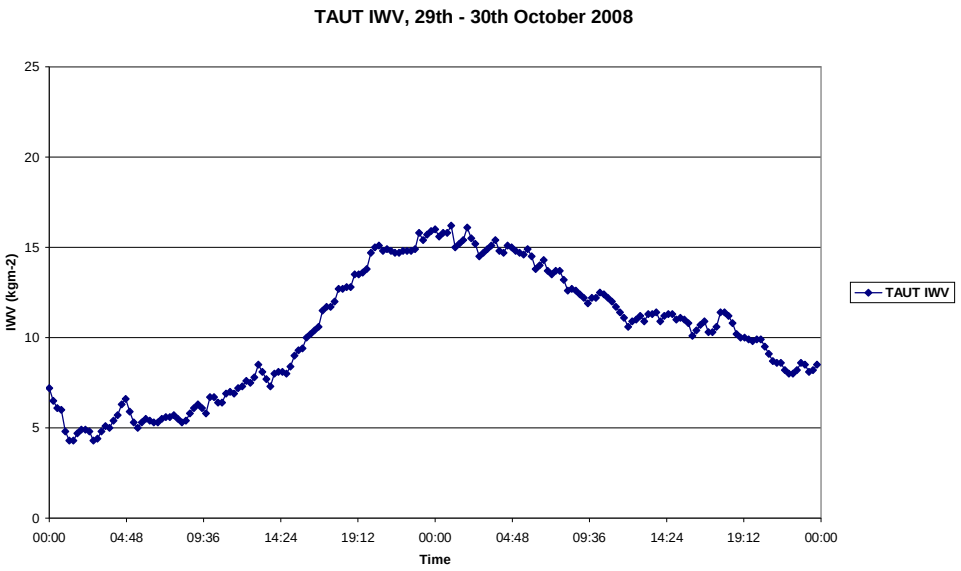

Figure 4.41 IWV time series, TAUT, 29th and 30th October 2008

From the time series comparison (Figures 4.39 to 4.41) it can be observed that the GPS receiver at Dunkeswell (DUNK) fails at midnight on the 30th. The cause for the outage is unknown, but may be due to a power failure relating to the storm.

When the 2D GPS water vapour images for the same time are compared (Figures 4.42 to 4.47), again we see a rise in IWV at the sites local to Ottery St Mary, but no dramatic rises typical of a convective storm of this severity. Also from the plots, extremely high IWV estimates from the GPS receiver at Kirkcudbright near Dumfries in Scotland are observed. The high values were traced through the METO system, and were found to be due to faulty pressure sensor at the nearby Met Office surface observations site at Dundrennan, from which data is used for ZTD to IWV conversion. The faulty sensor was then reported to the appropriate department at the Met Office for investigation and subsequent repair.

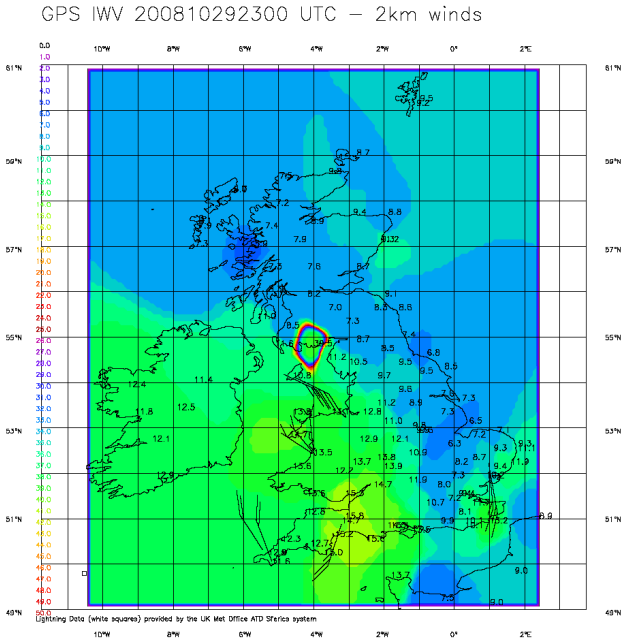

Figure 4.42 GPS water vapour plot, 23:00 UTC, 29th October 2008

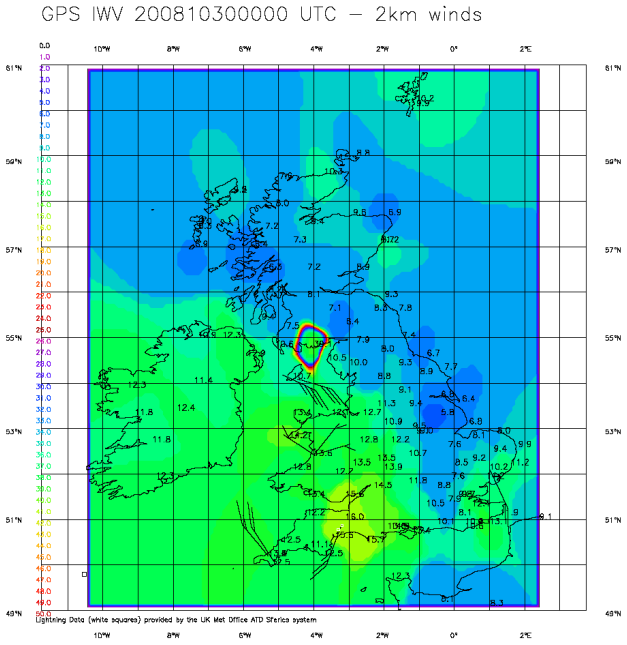

Figure 4.43 GPS water vapour plot, 00:00 UTC, 30th October 2008

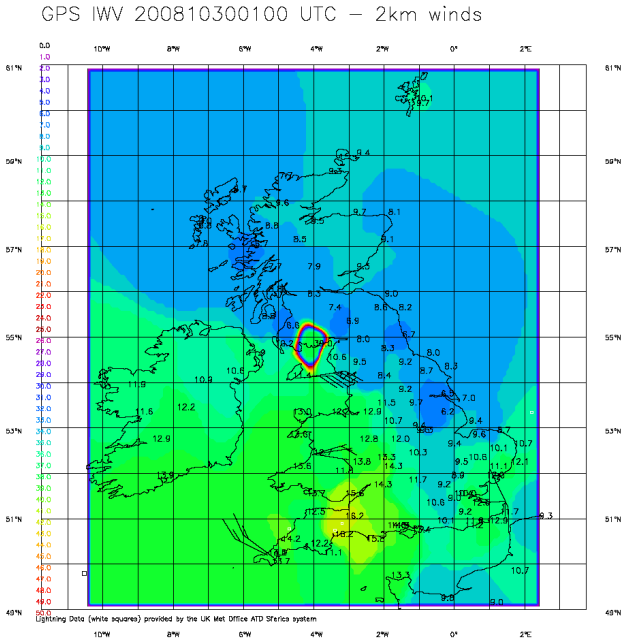

Figure 4.44 GPS water vapour plot, 01:00 UTC, 30th October 2008

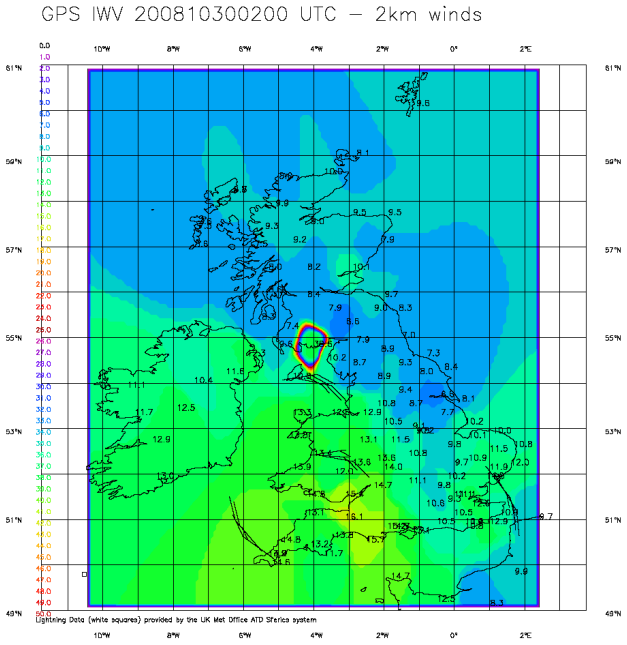

Figure 4.45 GPS water vapour plot, 02:00 UTC, 30th October 2008

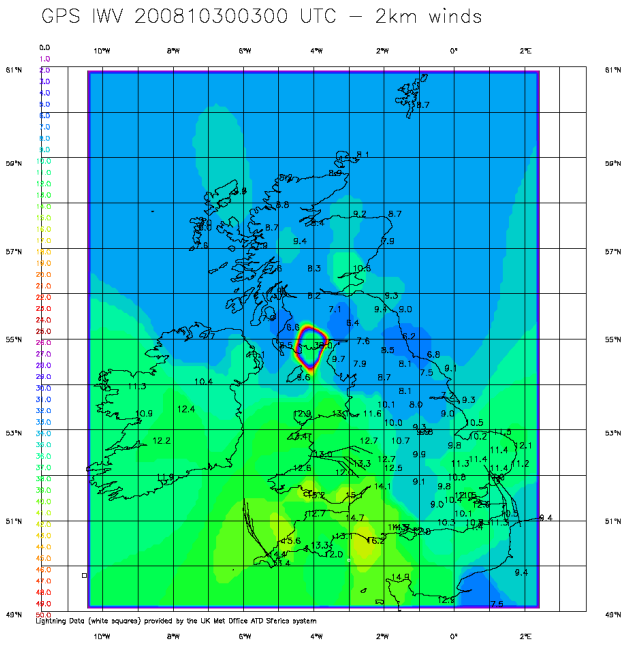

Figure 4.46 GPS water vapour plot, 03:00 UTC, 30th October 2008

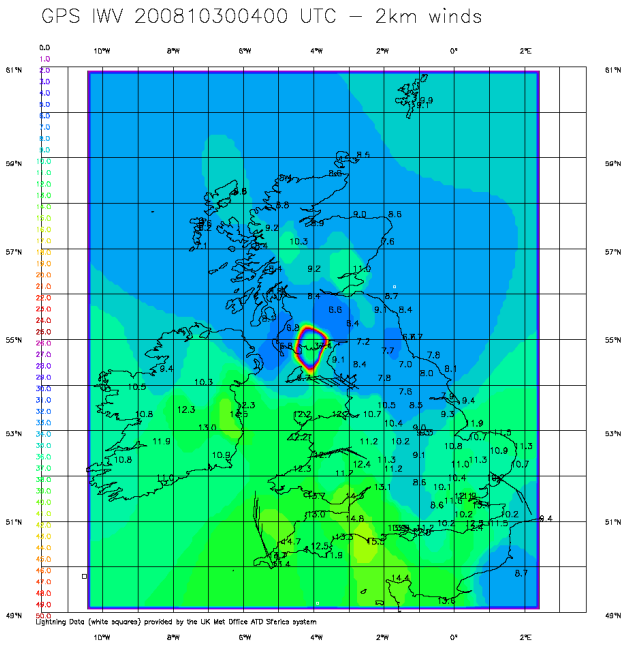

Figure 4.47 GPS water vapour plot, 04:00 UTC, 30th October 2008

This example illustrates that even a dense network of GPS receivers with a mean spacing of around 50km is still to coarse to resolve all small scale convective events. It is unrealistic that even in the future GPS networks will be dense enough to resolve all meteorological phenomena. However, even if the centre of the storm is not located directly over a GPS receiver, we still can see the influence of the storm on the nearest other receivers in the network. This demonstrates how important a network of receivers is, as opposed to observing from a single site.

4.3 Summary

The case studies presented here give excellent examples of how a network of GPS receivers used for the determination of near real-time water vapour can add new, previously unknown information to the forecasting community. By combination with other remote sensing instruments such as satellite water vapour, we can see how an integrated approach to remote sensing of the atmosphere can add value to observations. In the case of the dry intrusion we can see how using satellite and GPS water vapour together we can infer some vertical atmospheric structure where there was previously none evident.

The examples presented here demonstrate how the GPS water vapour maps should be classed as a new observing instrument in their own right. One GPS receiver might be able to give you atmospheric information at a specific site, and as we shall see in the next Chapter, be of potential use in identifying long term trends at that site. However, as we see here, when a whole network of GPS receivers are used, we are able to determine atmospheric features in the horizontal which is a new tool in itself. GPS water vapour is not an answer to all meteorologists problems, but in the future, if GPS water vapour fields can be integrated together with all other remote sensing and in situ observations, then the forecaster will have a better understanding of humidity structure in the horizontal than they have ever had previously.

Chapter 5 GPS as a Tool for Climate Monitoring

Water vapour is one of the key components in the climate system and is the most potent greenhouse gas (Philipona et al., 2005). Water in its condensed forms, liquid and ice, exerts a profound influence on both incoming solar and outgoing radiation and in the form of water vapour, is key to transporting energy around the atmospheric system. Water vapour moves quickly through the atmosphere and redistributes energy associated with its evaporation and condensation.

Climate models find that predictions of climate change are very sensitive to water vapour and cloud feedback. It has been estimated that water vapour feedback alone doubles the effect on temperature of an increase in other greenhouse gases (Cess, 2005) and approximately 70% of atmospheric warming can be attributed to water vapour acting as a greenhouse gas (Houghton et al., 2001; Solomon et al., 2007) due to its absorption of incoming sunlight, particularly in the infrared region. The International Panel on Climate Change (IPCC), AP4 numerical climate model currently predicts a 6.7% increase in IWV per degree C over the next few decades, whereas bias corrected, long-term radiosonde time series (Dai, 2009) predicts a ~4.8% rise in IWV per degree C rise in atmospheric temperature. However, there is much uncertainty in these calculations. Water vapour feedback occurs primarily in the upper troposphere where there is no physical link between water vapour and temperature. Climate models tend to suggest that the relative humidity of the upper troposphere will remain unchanged in a warmer atmosphere and as such absolute humidity will have to increase, but there is much uncertainty in the calculations. A better understanding of the distribution of atmospheric humidity is therefore one of the prime areas of concern in climate research.

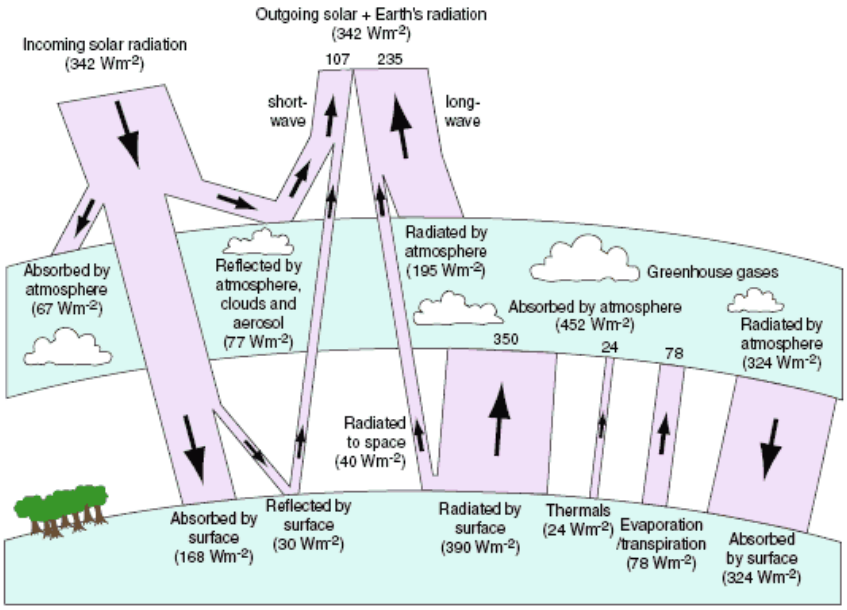

Figure 5.1 Earth radiation budget. All figures in W/m^2 (Houghten et al, 1996)

It is now well established that the top of the Earth's atmosphere receives a surface-averaged energy input from the Sun of approximately 342W/m^2 (Figure 5.1). Satellite measurements indicate that approximately 102 W/m^2 is immediately reflected back to space from cloud with the remaining 240W/m^2 of incoming solar radiation being absorbed by the Earth in some form and then emitted back to space as long wave radiation. As such the net gain is of course zero which must be the case as the Earth is neither inherently warming nor cooling. Modern radiative models suggest that the atmosphere is responsible for just 67 W/m^2 of the absorption with the remainder being absorbed by the ground and by the oceans. What is commonly known as the 'greenhouse effect' is essentially the difference between the long-wave radiation that is emitted by the Earth's surface and the upward thermal radiation that leaves the top of the atmosphere. However in effect this actually means the tropopause - the upper boundary of the troposphere. The greenhouse effect is around 146 W/m^2 in clear skies and approximately 30 W/m^2 higher under cloud cover, and it is this atmospheric absorption which permits life on Earth. The problem comes when the components of the atmosphere which are responsible for absorption of radiation (such as CH_4 or CO2) are increased due to anthropogenic activities, which causes an imbalance in the atmosphere system allowing more energy to be absorbed, thus heating up the atmosphere.

Current, state-of-the-art climate models predict that an increase in tropospheric temperature will lead to an increase in the water vapor content of the troposphere (Hansen et al., 1984). As surface temperature increases saturation vapour pressure increases exponentially with temperature and thus, more water can evaporate from the surface into water vapour. The increase in water vapor in turn leads to a further increase in temperature due to water vapour's ability to store more incoming long wave radiation, thus a positive feedback loop is established (Manabe and Wetherald, 1967).

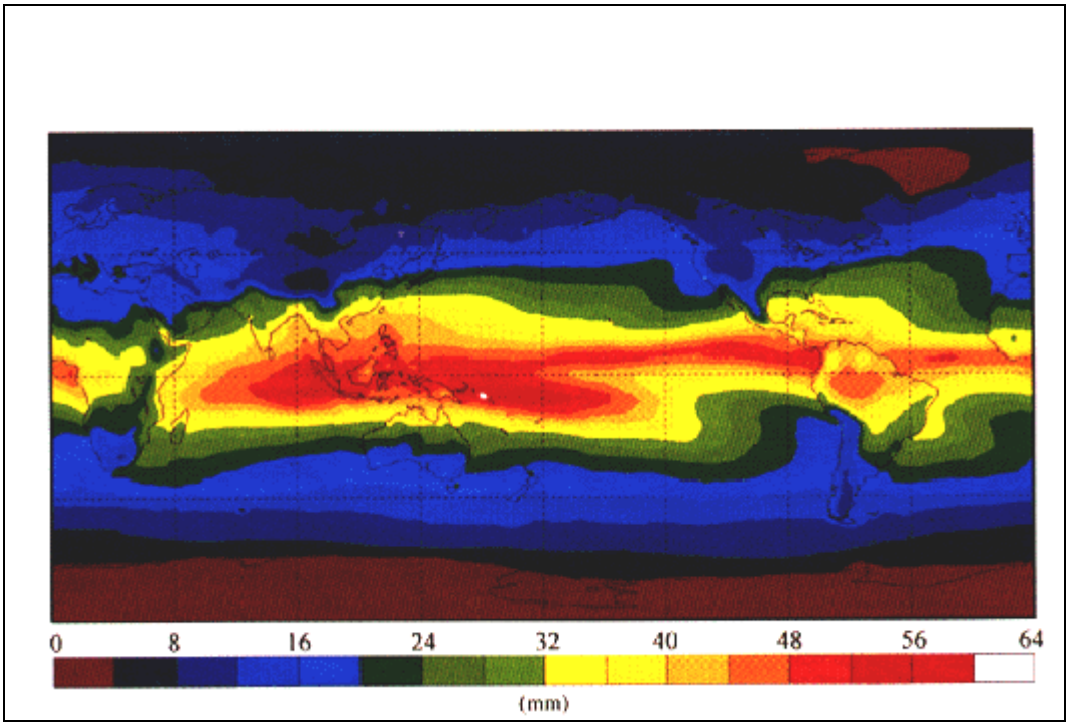

Figure 5.2 Mean distribution of Global IWV for 1992 taken from both satellite and radiosonde observations. (Image courtesy of Colorado State University)

As can be seen from Figure 5.2 the distribution of global water vapour is far from evenly distributed. The humid tropics (red regions) contain almost 100 times more water vapour than the dry polar regions (blue areas). Due to the widely dispersed nature of GNSS networks, water vapour measurements from GNSS can provide us with a new, low cost, accurate and well distributed observing tool. Furthermore the density and extent of GPS networks is constantly improving as countries are relying more and more on GPS as a cornerstone of national infrastructure. For example, over the course of the E-GVAP project the number of GPS sites contributing hourly data to the project increased from around 550 in 2003 to about 1000 in 2009 in the European region alone (Figure 5.3). Also, as GNSS is becoming more widely used around the globe, it gives us an opportunity to have long time series of water vapour from remote regions such as parts of the developing world and oceanic regions where traditional humidity observations are difficult and as such expensive.

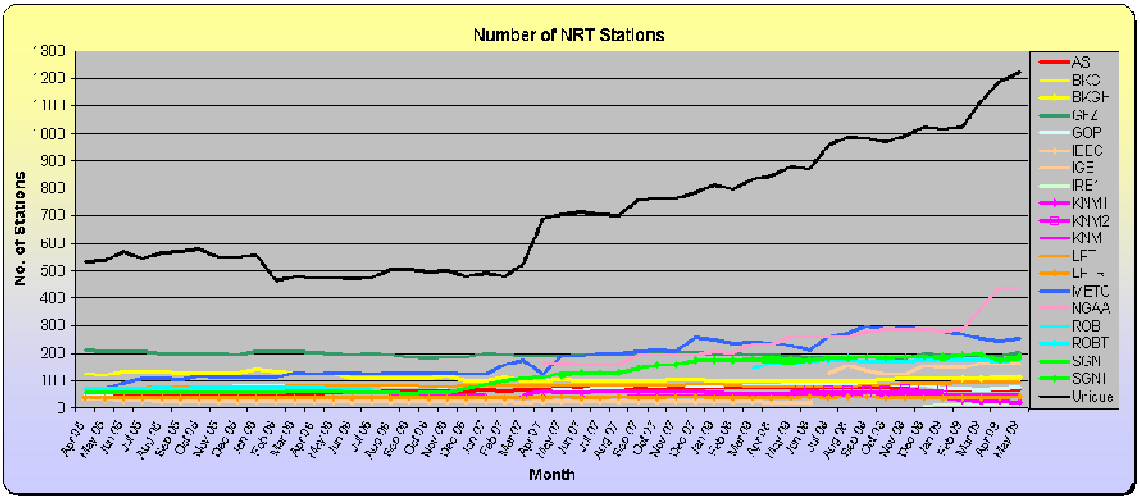

Figure 5.3 Time series of unique European GPS stations contributing near real-time data to the E-GVAP Project. (Image courtesy of the Met Office), coloured lines are individual ACs, black line is the total.

As can be seen from the E-GVAP map (Figure 5.4), the density of GNSS stations is much higher than that of the IGS network (Figure 5.5), and this does not necessarily include all commercial RTK networks. For future global observations of water vapour from GPS networks, more effort needs to be made to gain access from additional GPS stations throughout the world, and if a global GPS water vapour processing effort could be established, processing GPS data in a consistent manner for long time periods, this would be a great source of information to climate science.

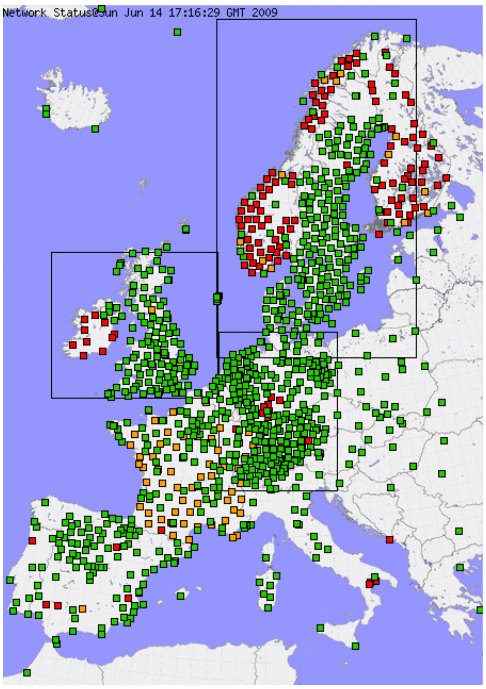

Figure 5.4 Map of European GNSS stations contributing data to the E-GVAP Project. Colours represent latency, see E-GVAP web page for more details, http://egvap.dmi.dk

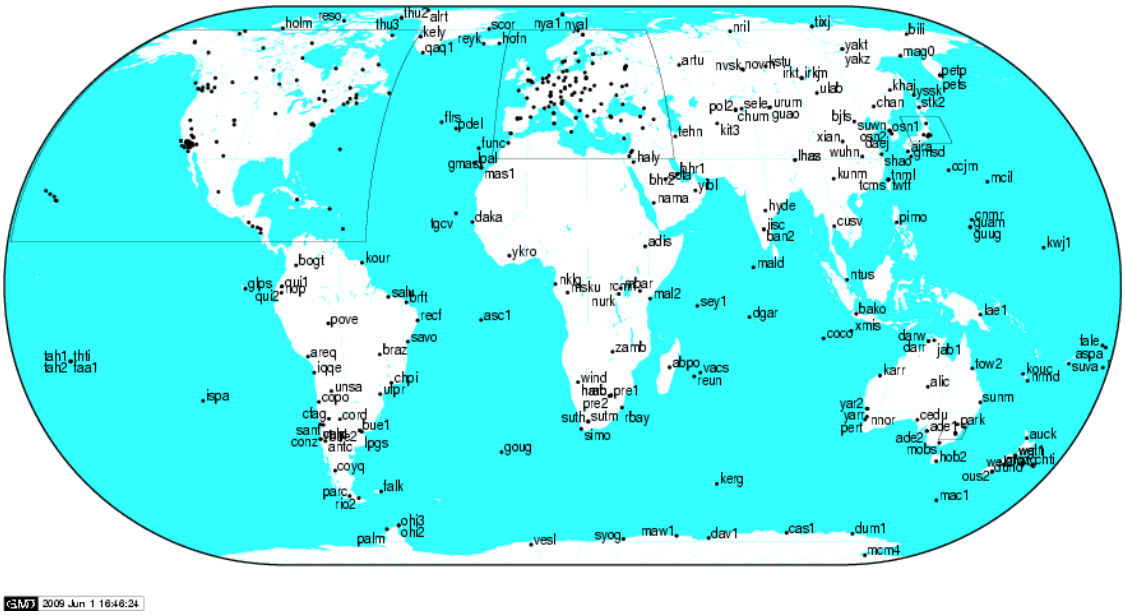

Figure 5.5 International GNSS Service (IGS) network map (Courtesy of the IGS)

This Chapter is concerned with determining if GPS water vapour measurements can be used for climate change applications. For this data back to 2001 in the UK is used and compared over 8-year time series against water vapour estimates from radiosonde data. From the analysis completed in Chapter 3 we now have the opportunity to bias correct the GPS and radiosonde on a site by site basis. This should be the most accurate method for reconstructing past time series of water vapour observations. We should then be able also to determine how accurate the bias corrections are by correlation of the reconstructed trends at the four UK sites used for comparison. Secondly, to truly remove all biases introduced with GPS processing changes over the last decade, a small network of European GPS stations were reprocessed by the author to identify any trends in the water vapour on a larger geographical scale. Finally the question of whether near real-time GPS water vapour estimates are accurate and stable enough to be used for climate studies, without the need of costly reprocessing campaigns, is addressed.

5.1 Bias Corrected Radiosonde and GPS IWV Time Series

For climate change studies it is essential to have a stable, long-term record of atmospheric water vapour as the distribution of global water vapour is a good general reflector of global temperature distribution. From previous studies (Emardson et al., 1998, Emardson et al., 2000; Gradinarsky et al., 2002), it has been demonstrated that reprocessed GPS data could be used for the determination of longer term climatic trends. From the Gradinarsky study in 2002 it was concluded, for the Nordic

region, that from 1993 to 2000 the amount of atmospheric water vapour was increasing, as current climate change theory would suggest, at a rate of approximately 0.1-0.2 kg/m^2 per year. To assess if this trend is still evident and indeed applicable to the UK, a long term GPS time series analysis was completed for four GPS sites in the UK collocated with operational radiosonde sites as used in Chapter 3 for the assessment of GPS/radiosonde bias. Based on the results of Chapter 3 we can apply site specific bias corrections to both the radiosonde and GPS water vapour estimates to remove any biases introduced with GPS processing changes or radiosonde instrument upgrades. The sites used for comparison in this study are Herstmonceux in East Sussex (HERS), Camborne in Cornwall (CAMB), Watnall near Nottingham (IESG) and Lerwick in Shetland (LERW). All of these sites were all installed over a decade ago, as such if any settlement of the GPS monument were to take place, it would be expected to have done so by now. Furthermore as the sites are well spread in latitude through the UK, any differences could indicate any latitude dependency of IWV trend.

Raw, uncorrected time series of both GPS and radiosonde IWV for all four sites are given as Figures 5.6 to 5.9. Data is plotted using whole annual data sets only to avoid any seasonal induced trends.

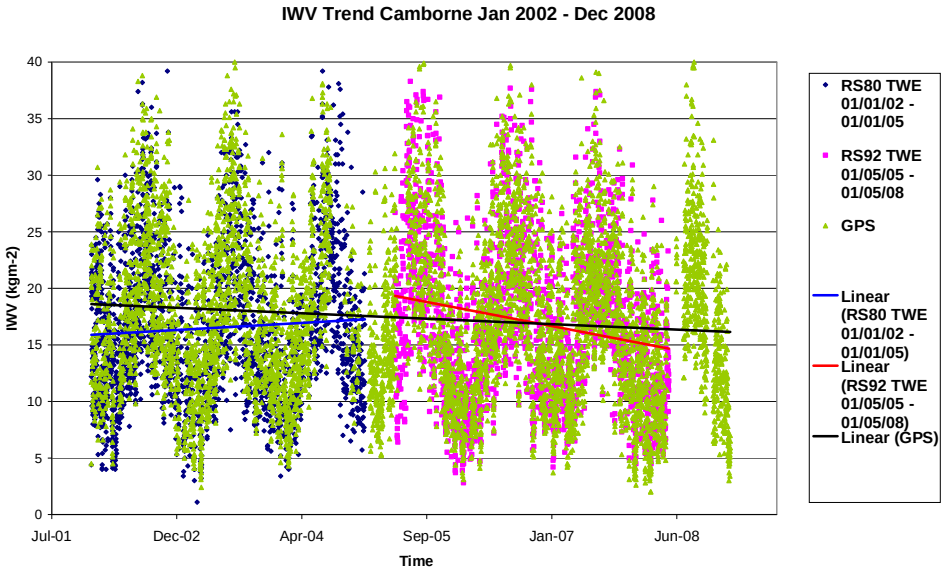

Figure 5.6 Raw Radiosonde and GPS IWV time series, Camborne, 2002 – 2008

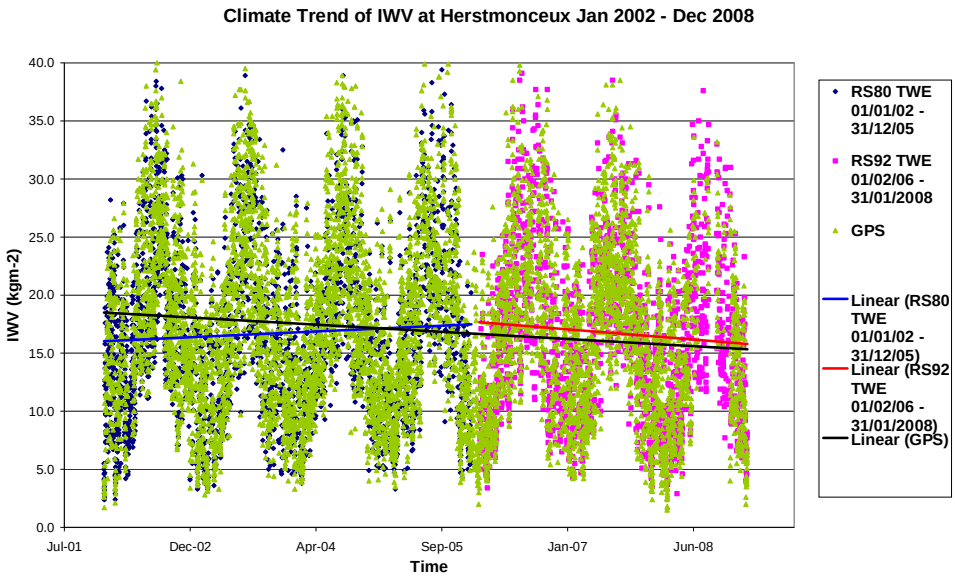

Figure 5.7 Raw Radiosonde and GPS IWV time series, Herstmonceux, 2002 – 2008

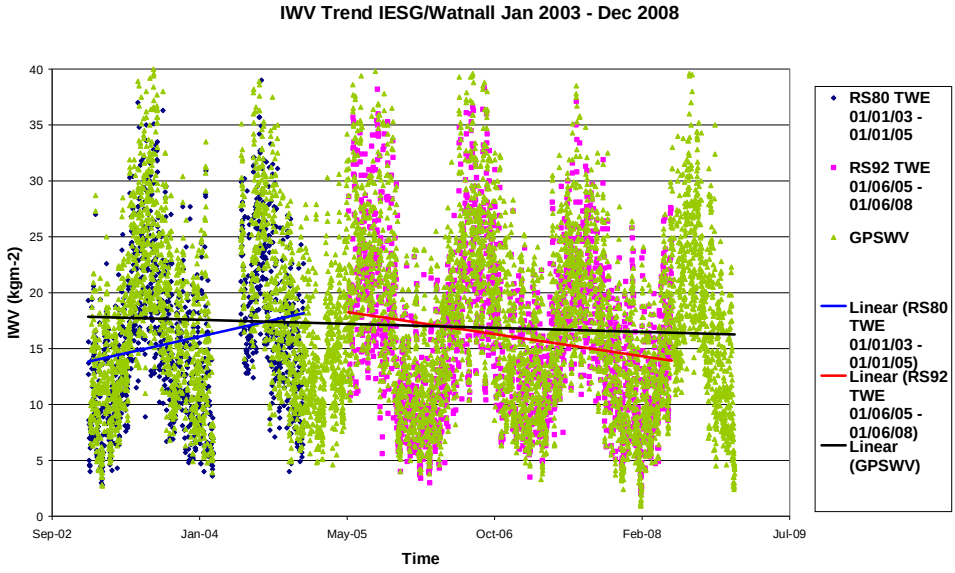

Figure 5.8 Raw Radiosonde and GPS IWV time series, Watnall/IESG, 2003 – 2008

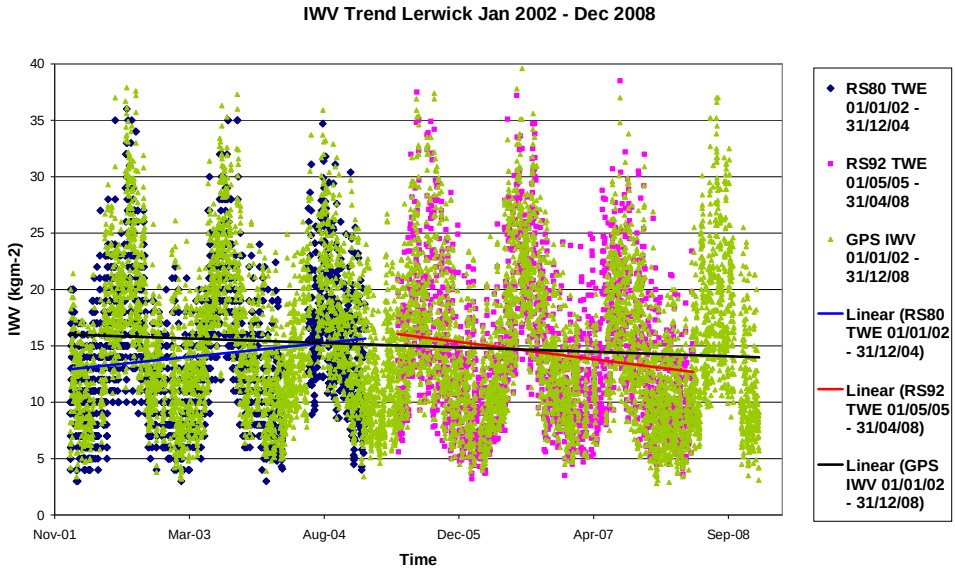

Figure 5.9 Raw Radiosonde and GPS IWV time series, Lerwick, 2002 – 2008

With the exception of Lerwick, all apparent trends in Figures 5.6 to 5.9 appear to be consistent with both the GPS and radiosonde time series showing a general increase in water vapour to ~2005 then a decrease since, and if a linear trend is plotted for the GPS time series we see an overall trend of water vapour decreasing by approximately 0.33 kg/m^2 per annum for Camborne for example. However from Chapter 3 we have seen that radiosonde instrument upgrades and changes in the GPS processing associated with the introduction of absolute antenna phase centre models can have had a profound impact on water vapour estimates. As such, to determine any long term climate trend in the data we must first bias correct the data according to the site specific biases calculated in Chapter 3. The bias corrections were applied to the data in a manner which made all data consistent with the most recent upgrades. Radiosonde data bias corrections were applied for the humidity sensor upgrade in July 2008, the temperature sensor upgrade in June 2007 as well as the RS80 to RS92 upgrade in ~2005. A correction was applied to the GPS time series to take account of the bias shift introduced with the upgrade to absolute antenna phase centre models in January 2007. A summary of the updates (Table 5.1) and biases at each stage of the radiosonde and GPS water vapour evolution (Table 5.2) are shown, as well as the bias corrections necessary to normalise all data to be consistent with the most recent GPS processing and most recent RS92 incarnation (Table 5.3).

Site	RS80 data from	RS92 from	AAPCV Since	New U	New T
Camborne/CAMB	June 2001	April 2005	Jan 2007	July 2007	July 2008
Herstmonceux/HERS	Jan 2002	Jan 2006	Jan 2007	May 2007	July 2008
Watnall/IESG	Jan 2003	May 2005	Jan 2007	June 2007	Aug 2008
Lerwick/LERW	June 2001	April 05	Jan 2007	June 2007	July 2008

Table 5.1 Overview of GPS processing and radiosonde upgrades during period of thesis

Site	RS80-GPS Bias (kg/m^2)	RS92 (Old T, Old U) - GPS (RAPCV) Bias (kg/m^2)	RS92 (Old T, Old U) - GPS (AAPCV) Bias (kg/m^2)	RS92 (New T, New U) - GPS(AAPCV) Bias (kg/m^2)	RS92 (new T new U) - GPS(AAPCV) Bias (kg/m^2)
Camborne/CAMB	-1.5033	-0.5075	+0.2896	+0.8323	+0.3975
Herstmonceux/HERS	-0.7838	+0.0134	+0.2918	+0.3803	+0.3118
Watnall/IESG	-1.8275	-1.2627	-0.6340	-0.9665	-0.3107
Lerwick/LERW	-1.2060	-0.5944	-0.5242	+0.6136	+0.2416
Mean Bias	-1.3302	-0.5878	-0.1442	+0.2149	+0.1601

Table 5.2 Overview of RS vs. GPS Bias evolution over the period of this thesis

Site	BC due to RS80 to RS92 (old U, old T)	BC due to introduction of new RS92 U sensor	BC due to introduction of new RS92 T sensor	RS92, New U, New T
Camborne/CAMB	+1.9008	+0.1079	-0.4257	0
Herstmonceux/HERS	+1.0956	+0.020	-0.0685	0
Watnall/IESG	+1.5168	+0.3233	+0.6658	0
Lerwick/LERW	+1.4476	+0.7658	-0.372	0

Table 5.3 Bias corrections due to radiosonde upgrades, normalised to most recent RS92

Bias corrections were applied to the whole time series of data for the four sites in the UK and the new data was plotted as time series in an attempt to identify any climatic trends. This data is presented as Figures 5.10 to 5.13. Again whole annual data sets are used to avoid any seasonally induced bias with all data starting on 1st of January and ending on the 31st of December.

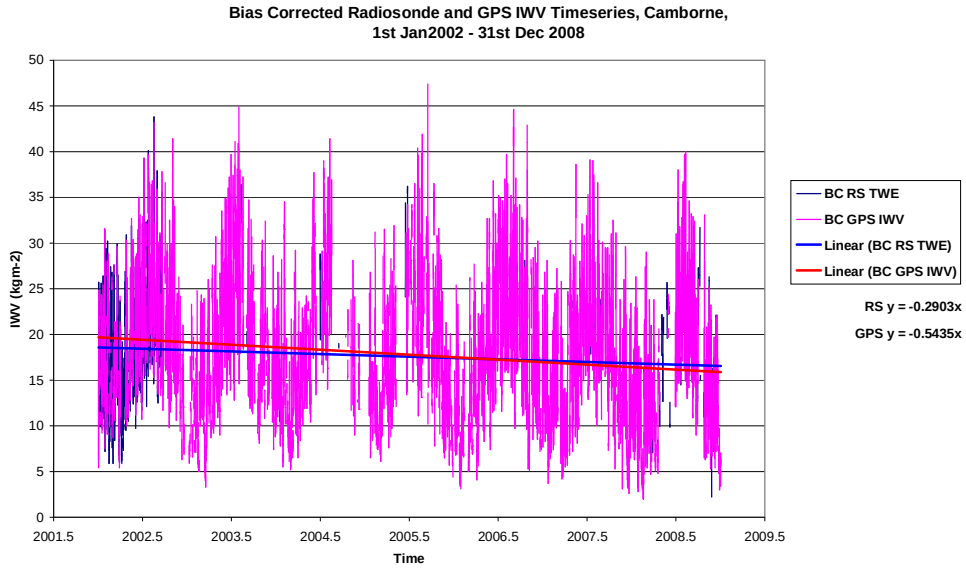

Figure 5.10 Bias corrected radiosonde and GPS IWV time series. Camborne 2002 – 2008

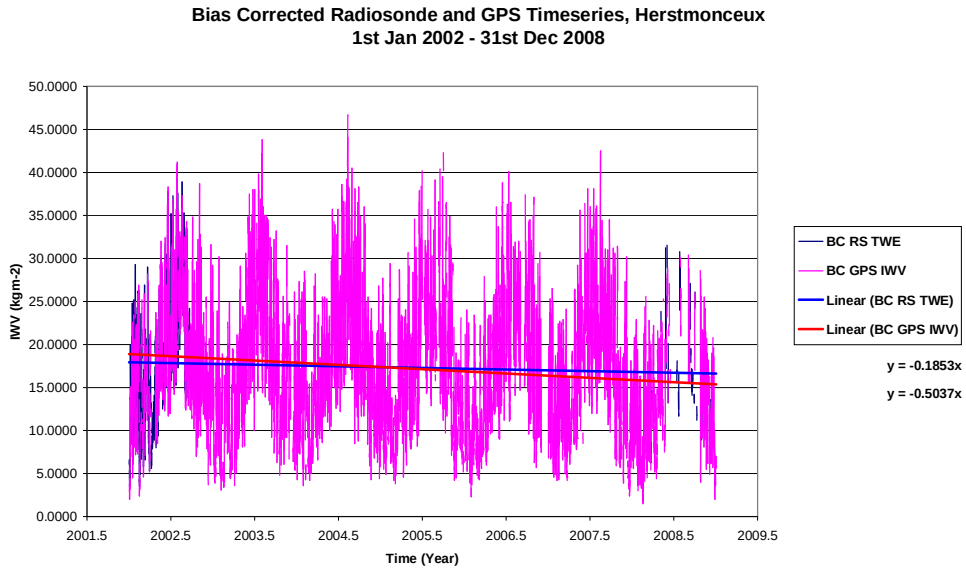

Figure 5.11 Bias corrected radiosonde and GPS IWV time series. Herstmonceux 2002 - 2008

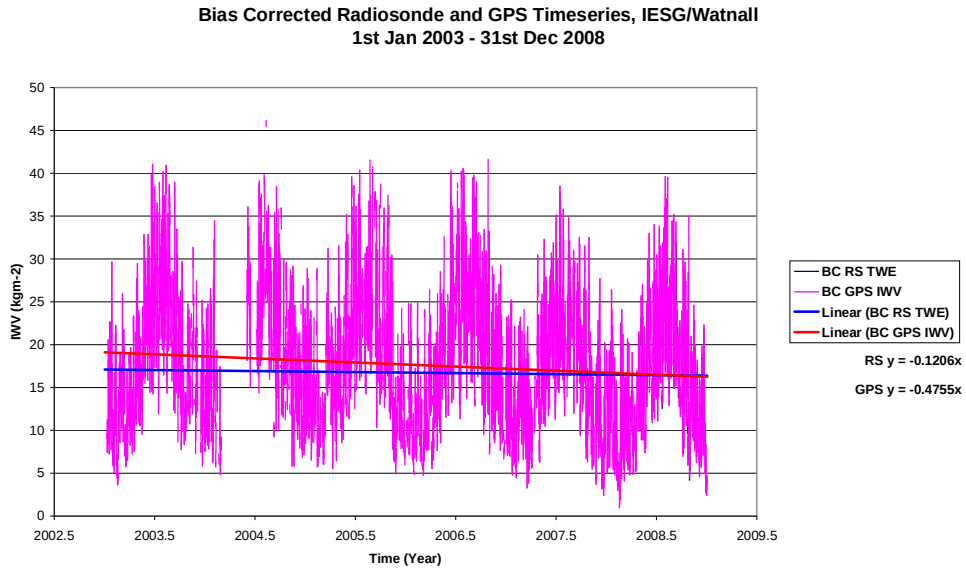

Figure 5.12 Bias corrected radiosonde and GPS IWV time series. Watnall/IESG 2003 – 2008

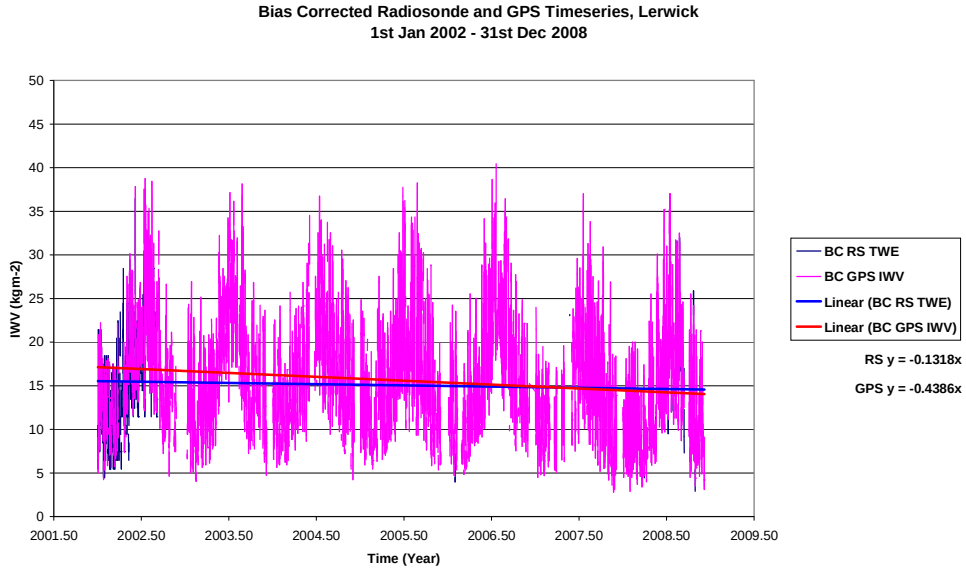

Figure 5.13 Bias corrected radiosonde and GPS IWV time series. Lerwick 2002 - 2008

As can be seen from Figures 5.10 to 5.13, we now see a slight negative trend in IWV data from both radiosonde and GPS data from all sites. It is important to remember that all data here has been bias corrected on a site by site basis with the data trained on the latest RS92 radiosonde and the latest GPS processing strategy. By comparison with the raw time series (Figures 5.6 to 5.9) we now see a consistent trend for all sites and no increase to 2005 then decrease since. This indicates the increase to 2005 is a radiosonde induced error relating to the RS80 to RS92 changeover. For all sites we now see a greatly reduced water vapour trend and this is summarised in Table 5.4.

Site	RS IWV Trend (kg/m^2 per year)	GPS IWV Trend (kg/m^2 per year)
Camborne/CAMB	-0.2903	-0.5435
Herstmonceux/HERS	-0.1853	-0.5037
Watnall/IESG	-0.1206	-0.4755
Lerwick/LERW	-0.1318	-0.4386

Table 5.4 Bias corrected annual IWV trends, 2002 – 2008

To assess whether there is a latitude dependency of the trends, annual water vapour trend is plotted against latitude in Figure 5.14. There does appear to be a vague latitude dependency with Camborne, the most southerly site exhibiting the greatest negative trend and Lerwick (the most northerly site) showing the least negative trend.

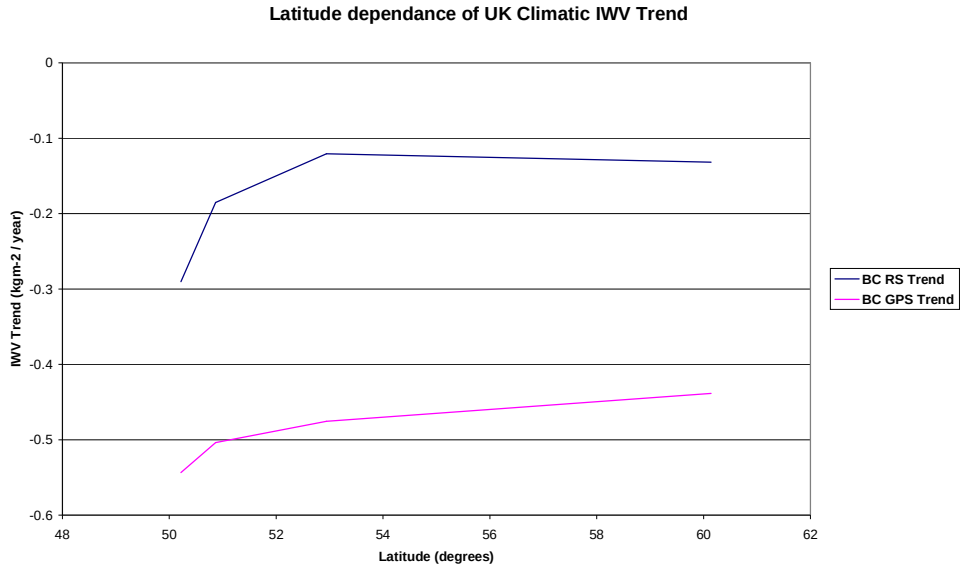

Figure 5.14 Apparent latitude dependency of negative IWV trend

To compare the apparent trend in IWV over the UK against temperature we can use the Central England temperature or CET record (Parker et al., 1992). Starting in 1659, the Central England Temperature Record is the world's longest continuous temperature record. The temperature is a monthly mean temperature based on three sites in the central UK. All sites are in rural locations to avoid biases introduced from urbanisation and are currently located in Hertfordshire, Staffordshire and Lancashire. The record does over-represent the warmer southern UK due to the locations of the sites and as such it cannot be used for comparison against Lerwick in this study. However the CET is a valuable guide to how temperatures have changed in the last 350 years for the UK and can be used in the context of this study to calculate the trend in IWV, per temperature change. Figure 5.15 is the whole CET time series.

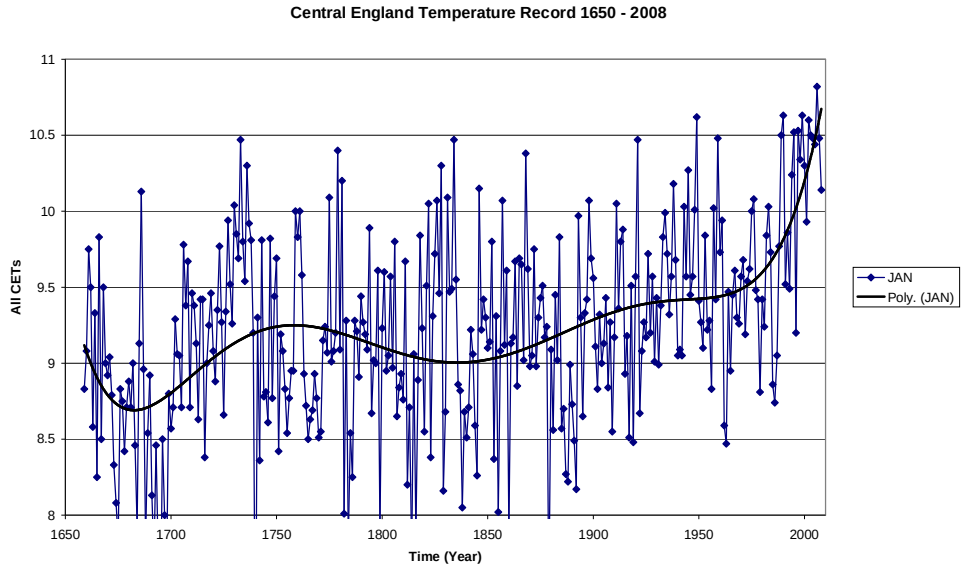

Figure 5.15 Met Office Hadley Centre CET Anomalies, 1772 - 2009

Although there is a clear signal in temperature in recent years from the CET record there has to be much doubt concerning the quality and bias of the observations prior to the mid-20th century as instrument technology has improved greatly over the last few decades. To eliminate instrument biases as far as possible, for the purposes of this study we only focus on data from a more recent timescale, from 1989 to 2009. The monthly mean CET data (^{o}C) from the last 20 years (1989 – 2009) is presented in Figure 5.16.

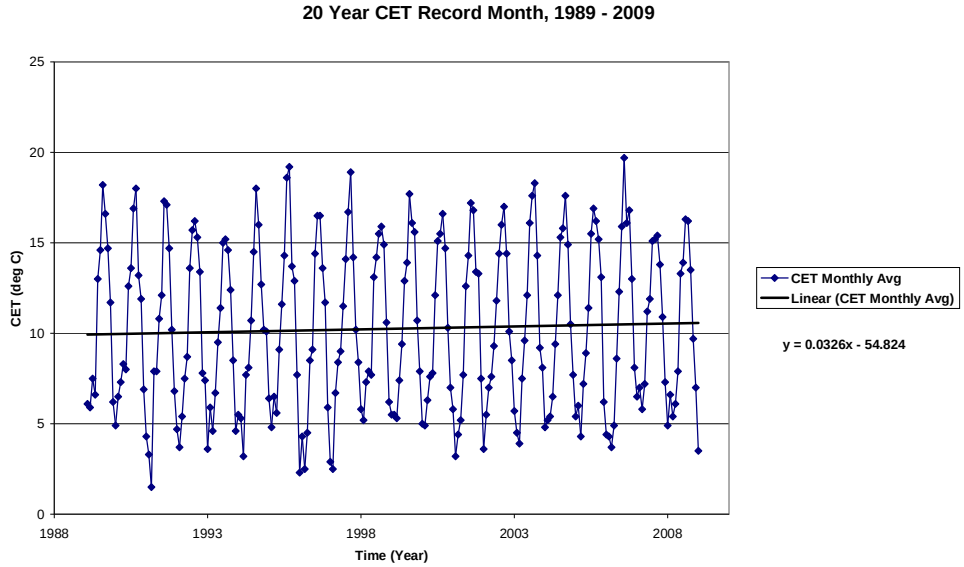

Figure 5.16 Monthly mean CET, 1989 – 2009

From Figure 5.16 we see a very small trend in increasing temperature over the UK over the last 20 years. When compared against the apparent decreasing water vapour trends calculated from bias corrected radiosonde and GPS estimates the results are very interesting as climate models generally predict a rise of atmospheric water vapour with increasing temperature. The bias corrections lead to similar trends at all sites in the UK which gives us confidence in the scale of the corrections. However, as good as a bias corrected reconstructed time series are, it is also possible to reprocess the entire time series of GPS data and account for changes that have occurred, for example relating to absolute antenna phase centre models

5.2 Reprocessed Climatological GPS Campaign

As stated above, the only way to truly remove processing changes in GPS data is to reprocess the whole time series. Only by reprocessing can we remove, as opposed to estimating, biases introduced with changes in GPS processing schemes. Apart form the change to absolute antenna phase centre models in January 2007, the effect on IWV of other more minor processing changes such as new OTL models can also be accounted for by a consistent reprocessing campaign.

Because reprocessing GPS data is a very time consuming process only a limited number of sites were chosen. The sites were chosen primarily for two main reasons. All sites are members of the EUREF permanent network (EPN), and as such are installed to geodetic standards. Also the sites were chosen because of their geographic spread across Europe. The aim of the reprocessing campaign was not so much to try and identify climate trends specifically for one geographic region or location, but more to try and identify water vapour trends on a European scale and in geographically diverse areas, and to compare the trends with those determined in Section 5.1. The sites chosen are shown as Figure 5.17.

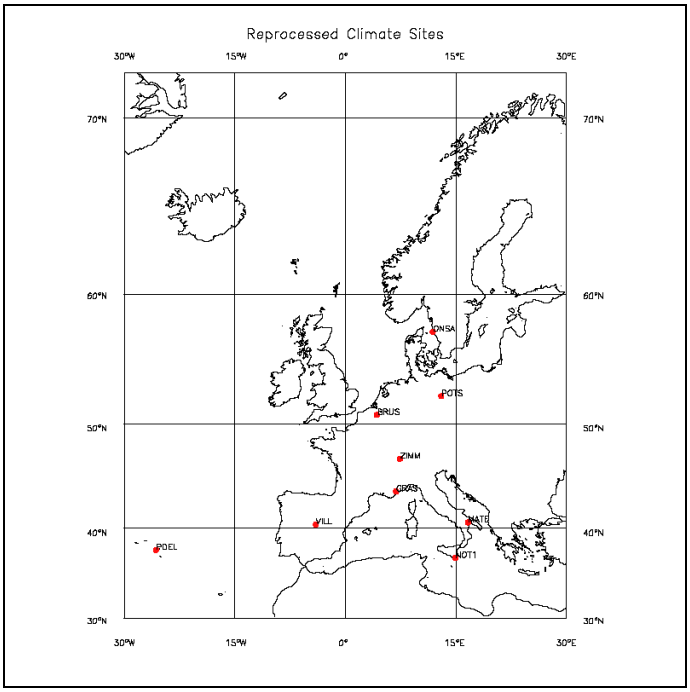

Figure 5.17 Map of sites in reprocessed climatological GPS campaign

The sites were reprocessed over an 8 year period from 1st January 2001 to 31st of December 2008 with the following processing parameters;

GPS Processing Software	Bernese v5.0
Strategy	Daily PPP
Orbits/Clocks	IGS Final Products
Antenna Phase Centres	Absolute
Ocean tide Loading Model	FES2004

Table 5.5 Overview of processing for reprocessed climatological GPS campaign

The decision was made not to convert ZTD to IWV for the reprocessing campaign. The decision was made on the basis that conversion to IWV would only introduce errors in the data as over time a number of different temperature and pressure sensors would have been used, for which biases would have had to been individually estimated.

The resulting reprocessing campaign output over 630,000 hourly ZTD estimates for the 9 sites over the 8-year period. Data was thinned by only using data from hour 12:00. This was chosen as it was a mid-point in the daily processed data set and would give consistent quality ZTD estimates. Also the maximum daily ZTD would have been from around mid-day and would give the maximum values to estimate any climate trend.

Data was quality checked using the standard Bernese value of SIGMA U in the output files. All data with greater than 2 times the standard deviation from the mean were excluded. The resulting data was plotted and the apparent linear climate trend for all sites can be observed. The time series of consistently reprocessed ZTD is given for all sites as Figures 5.18 to 5.25 and the results and trends are summarised as Table 5.6. Also in Table 5.6 are presented the Sigma U StDev after the outlier removal has taken place which gives an indication of ZTD quality over the reprocessed campaign for each site.

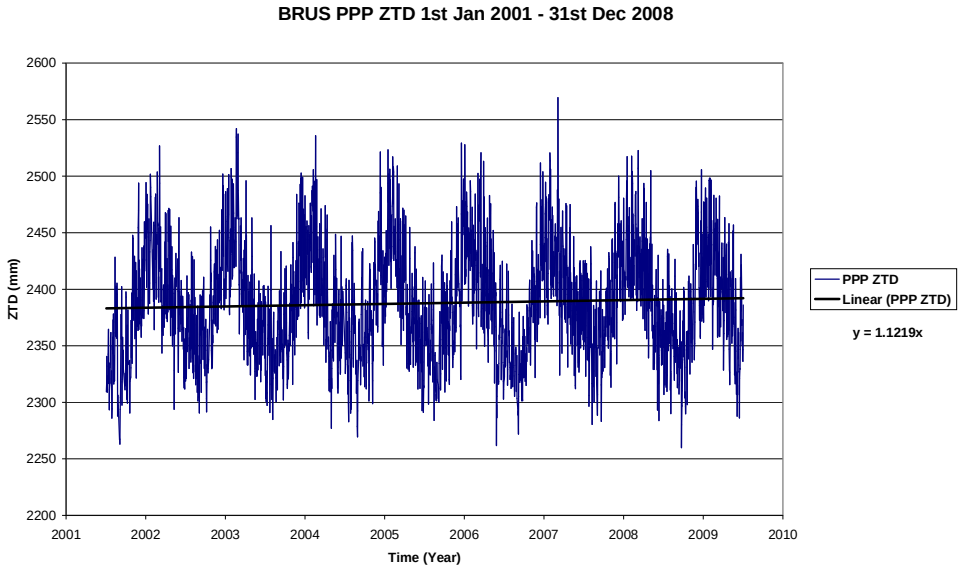

Figure 5.18 Reprocessed PPP ZTD time series. BRUS 2001-2008

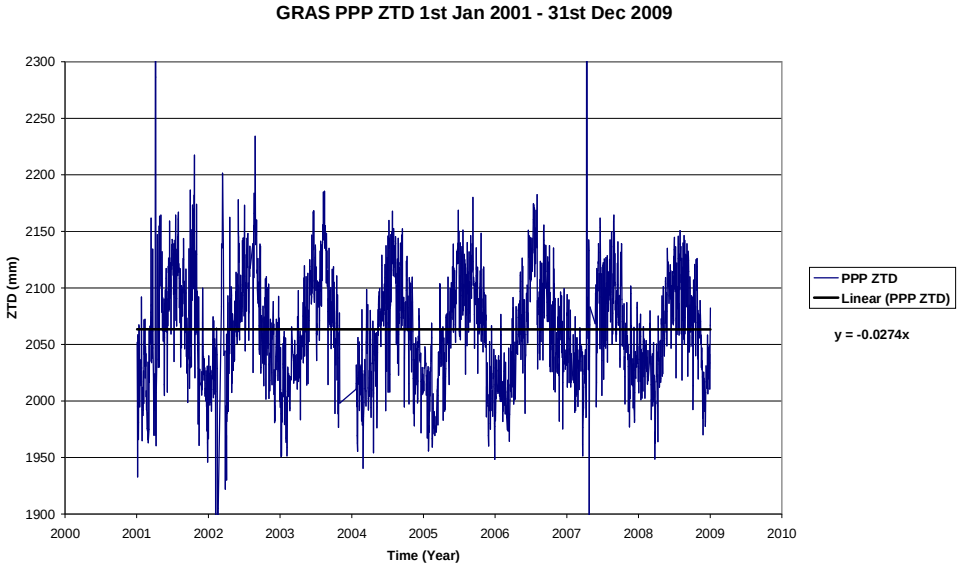

Figure 5.19 Reprocessed PPP ZTD time series. GRAS 2001-2008

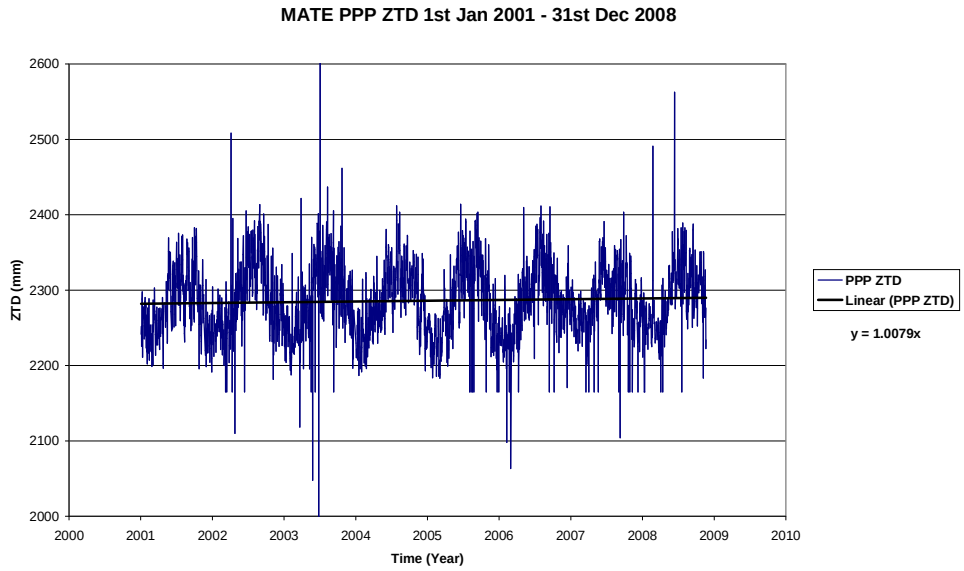

Figure 5.20 Reprocessed PPP ZTD time series. MATE 2001-2008

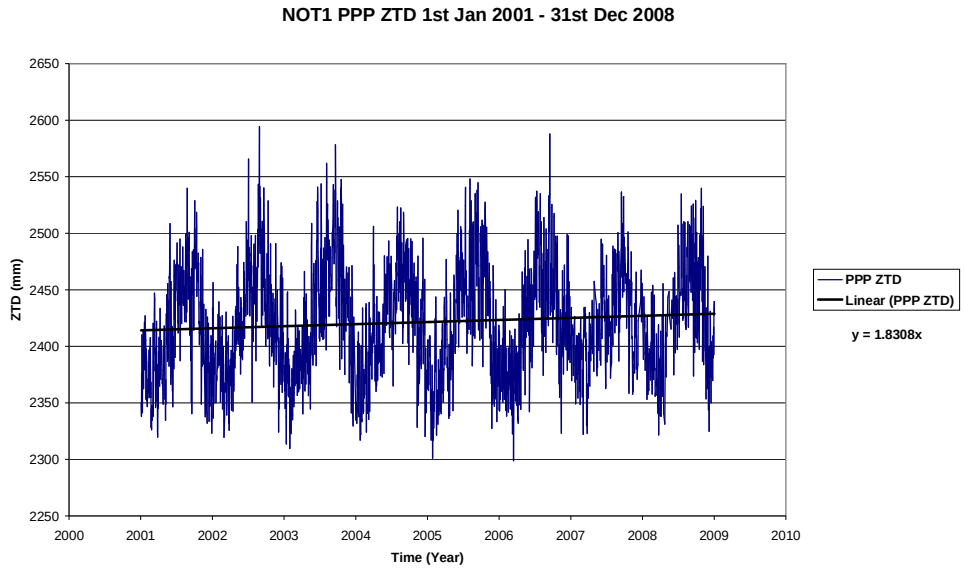

Figure 5.21 Reprocessed PPP ZTD time series. NOT1 2001-2008

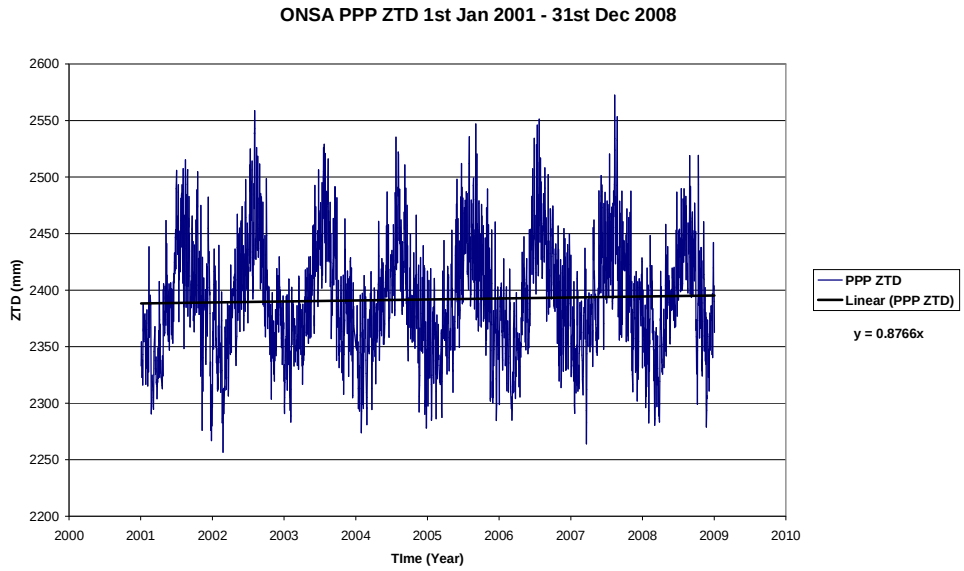

Figure 5.22 Reprocessed PPP ZTD time series. ONSA 2001-2008

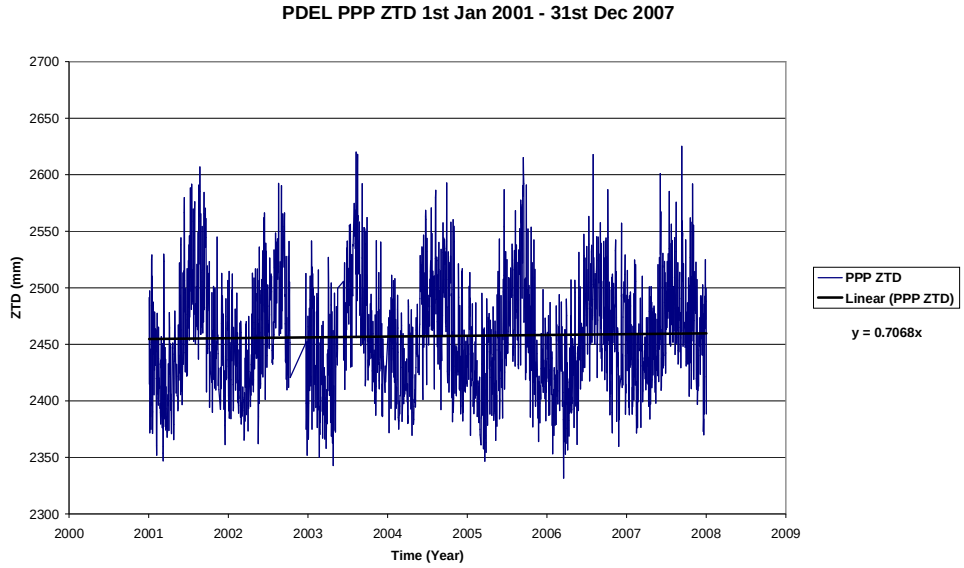

Figure 5.23 Reprocessed PPP ZTD time series. PDEL 2001-2007

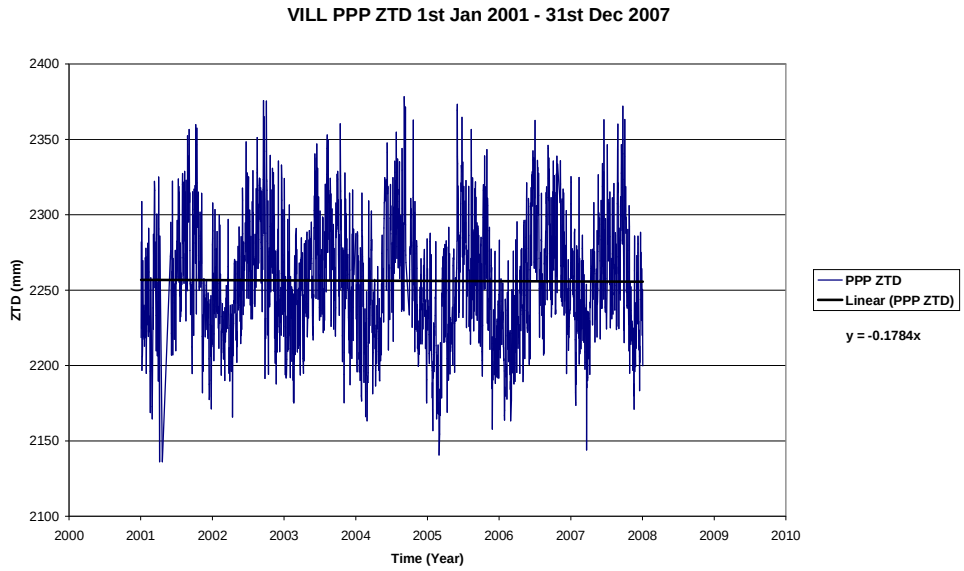

Figure 5.24 Reprocessed PPP ZTD time series. VILL 2001-2007

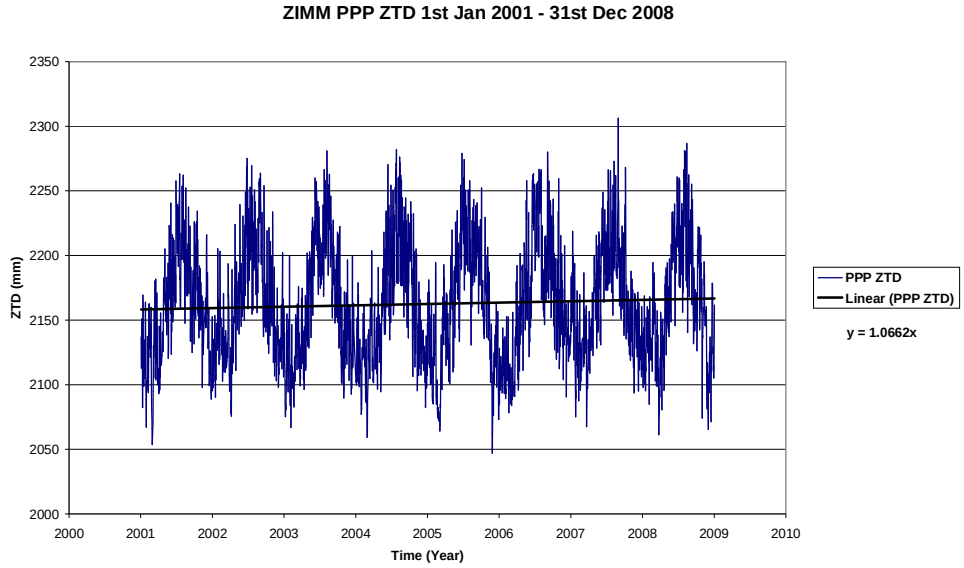

Figure 5.25 Reprocessed PPP ZTD time series. ZIMM 2001-2008

Site	Observations	StDev Sigma_U (mm)	Annual ZTD Trend (mm/yr)
BRUS	2841	0.1148	+1.1219
GRAS	2652	0.1947	-0.0274
MATE	2720	0.1041	+1.0079
NOT1	2722	0.0993	+1.8303
ONSA	2851	0.0932	+0.8766
PDEL	2332	0.1035	+0.7068
POTS	2468	0.0730	+1.0521
VILL	2391	0.1226	-0.1874
ZIMM	2859	0.1232	+1.0662

Table 5.6 Overview of climate trend at all reprocessed sites

From Table 5.6 it can be seen that with the exception of GRAS and VILL, all other sites have a positive trend with NOT1 having the largest positive trend of 1.8303mm/yr. To assess this trend further, a moving average trend line was applied to the time series and the results plotted as Figure 5.26. From the plot we can see that the maximum (summer) ZTD is actually decreasing, and it is the winter minimum which is actually increasing bringing up the mean ZTD as a whole. This shows that even though the overall ZTD trend is positive, the maximum ZTD values are either stable or decreasing.

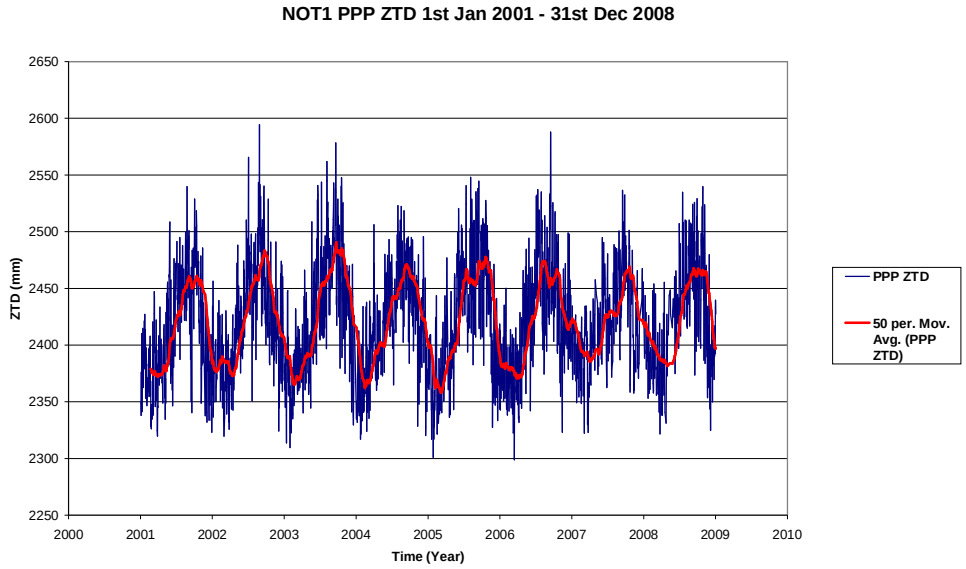

Figure 5.26 7-year ZTD trend, NOT1 with moving average trend line

In order to assess how much of the overall increasing ZTD trend is due to the minima and maxima trends, monthly mean ZTD for NOT1 was calculated and the month with the highest mean ZTD and lowest mean ZTD were identified. From the data, plotted as Figure 5.27, we can see even more clearly that it is the increasing ZTD minima, which is governing the trend of increasing ZTD.

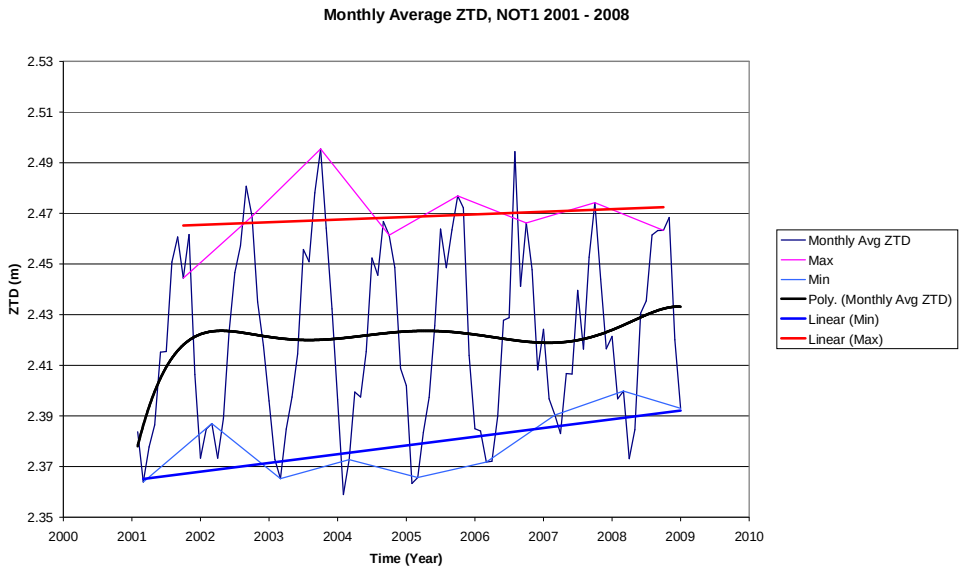

Figure 5.27 Mean monthly ZTD, NOT1, 2001 – 2008

The largest negative trend was observed from VILL in Spain with a drying trend of -0.1874mm/yr. The drying of some sites in this reprocessing campaign along with the apparent drying of the sites in the UK indicate that water vapour is not increasing all over Europe. Instead we may have some areas becoming moist whilst others are actually stable or drying. The trends from the reprocessing campaign are plotted on a map of Europe to assess their spatial distribution in Figure 5.28.

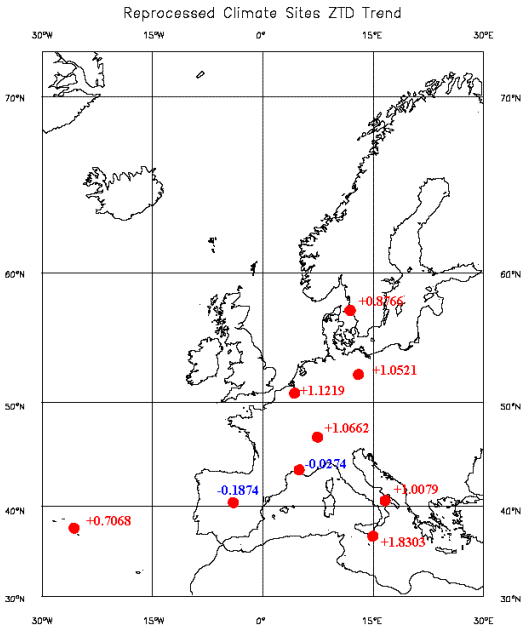

Figure 5.28 Map of reprocessed sites ZTD trends

So, it has been demonstrated here that reprocessed GPS data can indeed provide us with climatological trends in atmospheric delays which are in turn dictated mainly by changes in atmospheric water vapour. The other possibility, of course, is to use the wealth of data which is currently being processed in a near real-time manner to form time series, but the question is whether it is appropriate to do this?

5.3 NRT GPS Water Vapour for Climate Applications

As we have concluded, reprocessed GPS ZTD data does have its use in monitoring climate change. However, depending on the quality of near real time GPS ZTD and IWV this also may be useable for climate applications. If it is, it would remove the need for long, time consuming reprocessing campaigns. To assess the quality of NRT GPS data, the reprocessed PPP data is compared to the NRT data produced by the Met Office (METO) automated processing system. Hourly data is compared for all reprocessed GPS sites and further decimated to leave only the 12:00 ZTD estimates for all reprocessed sites used above for 2008. Of the sites reprocessed for the climate study, PDEL and POTS did not have enough NRT data to make any worthwhile comparison and as such they are excluded from the analysis. Coincident data points are compared and outliers are removed using the 2σ approach as used in Section 5.2. The results from the comparison are shown in Table 5.7.

Site	Observations	PPP-NRT Mean ZTD Bias (mm)	PPP-NRT Mean ZTD StDev (mm)	Scatter Plot Correlation
BRUS	225	2.4817	3.2481	0.9788
GRAS	212	2.6671	3.6942	0.9777
MATE	181	3.3134	6.0195	0.9555
NOT1	189	3.7120	5.5944	0.9621
ONSA	204	1.2233	2.6230	0.9900
VILL	140	3.0218	4.5476	0.9629
ZIMM	211	2.4582	4.3744	0.9751

Table 5.7 Results from long term comparison of post processed PPP ZTD against NRT DD ZTD

As can be seen from Table 5.7, there is a consistent bias for all sites with the PPP always estimating higher ZTD than the near real-time DD. The range of bias however is small with the maximum bias identified for the site NOT1 of ~3.7mm ZTD. This is consistent with comparisons carried out in Chapter 3 where PPP data as processed by GFZ does seem to over estimate atmospheric delay when compared to DD processed data.

Overall however the results were generally in very good agreement, with a linear trend drawn for all coincident data ranging 0.9555x for MATE up to 0.99x for ONSA. This indicates that although there is bias in the data, for the purpose of climate applications, NRT data could be of sufficient quality. Scatter distribution plots for ONSA and MATE are given as Figures 5.29 and 5.30 respectively.

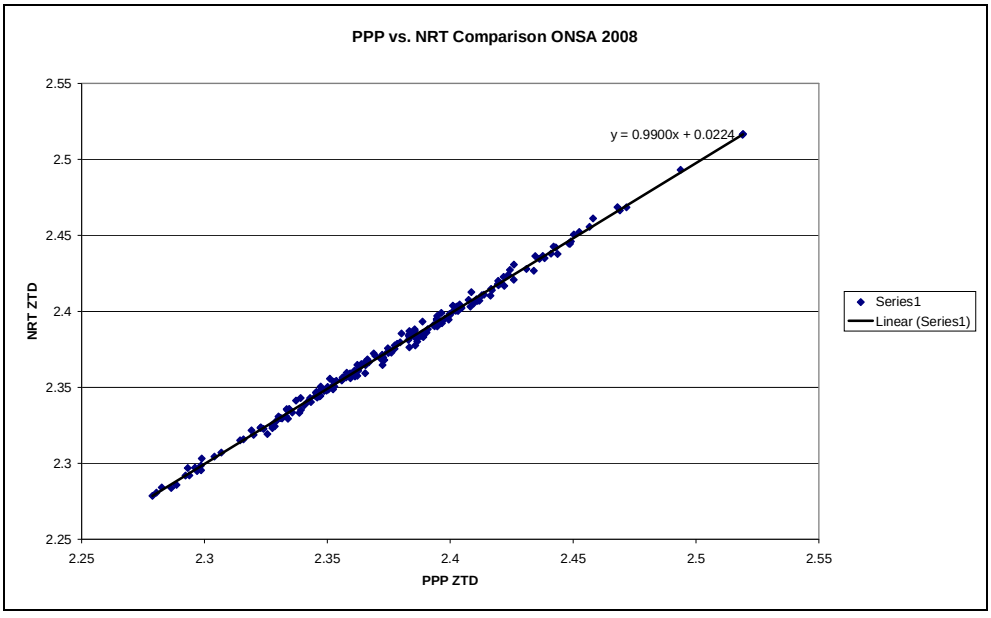

Figure 5.29 PPP ZTD vs. NRT ZTD scatter plot, ONSA, 2008

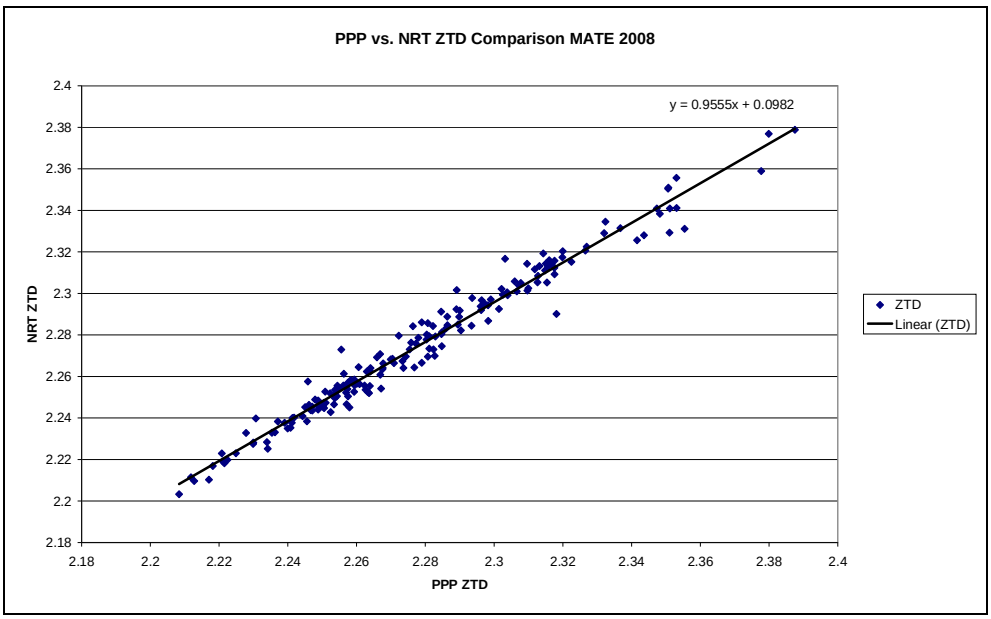

Figure 5.30 PPP ZTD vs. NRT ZTD scatter plot, MATE, 2008

To assess whether NRT GPS data is indeed suitable for climate applications without the need of reprocessing, we need to assess what impact instrument changes have on the ZTD time series. It is well known in the geodetic community that the introduction of a new antenna type can have an impact on coordinates but what, if any impact on ZTD can an antenna change have needs to be addressed here, to assess if NRT ZTD data sets can be used without the need of bias correction when a new antenna model is introduced. Fortunately all data relating to instrument changes is recorded by EUREF and is available in station log files through the EUREF website.

As can be seen from Table 5.8 a number of GPS sites have had the same antenna from the beginning to the end of the reprocessing campaign (BRUS, NOT1, ONSA and ZIMM), however there are also a number of sites (GRAS, MATE and VILL) which have had antenna changes during the period of reprocessing. To assess the impact on ZTD of the introduction of a new antenna type, we can compare GPS against NWP (the HIRLAM 11km model in this case) to assess if any ZTD bias shifts occurred at the time of antenna replacement. NWP data for MATE was not available in the database for the period of antenna change and as such must be omitted from the analysis. Bias against the HL11 model for GRAS and VILL was computed for the 30 days prior and post the antenna change and the results are plotted as Figures 5.31 to 5.36.

Site	Antenna Type	S/N	Radome	Date Antenna Installed	Date Antenna removed
BRUS	ASH701945B_M	CR519994604	None	2000-04-27T12:15z	N/A
GRAS	AOAD/M_T	219	None	1996-10-03	2003-04-22
	TRM29659.00	0220256858	None	2003-04-23	2004-10-20T11:00z
	ASH701945E_M	24222	None	2004-10-21T09:00z	N/A
MATE	TRM29659.00	10516	None	1999-06-18	2008-11-24
	LEIAT504GG	200668	None	2008-11-24	N/A
NOT1	TRM29659.00	11724	None	2000-09-15	N/A
ONSA	AOAD/M_B	020	OSOD	1999-02-02	N/A
VILL	AOAD/M_T	200	None	1994-11-12	2004-09-28T10:00z
	AOAD/M_T	152	None	2004-09-28T12:00z	2006-11-29T09:00z
	AOAD/M_T	CR620045041	None	2006-11-29T10:00z	2007-04-18T08:00z
	AOAD/M_T	CR620045041	None	2007-04-19T07:00z	N/A
ZIMM	TRM29659.00	99390	None	1999-07-02	N/A

Table 5.8 History of antenna changes at reprocessed GPS sites (N/A indicates that antenna is still in operation at time of thesis)

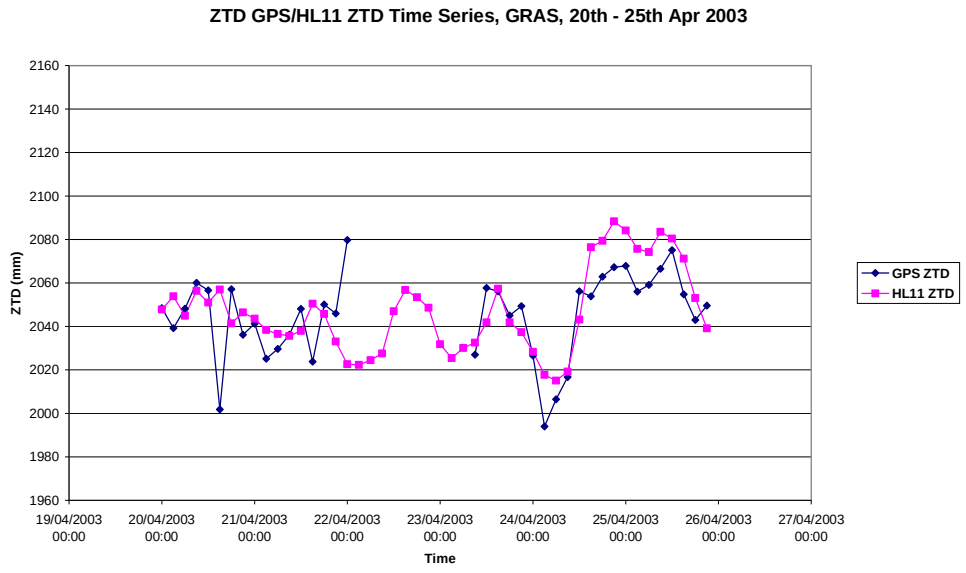

Figure 5.31 PPP ZTD vs. HL11 ZTD bias time series, GRAS, April 2003

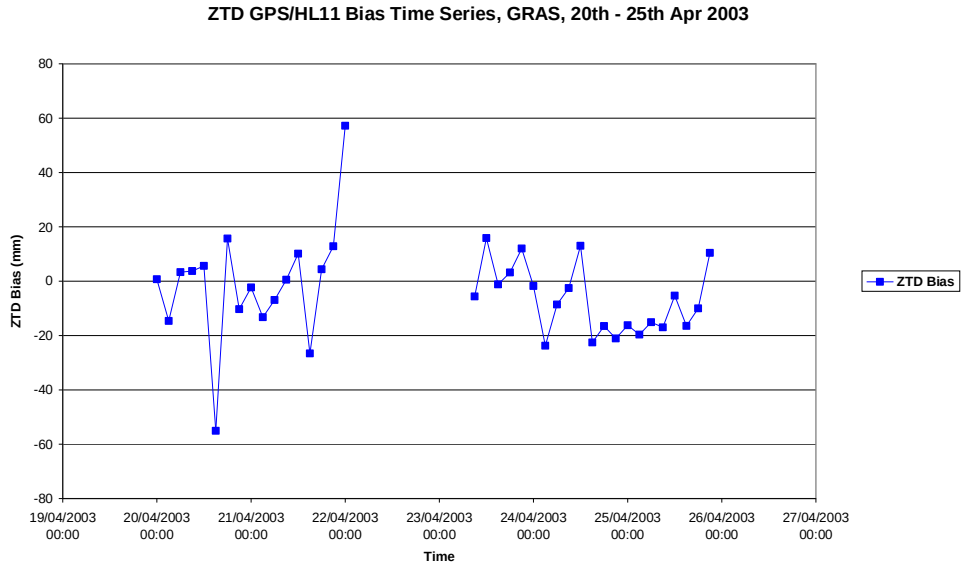

Figure 5.32 PPP ZTD minus HL11 ZTD bias time series, GRAS, April 2003

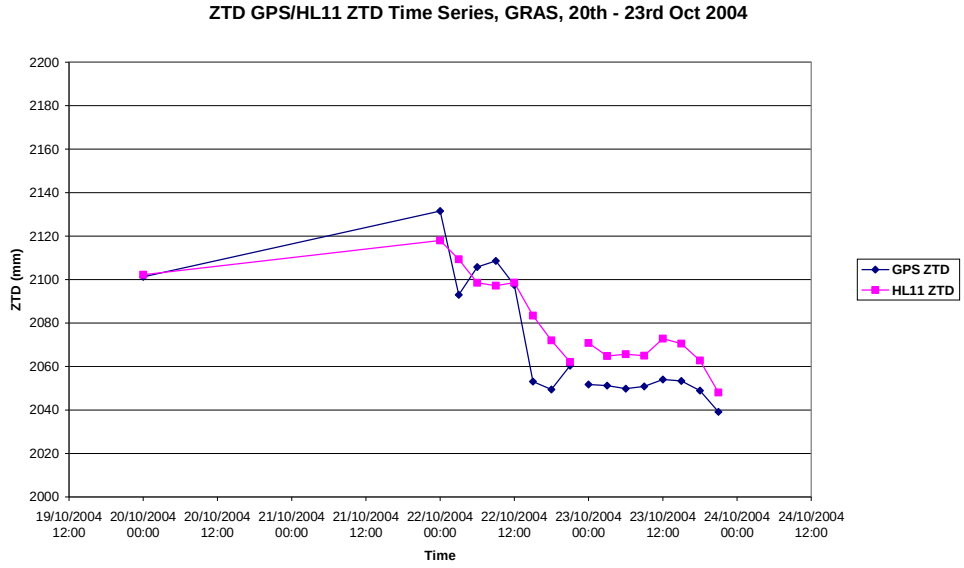

Figure 5.33 PPP ZTD vs. HL11 ZTD bias time series, GRAS, Oct 2004

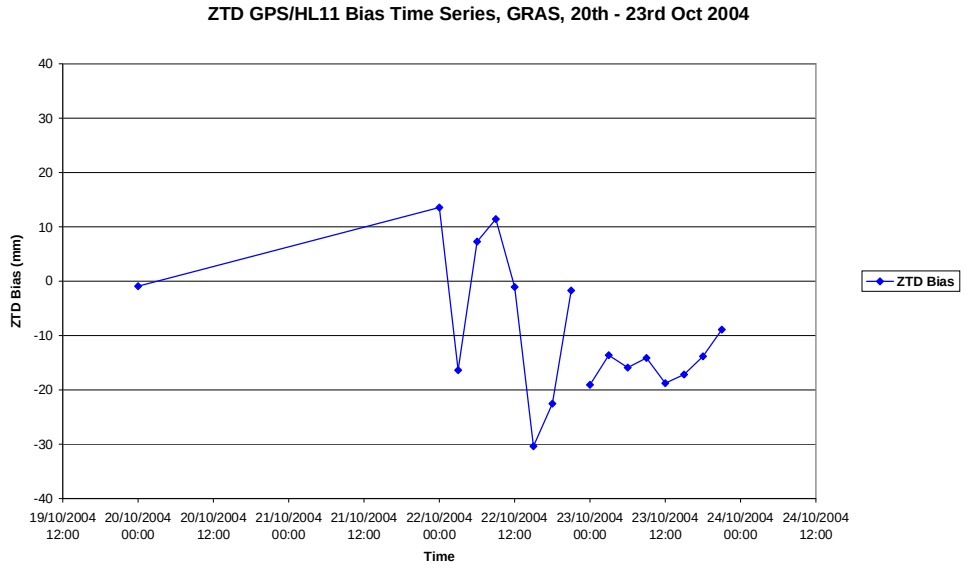

Figure 5.34 PPP ZTD minus HL11 ZTD bias time series, GRAS, Oct 2004

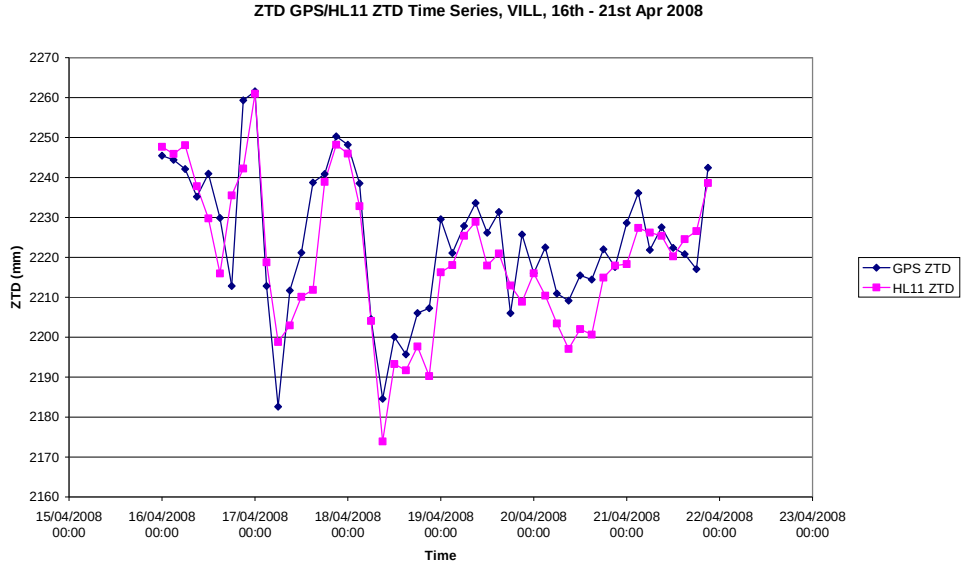

Figure 5.35 PPP ZTD vs. HL11 ZTD bias time series, VILL, April 2008

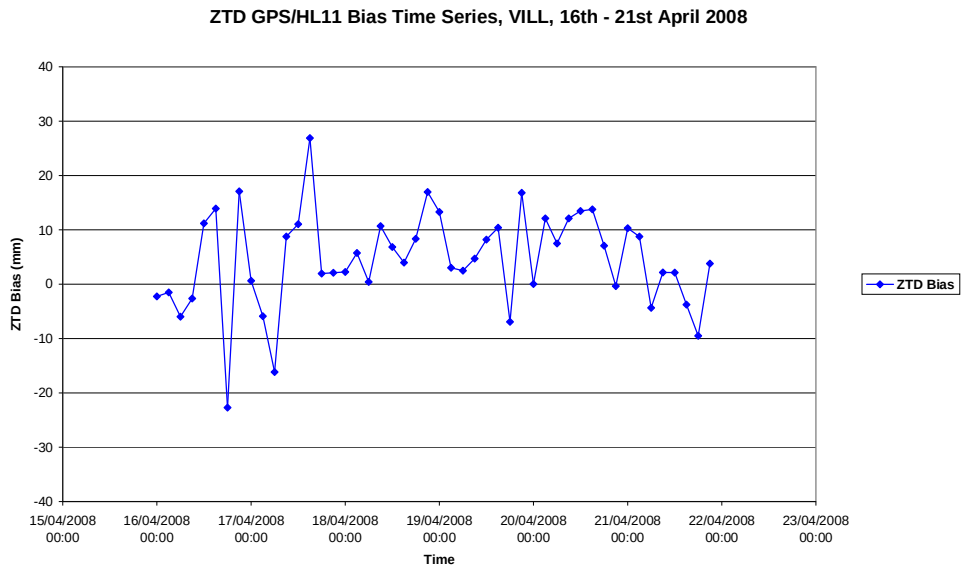

Figure 5.36 PPP ZTD minus HL11 ZTD bias time series, VILL April, 2008

If we compare the dates at which antennas were changed from Table 5.8 against the biases from Figures 5.31 to 5.36 we can see that there is no apparent bias shift with the introduction of a new antenna. This is consistent for all antenna changes for GRAS in either 2003 or in 2004, and for the antenna change at VILL in April 2008. This analysis suggests that antenna changes have a negligible effect on ZTD, and thus IWV. As such we may conclude that in the future, when GPS processing strategies become more fixed and consistent, near real-time GPS ZTD may indeed be suitable for climate applications, without the need for lengthy reprocessing campaigns.

5.4 Summary

In this section we have evaluated long-term radiosonde and GPS time series to assess their applicability as tools for monitoring climate change. From Section 5.1 we applied the site specific bias corrections determined in Chapter 3 to the four collocated GPS and radiosonde sites in the UK. Prior to correction we saw strong signals in the data with water vapour appearing to increase to ~2005 then showing a decreasing trend since, and furthermore the trends were not consistent across all sites. However when the site specific bias corrections were applied we saw generally very good agreement in the trends retrieved from the reconstructed time series data for all sites. All data then showed a consistent small decreasing trend in water vapour over the time periods used for re-analysis, with trends ranging from around -0.44 kg/m^2 to -0.54 kg/m^2.per annum for the four sites. The similarity in the reprocessed time series suggests the bias corrections are indeed correct, retrieving a consistent trend across the UK from four distinct sites.

When a set of high quality geodetic quality sites are reprocessed in a consistent manner we can clearly identify climate signatures. However, when the trends at the sites were compared, the trends were found to be far from consistent. Although there was an overall increase in tropospheric delay, this trend is not uniform with two out of the nine sites (GRAS and VILL) exhibiting an overall decrease in atmospheric delay over the reprocessed campaign. Also, when we investigate the overall increasing trend of the site showing the strongest increase (NOT1 with a +1.8303mm/yr trend) we see that although the overall atmospheric delay has increased, this is almost solely due to the winter minimum increasing with the maximum tropospheric delay parameters remaining relatively constant. From this we could conclude that it is the winters which are becoming more humid, and the summer time conditions are remaining almost constant over the campaign period.

The overall outcome from the reprocessing campaign was however, that reprocessed long time series of GPS derived atmospheric delay parameters should be a great source of information to the climate community. In order to confirm the trend seen here as well as to derive trends from other regions of Europe, a further reprocessing campaign should be undertaken, reprocessing a much denser European network, to see the true extent of the variation in climatic water vapour trends over Europe.

To assess the quality of near real time ZTD estimates versus a post processed routine, the results compare favorably. As such, the main problem with the use of NRT ZTD (and thus water vapour) is not so much the quality of the ZTD estimates, but as demonstrated in Chapter 3, processing changes over time as well as the meteorological data used for the ZTD to IWV comparison. Demonstrated here is the fact that while antenna changes have an impact on absolute positioning estimates, they do not have a noticeable effect on ZTD estimates. Thus we can conclude that if in the future, GPS tropospheric estimates are being derived from a near real-time processing system not undergoing any processing changes/updates, that data should also be sufficient quality to be used in climate applications.

Chapter 6 Conclusions, Outlook and Recommendations

Dense GNSS networks are now commonplace in many parts of the world, and as GNSS data is relied on more and more as a backbone to national infrastructure, spatial coverage is only going to increase. In regions such as Japan, North America and Europe dense GNSS networks are well established and have the potential to provide meteorology with a continuous stream of high quality water vapour estimates on a horizontal scale which is very useful to meteorology. In this Chapter the conclusions drawn from this thesis are presented as well as recommendations for future work in the field of GPS meteorology.

6.1 Conclusions

In Section 1.3 the objectives of this thesis were stated as answering two questions:

a) What is the true accuracy of water vapour estimates derived from networks of ground based GPS receivers when compared against NWP and other remote sensing instruments?

b) Are GPS signals effected by falling snow and can the errors be used for snowfall monitoring?

c) How well do near real-time GPS water vapour estimates represent real, short term atmospheric fluctuations?

d) Are 2D water vapour maps derived from networks of ground based GPS receivers useful of use to short-term forecasting?

e) Are estimates of tropospheric parameters derived from GPS networks suitable for climate science and are near-real time estimates of sufficient quality?

This section summarises the outcome of this thesis and demonstrates how these questions have been answered.

6.1.1 GPS Water Vapour Accuracy

In Chapter 3 a comprehensive review of all the main factors affecting biases both within GPS processing as well as biases between other instruments and numerical weather prediction models was presented.

Through the E-GVAP project the opportunity to assess data from a number of ACs using a variety of processing software and methods was demonstrated. On comparison, all ACs ZTD for the comparison period agreed well, but with those ACs using PPP typically under-estimating ZTD when compared to DD solutions provided by a number of other ACs by approximately 4mm. A comparison was also completed looking at the variability of NWP/GPS ZTD bias across Europe and a latitude dependant bias was identified. From comparison of GFZ and METO ZTD data against both the UK NAE model as well as against the European HIRLAM model, it appears that the bias is more likely to be related to the NWP model ZTD than within the GPS processing routines. Again there was a dry bias in the PPP GFZ solution, but as the same trends were observed when compared against both GPS solutions (which use different OTL models) the bias appears to originate in the NWP data. Furthermore the bias appears to be more pronounced when compared to the HIRLAM model. When the HIRLAM model is assessed in terms of its geographical coverage we see it has a smaller domain particularly to the South which could be the source of the added error.

To assess how well GPS data represents small scale atmospheric fluctuations a short time scale campaign was reprocessed a number of times using a variety of relative constraints limiting the random walk variability of successive water vapour estimates. When the resulting data is compared against a high resolution instrument such as a microwave radiometer at Payerne, Switzerland, it is clear that relative constraints do have a role in representing the real atmosphere. From the comparison study, it appears that the current operational constraint of 1mm is most likely too tight and limits GPS water vapour estimates from accurately representing smaller scale atmospheric fluctuations. The current limit on the amount of variability permitted in the solution is dictated by the operational targets at the UK Met Office relating to variability from NWP models. Due to NWP models' grid resolution being relatively coarse when compared to small scale phenomena such as smaller convective storms, NWP will never perform particularly well against sub-grid features until the grid resolution has been increased further. In the future with the advent of smaller scale models such as the UK 1.5km model, which should become the operational model for the UK in the next few years, we should have the ability to relax the constraints imposed on the GPS solutions and still get good agreement with NWP. Alternatively perhaps the optimum solution would be to have two GPS solutions. One, a tightly constrained solution for input into NWP with the other, a more loosely constrained solution for use in operational forecasting.

From the long term comparison against radiosonde data in the UK, a number of biases in the time series were identified and quantified. Firstly we saw the large improvement in RS-GPS bias with the introduction of the RS92 radiosonde in the UK, with mean biases improving from the order of around 1 kg/m^2 to around -0.5kg/m^2 with the newer RS92. Also with the transition from relative to absolute antenna phase centre models in the GPS processing we saw another large shift in bias of around 0.5 kg/m^2 taking the negative bias of around -0.5 kg/m^2 near to zero. However, since this time there have been two successive radiosonde upgrades which in turn have had their own effect on RS-GPS biases.

In conclusion, the importance of assessing each instrument and processing upgrade when trying to reconstruct a bias corrected time series for climate analysis cannot be underestimated, and it is clear that only from a study such as this it is possible to reconstruct site specific bias corrected radiosonde time series for the identification of climate trends.

In terms of trying to determine the absolute accuracy of GPS water vapour estimates, a number of comparisons against other remote sensing instruments were carried out. The results of the comparisons all displayed a common trend: water vapour estimates from GPS are lower than all other instruments used for comparison in this thesis. A dry bias in GPS exists even when compared against radiosondes, which historically have had a well known dry bias themselves. Since the introduction of the most recent incarnation of the Vaisala RS92 radiosonde we see a mean bias of around 0.3 kg/m^2 with the radiosonde measuring higher IWV than GPS. Again, from the annual comparison against the microwave radiometer at Payerne, Switzerland we saw a dry bias in the GPS compared to the WVR data, this time of around 2.5kg/m^2.

From the 2007 comparison at Izaña, we saw that the water vapour estimates from the CIMEL, FTIR and RS92 generally compare well with a relatively small overall spread of bias when compared against RS92 radiosonde data (~1 kg/m^2). When the GPS data is compared for the period in 2008 we yet again see a dry bias in the GPS water vapour estimates against all instruments, but this time with an even larger bias with the RS92-GPS bias is in the order of 3.3 kg/m^2. From the series of comparisons we can only come to one conclusion. Due to the fact that all other instruments used here for comparison estimate higher values of IWV than GPS, there seems to be overwhelming evidence that it is GPS which is in fact under-estimating atmospheric water vapour.

The question of whether falling snow affects GPS signals was also addressed. The study found that there was no correlation between falling snow and either the number of satellites observed or the signal to noise ratio.

Another very interesting point to come out of the comparisons was the importance of the meteorological data used for the ZTD to IWV conversion. Results showed that a more complicated interpolation of meteorological data could lead to large errors in IWV estimates if not monitored correctly. In the case study shown, biases of up to 15kg/m^2 IWV were observed by the introduction of non-representative pressure information. It was concluded that if water vapour data (as opposed to ZTD) is to be used for operational meteorology, a consistent approach needs to be developed to dictate where the meteorological data used for conversion is derived from. Only with a consistent approach will GPS IWV data be trusted by the forecasting community and thus used no an operational basis. Also when small scale fluctuations in IWV were assessed, hourly meteorological observations seemed to be valid for the whole hour for ZTD to IWV conversions. There do exist jumps in the IWV time series but the jumps are introduced by jumps in ZTD. Therefore it appears that producing smooth

transitions in ZTD between successive hourly campaigns is more of a limiting factor on deriving smooth, realistic IWV time series than the meteorological data which is used for conversion.

In summary we can say that:

a) GPS water vapour estimates are indeed of sufficient quality for operational use, however a dry bias does exist when compared against other remote sensing instruments which is worthy of further investigation

b) Falling snow does not affect GPS signals

c) The relative constraints imposed on the METO operational GPS solution are too tight to represent real atmospheric fluctuations, however at the present time the permitted variability of the GPS estimates is dictated by the NWP models which the data is going to be assimilated into. In the future with the advent of higher spatial resolution models a higher variability should be permitted

d) 2D water vapour maps derived from ground based GPS networks are indeed potentially very useful to the forecasting community, especially when used in conjunction with more traditional remote sensing instruments such as satellite water vapour estimates.

6.1.2 Applications of GPS Water Vapour for Forecasting and Climate Monitoring

The case studies presented in Chapter 4 give an overview of some of the conditions where the use of GPS water vapour maps could give new, previously unknown information to the forecaster. GPS water vapour fields were found to be able to identify smaller scale atmospheric features with the only limiting factor being the resolution of the GPS network itself. Aside from the identification of atmospheric features from GPS data alone, we saw how, when used in conjunction with other remote sensing instruments such as satellite water vapour, we were able to infer additional information such as a degree of vertical structure. The examples presented in Chapter 4 demonstrate how the GPS water vapour maps should be classed as a new observing instrument in their own right as when used in a network approach they can identify features which one GPS receiver alone could not identify.

With respect to the applicability of GPS water vapour for climate applications, we saw in Chapter 5 how when site specific bias corrections were developed (in Chapter 3) and applied to a long time series of data, it is possible to reconstruct a homogenous time series of radiosonde IWV data for the UK region. When the correct bias corrections were applied to radiosonde and to GPS data to account

for a number instrument changes and GPS processing changes, all sites' trends tended to agree very well. This leads to the conclusion that the bias corrections were in fact of the correct order and that the atmosphere in the UK is demonstrating a very slight drying trend over the period of study (2001 - 2009).

To truly remove as opposed to estimate biases in the time series, almost a decade's worth of GPS data was reprocessed producing over 630,000 ZTD estimates. Data was then thinned for ease of data manipulation leaving only the 12:00 ZTD estimates. From the reprocessed time series we saw that although much of Europe does show a positive ZTD trend, it is by no means uniform across Europe with two sites in Southern Europe actually exhibiting a drying trend, consistent with the UK. It can be concluded, therefore, that GPS does have a role to play in monitoring climate change and further, wider campaigns will be able to determine climate trends in more detail and over wider geographic regions.

When assessing the suitability of NRT GPS data for climate use, we firstly could conclude that there is very little bias between a NRT and a post-processed solution. To asses the impact of changes such as antenna replacement in the NRT time series we compared the GPS estimates against the HIRLAM 11km NWP model for periods prior and post antenna upgrade and found that there was no noticeable effect on ZTD. However, from the results of the analysis assessing the impact of the introduction of absolute antenna phase centre models we know that GPS processing model can have a large impact on IWV estimates. As such it was concluded that in the future when GPS processing strategies become more fixed and consistent, near real-time GPS ZTD may indeed be suitable for climate applications, without the need for lengthy reprocessing campaigns.

In summary we can say:

a) Atmospheric parameters derived from ground based GPS networks are indeed of sufficient quality for climate applications providing data has been processed in a consistent manner
b) Near real-time GPS water vapour estimates are also of sufficient quality for climate applications providing no processing changes have occurred in the time series
c) Antenna changes, whilst very important for coordinate time series are not of particular concern for climate monitoring of atmospheric parameters derived from GPS networks

6.2 Outlook and Recommendations

From the quality assessment carried out in Chapter 3 we determined that the GPS estimates are consistently lower than all other remote sensing instruments. To identify the source of the bias, it is recommended that data from a number of sites is reprocessed, possibly within the E-GVAP project

with a variety of processing options. Only by reprocessing the same data with different options can we identify where the source of the bias lies in the GPS processing and which processing models lead to the most accurate estimates of ZTD and IWV. Furthermore much care needs to be taken to use surface observations from as close to the GPS site as possible and maybe NWP data would be the best source for accurate surface parameters. Modern NWP schemes can predict surface pressure to an accuracy of around 2hPa which would lead in turn to errors in the region of around 0.5kg/m^2 IWV in most environments, which is certainly better than using poor quality surface data leading to errors as large as 15kg/m^2 which were observed in Section 3.6. Also, it is recommended that further assessment of GPS water vapour estimates at high altitude is carried out to assess the apparent large dry bias observed at Izaña, Tenerife.

GPS water vapour maps are, as was demonstrated, of great potential use to short term weather forecasting. However, it would make more sense to provide the forecaster with bias plots to help in the identification of areas where the model is over or under-estimating ZTD or IWV when compared to GPS estimates. The forecaster already has satellite and NWP water vapour fields and it might be of more value to the forecaster to display a 'divergence from the model field' as opposed to just another water vapour field image. Another potentially useful product might be plots of the rate of change in IWV as opposed to the IWV values directly. A plot such as this could indicate convective instability and might draw the forecaster attention to areas of interest.

Another point to note is that for the usefulness of water vapour maps to be fully realised, the data will have to be presented to the forecaster with a far shorter time delay than they are currently available. Under the current typical processing scheme, water vapour data is output, assuming an hourly batch processing method, with a time delay of between approximately 40 and 100 minutes from time of observation (relating to the end of the hour of observation and the start of the hour of observation respectively). If the time delay is to be brought down to a level where the water vapour data was to be considered near real-time by the forecaster, sub hourly processing routines would have to be adopted. With the advent of real time data transfer systems such as NTRIP, real time raw GPS data is widely available. One E-GVAP AC has already developed a test solution (KNM1 in the Netherlands) processing data in 15minute batches as opposed to the more commonly processed hourly batch. The solution is based on a longer period processed but time-slipped forward by 15minutes for successive processing solutions, with initial results appearing favourable with no apparent loss in data quality.

It has been demonstrated in Chapter 5 that GPS data is indeed suitable for climate applications. The added benefit of using GPS data is that water vapour may be estimated for anywhere where a GPS receiver is installed which is a far more cost effective solution than installing a microwave radiometer or radiosonde for example. Furthermore, as with GPS meteorology in Europe, the vast majority of observations are derived not from meteorological equipment but from that owned by geodetic and

mapping agencies, made available through a variety of agreements. If such a project as E-GVAP could be established on a Global scale, high quality humidity data from literally thousands of points around the World could be retrieved in near real-time for use in numerical and climate model analysis. If we look at the Pacific region for example we see that for an area which covers almost half the Globe there are only currently only around 22 IGS stations. Due to the use of GPS in national infrastructure and mapping, the number of GPS sites in the Pacific region must be far greater than just the IGS sites and if access to the raw GPS data can be facilitated, the impact to meteorology could be great. Not only could GPS water vapour have a role in providing near real-time humidity information to Global models but could be of particular importance in conventionally data sparse regions of the world.

GPS offers a robust and relatively cheap tool for the retrieval of accurate and continuous water vapour estimates and access to such observations can only be a positive thing for weather forecasting.

References

Alexandrov, M. D., A. Marshak, B. Cairns, A. A. Lacis, and B. E. Carlson, 2004: Automated cloud screening algorithm for MFRSR data, Geophys. Res. Lett., 31, 4, L04118, doi:10.1029/2003GL019105.

Alexandrov, M. D., B. Schmid, D. D. Turner, B. Cairns, V. Oinas, A. A. Lacis, S. I. Gutman, E. R. Westwater, A. Smirnov, and J. Eilers, 2009: Columnar water vapor retrievals from multifilter rotating shadowband radiometer data, J. Geophys. Res., 114, D02306, doi:10.1029/2008JD010543.

Askne, J., and H. Nordius, 1987: Estimation of tropospheric delay for microwaves from surface weather data, Radio Sci., 22(3), 379–386.

Atkins, N. T., and R. M. Wakimoto, 1997: Influence of the Synoptic-Scale Flow on Sea Breezes Observed during CaPE. Monthly Weather Review, Vol. 125, pp. 2112-2130.

Bevis, M., S. Businger, T.A. Herring, C. Rocken, R.A. Anthes, and R.H.Ware, 1992: GPS meteorology: Sensing of atmospheric water vapor using the global positioning system, J. Geophys. Res., 97, 15787-15801.

Bevis, M., S. Businger, S. Chiswell, T. A. Herring, R. A. Anthes, C. Rocken, and R. H. Ware, 1994: GPS meteorology: Mapping zenith wet delays onto precipitable water, J. Appl. Met., 33, 379-386.

Blewitt, G. 1997: Basics of the GPS technique: observation equations. Pp 9-54 in Geodetic applications of GPS, edited by B. Jonsson. National Land Survey of Sweden.

Bruegge, C. J., J. E. Conel, R. O. Green, J. S. Margolis, R. G. Holm, and G. Toon, 1992: Water vapor column abundances retrievals during FIFE, J. Geophys. Res., 97, 18759–18768.

Businger, S., S.R. Chiswell, M. Bevis, J. Duan, R.A. Anthes, C. Rocken, R.H. Ware, M. Exner, T. VanHove, and F.S. Solheim, 1996: The promise of GPS in atmospheric monitoring, Bull. Amer. Meteor. Soc., 77, 5-18.

Cess, R. D., 2005: Water Vapour Feedback in Climate Models, Science, Vol 310, no5749, pp795-796.

Colman, R., 2003. A comparison of climate feedbacks in general circulation models. Climate Dynamics, 20, 865-873.

Dach, R., U. Hugentobler, P. Fridez, and M. Meindl, (Eds.) 2007: Bernese GPS Software Version 5.0, Astronomical Institute, university of Bern, Switzerland.

Dai, A., 2009: US National Centre for Atmospheric Research, report to Met Office.

Duan, J., M. Bevis, P. Fang, Y. Bock, S. Chiswell, S. Businger, C. Rocken, F. Solheim, T. Van Hove, R. H. Ware, S. Mc-Clusky, T. A. Herring, and R. W. King, 1996: GPS meteorology: Direct estimation of the absolute value of precipitable water, J. Appl. Met., 35, 830-838.

Elgered, G., H -P. Plag, S. Barlag, and J. Nash, 2004: COST716 national report, European Union, 252 pp.

Emardson, T. R., G. Elgered, and J. M. Johanson, 1998: Three months of continuous monitoring of atmospheric water vapor with a network of global positioning system receivers, J. Geophys. Res., 103, 1807-1820.

Emardson, T. R., J. M. Johanson, and G. Elgered, 2000: The systematic behaviour of water vapor estimates using four years of GPS observations, Trans. IEEE Geosci. and Rem. Sensing, GE-3, 24-329.

Falvey, M., and J. Beavan, 2002: The impact of GPS precipitable water assimilation on mesoscale model retrievals of orographic rainfall during SALPEX'96. Mon. Wea. Rev, 130, 2874-2888.

Gradinarsky, L. P., J. M. Johansson, H. R. Bouma, H.-G. Scherneck, and G. Elgered, 2002: Climate monitoring using GPS, Phys. Chem. Earth, 27, 225-340.

Grody, N., J. Zhao, R. Ferraro, F. Weng, and R. Boers, 2001: Determination of precipitable water and cloud liquid water path over oceans from the NOAA 15 advanced microwave sounding unit, J. Geophys. Res., D3, 2943-2953.

Guerova, G., E. Brockmann, J. Quiby, F. Schubiger, and C. Matzler, 2003: Validation of NWP mesoscale models with Swiss GPS network AGNES, J. Appl. Met., 42, 141-150.

Guerova, G., J. M. Bettems, E. Brockmann, and C. Matzler, 2006: Assimilation of COST-716 near real-time GPS data in the nonhydrostatic limited area model used at MeteoSwiss. Meteorol. Atmos. Phys., 91, 149-164.

Haan, S. de, S.J.M. Barlag, H. Klein Baltink, F. De Bie and H. van der Marel, 2004: Synergetic use of GPS water vapor and Meteosat images for Synoptic Weather Forecasting J. Appl. Meteorol., 43, 514-518.

Haan, S. de, 2006: Measuring atmospheric stability with GPS, J. Appl. Met., 3, 467-475.

Haan, S. de, 2008: GPS processing, Technische Rapport, Koninklijk Nederlands Meteorologisch Instituut.

Hagemann S., L. Bengtsson, and G. Gendt, 2003: - On the determination of atmospheric water vapour from GPS measurements, J. Geophysical Research, 108 (D21), 4678, doi:10.1029/2002JD003235,.

Hansen, J., A. Lacis, D. Rind, G. Russell, P. Stone, I. Fung, R. Ruedy, and J. Lerner, 1984: Climate sensitivity: Analysis of feedback mechanisms. In Climate Processes and Climate Sensitivity, AGU Geophysical Monograph 29, Maurice Ewing Vol. 5. J.E. Hansen and T. Takahashi, Eds. American Geophysical Union, pp. 130-163.

Harrison, L., J. Michalsky, and J. Berndt, 1994: Automated multifilter rotating shadow-band radiometer: an instrument for optical depth and radiation measurements, Appl. Opt., 33, 5118–5125.

Hase, F., Hannigan, J.W., Coffey, M. T., Goldman, A., Hopfner, M., Jones, N. B., Rinsland, C. P., and Wood, S. W., 2004: Intercomparison of retrieval codes used for the analysis of high-resolution, ground-based FTIR measurements, J. Quant. Spectrosc. Ra., 87, 25–52.

Healy, S. B., A. M. Jupp, and C. Marquardt, 2005: Forecast impact experiment with GPS radio occultation measurements, Geophys. Res. Lett., 32.

Hewison, T. J., 2006: Profiling Temperature and Humidity by Ground-based Microwave radiometers, PhD Thesis, Dept of Meteorology, Reading University.

Holben, B. N., T. F. Eck, I. Slutsker, D. Tanr´e, J. P. Buis, A. Setzer, E. Vermote, J. A. Reagan, Y. J. Kaufman, T. Nakajima, F. Lavenu, I. Jankowiak, and A. Smirnov, 1998: AERONET—A Federated Instrument Network and Data Archive for Aerosol Characterization, Remote Sens. Environ., 66, 1–16.

Holleman, I., 2005: Quality control and verification of weather radar wind profiles, J. Atmos. Ocean. Technol., 22, 1541-1550.

Holton, J. R., 1992: An Introduction to Dynamic Meteorology, Academic Press, 511 pp.

Houghton, J. T., L. G. Meira Filho, B. A. Callander, N. Harris, A. Kattenberg, and K. Maskell, 1996: Climate Change 1995: The science of climate change, Cambridge University Press, Cambridge, UK.

Houghton, J.T., Y. Ding, D.J. Griggs, M. Noguer, P.J. van der Linden, X. Dai, K. Maskell, and C.A. Johnson, (eds), 2001: Climate Change 2001: The Scientific Basis. Contribution of Working Group I to the Third Assessment Report of the Intergovernmental Panel on Climate Change, Cambridge University Press, Cambridge, UK.

Jaldehag R. T. K., J. M. Johansson, J. L. Davis, and P. Elosegui, 1996: Geodesy using the Swedish permanent GPS network: Effects of snow accumulation on estimates of site positions. Geophysical research letters, vol. 23, n°13, pp. 1601-1604.

Jupp, A., 2006: Met Office assimilation results, TOUGH Deliverable D48, Danish Meteorological Institute, http://tough.dmi.dk

Kouba, J. and Heroux, P., 2001: Precise point positioning using IGS orbit and clock products, GPS Solutions 5 (2): 12-28

Larson, K. M., E. E. Small, E. D. Gutmann, A. L. Bilich, J. J. Braun, and V. U. Zavorotny, 2008: Use of GPS receivers as a soil moisture network for water cycle studies, Geophys. Res. Lett., *35*, L24405, doi:10.1029/2008GL036013.

Leiterer, U., H. Dier, and T. Naebert, 1997: Improvements in radiosonde humidity profiles using RS80/RS90 radiosondes of Vaisala, Beitr. Phys. Atmosph., 124, 319-336.

Liou, Y. A., Y. T. Teng, T. van Hove, and J. C. Liljegren, 2001: Comparison of precipitable water observations in the near tropics by GPS, microwave radiometer, and radiosondes, J. Appl. Met., 40, 5-15.

Lorenc, A.C., D. Barker, R.S. Bell, B. Macpherson, and A.J. Maycock, 1996: On the use of radiosonde humidity observations in mid-latitude NWP, Meteor. Atmos. Phys., 60, 3-17.

Manabe, S., and R.T. Wetherald, 1967: Thermal Equilibrium of the Atmosphere with a Given Distribution of Relative Humidity. *J.* Atmos. Sci., 24, 241–259.

McClatchey, R. A., R. W. Fenn, J. E. A. Selby, F. E. Volz, and J. S. Garing, 1971; Optical properties of the atmosphere. Report AFRCL-71-0279, pp85, Air Force Cambridge Research Laboratories.

Moncrieff, M. W., and M. J. Miller, 1976: The dynamics and simulation of tropical cumulonimbus and squall lines. Quart. J. Roy. Meteor. Soc., 102, 373-394.

Nash, J., C. Gaffard, T. Hewison, E. Norton, J. Agnew, E. Walker, J. Jones, M. Smees, M. Ramatschi, and G. Dick, 2006: Humidity Evaluation using GPS, Radiometer, Wind Profiler and UV Lidar During CSIP Associated with Thunderstorms, Proceedings of COST720 Final Symposium.

Niell, A. E., 1996: Global mapping functions for the atmospheric delay at radio wavelengths, J. Geophys. Res., 101, 3227-3246.

Niell, A. E., 2000: Improved atmospheric mapping functions for VLBI and GPS, Earth Planets Space, 699-702.

Orliac E. J., R. M. Bingley, and A. H. Dodson, 2003; An assessment of Near Real-Time and Post-Processing Strategies for Tropospheric Delay Estimation from a Planned CGPS Network in the UK. Atmospheric Remote Sensing using Satellite Navigation Systems, Special Symposium of the URSI Joint Working Group FG, 13-15 October 2003, Matera, Italy

Pacione, R., C. Sciaretta, C. Faccani, R. Ferretti and F. Vespe, 2001: GPS WV assimilation into MM5 with the nudging technique. Phys. Chem. Earth (A), 26, 481-485.

Parker, D.E., T.P. Legg, and C.K. Folland. 1992. A new daily Central England Temperature Series, 1772-1991. Int. J. Clim., Vol 12, pp 317-342.

Paukkunen, A., V. Antikainen, and H. Jauhiainen, 2001; Accuracy and Performance of the New Vaisala RS90 Radiosonde in Operational Use , Proceedings from 11th Symposium on Meteorological Observations and Instrumentation, 14-19 Jan. 2001, New Mexico, AMS

Paukkunen A, 2002: Measurement Accuracy and Repeatability of Vaisala RS90 Radiosonde. Vaisala News no 159, pp11-13.

Philipona, R., B. Dürr, A. Ohmura, and C. Ruckstuhl, 2005: Anthropogenic greenhouse forcing and strong water vapour feedback increase temperature in Europe, Geophys. Res. Lett., 32, L19809, doi:10.1029/2005GL023624.

Pielke, R. A., 1981: An overview of our current understanding of the physical interactions between the sea- and land-breeze and the coastal waters. Amsterdam, Ocean Manage, Vol. 6, p. 87-100.

Poli, P., P. Moll, F. Rabier, G. Desroziers, B. Chapnik, L. Berre, S. B. Healy, E. Andersson, and F.-Z. El Guelai, 2007: Forecast impact studies of zenith total delay data from European near real-time GPS stations in Meteo France 4DVAR, J. Geophys. Res., 112, 1-16.

Rocken, C., R. Ware, T. VanHove, F. Solheim, C. Alber, J. Johnson, M Bevis, and S. Businger, 1993: Sensing atmospheric water vapor with the global positioning system, Geophys. Res. Lett., 20, 2631-2634.

Rocken, C., T. Van Hove, J. Johnson, F. Solheim, R. Ware, M. Bevis, S. Chiswell, and S. Busingerb, 1995: GPS/STORM - GPS sensing of atmospheric water vapor for meteorology, J. Atmos. Ocean. Technol., 12, 468-478.

Rocken, C. R., T. van Hove, and R. H. Ware, 1997: Near real-time GPS sensing of atmospheric water vapor, Geophys. Res. Lett., 24, 3221-3224.

Rodgers, C. D., 2000: Inverse Methods for Atmospheric Sounding: Theory and Practice, World Scientific Publishing Co., Singapore, ISBN 981-02-2740-X, 1223-1225.

Rosenkranz, P.W., 1998: Water vapor microwave continuum absorption: A comparison of measurements and models. Radio Sci., 33, 919-928.

Rothacher, M., and L. Mervart, 1996: Bernese GPS software version 4.0, Technical report, Astronomical Institute, Berne University, Switzerland.

Saastamoinen, J., 1972: Atmospheric correction for the troposphere and stratosphere in radio ranging of satellites, Geoph. Monograph Series, 15, 247-251.

Schmid, B., J. J. Michalsky, D. W. Slater, J. C. Barnard, R. N. Halthore, J. C. Liljegren, B. N. Holben, T. F. Eck, J. M. Livingston, P. B. Russell, T. Ingold, and I. Slutsker, 2001: Comparison of columnar water-vapor measurements from solar transmittance methods, Appl. Opt., 40, 1886–1896.

Schneider, M., Hase, F., and Blumenstock, T, 2006: Ground-based remote sensing of HDO/H2O ratio profiles: introduction and validation of an innovative retrieval approach, Atmos. Chem. Phys., 6, 4705–4722.

Schneider, M. and F. Hase, 2009: Reviewing the development of a ground based FTIR water vapour profile analysis, submitted to Atmos. Meas. Tech.

Senior, C., and J. Mitchell, 1993: Carbon Dioxide and Climate. The Impact of Cloud Parameterization. J. Climate, 6, 393–418.

Smith, E. K., and S. Weintraub, 1953: The constants in the equation for atmospheric refractive index at radio frequencies, Proc IRE, 41, 1035-1037.

Smirnov, A., B. N. Holben, T. F. Eck, O. Dubovik, and I. Slutsker, 2000: Cloud screening and quality control algorithms for the AERONET database, Remote Sens. Environ., 73, 337-349.

Soden B.J., and I.M. Held, 2006: An assessment of climate feedbacks in coupled ocean-atmosphere models. J Climate 19, 3354-3360.

Solheim, F. S. J. Vivekanandan, R. H. Ware, C. Rocken, 1999: Propogation delays induced in GPS signals by dry air, water vapour, hydrometers and other particulates, J. Geophys. Res., Vol 104, No. D8, p.9663-9670.

Solomon, S., D. Qin, M. Manning, Z. Chen, M. Marquis, K.B. Averyt, M. Tignor, and H.L. Miller, (eds), 2007: Climate Change 2007: The Physical Science Basis. Contribution of Working Group I to the Fourth Assessment Report of the Intergovernmental Panel on Climate Change, Cambridge University Press, Cambridge, United Kingdom and New York, NY, USA, 996 pp.

Stainforth D. A., T. Aina, C. Christensen, M. Collins, N. Faull, D. J. Frame, J. A. Kettleborough, S. Knight, A. Martin, J. M. Murphy, C. Piani, D. Sexton, L. A. Smith, R. A. Spicer, A. J. Thorpe and M. R. Allen, 2005: Uncertainty in Predictions of the Climate Response to Rising Levels of Greenhouse Gases. Nature, Vol. 433: 403:406.

Thayer, G. D., 1974: An improved equation for the radio refractive index of air, Radio Sci., 9, 803-807.

Thompson, A. R., J. M. Moran, and G. W. Swenson, 1986: Interferometry and Synthesis in Radio Astronomy, John Wiley and Sons, New York, 720 pp.

Unden, P., L. Rontu, H. Jarvinen, P. Lynch, J. Calvo, G. Cats, J. Cuhart, and K. Eerola, 2002: HIRLAM-5 scientific documentation, Technical report, HIRLAM-project, Norrkopping.

Vespe, F., and R. Pacione, 2007: GPS Tropospheric Processing for NRT and Post-Processing Applications at ASI. Presentation: EUREF Symposium, London England.

Vomel, H., H. Selkirk, L. Miloshevich, J. Valverde, J. Valdes, E. Kyro, R. Kivi, W. Stolz, G. Peng, and J. A. Diaz, 2007: Radiation dry bias of the Vaisala RS92 humidity sensor, J. Atmos. Oceanic Technology., 24, 953–963.

Wang, J., and L. Zhang, 2008: Systematic errors in global radiosonde precipitable water data from comparisons with ground-based GPS measurements. J. Climate, Vol. 21, n°10, pp. 2218-2238

Webb, F. H., and J. F. Zumberge, 1993: An introduction to GIPSY/ OASIS-II, JPL publication D-11088, Jet Propulsion Laboratory, Pasadena, California.

Webb M. J., C. Senior, D. Sexton, W. Ingram, K. Williams, M. Ringer, B. Mcavaney, R. Colman, B. Soden, R. Gudgel, T. Knutston, S. Emori, T. Ogura, Y. Tsushima, N. Andronova, B. Li, S. Bony and K. Taylor, 2006: On the contribution of local feedback mechanisms to the range of climate sensitivity in two GCM ensembles. Clim Dyn Vol. 27, pp17-38

Weldon, R. B., and S. J. Holmes, 1991: Water vapor imagery interpretation and applications to weather analysis and forecasting, NOAA technical report NESDIS, US Department of Commerce National Oceanic and Atmosperic Administration, Washington DC.

Westwater, E., 1965; Ground-based passive probing using the microwave spectrum of oxygen, Radio Sci., 69D, 1201-1211.

Yokohata, T., S. Emori, T. Nozawa, Y. Tsushima, T. Ogura, and M. Kimoto, 2005: A simple scheme for climate feedback analysis, Geophys. Res. Lett., 32, L19703, doi:10.1029/2005GL023673.

Appendix A - Calculation of Solar Elevation

To calculate solar elevation for a specific date and latitude and longitude we must firstly calculate a

$$X = \left(\frac{2\pi}{360}\right) \qquad \text{and} \qquad Q1 = \left(\frac{H}{24 + DN}\right)0.9863$$

Where H is the decimal hour of day (05:30am = 5.5) and DN is the day of year.

$$D = SIN\left(X\left(Q - 80.877\right)\right)23.43$$

$$W = SIN\left(QX\right)$$

$$Q2 = SIN\left(\left(2QX\right) + 20\right)$$

$$Y = \left(W + 1.855\right) + \left(2.525Q\right)$$

$$Z = \left(15H\right) - Y$$

$$T = Z + \lambda$$

Where λ = Longitude

$$C = SIN\left(\varphi X\right)SIN\left(DX\right)$$

Where φ =latitude

$$B = COS\left(DX\right)COS\left(\varphi X\right)$$

$$Q3 = C - COS\left(TX\right)B$$

$$SolarElevation = \frac{ATN\left(\frac{Q}{\sqrt{(1-Q)Q}}\right)}{X}$$

Where ATN is the Arctan. As such we can accurately estimate the sun's elevation for any latitude, longitude or time.

Appendix B - Further Examples of GFZ/METO IWV Bias

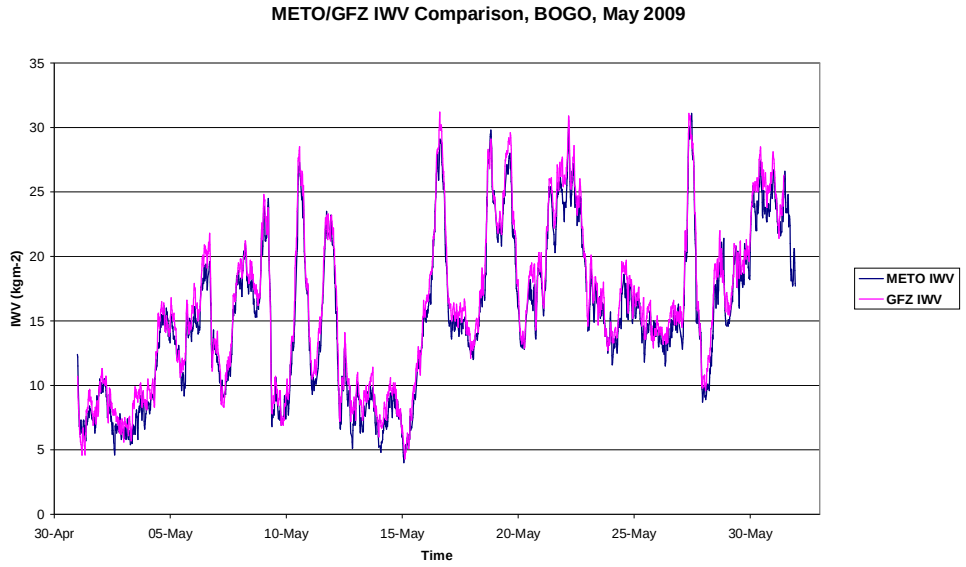

Figure A2.1 Time series of BOGO IWV from GFZ and METO, May 2009

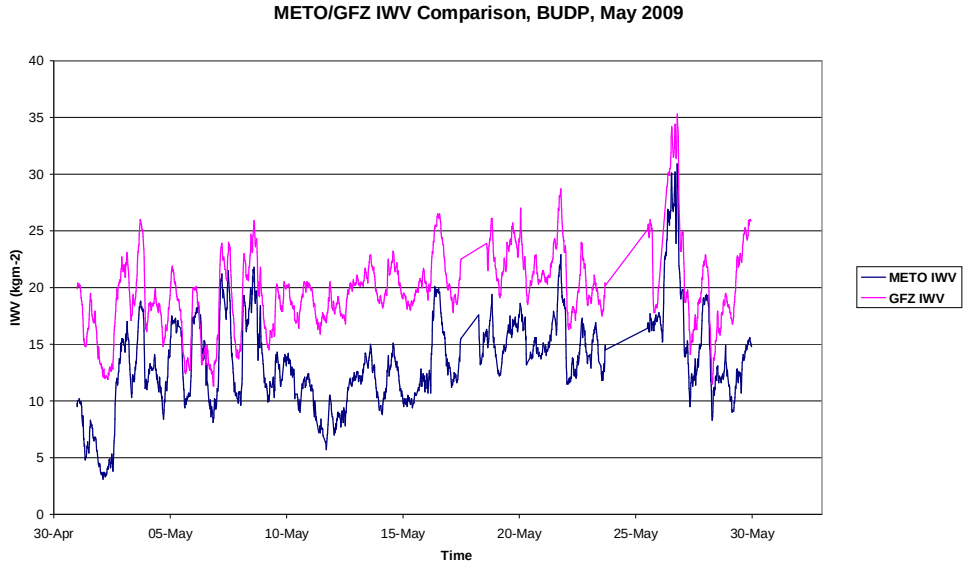

Figure A2.2 Time series of BUDP IWV from GFZ and METO, May 2009

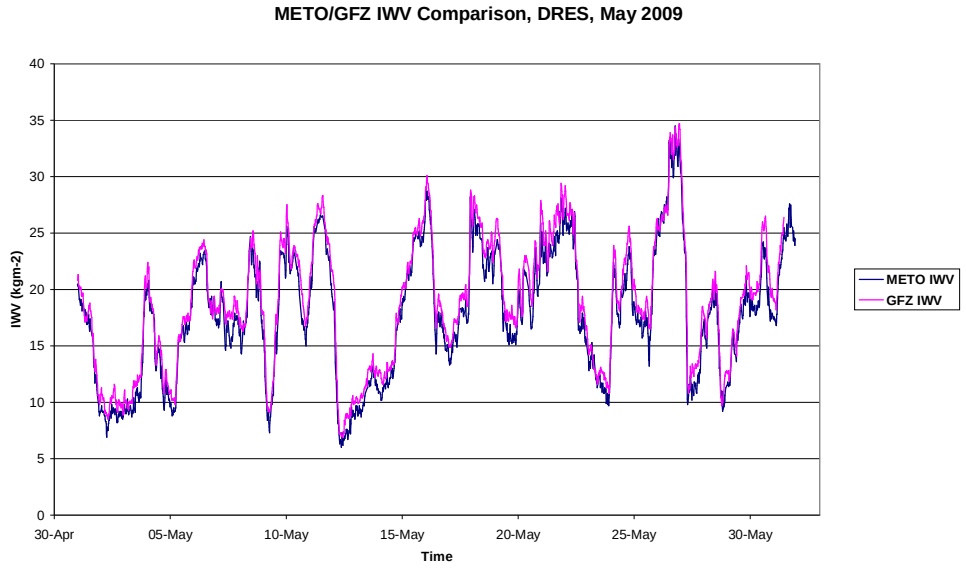

Figure A2.3 Time series of DRES IWV from GFZ and METO, May 2009

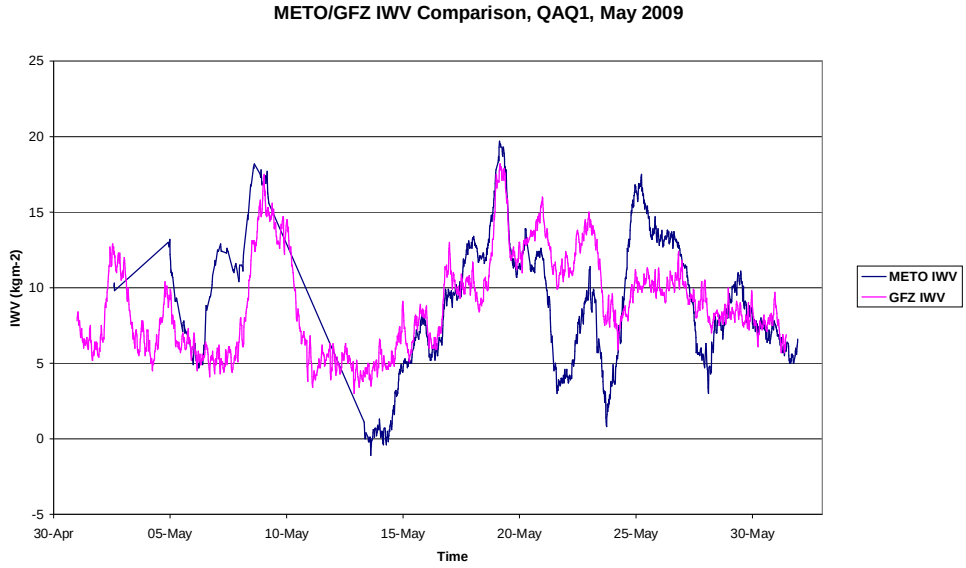

Figure A2.4 Time series of QAQ1 IWV from GFZ and METO, May 2009

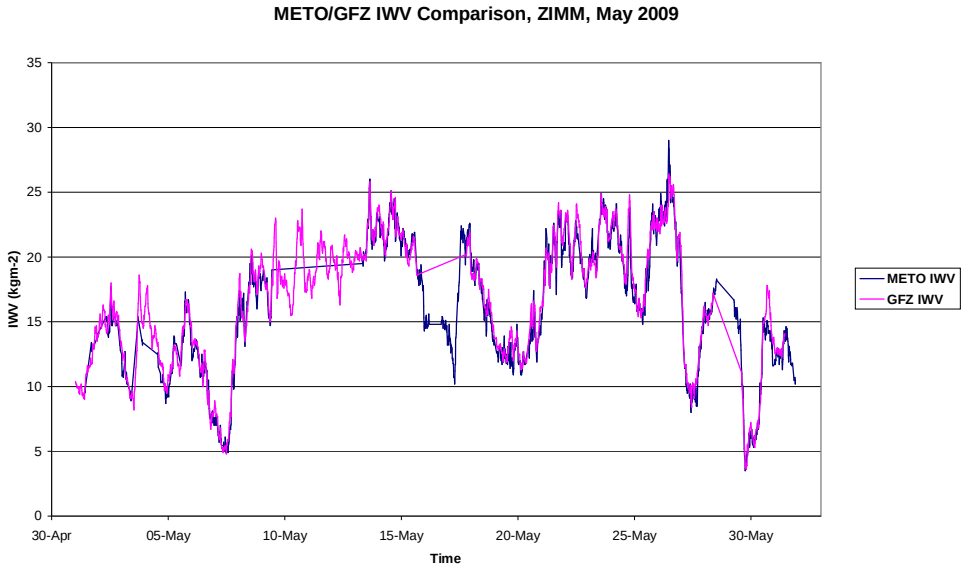

Figure A2.5 Time series of ZIMM IWV from GFZ and METO, May 2009

Appendix C - Bernese v5.0 GPS Processing software

Bernese software v5.0 (BSW5.0) is a highly accuracy, highly flexible suite of programs designed for post processing of radio positioning data. Although the software can process other forms of data such as GLONASS as well as VLBI data, in this thesis and with regards to the METO system, only GPS signals are processed. BSW5.0 is in fact a whole suite of programs which, when used in sequence, can provide high quality coordinate, and more importantly for the subject of this thesis, tropospheric estimates.

Role of the BPE

Although the software was initially designed for manual post-processing applications, the scripts and programs may be controlled by the Bernese Processing Engine (or BPE) to make the software run on an automated basis. This is essential for operational applications such as near real-time tropospheric applications as it would be far too cumbersome to process the data on a manual basis. The BPE is called from a script set up as a cron on the Linux server which in turn calls the Process Control File (PCF) which in turn calls the individual programs to enable automated processing.

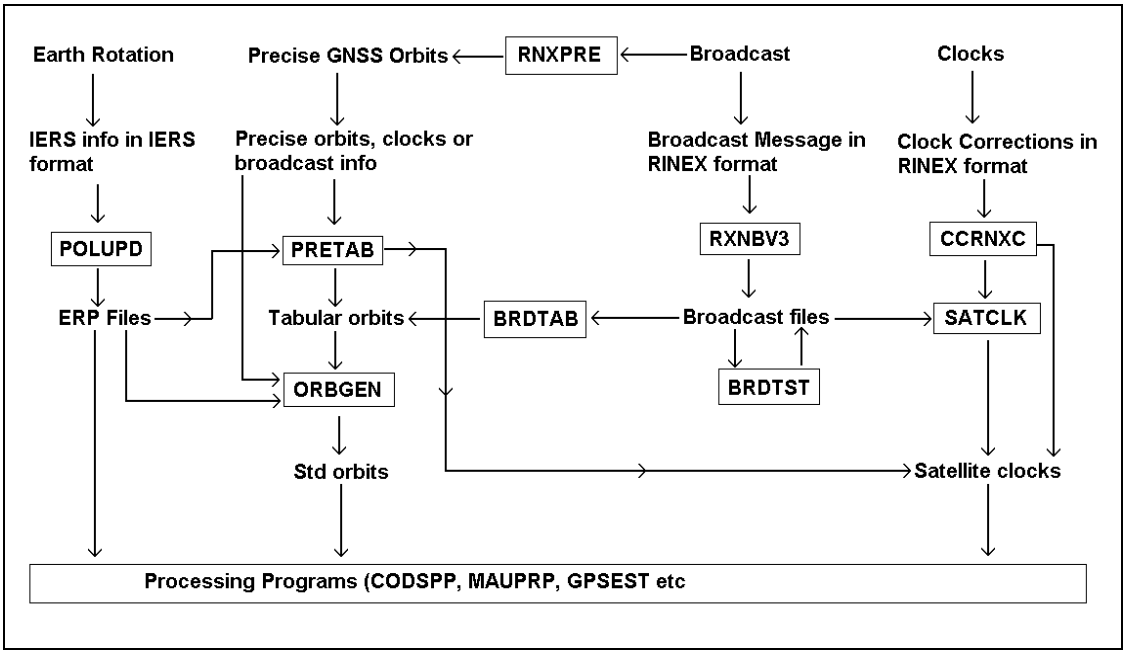

Figure A3.1 Flow diagram of Bernese Preparation of Orbits, Clocks and ERPs

Below is a list of the packages used in a typical METO near real-time processing solution as well as a brief overview of the role of each:

CAMPAIGN SETUP (Generate a-priori coordinates and import observations)

COOVEL– Used to extrapolate a set of coordinates from a reference epoch to the epoch that is to be processed using the corresponding station velocities

RXOBV3 – Import the RINEX observation files to Bernese (binary) format – output is code and phase zero difference headers and observations, i.e. .CZH, .CZO, .PZH and .PZO files

PREPARE POLE INFORMATION

POLUPD – Creates or updates a pole information file (transforms IGS .IEP files into BSW5.0 .ERP files)

PRETAB – Transforms the precise orbit files from the IGS (.PRE or SP3) which are in a terrestrial reference frame into tabular orbits in a celestial reference frame. Creates Tabular orbits (.TAB)

ORBGEN – Prepares the standard orbit files (.STD) using the outputs of PRETAB

DATA PREPROCESSING

CODSPP – Code based clock synchronisation. Main task is to compute the receiver clock corrections

SNGDIF – Creates single difference baselines

MAUPRP – Pre-processing of the phase baseline files. Main task is to detect and correct cycle slips and outliers. Also updates the phase ambiguities of the observation

DATA PROCESSING

GPSEST – Processes individual sessions

GPSEST (again) – Makes a first network solution and generates a ionosphere free solution (L3)

GPSEST (again) – Ambiguity resolution (Quasi Ionosphere Free (QIF) solution)

FINAL NETWORK SOLUTION

GPSEST (again!) – Used in session mode. Ambiguities resolved in the previous run using the QIF strategy are introduced as known. Save the normal equation or NQ0 files

ADDNEQ2 – Check the coordinates of the fiducial sites by performing a minimum constraint solution by combining the normal equation files output by either GPSEST or ADDNEQ2 based on least squares estimation techniques

For more information on the BPE package, please refer to Dach et al., 2007